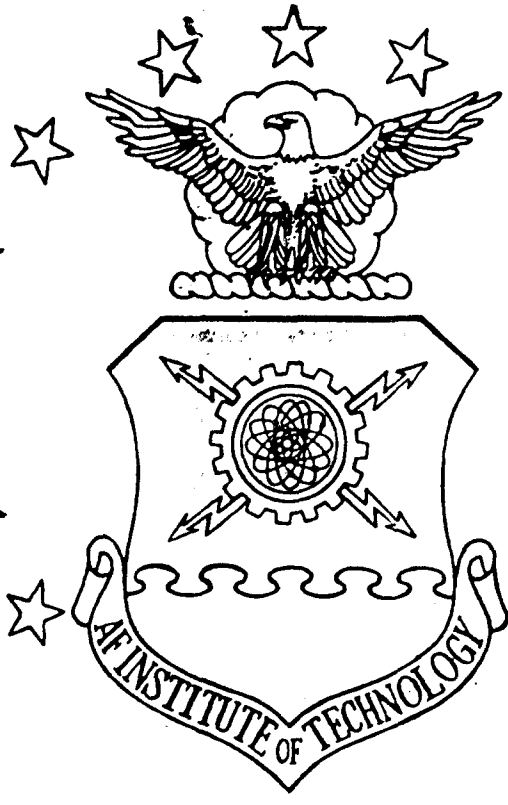

DEPARTMENT OF THE AIR FORCE

AIR UNIVERSITY

AIR FORCE INSTITUTE OF TECHNOLOGY

Wright-Patterson Air Force Base, Ohio

AFIT/GE/ENG/91D-55

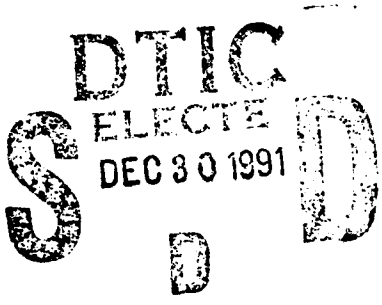

Evaluation of an Interdigitated Gate Electrode Field-Effect Transistor (IGEFET) for *In Situ* Resin Cure Monitoring

THESIS

Thomas E. Graham
Captain, USAF

AFIT/GE/ENG/91D-55

Approved for public release; distribution unlimited

AFIT/GE/ENG/91D-55

Evaluation of an Interdigitated Gate Electrode Field-Effect Transistor (IGEFET) for *In Situ* Resin Cure Monitoring

THESIS

Presented to the Faculty of the School of Engineering

of the Air Force Institute of Technology

Air University

In Partial Fulfillment of the

Requirements for the Degree of

Master of Science in Electrical Engineering

Thomas E. Graham, B.S.E.E.

Captain, USAF

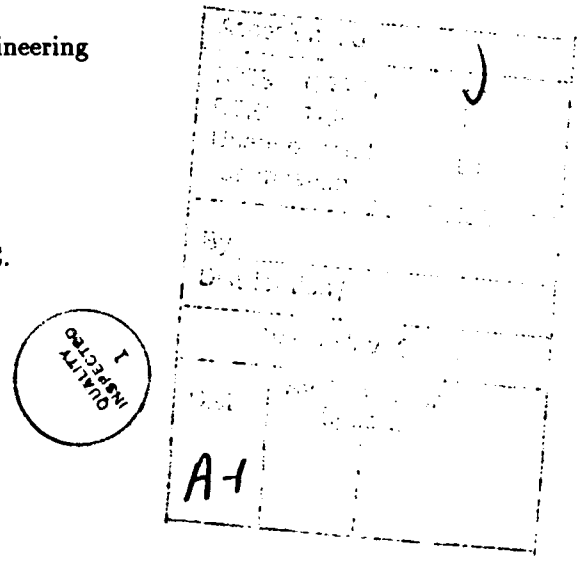

15 November 1991

Acknowledgments

This thesis has been the most ambitious undertaking of my life. Without the knowledge, help, and support of several individuals, this thesis would not have been possible. I deeply appreciate the assistance I received.

I am grateful to my advisor, Lt Col Edward Kolesar, for his patience and his positive attitude. His continual interest in my work kept me going when little else would. I owe Ms Francis Abrams at the Wright Research and Development Center's Non-Metallic Materials Laboratory thanks for making her personnel, equipment, and expertise available to me. I also owe a debt of gratitude to Capt John Wiseman and Capt Thomas Jenkins for their advice and assistance, and to Capt Anthony Moosey, Capt Rocky Weston, and Capt Charles Brothers for their moral support. I would also like to thank the AFIT Electronics and Materials Cooperative Laboratory Staff for their help with the facilities and equipment used in this thesis.

Finally, I would like to thank my wife, Marisa, and my son, Chistopher for their love, understanding, and support through this experience.

Thomas E. Graham

Table of Contents

List of Figures

List of Tables

Abstract

The purpose of this study was to design an Interdigitated Gate Electrode Field-Effect Transistor (IGEFET) and evaluate its performance as an *in situ* resin cure monitor. A commercially available resin was selected for the research, and rheological studies were performed to establish the optimal range of cure temperatures. Additional rheological studies were performed to identify the resin's gelation point during isothermal cures at two selected temperatures, and to determine the resin's glass transition temperature. The interdigitated gate electrode of the IGEFET was coated with samples of the resin, and electrical measurements were performed while the resin cured. The chemical changes which occur in the resin as a result of curing were manifested in the interdigitated gate electrode's electrical characteristics. The results reveal that the IGEFET is capable of sensing the electrical impedance changes, and hence the chemical changes, which occur during the resin's cure. In particular, the chemical changes due to gelation are evident in the IGEFET's electrical response data. In addition, the resin which was cured at the higher temperature was close to its glass transition temperature, and hence softer than the resin cured at the lower temperature, and the IGEFET was capable of detecting this differnce.

Evaluation of an Interdigitated Gate Electrode Field-Effect Transistor (IGEFET) for *In Situ* Resin Cure Monitoring

I. Introduction

Background

The development of sensors for monitoring the cure of epoxy resin compounds has been an active area of research for many years. With the advent of composite material aircraft structures, the military could benefit from the development of ***in situ*** sensors which are capable of measuring the cure rate of epoxy resins. Potentially, such devices could be utilized in a system that would be able to detect critical processing events, such as the gelation point, and use these milestones to determine the optimum cure process for a given resin or composite material.

Composite materials are more complicated compared to stand-alone resins. Aircraft structures which utilize advanced composite materials are typically manufactured with carbon fiber mats which have been pre-impregnated with a resin. The mats, called "prepregs", are usually stacked and trimmed to a desired configuration, and they are usually cured at an elevated temperature under vacuum (1:4). The result is an inhomogeneous laminate material. The mechanical properties of resins and laminates are highly process dependent (2:275), and the development of a sensor capable of inter-laminar, real-time measurement of the cure of composite materials for the purpose of increasing process control has an immediate military application.

The interdigitated gate electrode field-effect transistor (IGEFET) is a sensor which is potentially capable of performing this task. An IGEFET is a metal-oxide-semiconductor field-effect transistor (MOSFET) with an interdigitated gate electrode (IGE) structure. Its potential utility as a solid-state sensor for certain environmentally-sensitive gases, as well as its

potential as an *in situ* sensor for measuring a resin's cure rate have been investigated at the Air Force Institute of Technology (AFIT) (3, 4, 5, 6). Because the IGEFET is small in size (7.9 x 9.2 mm), it may be unobtrusively implanted in a resin or composite material whose cure is to be monitored. By direct extension, it is also envisaged that the implanted sensor could provide long-term information concerning the mechanical and physical integrity of the material while it is being used.

The gate electrode structure of an IGEFET consists of two interdigitated conductors, as illustrated in Figure 1.1. The floating-electrode, which serves as the gate contact for the MOSFET, is electrically and physically isolated from the driven-electrode. When the device is used to detect a specific environmentally-sensitive gas, the IGE structure is coated with an organic semiconductor polymer (for example, a metal-doped phthalocyanine) that changes its composition, and hence its electrical conductivity, in the presence of the challenge gas (3, 4, 5). The change in the polymer's electrical conductivity causes a corresponding change in the characteristic response of the IGE structure to an electrical stimulus.

The chemical structure and electrical characteristics of an epoxy resin are known to change continuously during its cure (8, 9). As the resin cures, the polymer chains which constitute its chemical structure increase in size. Consequently, the ability of the polymer chain's molecular dipoles to orient themselves in the presence of an electric field becomes increasingly limited as the cure process progresses. In addition, the mobility of ions in the material correspondingly decreases. The overall effect is a decrease in the relative permittivity and dielectric loss of the resin as it cures (9:448, 10:88). These changes in the dielectric characteristics of the resin during its cure can be detected by the IGEFET. Introductory work by Kolesar and Wiseman has demonstrated the IGEFET's utility in this application (3, 6).

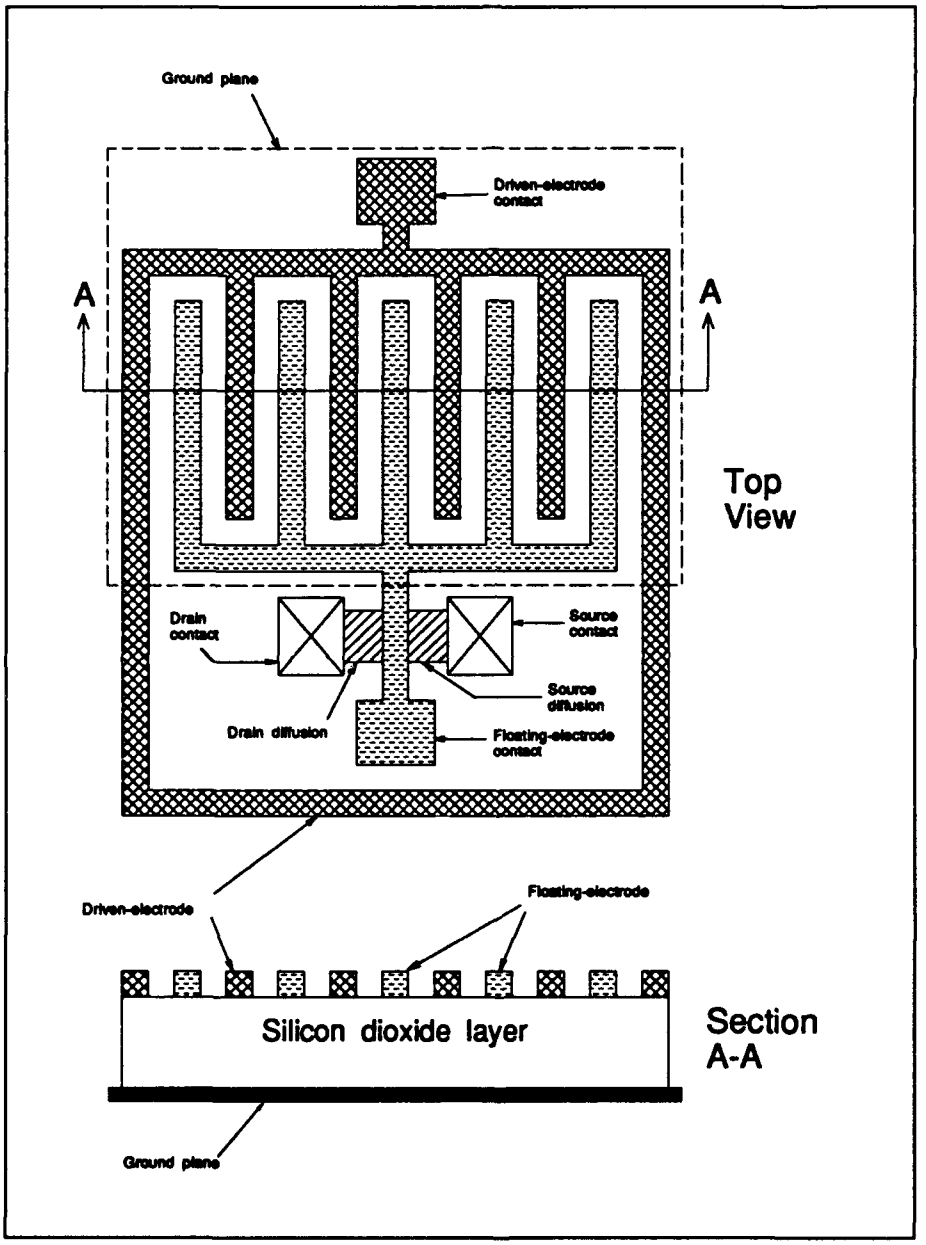

Figure 1.1. Illustration of the IGEFET (7).

Problem Statement

A more comprehensive investigation of the IGEFET's response to changes in the electrical properties of epoxy resins has been motivated by preliminary research.

Justification. A closer examination of the IGEFET's response to resin cure, with a goal of locating the characteristic gelation point by analysis of the IGEFET's response data, is warranted. In his IGEFET research, Wiseman investigated the feasibility of using the IGEFET to monitor a resin's cure rate (3). He used a well-characterized epoxy resin (Epon 828, Miller-Stephenson Chemical Co., Danbury, CT), and applied it as a thick film to the IGE structure. Wiseman was able to show that the IGEFET's response to a thick film of epoxy resin could be attributed to the changing permittivity of the resin as it cured. Epoxy resins, in general, display a dramatic change in electrical conductivity when their characteristic gelation point is attained (11:188).

Scope. The purpose of this thesis is to characterize the response of the IGEFET sensor to a thermosetting epoxy resin system. The cure of this resin has been characterized with respect to two different isothermal temperature profiles. The data collected was direct current (dc) resistance of the IGE structure, alternating current (ac) impedance (magnitude and phase) of the IGE structure, and the transient (time-domain) and spectral (frequency-domain) responses of the IGEFET to a voltage pulse excitation. The resin was applied directly to the IGE structure, and the data collected was analyzed to identify its gelation point. Rheological studies of the resins used in the IGEFET sensor studies were also conducted for the same isothermal temperature profiles, and the measured viscosity data was used to locate the gelation point of the resin. All electrical characteristics, measured with respect to time, were compared to the viscosity data, which were also measured with respect to time. A dramatic change in the electrical characteristics of the resin was expected to occur as a result of the resin's gelation.

Definitions. In the interest of improving clarity for this multi-disciplinary research topic, several fundamental definitions of the key terminology are presented.

An *epoxy group*, also called an epoxide, is defined as an oxygen atom bound to two carbon atoms which are also connected in some manner (12:1-1). This term is often used interchangeably with the term *resin*.

A *resin* is a molecule which contains more than one epoxy group (12:1-2). In this thesis, the terms *epoxy resin* and *resin* will be used interchangeably.

The *gelation point* (or *gel point*), of a resin can be defined many ways. An abstract, microscopic definition is that the gelation point corresponds to the moment an infinitely long polymer chain has been produced (8:272). From a macroscopic and practical perspective, the gelation point is defined as the moment the resin loses its fluidity, or becomes rubbery. At this point, bubbles can no longer rise through the material (8:274). A consequence of the differing definitions for the gelation point is that interpretations of its occurrence in a resin can differ, given identical sets of data. Therefore, the establishment of a technique for identifying the gelation point is somewhat arbitrary. The method used in this thesis effort will be to locate the point at which the storage modulus of the resin (G') is equal to the loss modulus (G'') (13:571). In general, the complex shear modulus (G^*) is given by, $G^* = G' + jG''$, and it is related to complex viscosity (η^*) by the expression $\eta^* = G^*/\omega$, where ω is the angular frequency at which the material is physically twisted. Additionally, the mechanical *loss tangent* ($\tan\delta_m$) is defined to be the ratio between the loss modulus and the storage modulus ($\tan\delta_m = G''/G'$).

Whenever a dielectric material becomes electrically lossy, its permittivity becomes complex. The *complex permittivity* consists of a real part (the relative permittivity, denoted by ϵ'), and an imaginary part (the loss factor, denoted by ϵ'') (14:4).

Approach

The critical milestones implemented in this investigation included a redesign of the IGEFET, qualification of the revised IGEFET after fabrication, and collection of the resin cure performance data. These steps are described in the following sections.

IGEFET Redesign. The previous IGEFET designs contributed by Jenkins and Shin (4, 5) were largely successful, so the accomplishment of the redesign of the IGEFET was, for the most part, an exercise of combining the best features from each design.

A block diagram of the IGEFET circuit is illustrated in Figure 1.2. The revised integrated circuit consists of:

1. 3 x 3 matrix of IGEFET sensor elements. Each sensor element is composed of an IGE structure and a sensor element amplifier.
2. Ground plane. This dielectrically-isolated ground plane, realized from first-level metal, passes beneath the signal lines an the IGE structures.
3. Demultiplexer. This circuit determines which of the nine sensor elements will be connected to the input.
4. Multiplexer. This circuit selects the output of one of the sensor element amplifiers.
5. Output interface. Two such interfaces are available at the discretion of the user: first, a voltage follower, or second, a five-stage operational amplifier which provides additional gain.
6. Reference element. The reference element is composed of a sensor element amplifier (identical to those fabricated for the IGEFET sensor elements) whose input is tied to a solid, second-level metal electrode. The area of this electrode is approximately equal to the combined areas of the driven- and floating-electrodes which compose the IGE structure. During the collection of IGEFET response data (gain and phase delay, and frequency-domain response to a voltage pulse excitation), identical sets of data were

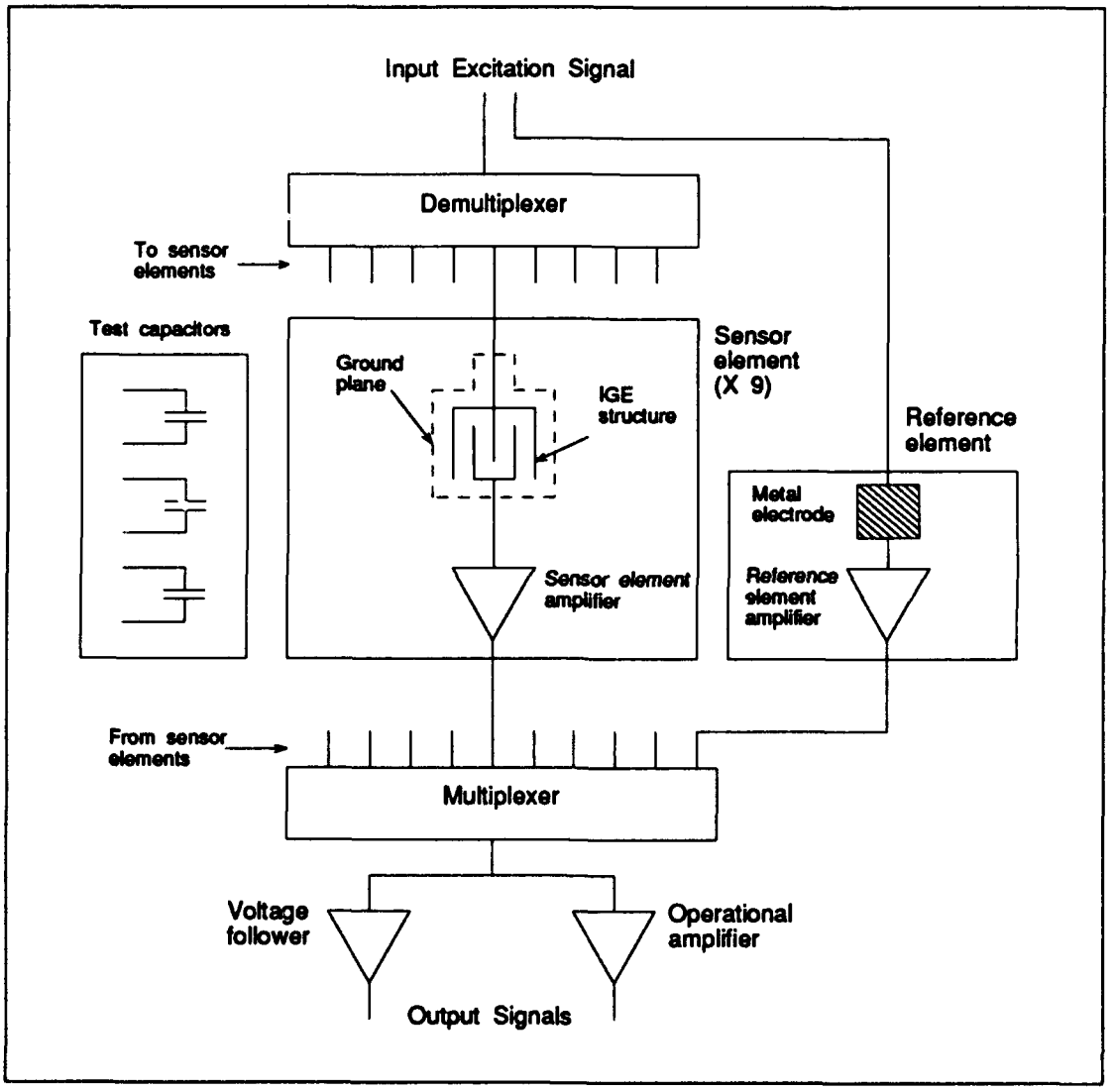

Figure 1.2. Block diagram of the IGEFET sensor system.

collected for the reference element. Comparison of the IGEFET and reference element data provided information concerning the effect of the experimental conditions on the IGEFET electronics. In particular, the spectral response of the reference element was subtracted from the spectral response of the IGEFET to provide the difference Fourier transform spectrum. The difference Fourier transform spectrum provided information concerning the spectral response of the IGE structure without the effects of the IGEFET electronics or the effects of the electrical parasitics in the measurement system.

7. Three parallel-plate test capacitors. These passive elements facilitated characterizing the field-oxide layer which isolates the ground plane from the IGE structure.

A number of areas have been intentionally exposed on the integrated circuit (IC) die to facilitate excision of inoperative circuits with an ultrasonic microprobe cutter. In addition, most important internal nodes are accessible via microprobe bonding pads.

IGEFET Qualification. This milestone was initiated when the IGEFET integrated circuit packages were received from the Metal-Oxide-Semiconductor Implementation System (MOSIS) fabrication service. The following steps were accomplished to ensure proper operation of the IGEFET sensors. A randomly selected sample package was evaluated, and it satisfied the following criteria:

1. Physical and electrical isolation of the driven- and floating-electrodes was verified by visual inspection and by requiring a minimum of 30 dB of isolation between them.
2. Proper operation of the multiplexer and demultiplexer was verified. This requirement was established because each circuit had to provide a minimum isolation of 30 dB relative to each non-selected signal line.
3. The sensor element amplifier and voltage follower were checked for proper operation relative to the specified design constraints. Since a previous design was being utilized, the expected

performance was anticipated to be comparable to the performance realized in that design effort. As a result, the measured gain at the voltage follower output was approximately 20 dB with a 3-dB cutoff frequency of approximately 450 KHz (4:5-4).

4. The 5-stage operational amplifier was evaluated for proper operation within the specified design constraints. Only the first stage of the operational amplifier was utilized, and it yielded an overall gain of approximately 20 dB with a 3-dB cutoff frequency of approximately 850 KHz.

Faulty components could be bypassed or isolated by trimming the appropriate metal signal lines with an ultrasonic microprobe cutter and supplementing the remaining circuit with wire bonds and externally configured electronics.

Performance Data Collection. The resin used in this thesis effort was Epoxy 907 (Miller-Stephenson Co., Danbury, CT), a thermosetting resin with a dielectric filler material. This resin was selected because of its relatively high viscosity in the uncured state, its low cure temperature, and its availability. The resin was subjected to electrical and mechanical tests. The electrical tests, which utilized the IGEFET sensor, are detailed in Table 1.1, and the mechanical tests are detailed in Table 1.2.

Mechanical Performance Tests. A separate effort was implemented to collect the mechanical performance data on the resin. The rheological studies were conducted using instrumentation available at the Materials Division of the Wright Laboratory (WL/MLB). Two types of tests were conducted: parallel plate analysis and torsional bar analysis. The purpose of the parallel plate analysis was to obtain an estimate of the gelation time for the resin, and the purpose of the torsional bar analysis was to estimate its glass transition temperature.

Electrical Performance Tests. A separate test was conducted for each electrical characteristic measured (see Table 1.1) to minimize the time interval between data points. For

Table 1.1. Electrical measurements.

Structure	Measurement
IGE structure	DC resistance • with respect to time • with respect to applied bias AC impedance with respect to frequency • magnitude • phase Transfer function with respect to frequency • gain • phase
IGEFET	Transfer function with respect to frequency • gain • phase Voltage pulse excitation response • time-domain • frequency-domain

each test, a small sample of the uncured resin was applied to a single IGE structure, and the resin's electrical characteristics were measured well beyond its estimated gelation time.

Experimental Data Reduction. After the first complete set of test data was collected, the data reduction process was implemented. The primary goal of the data reduction exercise was to locate the gelation point of the resin by correlating the results obtained with the electrical and mechanical measurements.

Plan of Development

Chapter II contains a literature review concerning MOS-based sensors applied to resin cure monitoring. The theory of resin cure dielectric analysis is discussed in Chapter III. The redesign of the IGEFET sensor, the test fixture, and the experimental methodology are described in

Table 1.2. Mechanical measurements.

Structure	Measurement
Parallel Plate	Storage Modulus (G') Loss Modulus (G'') Complex Viscosity (η^*) • with respect to time for isothermal cure profiles • with respect to temperature for ramped cure profiles
Torsional Bar Analysis	Storage Modulus (G') Loss Modulus (G'') Mechanical Loss Tangent ($\tan \delta_m$) • with respect to temperature

Chapter IV. Chapter V reports the results and findings. The conclusions and recommendations are presented in Chapter VI.

II. Literature Review of Sensors for In Situ *Resin Cure Monitoring*

Introduction

The purpose of this literature review is to discuss recent research concerning sensors for *in situ* resin cure monitoring. The ability to unobtrusively embed a small sensor in a resin for the purpose of real-time cure monitoring will facilitate greater control over the cure process and enhance production of higher quality materials and fabricated parts. This is especially true for the application of monitoring the cure of advanced composite materials whose mechanical properties are highly process dependent (2:275).

A number of techniques exist which facilitate the characterization of the resin cure process. These include Differential Scanning Calorimetry (DSC), Thermal Stimulated Current (TSC), Relaxation Map Analysis (RMA) spectroscopy, Torsional-Braid Analysis various techniques which measure electrical impedance characteristics of the resin, and the measurement of optical characteristics of curing resin systems. However, many of these techniques do not lend themselves to *in situ* resin cure monitoring. In this chapter, the development of the techniques and sensors which facilitate *in situ* resin cure monitoring is presented.

Fluorescence Sensors

In recent years, a considerable body of research has been performed in the area of fluorescence monitoring of chemical and viscosity changes that occur during the cure of epoxy resins. The techniques used by different researchers include the use of dyes which dissolve in the resin being monitored and the use of dyes which react with epoxide groups, called reactive dye labelling. The following sections describe the research performed in these areas.

Fluorescence Monitoring with an Internal Standard. Wang and others at the National Bureau of Standards have been researching the fluorescence monitoring of resin cure for several

years. Their technique incorporates a viscosity-insensitive internal standard dye in conjunction with a dye which is sensitive to changes in local viscosity (15). As the polymerization reaction proceeds, the fluorescence intensity of the viscosity sensitive dye increases, while the fluorescence intensity of the viscosity-insensitive dye remains constant. Using a viscosity-insensitive dye eliminates the reliance upon absolute measures of fluorescence intensities. The researchers contend that the ability to measure relative intensities is more practical in an industrial setting (15:455). The results of their research has demonstrated that this technique is capable of monitoring resin cure throughout the entire cure cycle.

Fluorescence Monitoring with Reactive Dye Labels. A technique which has demonstrated considerable capability has been developed by Sung and others (16). The method utilizes dyes which react with the epoxide groups in the resin and mimic the action of the cure agents. As these dyes react with the resin, their fluorescence intensity changes. In particular, the dyes exhibit shifts in their absorption spectra due to their reaction with the resin. Using this technique, Sung has been able to monitor the cure of resins beyond the gelation point. Figure 2.1 is a chart of fluorescence intensity versus time for a resin cured at two temperatures. The onset of gelation occurs at the bottom knee portion of the sigmoidal-shaped plot. The vitrification of the resin occurs in the area at the top of the plot where the intensity starts to saturate.

Sung has further developed this method to facilitate true *in situ* resin cure monitoring using fiber optic probes (17). This technique facilitates the measurement of the fluorescence intensity at the probe-resin boundary, and the results are similar to those illustrated in Figure 2.1.

Electrical Sensors

Dynamic Dielectric Analysis. A large body of research has been produced by Kranbuehl and others at the College of William and Mary (18). Using an undescribed probe, Kranbuehl has measured the capacitance and conductance of resins, and he has used these measurements to

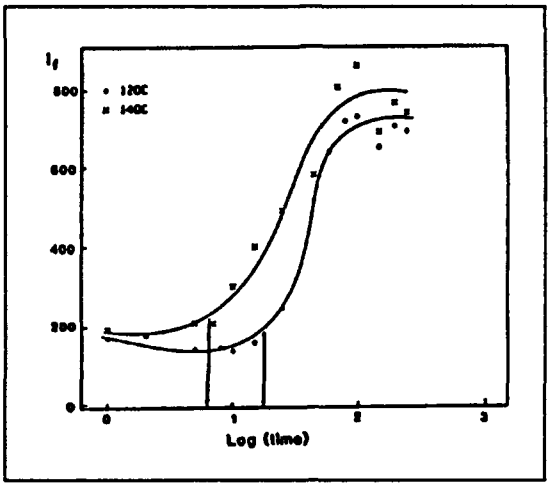

Figure 2.1. Fluorescence intensity (I_f) at 418 nm as a function of cure time for a resin cured at two different temperatures (16:477).

calculate the relative permittivity and loss factor of the material. The thrust of his research has been to use these measured and calculated parameters to characterize the extent of the reaction as a function of time and temperature (18:344). Since the probe design is not unobtrusive, the samples used in his experiments required considerable preparation.

Chemiresistor. A device designed to detect electron donor vapors at low concentrations, called the chemiresistor, has been developed by Wohltjen and others at the U.S. Naval Research Laboratory (19). The device relies on two components: an interdigitated gate electrode (IGE) structure and a chemically-sensitive semiconductor film, typically a metal-substituted phthalocyanine. The semiconductor film is deposited on the IGE structure, which is fabricated on an insulating substrate, as illustrated in Figure 2.2. The conductance of the semiconductor film changes upon exposure to a specific vapor, and the change can be detected by applying a direct-current bias voltage across the IGE structure and measuring the change in the current.

IGE structures similar to the chemiresistor have been used extensively as the basis for making impedance measurements of curing resin systems, as will be discussed later in this chapter. IGE structures have two main advantages. First, the electrodes in these structures are

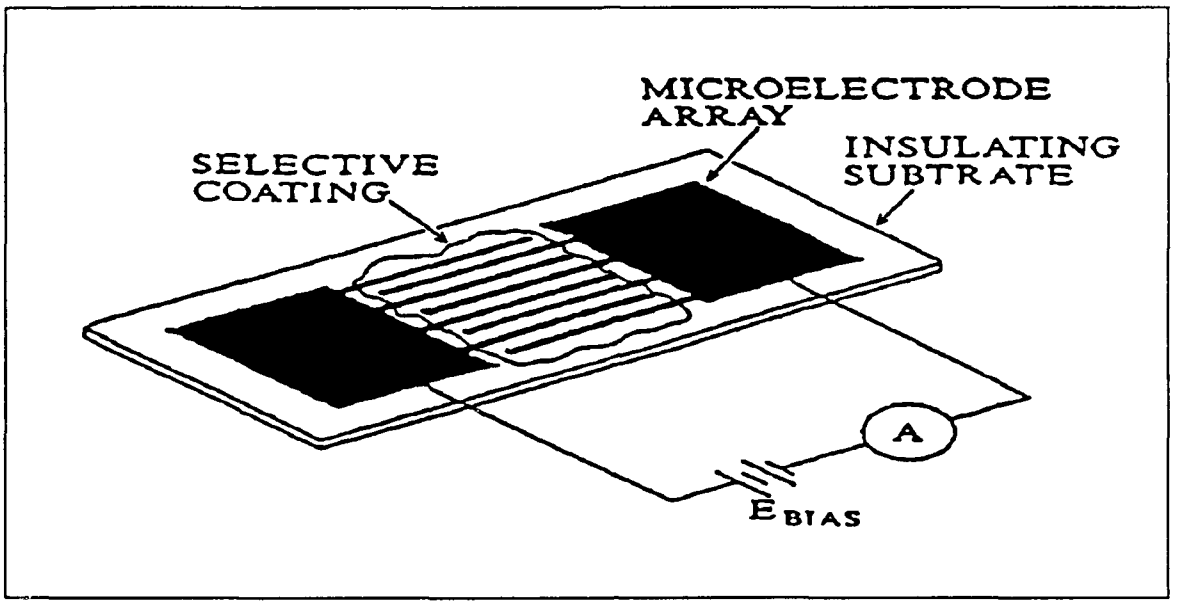

Figure 2.2. Diagram of the chemiresistor (19).

fixed. The volumetric shrinkage that most resin systems experience during cure causes the spacing between electrodes in many other structures (most notably parallel-plate structures) to change. Changes in electrode spacing make measurements of permittivity and loss factor difficult. Second, IGE structures are easily fabricated on a microscopic scale using standard integrated circuit vacuum deposition and photolithographic processes.

Metal-Oxide-Semiconductor (MOS)-Based Sensors. Sensors incorporating the MOS structure have been developed to detect a multitude of chemical species and to sense changes in the electrical properties of materials due to chemical reactions. In general, MOS sensors can be divided into two major classes: chemical sensors and charge-flow sensors (20:507).

Chemical sensors are those which respond to changes in the chemical potential of the gate structure of the MOS device. In this class of MOS sensors, the gate material of a typical MOSFET (which is normally a metal or polysilicon) is replaced by the material to be monitored.

The Ion-Sensitive Field-Effect Transistor (ISFET) is a typical MOS-based chemical sensor configuration, and it is illustrated in Figure 2.3.

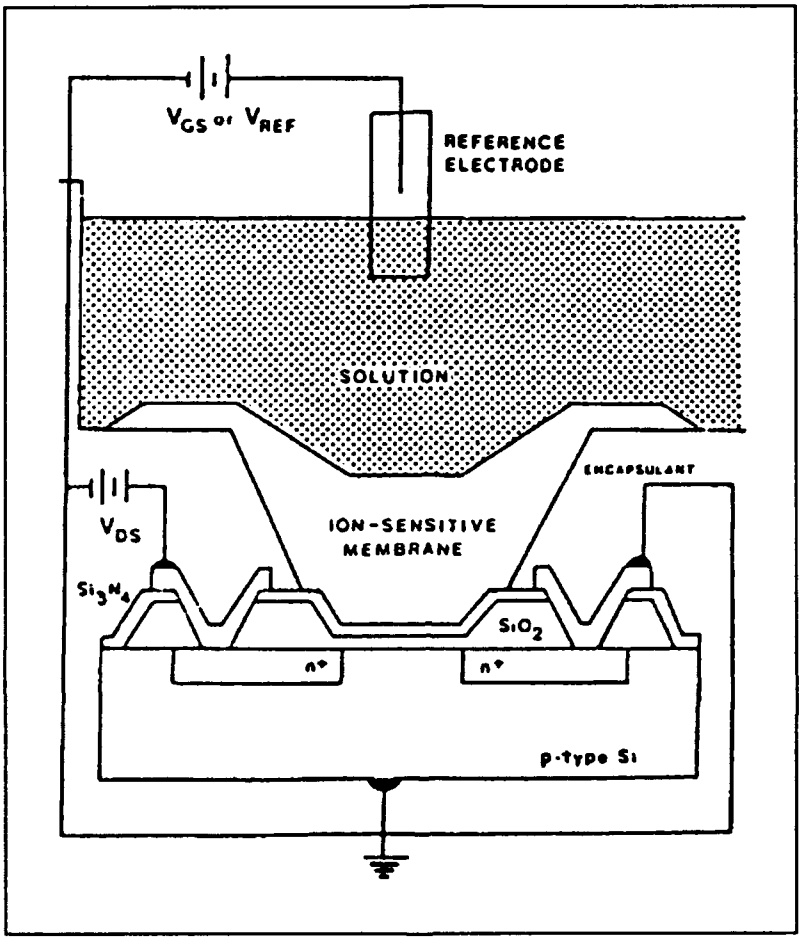

Figure 2.3. Diagram of an Ion-Sensitive Field-Effect Transistor (ISFET) (21:132).

Charge-flow sensors comprise the second major class of MOS-based sensors. Their operation can be explained based upon the charge-imaging property of the MOS structure. That is, the conducting channel of a MOSFET is modulated by the charge on its gate. This charge is typically established by a sensing membrane which responds to changes in its environment by altering its chemical structure and electrical characteristics. Figure 2.4 depicts a typical charge-flow sensing FET.

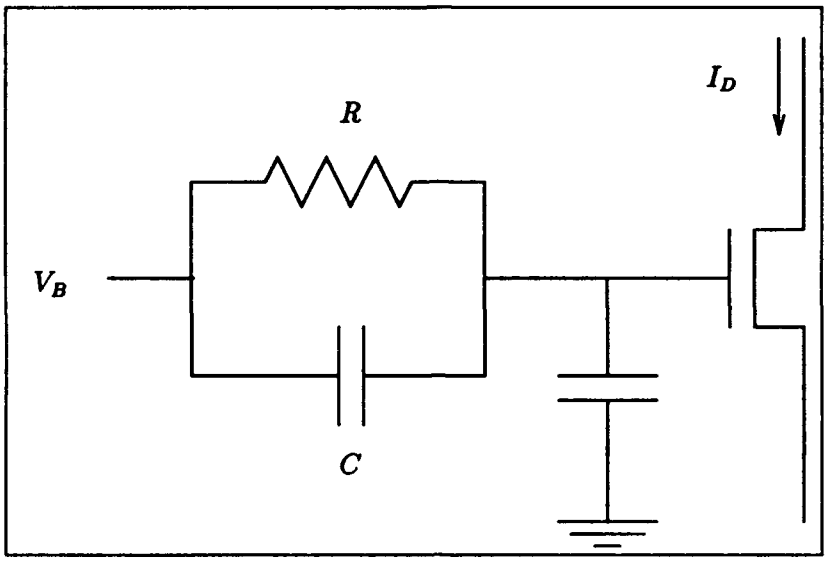

Figure 2.4. Diagram of a typical charge-flow sensing FET with a property-dependent RC network coupling a bias voltage (V_B) to the gate of the FET (20:521).

The Charge-Flow Transistor (CFT). A chemical sensor for detecting changes in humidity, called the charge-flow transistor (CFT), was developed by Senturia and his co-workers at the Massachusetts Institute of Technology (MIT) in the mid-1970s (22). The CFT is fabricated similar to a standard MOS field-effect transistor (MOSFET), except the conventional gate material is replaced with a material which changes its electrical characteristics as a result of a chemical reaction. The CFT is illustrated in Figure 2.5. In the humidity sensor application, the gate material used was poly(p-aminophenylacetylene), which is a humidity-(ACsensitive polymer. In addition, the CFT was evaluated for potential use as a photodetector. When a photosensitive polymer was applied as a gate material, photoconductivity was observed (22:107).

According to Senturia *et al.* the possibility of monitoring the cure of a resin with the CFT was first proposed by Dr. L. H. Peebles from the Office of Naval Research, and the correlation between the CFT's response and major events in the cure cycle was established by Appleman (23:1). The resin to be monitored was placed in the gap region of the CFT's gate electrode. The

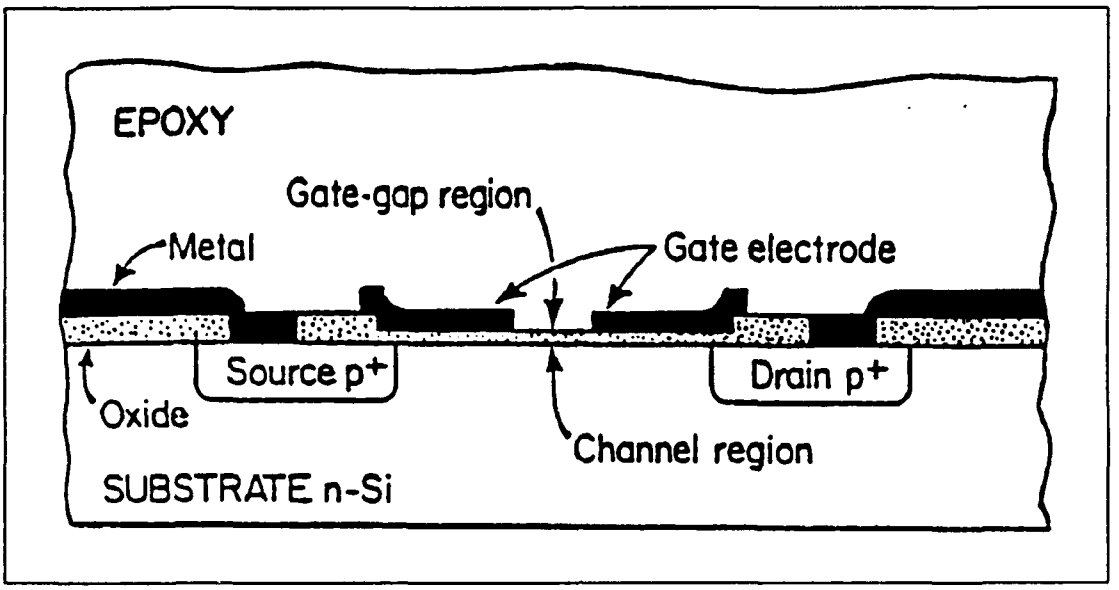

Figure 2.5. Illustration of the charge-flow transistor (CFT) (23:2).

changing electrical characteristics of the curing resin manifested themselves when an electrical signal was applied to the gate electrode of the CFT.

In their work with the CFT, Senturia *et al.* applied a direct current (dc) bias to the drain of the device and a low-frequency square wave to the gate electrode. The square wave alternated between ground potential and a potential just slightly greater than the threshold voltage of the MOSFET device. The period of the square wave was one minute, and a fifty percent duty cycle was utilized. The output current waveforms displayed peaks, which were attributed to capacitive coupling between the gate electrode and the channel region. Also, the device response was asymmetrical. However, the turn-off time was much shorter than the turn-on time because a portion of the metal gate electrode overlapped the channel region (see Figure 2.5). These waveforms are depicted in Figure 2.6. The charge required to produce a conducting channel could be provided much more quickly by the gate electrode compared to the material in the gate-gap region. Therefore, realization of a conducting channel was limited by the time required for the gate material to produce the required charge. Conversely, the charge could be removed more

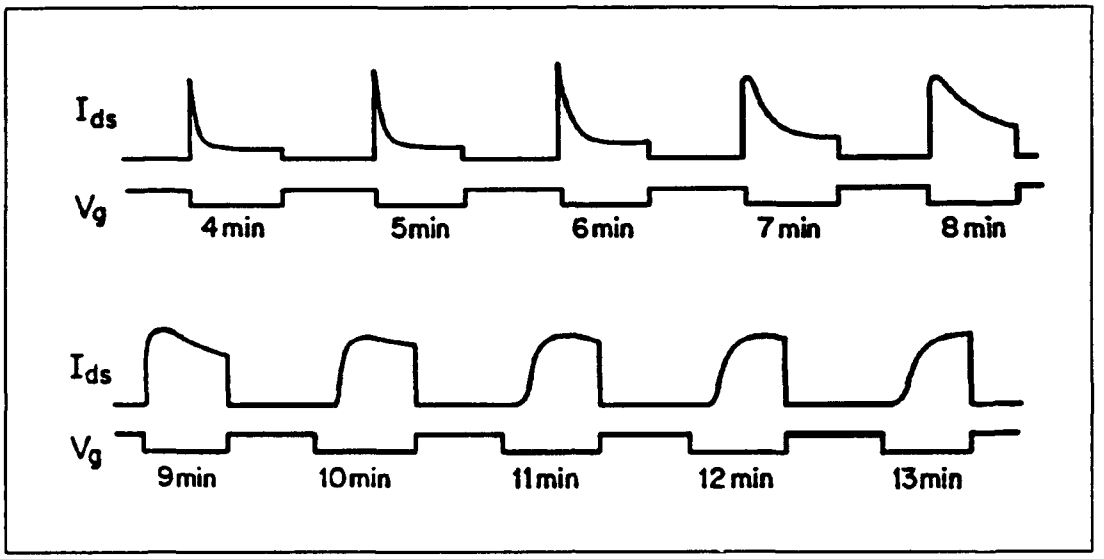

Figure 2.6. Current waveforms for the charge-flow transistor (CFT) (23:4).

quickly from the metal gate electrode than from the material in the gate-gap region. Consequently, the conducting channel was very quickly pinched-off. A modified CFT was fabricated which eliminated the gate electrode overlap (see Figure 2.7). Subsequent testing demonstrated that the peaks in the response had been eliminated, and the device's response became symmetrical. The current waveforms for the modified CFT are given in Figure 2.8.

A monolithic version of the CFT was reported in 1981 (24). In this implementation, the gate electrode was completely removed from the channel region in order to provide symmetrical turn-on and turn-off characteristics (see Figure 2.9).

Floating-Gate Charge-Flow Transistor. A MOS-based charge sensor developed in conjunction with the CFT, originally known to as the floating-gate CFT, and subsequently referred to as the surface impedance measurement (SIM) device, or microdielectrometer, has been developed (23, 25, 26). It was originally designed to measure the low-frequency dielectric constant of the material being monitored by the CFT (23:6). These measurements were necessary to facilitate modeling the CFT's performance. An illustration of the original floating-gate CFT is

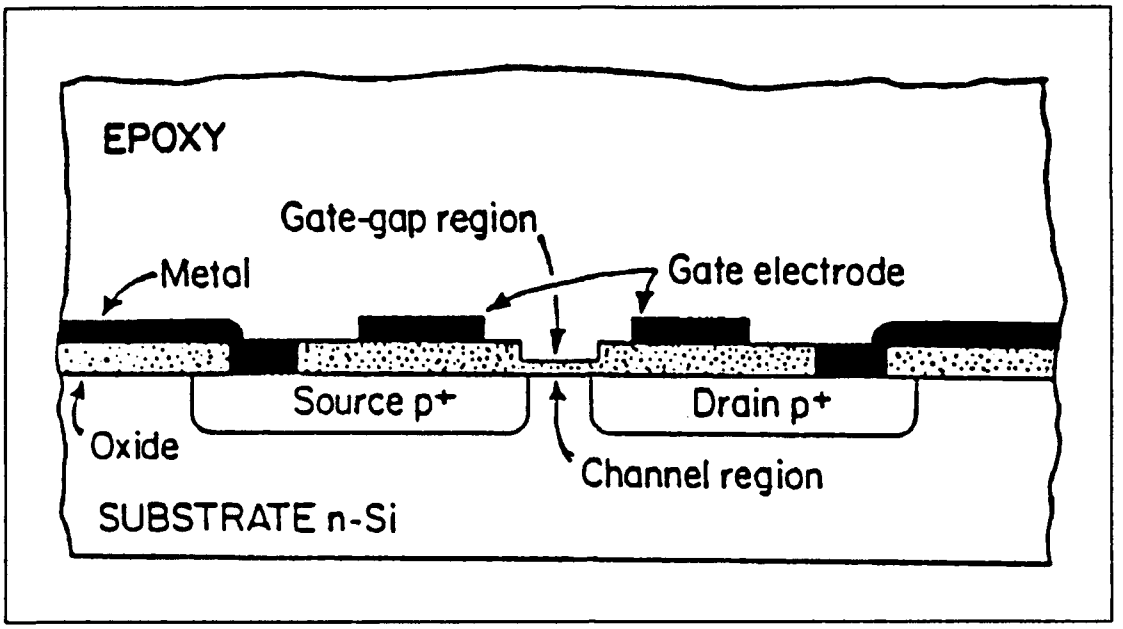

Figure 2.7. Illustration of the modified CFT structure (23:9).

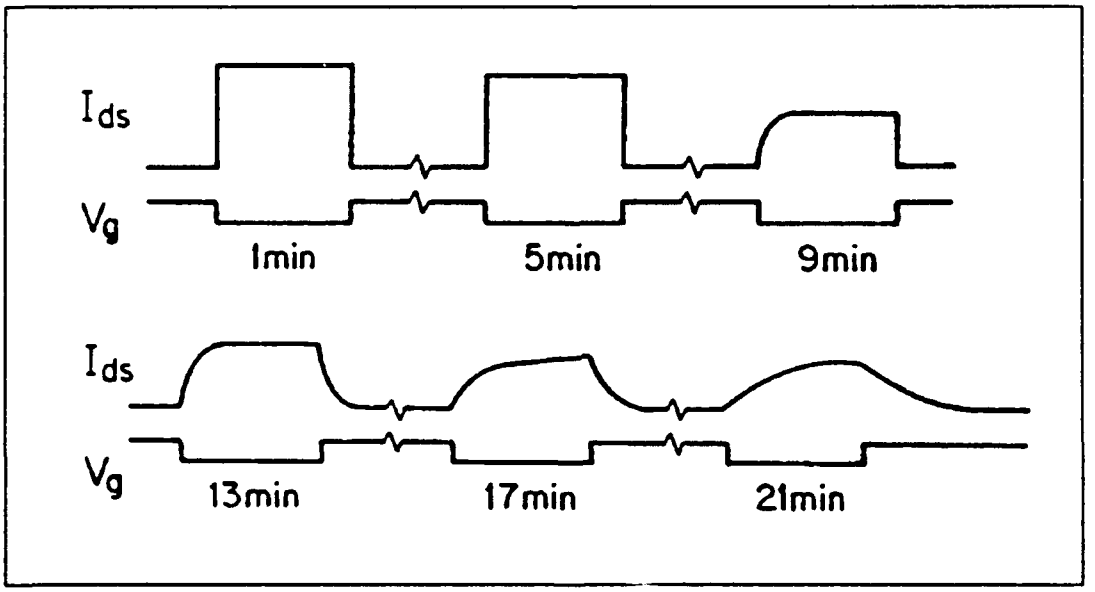

Figure 2.8. Current waveforms for the modified charge-flow transistor (CFT) (23:14).

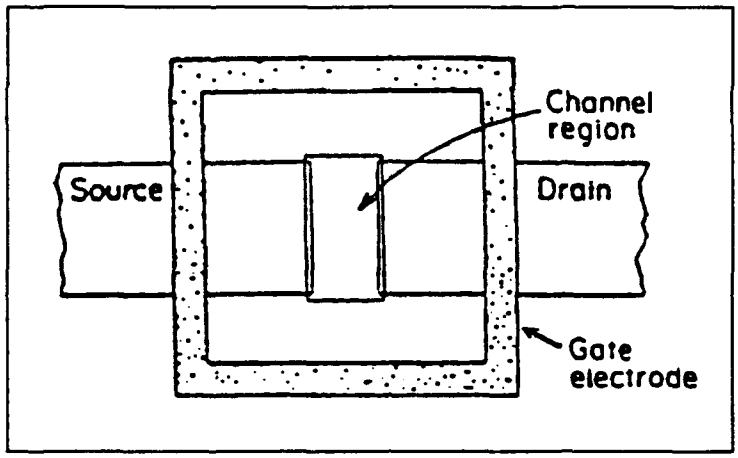

Figure 2.9. The CFT structure utilized in the monolithic circuit (24:66).

presented in Figure 2.10. The interdigitated electrode structure (IGE) illustrated in Figure 2.10 was utilized in the feedback loop of an operational amplifier. The structure was coated with the material to be monitored, and an alternating current signal was used as the excitation source. The conductance and capacitance were measured, and these values were used to calculate the relative permittivity, loss factor, and loss tangent. Experiments conducted to evaluate the device's performance as a resin cure monitor revealed that a sharp decrease in the calculated relative permittivity and loss factor of the resin being monitored occurred at the resin's gelation point (23:16).

The original CFT design had several disadvantages. It was difficult to calibrate, and the sensor's output signal was nonlinear. In contrast, the floating-gate CFT could be accurately calibrated and linear device models could be used to analyze the output signal (26). Most of the continuing research at MIT concerning resin cure monitoring has utilized the floating-gate CFT, and in 1983, a commercial version of the device became available (27).

Interdigitated Gate Electrode Field-Effect Transistor (IGEFET). A device similar to the CFT is the chemically-sensitive field-effect transistor (CHEMFET), developed by Janata and his co-workers at the University of Utah (28). The goal of their research was to develop a

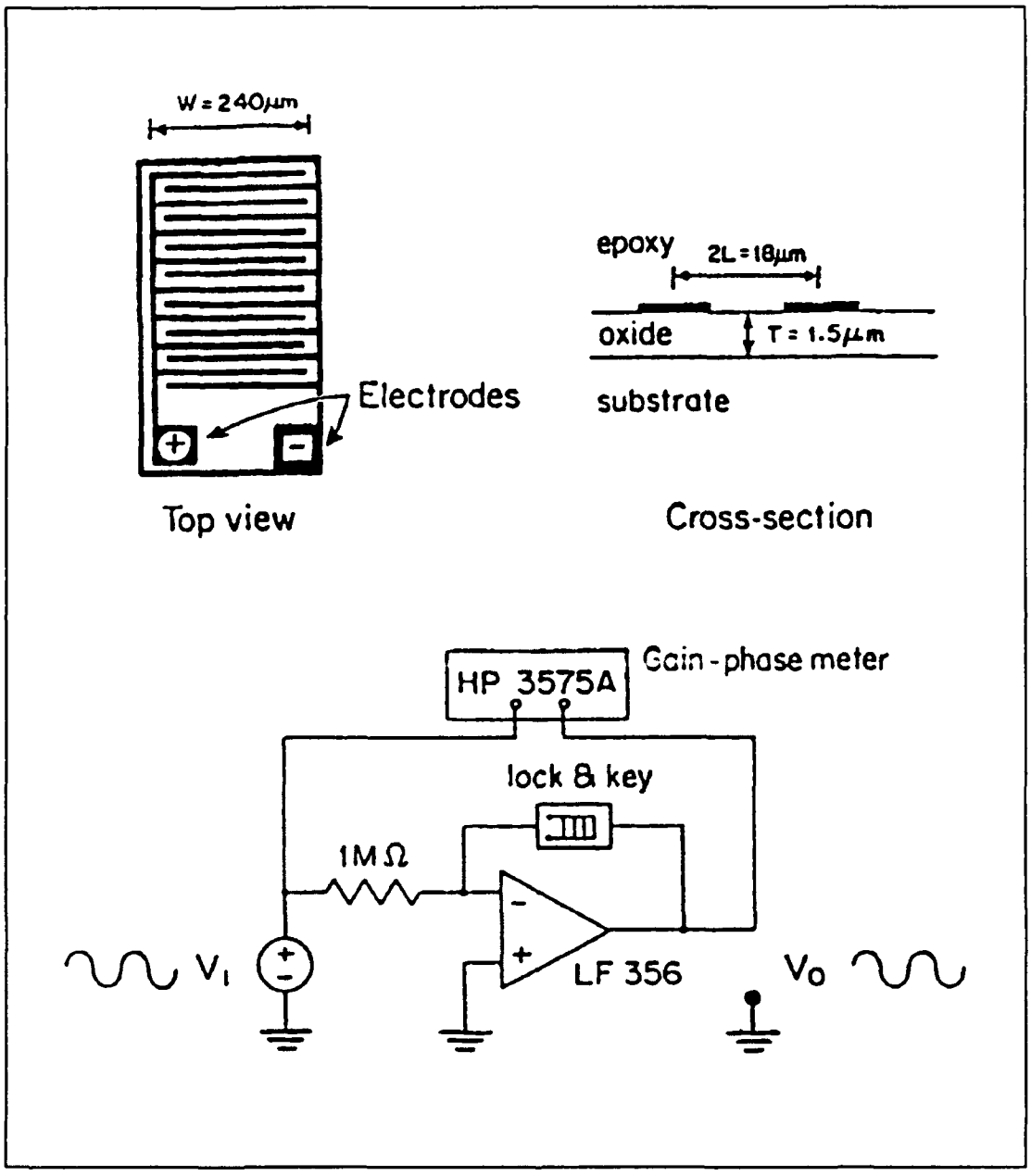

Figure 2.10. Diagram of the floating-gate CFT (23:7).

MOS-based chemical sensor for the detection of organophosphorus compounds and pesticides. Four types of CHEMFETs were evaluated: enzyme-coupled, galvanostatic, catalytic, and work function. The criteria for selecting an optimum configuration included: a concentration sensitivity of 1–10 parts-per-billion, a response time of less than ten seconds, complete reversibility in thirty seconds, a shelf life of six months, and an operational life of ten days of continuous use (28:666). Based on these criteria, the work function CHEMFET configuration was chosen.

A diagram of the work function CHEMFET is presented in Figure 2.11. In order for the

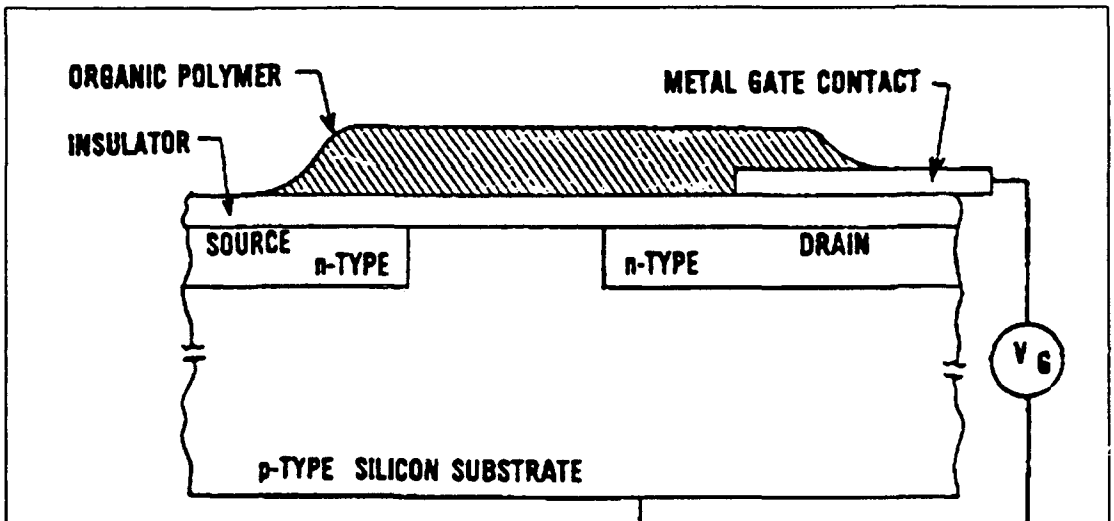

Figure 2.11. Diagram of the work function CHEMFET (28:669).

CHEMFET to provide acceptable results, it would be necessary to use a material for the gate electrode whose work function varied to a measurable degree upon exposure to small concentrations of the chemical being detected. Based upon this requirement, it was determined that an organic semiconducting polymer should be used as the gate material (28:668–669). Positive detection of the challenge gas was to be determined by measuring the work function difference between the organic polymer gate material and the substrate (29:7). This concept

required that the resistive effects of the gate electrode contacts be negligible; that is, ohmic gate-to-polymer contacts were needed. However, ohmic contacts to organic materials are difficult to realize. Experiments to determine an optimum contact material revealed that the observed change in the dc resistance of the CHEMFET was primarily due to the change of the contact resistance upon exposure to the challenge gas. Since changes in the contact resistance could not be separated from changes in the work function difference between the gate material and the substrate, it was determined that the CHEMFET work function difference configuration would not function for the detection of organophosphorus compounds.

As a result of this apparent setback, Janata and Gehmlich decided that impedance measurements should be studied as an alternative approach (29:8). Gehmlich designed an interdigitated copper electrode structure on a printed circuit board that was similar to the floating-gate CFT. The interdigitated electrode structure was coated with a film of polymeric material known to be sensitive to organophosphorus compounds. Tests performed with this device revealed improved sensitivity (at low frequencies) to varying concentrations of organophosphorus compounds (29:11).

An improved version of the fundamental interdigitated electrode structure is realized with the interdigitated gate electrode field-effect transistor (IGEFET). The IGEFET is essentially a MOSFET with an interdigitated gate electrode structure, as illustrated in Figure 2.12. Thesis research by Wiseman, Jenkins, and Shin has shown the IGEFET to be sensitive to very small concentrations of organophosphorus compounds and nitrogen dioxide when thin films of metal-doped phthalocyanines were deposited on the IGE structure (3, 4, 5).

Preliminary research by Wiseman indicates that the IGEFET may be useful as a resin cure monitoring sensor (3:6-4). Of particular interest was the spectral response of the IGEFET to a pulsed voltage excitation signal. The greatest degree of change in the spectral response occurred with the low frequency harmonics of the input signal, which was a voltage pulse.

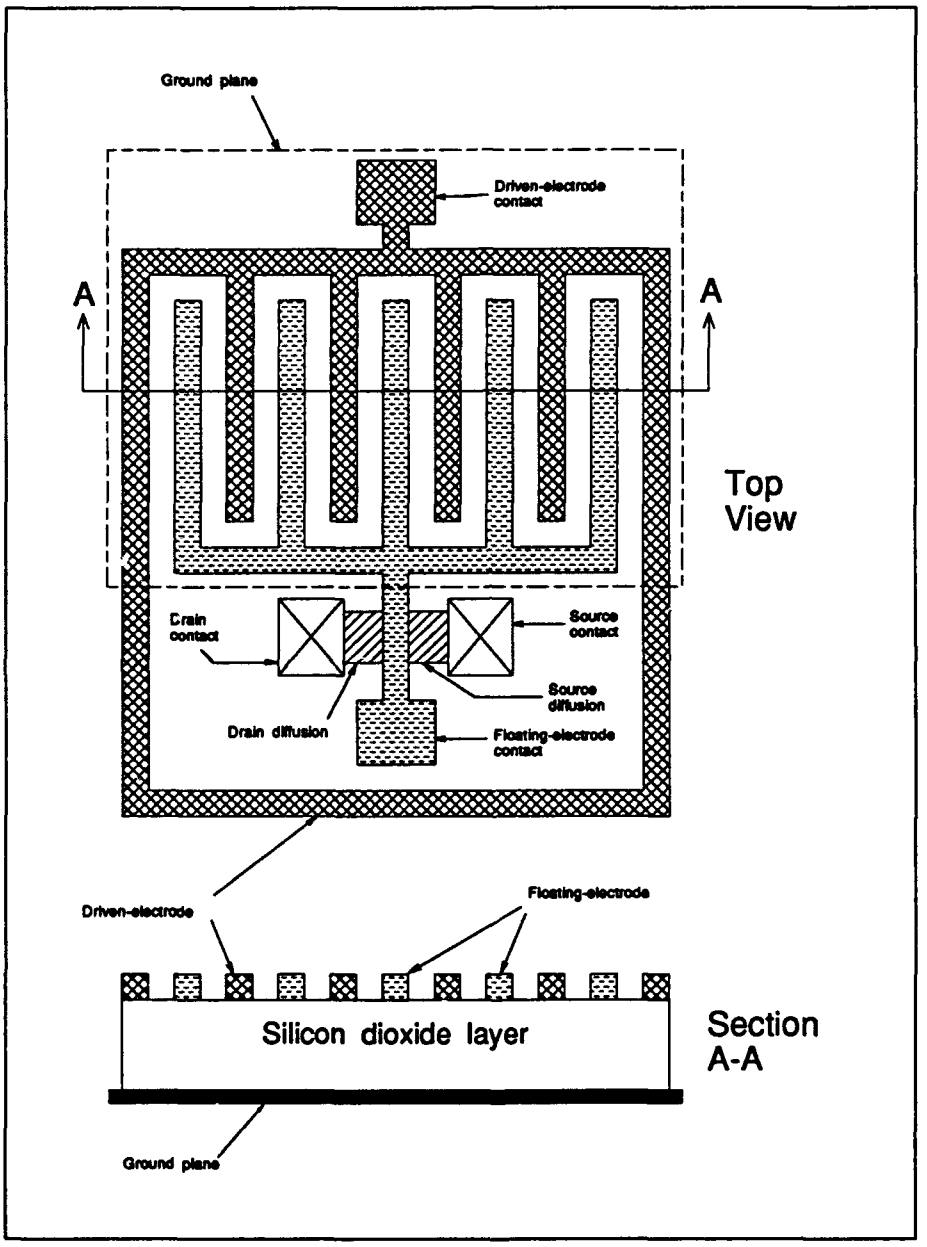

Figure 2.12. Diagram of the IGEFET (7).

Summary

Several sensors and techniques have been investigated for monitoring the cure of epoxy resins. In particular, two basic classes of sensors were described: fluorescence intensity monitors and electrical impedance monitors.

Fluorescence monitors show great promise, but the use of a fiber-optic cable to realize a compact sensor configuration using this technique is still under development.

Two broad categories of electrical impedance resin cure monitoring techniques were discussed: dynamic dielectric analysis and MOS-based sensors. Dynamic dielectric analysis is primarily used to characterize the cure of resins, and it could be used in quality control processes. The probe described is not unobtrusive. One MOS-based chemical sensor for monitoring resin cure is the charge-flow transistor (CFT), but the CFT technology has not been rigorously pursued due to the device's nonlinear response and difficulties encountered in its calibration. Another MOS-based charge sensor developed at the same time as the CFT is the floating-gate CFT, or microdielectrometer. It has proven effective as a device for monitoring resin cure, but it possesses limitations which restrict its practical utility. Another charge sensor for monitoring resin cure is the interdigitated gate electrode field-effect transistor (IGEFET), which is an evolutionary extension of research concerned with the work function chemically-sensitive field-effect transistor (CHEMFET).

III. Theory of IGEFET Resin Cure Monitoring

Introduction

The research in this thesis involved the measurement of the electrical and mechanical (physical) characteristics of a curing resin system. To explain the measurements requires an understanding of the underlying physical processes manifested when a resin cures. To this end, this chapter includes a discussion of the electrical processes at work in a curing resin, and an overview of the dynamic physical mechanisms involved.

Polarization Mechanisms in Dielectric Materials

In the presence of an electric field, the response of a dielectric material is manifested through a mechanism called polarization. That is, the electric dipoles in the material tend to align themselves parallel to the direction of an externally applied electric field. Assuming that the dielectric is isotropic, a vector, $\mathbf{P}$, known as the polarization, can be assigned to the material, where each incremental volume, dV, has associated with it, an incremental dipole moment, $\mathbf{P}_i$. Integrating the quantity $\mathbf{P}_i dV$ over the volume of the material contained between the electrodes used to apply the electric field yields the polarization, $\mathbf{P}$, which describes the magnitude and direction of the net dipole moment per unit volume.

The mechanisms which contribute to polarization include electronic polarization, atomic polarization, orientational polarization, and interfacial polarization (30:18). A schematic representation of the polarization mechanisms is presented in Figure 3.1. These mechanisms will now be discussed.

Electronic Polarization. This type of polarization is caused by a displacement of the electrons of an atom with respect to its nucleus. This usually occurs at high frequencies (typically

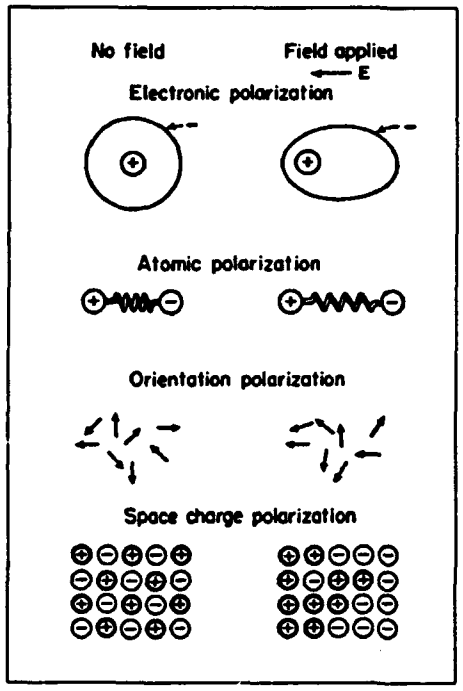

Figure 3.1. Mechanisms of polarization (14:96).

in the range of 10^{12}– 10^{15} Hz), and for that reason, it is also called optical polarization. Electronic polarization is responsible for the refraction of light (30:18).

Atomic Polarization. This mechanism arises when molecular positions are distorted by an externally applied electric field. That is, the equilibrium positions of atoms in a molecule are changed with respect to each other. Due to the large size of the atomic nuclei with respect to their electrons, atomic polarization normally occurs at lower frequencies compared to electronic polarization, typically on the order of 10^{10}–10^{12} Hz.

Orientational Polarization. Many molecules contain macroscopic dipole moments. When these dipole moments are acted upon by an externally applied electric field, the molecules will attempt to orient themselves in the direction of the field. This phenomena occurs for frequencies below approximately 10^{9} Hz, and it is the primary polarization mode for resins, since the resin molecules are large.

Interfacial Polarization. This mechanism, also called *space-charge* polarization, occurs when charge carriers accumulate at a molecular-level discontinuity in the structure of the material. This localized charge is mirrored at an adjacent electrode, creating a dipole moment (31:52). Since the distances over which the charge carriers must migrate is very large, the frequencies involved approach 0 Hz.

The relative magnitudes of these mechanisms and the frequencies over which they typically occur are illustrated in Figure 3.2.

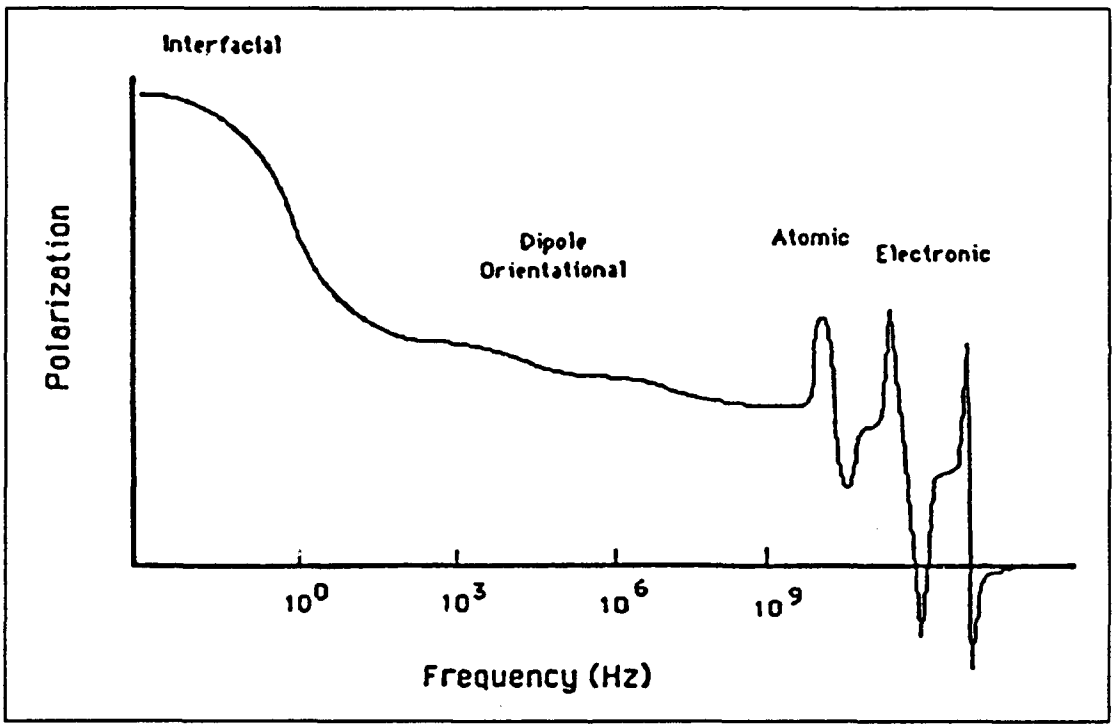

Figure 3.2. Magnitudes of the four polarization mechanisms with respect to frequency (10:32).

Dielectric Relaxation

In the previous discussion, an externally applied electric field was used to introduce the concept of polarization. This section considers the application of a harmonic, time-varying electric field to a lossy dielectric.

Complex Permittivity. An externally applied, harmonically-varying electric field acting on a dielectric may be described as:

$$\mathbf{E} = \mathbf{E}_0 \cos \omega t \tag{3.1}$$

where $\mathbf{E}$ is the vector representing the applied electric field, $\mathbf{E}_0$ is the amplitude of the applied electric field, ω is its radian frequency, and t is time. If the dielectric is ideal, that is, if it is a lossless material, the current flow through the material will only be displacement current. In this case, the permittivity associated with the material is a pure real number. If, however, the material is lossy (non-ideal), a complex permittivity results. Demonstration of this concept can be supported by applying basic electromagnetic theory. That is, the time-varying electric field has associated with it, a time-varying magnetic field, $\mathbf{H}$. The total current density, $\mathbf{J}_T$, induced by this magnetic field is given by Maxwell's representation of Ampere's Law in point form:

$$\nabla \times \mathbf{H} = \mathbf{J}_T. \tag{3.2}$$

For an ideal dielectric, $\mathbf{J}_T$ can be expressed as:

$$\mathbf{J}_T = \frac{\partial \mathbf{D}}{\partial t} \tag{3.3}$$

where $\mathbf{J}_T$ becomes the displacement current density in the dielectric, and $\mathbf{D}$ is the electric flux density. In a more general sense, though, some loss will be experienced in the form of conduction current density, $\mathbf{J}_C$, and Equation 3.3 becomes:

$$\mathbf{J}_T = \mathbf{J}_C + \frac{\partial \mathbf{D}}{\partial t}. \tag{3.4}$$

Substituting the previous relationship into Equation 3.2 yields:

$$\nabla \times \mathbf{H} = \mathbf{J}_C + \frac{\partial \mathbf{D}}{\partial t}. \tag{3.5}$$

In phasor notation (harmonic field variations), this can be rewritten as:

$$\nabla \times \mathbf{H} = \mathbf{J}_C + \jmath\omega\mathbf{D} \tag{3.6}$$

where $\jmath$ represents the unit imaginary number, given by, $\jmath = \sqrt{-1}$.

The electric flux density is given by:

$$\mathbf{D} = \epsilon'\epsilon_0\mathbf{E} \tag{3.7}$$

where ϵ' is the relative permittivity of the material, and ϵ_0 is the permittivity of free space. Substituting this relationship into Equation 3.6 gives:

$$\nabla \times \mathbf{H} = \mathbf{J}_C + \jmath\omega\epsilon'\epsilon_0\mathbf{E}. \tag{3.8}$$

Ampere's Law in point form states that $\mathbf{J}_C = \sigma\mathbf{E}$, where σ is the electrical conductivity of the dielectric. Substituting this expression into Equation 3.8 yields:

$$\nabla \times \mathbf{H} = \sigma\mathbf{E} + \jmath\omega\epsilon'\epsilon_0\mathbf{E}. \tag{3.9}$$

Rearranging Equation 3.9 gives:

$$\nabla \times \mathbf{H} = \jmath\omega\epsilon_0\mathbf{E}\left(\epsilon' - \jmath\frac{\sigma}{\omega\epsilon_0}\right). \tag{3.10}$$

Consistent with the prior discussion, the quantity $\sigma/\omega\epsilon_0$ is related to the material's dielectric loss. Therefore, the *loss factor* of the material is defined as, $\epsilon'' = \sigma/\omega\epsilon_0$. Equation 3.10 then becomes:

$$\nabla \times \mathbf{H} = \jmath\omega\epsilon_0\mathbf{E}(\epsilon' - \jmath\epsilon''). \tag{3.11}$$

The complex relative permittivity, ϵ^*, is then defined by:

$$\epsilon^* = \epsilon' - \jmath\epsilon''. \tag{3.12}$$

A related figure of merit, the loss tangent, is given as:

$$\tan\delta_e = \frac{\epsilon''}{\epsilon'} \tag{3.13}$$

where δ_e is the phase angle associated with the total current density vector, $\mathbf{J}_T$. The sub-script "e" is used to prevent confusion between the loss tangent associated with the total current density, and the mechanical loss tangent, which will be described later in this chapter.

Debye Equations. If a static electric field is applied to a dielectric and the material is allowed to respond via the polarization mechanisms discussed earlier in this chapter, and then the field is instantaneously removed, the polarization decays towards its equilibrium value according to a decay factor, $\alpha(t)$, which was described by Debye as (32:84):

$$\alpha(t) = \alpha(0)e^{-t/\tau} \tag{3.14}$$

where $\alpha(0)$ is the value of $\alpha(t)$ at $t = 0$ (due to molecular dipole orientation), and τ is the characteristic relaxation time of the material. The characteristic relaxation time (τ) may depend upon temperature, but not on time (31:68).

If a time-varying field is applied to the dielectric, the material will change to achieve maximum polarization, but if the frequency is too high, the material will not have sufficient time to attain its maximum value. Consequently, the permittivity of the material is said to be relaxed. Thus, the permittivity of the material is a frequency-dependent quantity, and this dependence is demonstrated by the equation (31:67):

$$\epsilon^*(\omega) = \epsilon_\infty + \int_0^\infty \alpha(t) e^{j\omega t} dt \tag{3.15}$$

where ϵ_∞ is a constant equal to the value of the permittivity at infinite frequency. Physically, ϵ_∞ corresponds to the permittivity value which is attained instantaneously when the external electric field is applied. This quantity is also called the optical dielectric constant, because it can be described by the optical (electronic) polarization mechanism (14:175).

Substituting the exponential description of the decay factor into Equation 3.15 yields:

$$\epsilon^*(\omega) = \epsilon_\infty + \int_0^\infty \alpha(0) e^{-t/\tau} e^{j\omega t} dt. \tag{3.16}$$

Integrating this expression gives:

$$\epsilon^*(\omega) = \epsilon_\infty + \frac{\alpha(0)}{\frac{1}{\tau} - j\omega}. \tag{3.17}$$

The static permittivity of the material, ϵ_s, can be determined by setting $\omega = 0$ in Equation 3.17. That is,

$$\epsilon_s = \epsilon_\infty + \tau\alpha(0). \tag{3.18}$$

Rearranging Equation 3.18 yields the value of $\alpha(0)$:

$$\alpha(0) = \frac{\epsilon_s - \epsilon_\infty}{\tau}. \tag{3.19}$$

Substituting this result into Equation 3.14, yields:

$$\alpha(t) = \frac{\epsilon_s - \epsilon_\infty}{\tau} e^{-t/\tau}. \tag{3.20}$$

Similarly, substituting Equation 3.20 into Equation 3.16 again gives:

$$\epsilon^*(\omega) = \epsilon_\infty + \int_0^\infty \frac{\epsilon_s - \epsilon_\infty}{\tau} e^{-t/\tau} e^{j\omega t} dt \tag{3.21}$$

$$= \epsilon_\infty + \int_0^\infty \frac{\epsilon_s - \epsilon_\infty}{\tau} \exp\left[\left(j\omega - \frac{1}{\tau}\right) t\right] dt \tag{3.22}$$

$$\epsilon^*(\omega) = \epsilon_\infty + \frac{\epsilon_s - \epsilon_\infty}{1 - j\omega\tau}. \tag{3.23}$$

For an ideal dielectric (lossless), this last equation is valid for describing the material's relative permittivity. However, for a lossy dielectric, the complex relative permittivity is, $\epsilon^* = \epsilon' - j\epsilon''$. Therefore, equating the real and imaginary components of the last two expressions yields:

$$\epsilon' = \epsilon_\infty + \frac{\epsilon_s - \epsilon_\infty}{1 + \omega^2\tau^2} \tag{3.24}$$

and

$$\epsilon'' = \frac{(\epsilon_s - \epsilon_\infty)\omega\tau}{1 + \omega^2\tau^2}. \tag{3.25}$$

The loss tangent is given by:

$$\tan\delta_e = \frac{\epsilon''}{\epsilon'} \tag{3.26}$$

or

$$\tan\delta_e = \frac{(\epsilon_s - \epsilon_\infty)\omega\tau}{\epsilon_s + \epsilon_\infty\omega^2\tau^2}. \tag{3.27}$$

The equations for ϵ', ϵ'', and $\tan\delta_e$ are called the Debye equations (31:68). For dielectrics with a single characteristic relaxation time, these relationships are valid. The behavior of ϵ' and ϵ'' are plotted in Figure 3.3. A plot of ϵ' versus ϵ'' is illustrated in Figure 3.4. The values of ϵ' and ϵ'' are

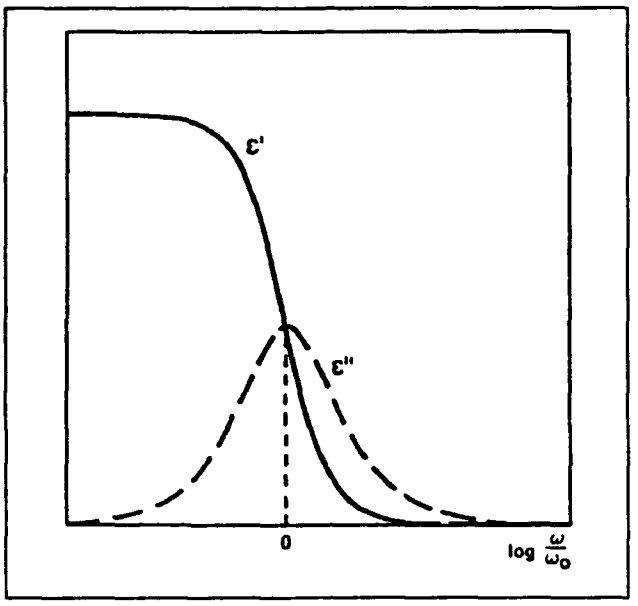

Figure 3.3. Real and imaginary components of the complex relative permittivity of a dielectric as a function of frequency (33:34).

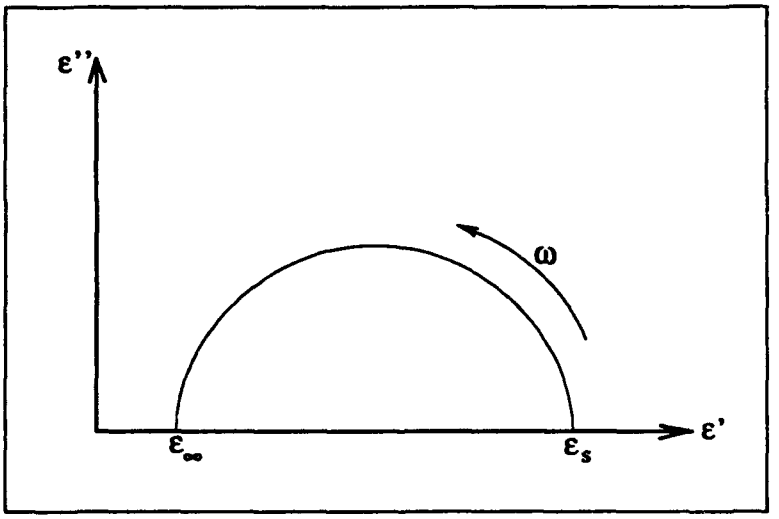

Figure 3.4. Plot of ϵ' versus ϵ'' for a system with a single relaxation time (ω increases from a value of zero at $\epsilon' = \epsilon_s$ and increases in a counter-clockwise direction) (30:44).

measured as a function of frequency. The point corresponding to $\omega = 0$ is ϵ_s. Since ϵ_∞ can not be measured directly, the curve is usually extrapolated, and the value is determined graphically (numerically). The resultant plot in Figure 3.4 is called a *Debye semicircle*, and it is useful to determine if a system has only one characteristic relaxation time.

Cole-Cole Model. In general, experimental data for real dielectrics will not fit the Debye model (33:16). Debye's equations were developed for polar liquids and assumed that the dielectric's constituent molecules were spherical (32:83–85). By analysis of experimental data, Cole and Cole found that for most dielectric materials, the plot of ϵ' versus ϵ'' can be fitted to a circular arc whose center is located below the ϵ' axis (Figure 3.5) (34:344). The expression for the complex relative permittivity, as given in Equation 3.23, was modified by Cole and Cole to account for the difference between the Debye equations and the experimental data (34:346). That is:

$$\epsilon^*(\omega) = \epsilon_\infty + \frac{\epsilon_s - \epsilon_\infty}{1 - (j\omega\tau_0)^{(1-\alpha)}}, \tag{3.28}$$

where τ_0 is a generalized relaxation parameter, and the $(1 - \alpha)$ parameter is used to fit the plot. The resultant plot is called a *Cole-Cole* plot, and it is illustrated in Figure 3.5. The parameter τ_0 is given by, $\tau_0 = 1/\omega$, where the value of ω corresponds to the maximum value of ϵ''. The value of α is determined by measuring the angle (θ) between the center of the arc and the ϵ' axis at either ϵ_∞ or ϵ_s, as illustrated in Figure 3.5. Once θ is known, α is given by (31:76):

$$\alpha = \frac{2\theta}{\pi} \tag{3.29}$$

where θ is the measured angle in radians.

Cole and Cole suggested the concept of a distribution of relaxation times in the material to account for the observed deviations from the Debye model. In this case, the generalized relaxation parameter, τ_0, is the mean of the relaxation times. The distribution function, $F(s)$, is given by

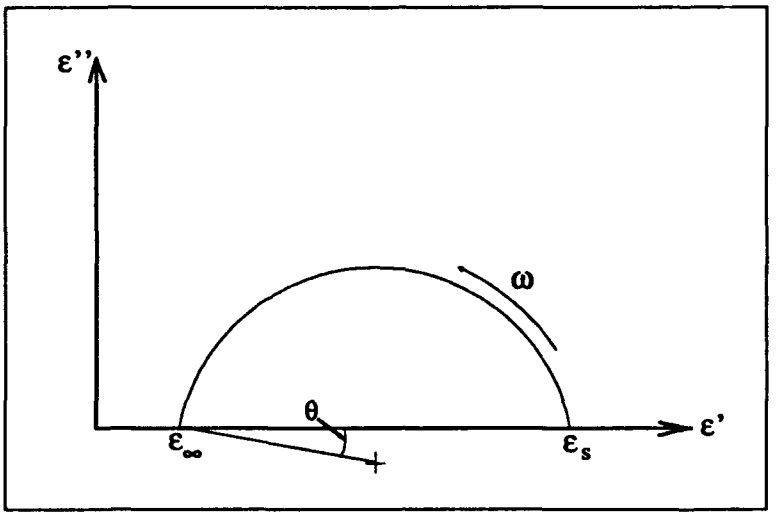

Figure 3.5. Cole-Cole plot of a dielectric (31:76).

(34:350):

$$F(s) = \frac{1}{2\pi} \frac{\sin \alpha\pi}{\cosh(1-\alpha)s - \cos \alpha\pi} \tag{3.30}$$

where $s = \ln(\tau/\tau_0)$. This distribution is plotted in Figure 3.6 for different values of α. Cole and Cole mention that, while Equation 3.30 is an exact representation of the circular arc, it is difficult to satisfactorily account for such a distribution (34:350–351).

The representations of the relationship between the relative permittivity, loss factor, and frequency are useful when attempting to characterize the nature of the relaxation time, or distribution of relaxation times, of a dielectric material. While it is difficult to measure the relative permittivity and loss factor directly, this information is embedded in the impedance of the material. A plot of the real part of the impedance versus the imaginary part of the impedance in given in Figure 3.7.

Epoxy Resin Systems

The term *epoxy* is actually a corruption of the word *epoxide*. The base of the word is *oxygen*, and the prefix is derived from the Greek, and means *over* or *between*. The meaning of the word is,

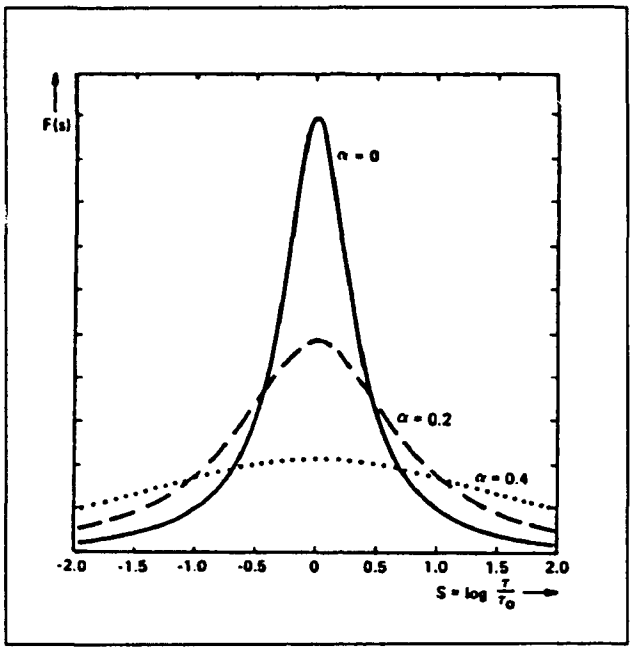

Figure 3.6. The function $F(s)$ describing the distribution of relaxation times for the Cole-Cole model of complex permittivity (33:38).

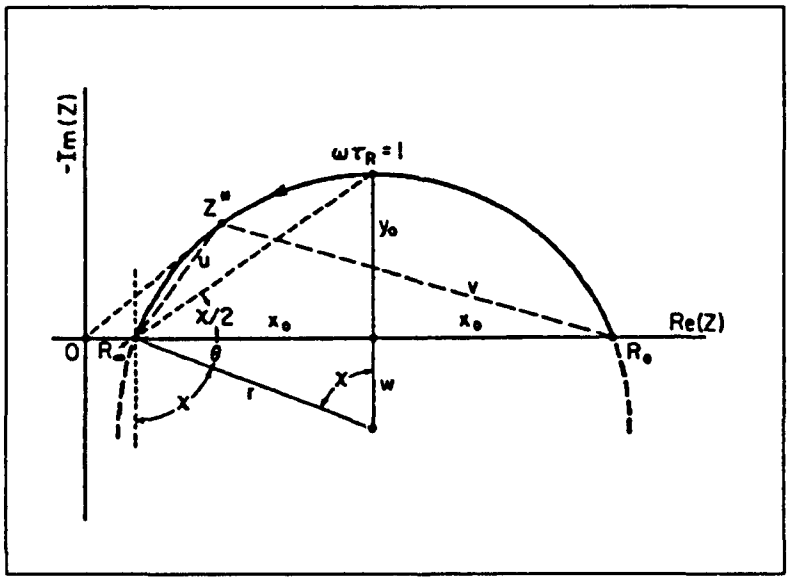

Figure 3.7. Cole-Cole plot in the impedance plane (33:17).

therefore, "oxygen between compound" (35:1). The term epoxy is usually used to refer to a chemical group consisting of an oxygen atom bonded to two carbon atoms, which are already bonded together in some fashion (12:1-1). An epoxy resin is defined as a molecule containing at least one epoxy group (12:1-2). Epoxy resins belong to the larger family of thermosetting resin systems. Thermosetting resins are characterized by an irreversible molecular change with heat from a soluble material to one that is insoluble and infusible (8:468). This characteristic contrasts that of thermoplastic materials, which tend to soften and flow with the addition of heat.

The most prevalent epoxy resins are those produced by condensing epichlorohydrin with bisphenol-A. The resin used in this research (Epoxy 907, Miller-Stephenson Chemical Company, Danbury, CT) is of this type. The product of the reaction between these two compounds is the diglycidyl ether of bisphenol-A (DGEBA). The reaction which produces DGEBA is illustrated in Figure 3.8.

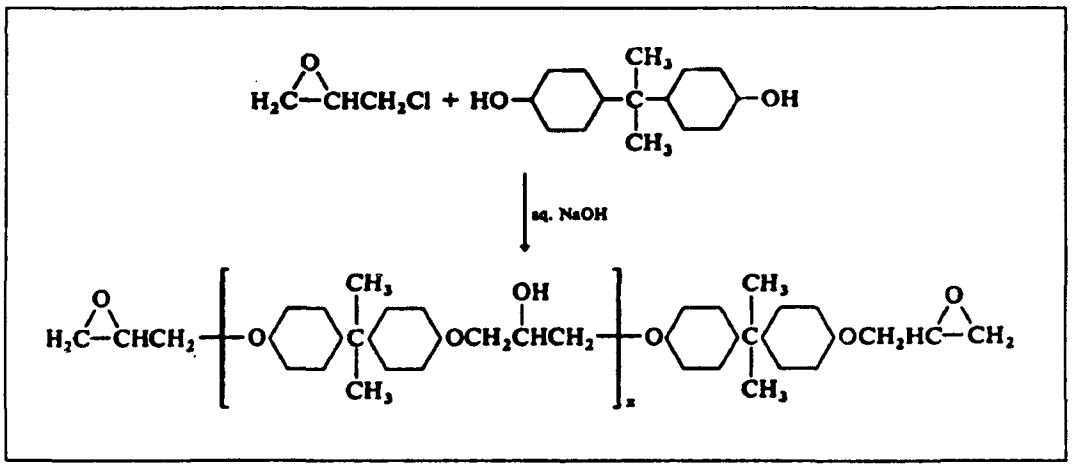

Figure 3.8. Reaction of epichlorohydrin with bisphenol-A to produce DGEBA (8:479).

The process by which a thermosetting resin attains its solid, brittle state is called *curing*. During cure, the resin is cross-linked, resulting in a material with a continually increasing molecular weight. This process is facilitated by the addition of a compound called a curing agent. Some curing agents are catalysts, and others become bound in the resin chains (12:5-1). Curing

agents include polyamines, polyamides, polysulfides, and acids or acid anhydrides (8:479). A reaction with a polyamine is depicted in Figure 3.9. The curing agent used in this thesis effort was a polyamide resin. This simplified illustration shows the process of cross-linking, in which

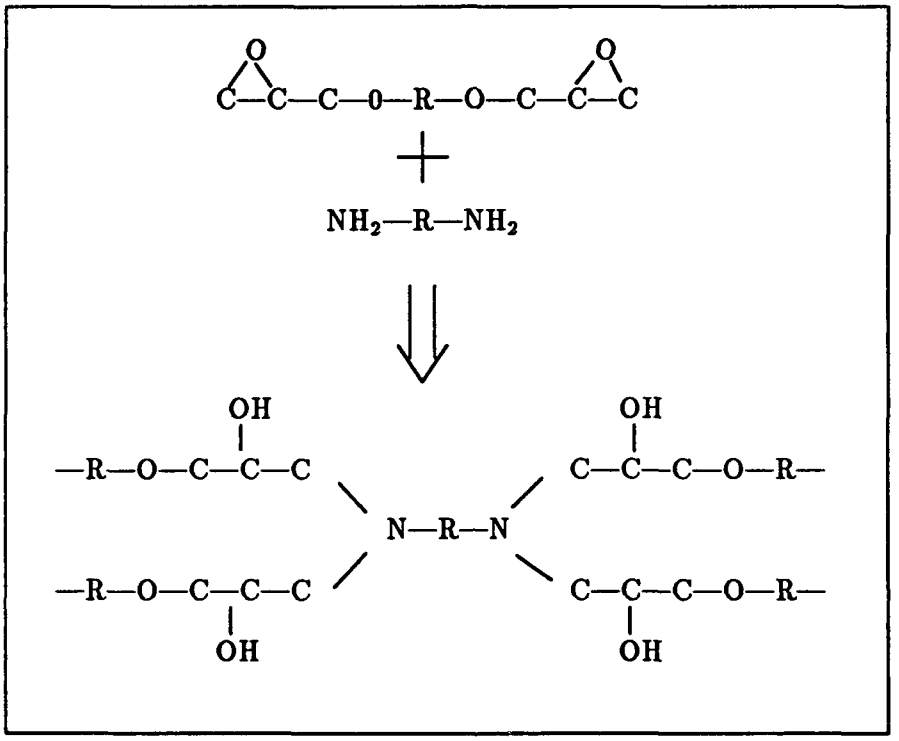

Figure 3.9. The cross-linking reaction between DGEBA and a polyamine (35:11).

resin molecules are joined together by reaction with the curing agent.

The curing, or polymerization process, is characterized by three "phases." In the uncured state, the resin is a liquid. With the addition of heat, the polymerization reaction proceeds. The gelation point occurs when the material passes from the liquid state to a rubber state. At the glass transition point, the material becomes vitreous. These phases are illustrated in Figure 3.10. There are some interesting points to be made upon examination of Figure 3.10. At high temperatures, the resin gels but does not vitrify. At low temperatures, the resin can pass from its

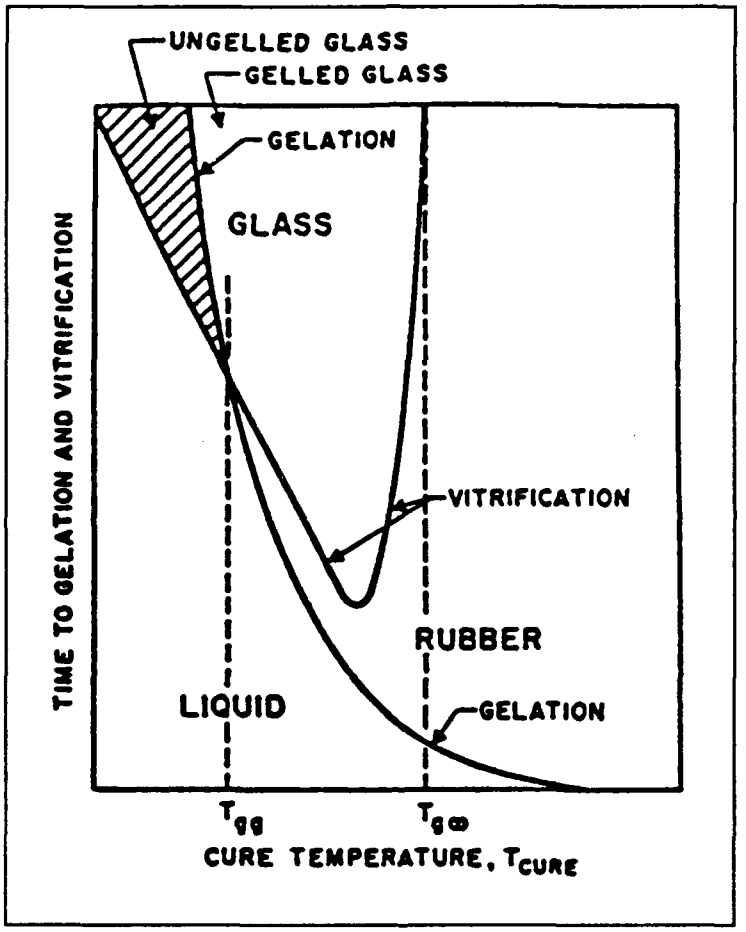

Figure 3.10. Time-to-gelation and time-to-vitrication versus isothermal cure temperature for an epoxy resin (40:63).

liquid state directly into its vitrified state without having gelled. At the range of temperatures between T_{gg} and $T_{g\infty}$, the system first gels and then vitrifies (40:64).

The definitions of the gelation point and glass transition temperature, two important figures of merit for thermosetting resins, are now discussed.

Gelation Point. The gelation point of a resin, or the point at which it passes from the liquid state into the rubber state, is not analogous to a phase change associated with a compound such as water. There are many definitions and interpretations of this concept. In general, however, the gelation point is characterized by a sudden loss of resin fluidity (8:274). Another definition is that the gelation point corresponds to the point at which an essentially infinite degree of polymerization has been attained (8:277).

From an electrical perspective, the gelation point is marked by a sudden variation in the rate of change of the measured electrical characteristics. This behavior can be understood by referring to the orientational polarization mechanism discussed earlier. Once the reaction attains gelation, there is a sudden rise in viscosity and a corresponding loss of fluid flow (36). This behavior reduces the polarizability of the polymer molecules because they are bound more rigidly in the resin and cannot respond as readily to electromagnetic stimuli.

At the gelation point, the rate of change of the mechanical characteristics is markedly decreased since the opportunities for polymer chain growth are severely limited (36). Hence, the electrical characteristics should manifest a corresponding decreasing rate of change.

Glass Transition Temperature. The glass transition temperature is loosely defined as the temperature at which the onset of brittleness occurs. All polymers will assume a vitrified state at a sufficiently low temperature. At temperatures above the glass transition temperature, the resin softens. Below the glass transition temperature, the resin assumes a glassy state. In the glassy state, large-scale molecular motion does not take place (8:209).

Viscosity. The term *viscosity* comes from a Latin word which means "stickiness" (37:12). According to Newton, the ratio of stress to the shear rate in a material is constant (all other things being equal). This ratio is called the viscosity of the material, and is denoted by η. Shear is defined as a deformation that is parallel to a stationary plane.

If a sinusoidal torque is applied to a perfectly elastic material, the *shear modulus*, or the ratio of torque/shear (denoted by G), is a constant with respect to the applied torque's frequency (ω). That is, the torque and the shear will be in phase. However, if the material is purely viscous (or *Newtonian*), the shear will lag the torque by 90 degrees. Most real materials display *visco-elastic* behavior, since they exhibit elasticity and viscosity characteristics simultaneously. In this case, the shear modulus, G^*, is complex, and is given by:

$$G^* = G' + jG'' \tag{3.31}$$

where G' is the *storage modulus* and G'' is the *loss modulus*. The storage modulus is related to the elastic behavior of the material, since the applied energy is stored elastically. The loss modulus is related to the viscosity of the material, since the applied energy is dissipated as heat (37:39–40). The viscosity, η^*, in a visco-elastic material is also complex, and is given by,

$$\eta^* = \eta' + j\eta''. \tag{3.32}$$

The viscosity is related to the shear modulus by, $G^* = \eta^*\omega$. These relationships are similar to the electrical properties of dielectrics that were discussed earlier. The plot of the real and imaginary components of the complex shear modulus (G^*) is given in Figure 3.11. Figure 3.11 is very similar to the plot of the real and imaginary components of the relative permittivity (Figure 3.3).

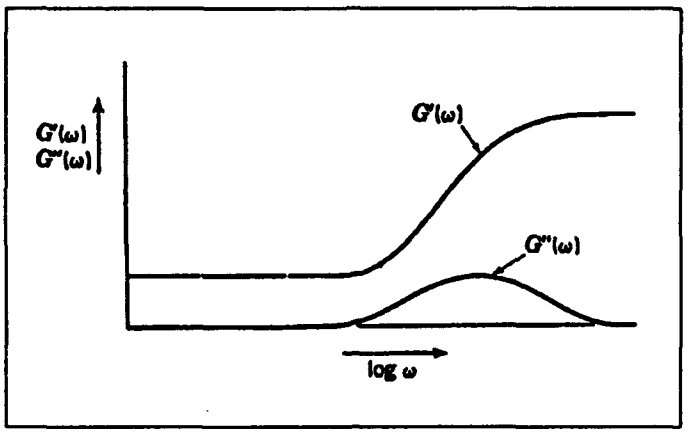

Figure 3.11. Real and imaginary components of the shear modulus (G^*) as a function of frequency (38:22).

Another similar figure of merit is the mechanical loss tangent ($\tan \delta_m$), given by:

$$\tan \delta_m = \frac{G''}{G'}. \tag{3.33}$$

By direct analogy with the impedance parameters for dielectric materials, it should also be possible to represent the viscosity information as a circular locus (similar to the Debye semicircle and the Cole-Cole plot). A circular locus plot of the complex shear modulus may provide information useful for mechanical "equivalent circuit" models of a material's visco-elastic behavior. The shear modulus data in this thesis was collected as a function of temperature rather than frequency, and thus, it did not display the characteristic semicircle of a Debye plot.

Equivalent Circuit Representation of the IGEFET-Resin System

A curing resin system's electrical behavior is quite complex. The permittivity of the resin is frequency dependent, and it also changes with cure time. Therefore, it is not possible to represent the system as a simple combination of passive electrical elements, unless the representation is specified for a known frequency and a known cure time. However, a lumped-element model of the

IGE-resin system is useful as an aid for illustrating the system's electrical characteristics for a given frequency and cure time.

During the IGEFET experiments, the IGE structure was coated with an essentially infinitely thick layer of resin (with respect to the thickness of the electrodes). The IGE-resin system can be modeled as a lumped-element circuit (at a known frequency and cure time), as illustrated in Figure 3.12. In this figure, C_e and C_{ox} correspond to the capacitance of the epoxy and SiO_2 layer,

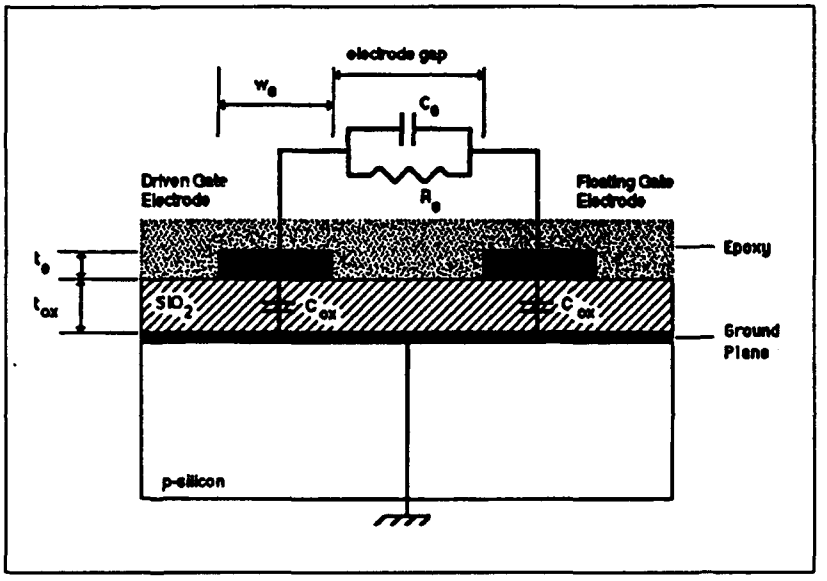

Figure 3.12. A lumped-element equivalent circuit model of the IGE-resin system.

respectively. R_e represents the resistance of the epoxy, w_e is the width of an electrode, t_e represents the thickness of an electrode, and t_{ox} corresponds to the thickness of the SiO_2 layer. As the cure reaction proceeds, the electrical characteristics of the epoxy, and hence C_e and R_e, will change. Based on the polarization mechanisms discussed earlier in this chapter, particularly orientational polarization, the permittivity of the resin should decrease because the cross-linking process causes the average molecular weight of the resin to increase. Consequently, the resin's polarizability correspondingly decreases. If the resin were an ideal dielectric, that is, if there were no loss mechanisms present, R_e should approach a value of zero. However, there will always be

some degree of loss in a resin system, which is attributable primarily to ionic conduction (9). These ions can include unreacted materials present in the resin and byproducts of the resin's synthesis (for example, sodium). As the cure proceeds, there will be fewer unreacted species in the material, and the mobility of these and other the ionic materials will correspondingly decrease. This behavior will result in a decrease in R_e as the cure proceeds.

Summary

In this chapter, the theory of the mechanics of resin cure and the electrical characteristics associated with the process have been presented. The concept of polarization was discussed. Complex electrical permittivity was introduced to account for loss in the resin, and the Debye equations were derived. The Cole-Cole plot's significance was stressed. The basic physical mechanisms involved in the cure of epoxy resins was discussed and related to previously discussed electrical characteristics.

IV. IGEFET Sensor Design, Instrumentation Configuration, and Experimental Methodology

IGEFET Sensor Design and Characterization

The purpose of this chapter is to detail the design of the IGEFET sensor and to present a preliminary assessment of its operating characteristics. An overview of the design goals and rationale will first be presented, followed by a detailed description of the design process and sub-circuits included to realize the sensor. Finally, the expected operating characteristics of the design, based upon computer simulations, will be presented.

Design Goals. As discussed in Chapter 1, the design of the IGEFET sensor used in this thesis effort was essentially an exercise of combining several sub-circuits designed in previous theses. No new active electronic devices were designed for the IGEFET sensor. However, the primary new features included in this design are detailed below:

1. The IGE structure is square, and the individual structures are separated by a distance greater than previously utilized. This arrangement facilitates deposition of epoxy resin and other chemicals onto the surface of each IGE structure without interfering with adjacent structures.
2. A ground plane was added beneath each IGE structure and the driven-electrode (DE) input line to reduce noise and to facilitate characterizing the oxide layer which separates the IGE structure and the ground plane.
3. The size and spacing of the electrode fingers has been changed.
4. Nine sensor elements (SEs) are arranged in a 3 x 3 matrix which comprises an approximately square configuration on the surface of the integrated circuit.
5. Three test capacitors have been included to permit characterization of the oxide layer between the two levels of metal.

6. A demultiplexer was added to facilitate switching the input excitation signals between individual DEs.

The IGEFET was designed at AFIT using computer-aided design tools located in the AFIT Very Large Scale Integration (VLSI) laboratory. Several subcircuits used to design the IGEFET were extracted from the CHEMFET designs of Jenkins (4) and Shin (5).

Interdigitated Gate Electrode Structure Design. Due to difficulties experienced in applying certain polymers to the IGE structure in previous experimental efforts (5:VI-6), a square IGE structure was designed in this thesis effort. The previous designs had been rectangular in shape, with very little space provided between adjacent structures. Prior experience also suggested the optimal width of the fingers in the IGE structure and their spacing. The fingers were designed to be 10 μm wide and spaced 10 μm apart, as illustrated in Figure 4.1. The DE consisted of 30 such fingers, and the floating-electrode (FE) consisted of 29 fingers. To facilitate the application of certain resins and polymers, the design of the IGE structures was approximately square. This modification required the fingers to be 1170 μm long. The IGE structures designed in this manner were placed approximately 700-to-1000 μm apart, depending upon their location on the IC die.

In addition to the change in the design of the IGE fingers, it was decided that a ground plane be included in the revised design. The ground plane would serve a dual purpose. First, it would provide some degree of noise immunity to the SE. Second, it would make modelling the electrical characteristics of the IGE structure much simpler (the cumbersome capacitance-voltage characteristics of the semiconductor could be eliminated). The ground plane was fabricated in first-level metal, while the IGE structure was fabricated in second-level metal. The addition of several capacitors in the design facilitated characterizing the oxide between the two metal layers. The values for the electrical properties of this oxide could then be utilized to create a mathematical equivalent electrical circuit model of the IGEFET.

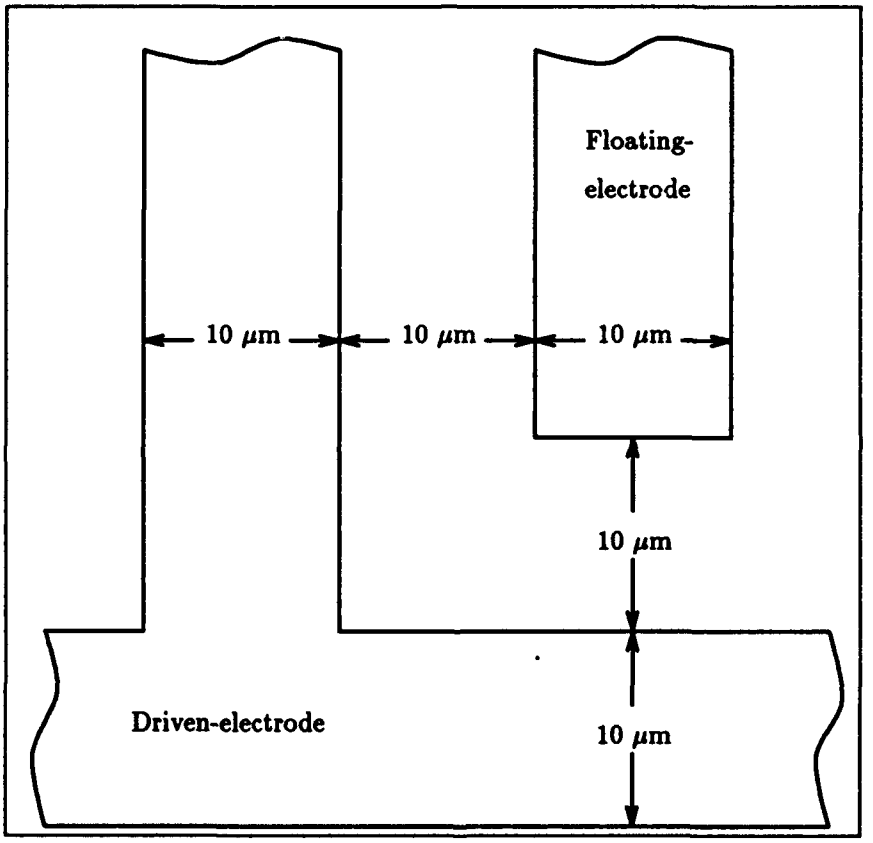

Figure 4.1. Dimensions of the interdigitated gate electrode structure fingers.

Sensor Element Amplifier Design. The SE amplifier was designed by Jenkins (4:4-3–4-7). A schematic diagram of the amplifier is illustrated in Figure 4.2. The amplifier is a 3-stage NMOS

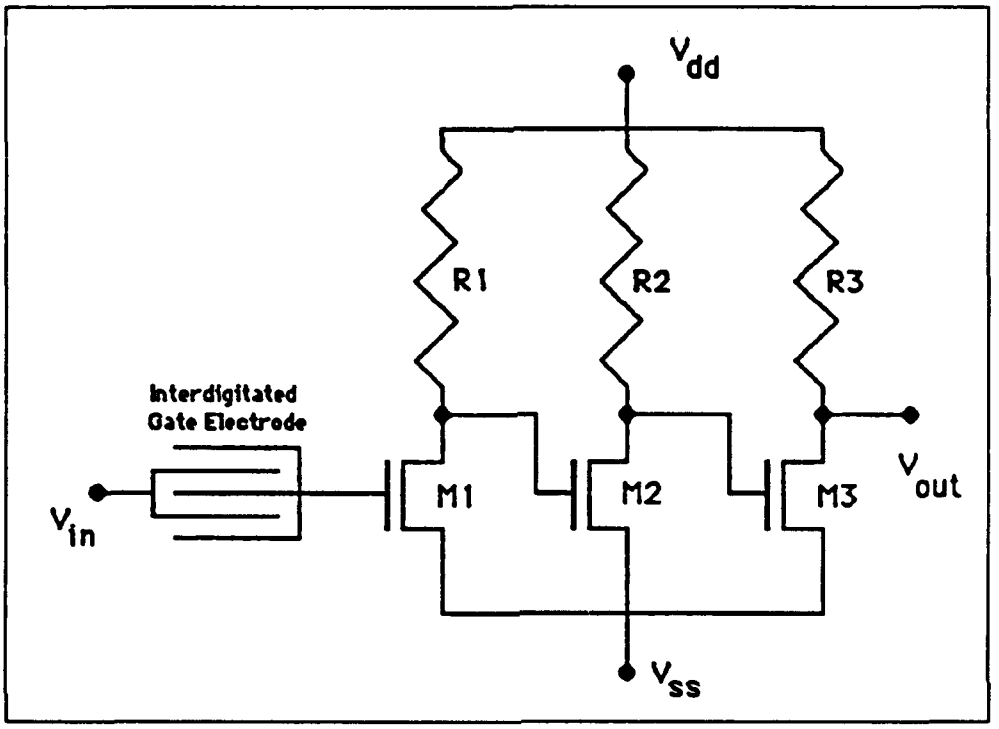

Figure 4.2. Schematic diagram of the sensor element amplifier (4:4-4).

enhancement-mode device. The resistors used to bias the MOSFET transistors were scaled as follows: R1 had a width of 3 μm and contained 326 squares for a typical resistance value of approximately 6700 ohms. R2 had a width of 3 μm and contained 486 squares for a typical resistance value of approximately 10 Kohms. R3 was also 3 μm wide and contained 364 squares for a typical resistance value of approximately 7500 ohms. The MOSFET transistors all had gate lengths of 3 μm. M1 had a 9 μm wide gate, M2 had an 11 μm wide gate, and M3 had a 12 μm wide gate. The layout of the SE amplifier is illustrated in Figure 4.3. Jenkins designed the amplifier in SPICE3 (U.C. Berkeley), and the code used in the SPICE simulation is listed in Appendix A.

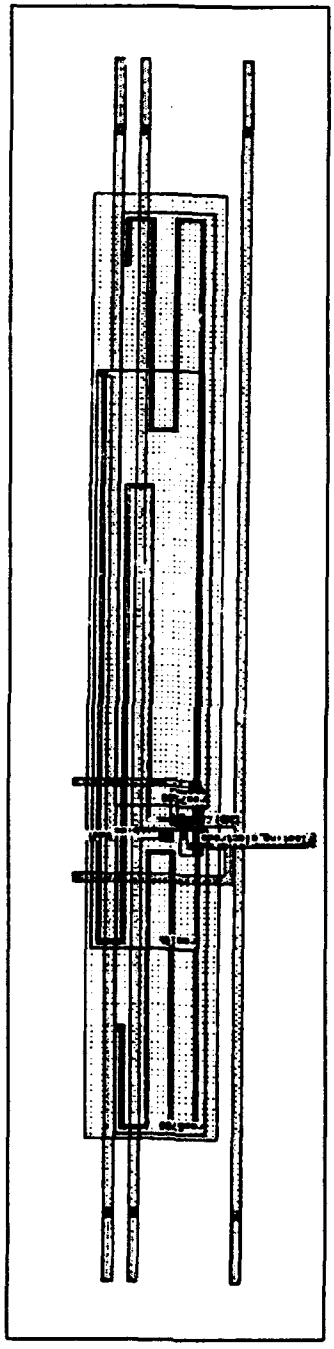

Figure 4.3. Layout of the sensor element amplifier.

Reference Element Design. The design approach for the reference element was the same in this research effort as was used in the past. The amplifier utilized was identical to the SE amplifier. However, the gate electrode structure was no longer interdigitated. Since the purpose of the reference element was to provide compensation for environmental effects on the SE amplifier, it was necessary to simulate the SE amplifier accurately. This configuration required the addition of parasitic capacitance which was approximately equal to that provided by the IGE structure. This was accomplished by fabricating an electrode of solid, second-level metal, whose area was approximately equal to the effective (metallized) area of the IGE structure.

Multiplexer and Demultiplexer Circuit Designs. The multiplexer (MUX) and demultiplexer (DEMUX) circuits were also used in Jenkin's design (4:4-12–4-18). The basic design, however, was derived from previous designs by several students in AFIT VLSI classes (4:4-12). The MUX and DEMUX circuits were identical. The difference between the two only concerned their implementation. The signal input and signal output lines were interchanged in the two circuits. Therefore, to simplify the narrative, only the MUX will be mentioned in this section unless the DEMUX is specified.

The MUX consisted of two basic sections: a decoder and switches. The decoder utilized four logic inputs, denoted A, B, C, and D. This feature implies that the maximum number of switches that could be controlled by the decoder was 16. Because only 9 SE output signals and an additional reference element output needed to be switched, the MUX required only 10 switches. The logic decoder design was pseudo-NMOS, as illustrated in Figure 4.4. The p-channel pull-up MOSFET is provided with a constant V_{SS} supply so that it is always conducting. The four n-channel pull-down MOSFETs act as the logic decoders. If any one of the four gates of these transistors is provided with V_{DD}, the output signal is driven to V_{SS}. Otherwise, the output signal is pulled-up to almost the V_{DD} level. Jenkins performed a "switch-level" simulation of the circuit to ensure its proper operation (4:4-14).

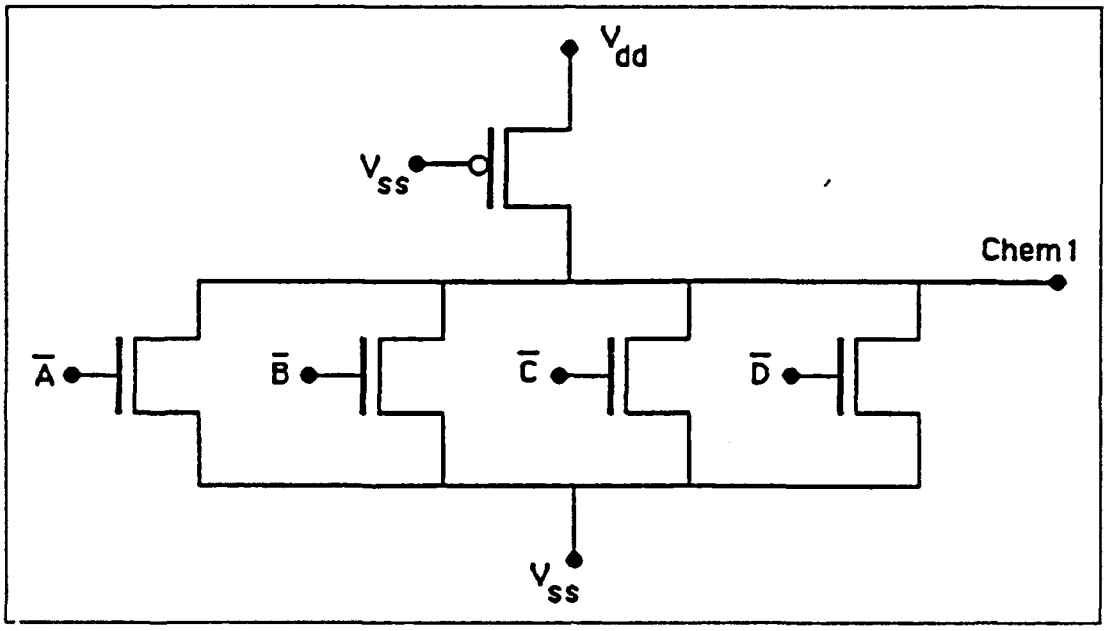

Figure 4.4. Schematic diagram of one bit-slice of the logic decoder (4:4-13).

An inverting buffer was also included in the design of the MUX circuit. The purpose of the inverting buffer was to provide the correct logic levels for the operation of the switches at the output of the MUX. It was necessary for the buffer to provide a control signal and its complement, as illustrated in Figure 4.5. Since the decoder section of the MUX was designed in pseudo-NMOS, the logic levels provided at its outputs were not exactly V_{DD} and V_{SS}. Consequently, the buffer was used to restore the logic levels to V_{DD} and V_{SS}.

The final stage of the MUX circuit was a transmission gate (T-gate), and it is depicted in Figure 4.6. The purpose of the gate is to either pass the selected signal or block unselected signals. Therefore, it acted as an analog switch. The only difference between the MUX and the DEMUX was in the implementation of the input and output signals. That is, the MUX circuit selected one of ten inputs and passed it to the output, while the DEMUX passed its input to one of nine outputs. The controlling logic for this circuit was the output of the decoder section and its complement, which were derived in the inverting buffer section. The gate dimensions of the

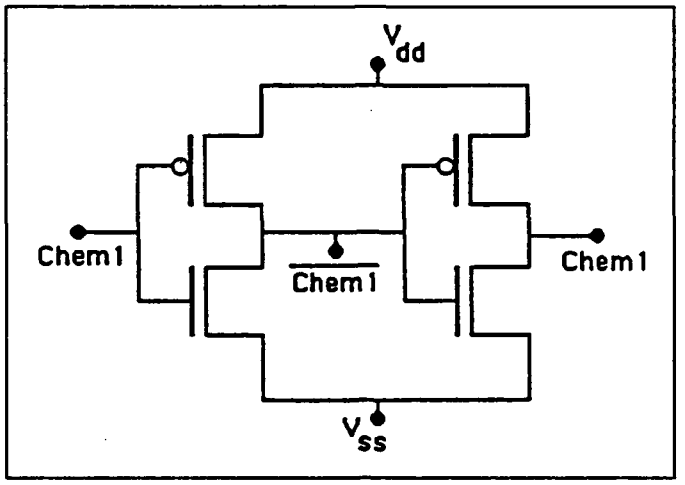

Figure 4.5. Schematic diagram of the inverting buffer (4:4-14).

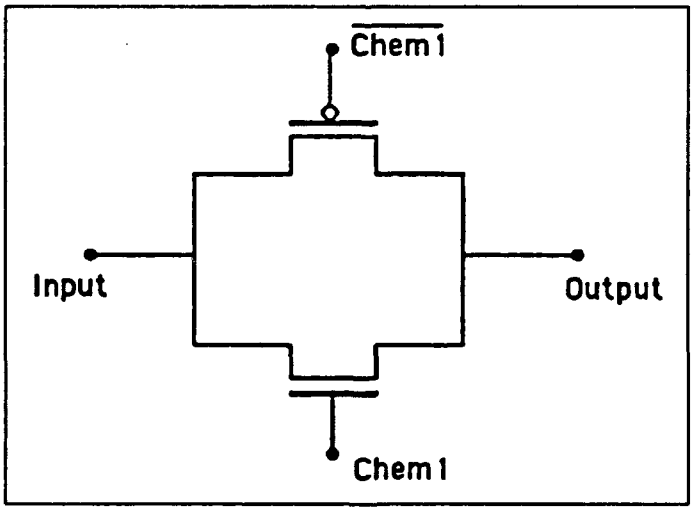

Figure 4.6. Schematic diagram of the T-gate switch (4:4-14).

n-channel and p-channel transistors in the transmission gates were 3 μm long and 15 μm wide. The layout of the entire MUX circuit is illustrated in Figure 4.7.

Voltage Follower Circuit Design. The voltage follower was also designed by Jenkins (4:4-16). Its purpose was to isolate the IGEFET electronics from the external electrical environment. The design, depicted in Figure 4.8, is based upon a standard analog comparator design. The sizes of the transistors used in the design were determined by simulating the circuit. For proper operation of an operational amplifier, it is necessary to have M1 and M2 be the same size, and M3 and M4 be the same size. M1 and M2 were p-channel transistors with gates 6 μm long and 36 μm wide. M3 and M4 were n-channel transistors whose gates were 3 μm long and 24 μm wide. N-channel transistor M5 was biased with V_{DD} to provide a constant "on" resistance, and it was designed with a gate that was 3 μm long and 12 μm wide. The layout of the voltage follower is illustrated in Figure 4.9.

Operational Amplifier Circuit Design. The operational amplifier section of the IGEFET electronics was designed by Shin (5:III-4–III-5). The basic design is based on an analog comparator, just as the voltage follower design was. This basic circuit is illustrated in Figure 4.8. The operational amplifier was a five-stage design, and each stage incorporated feedback. The first four stages were identical, and the fifth stage was slightly different, as shown in Figure 4.10. Based on SPICE simulations, the operational amplifier stage was predicted to provide 32 dB of gain with a 3-dB cutoff frequency of 10 MHz (5:III-6).

Final Design. The final design of the IGEFET integrated circuit consisted of positioning the individual sub-circuits in their proper places, designing the ground plane, providing interconnections between the sub-circuits, incorporating the bonding pads, locating the glass cuts, and including the three parallel-plate test capacitors on the IC die.

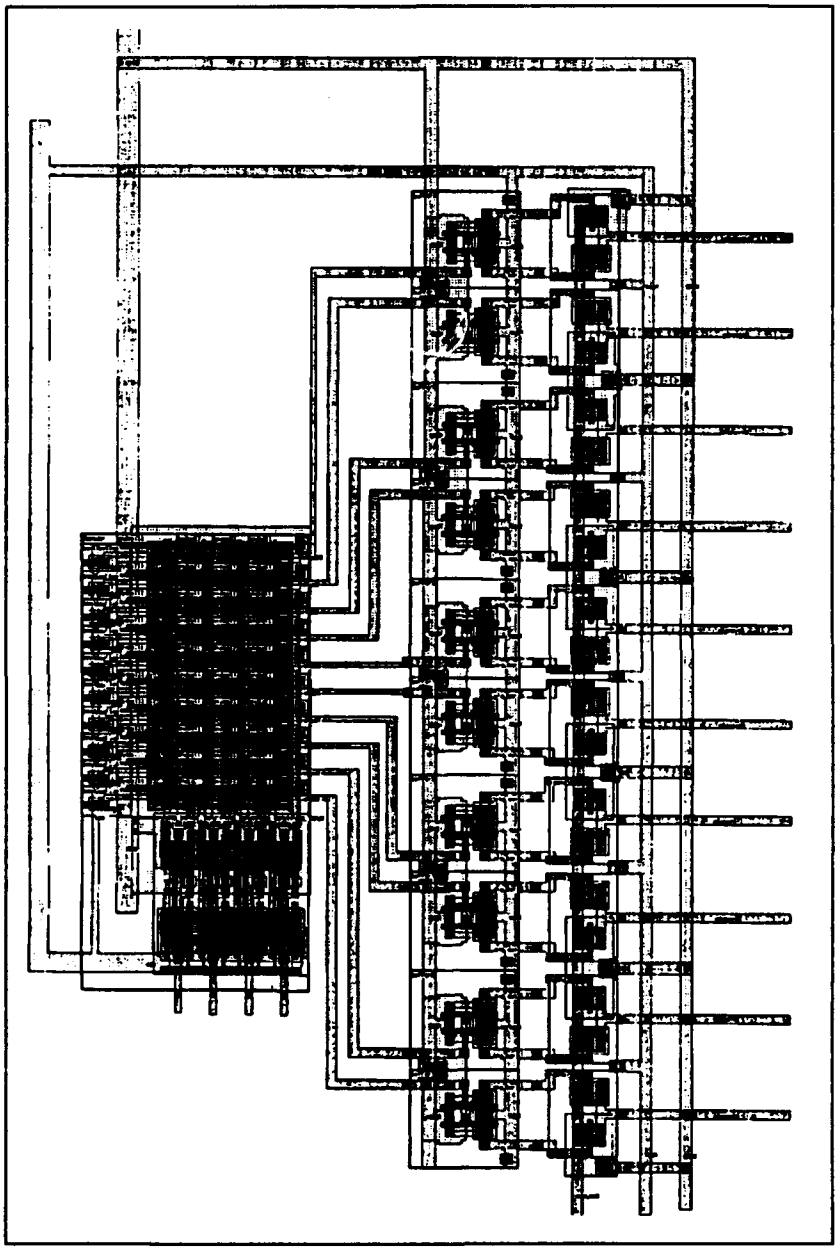

Figure 4.7. Layout of the multiplexer and demultiplexer circuits (4:4-17).

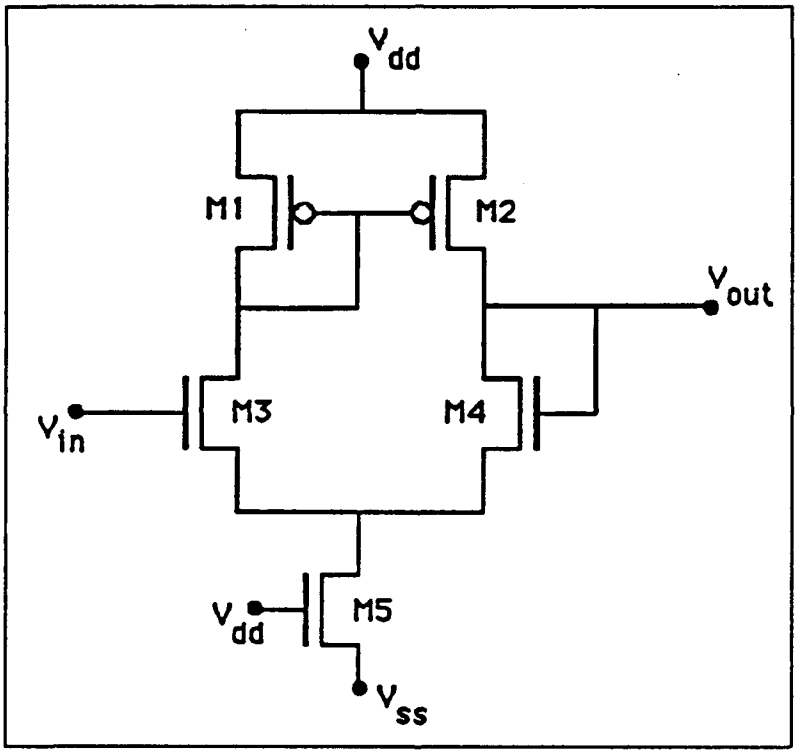

Figure 4.8. Schematic diagram of the voltage follower circuit (4:4-18).

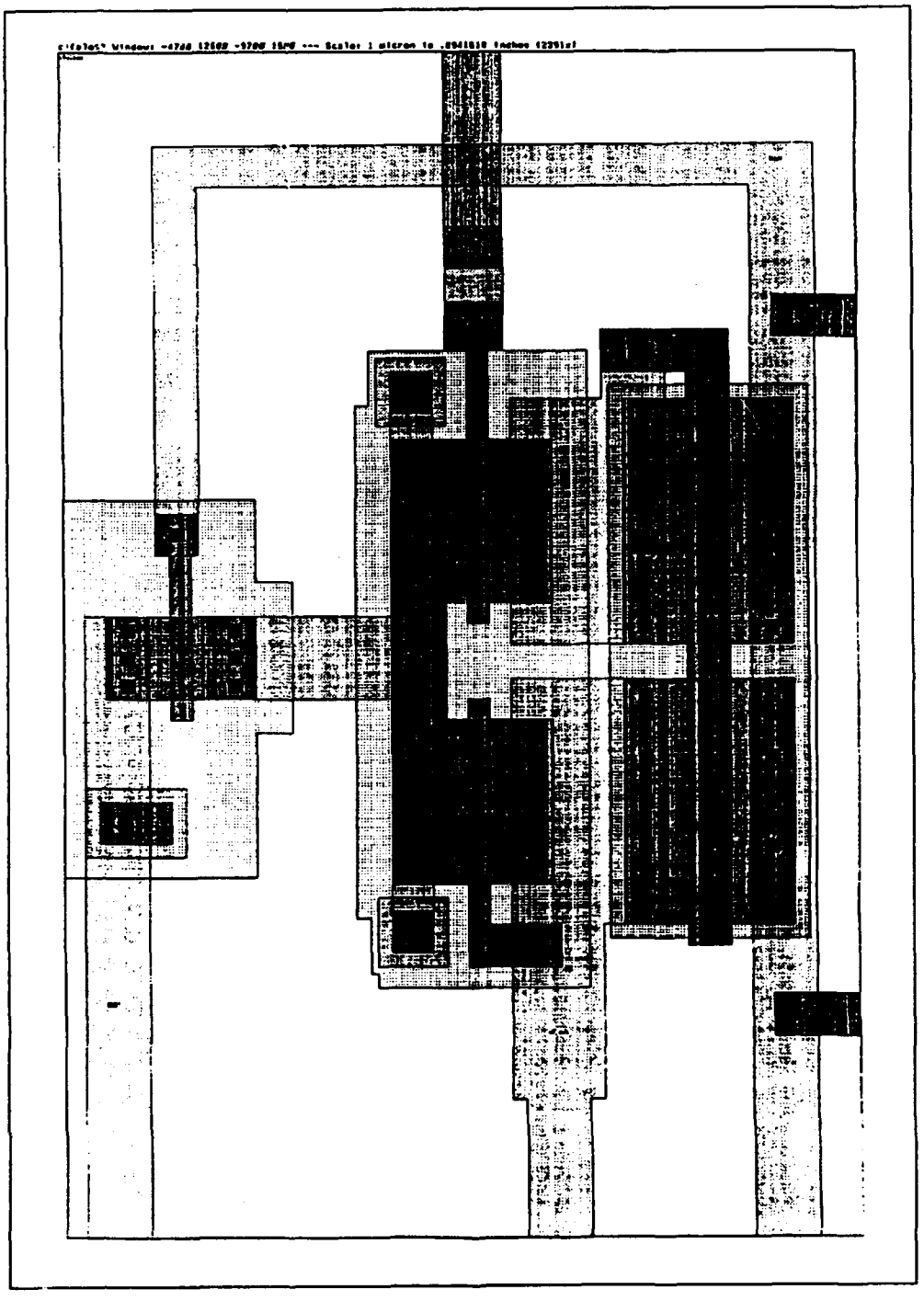

Figure 4.9. Layout of the voltage follower circuit (4:4-18).

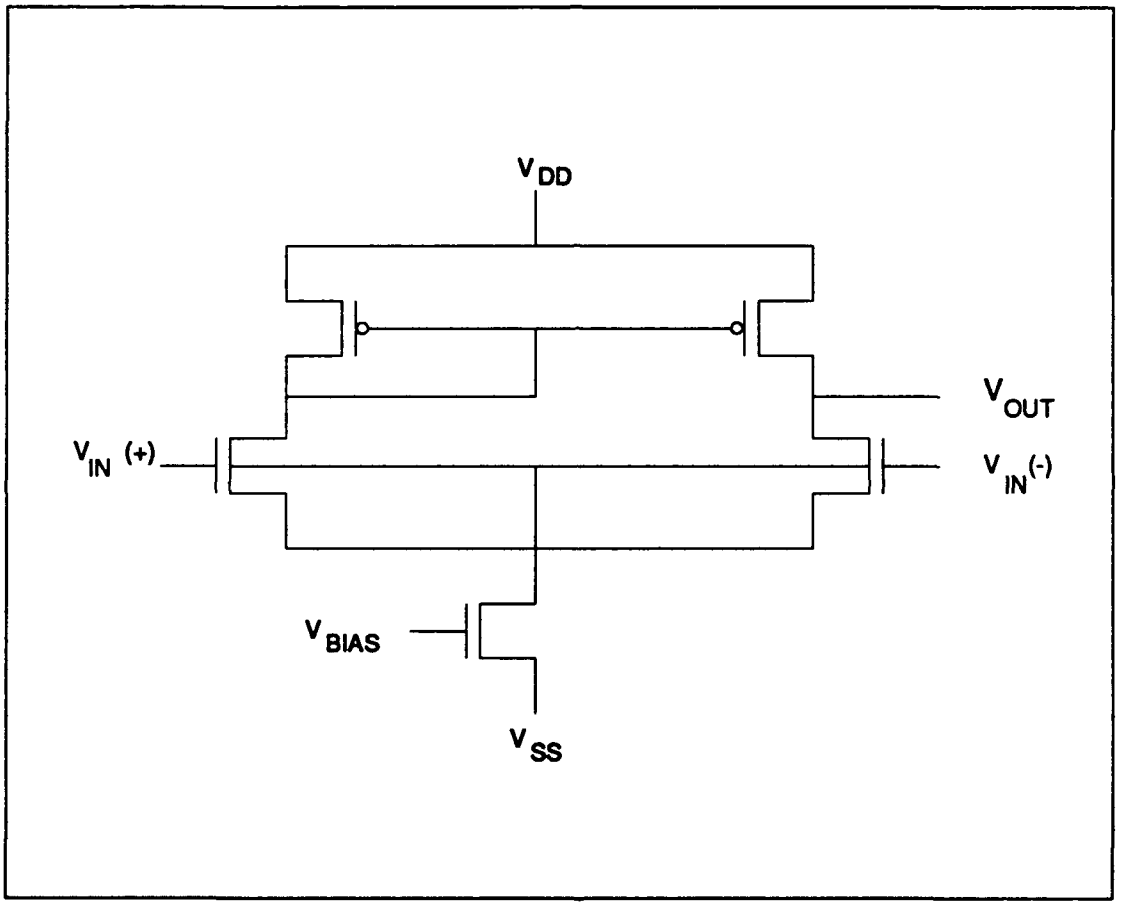

Figure 4.10. Schematic representation of one of the operational amplifier stages (5:III-5).

As mentioned earlier, the individual sensor elements were arranged in a 3 × 3 matrix in the integrated circuit design. The reference element, MUX, voltage follower and operational amplifier were located adjacent to this matrix. The DEMUX was located in another part of the circuit. A diagram depicting the locations of the individual sub-circuits is provided in Figure 4.11.

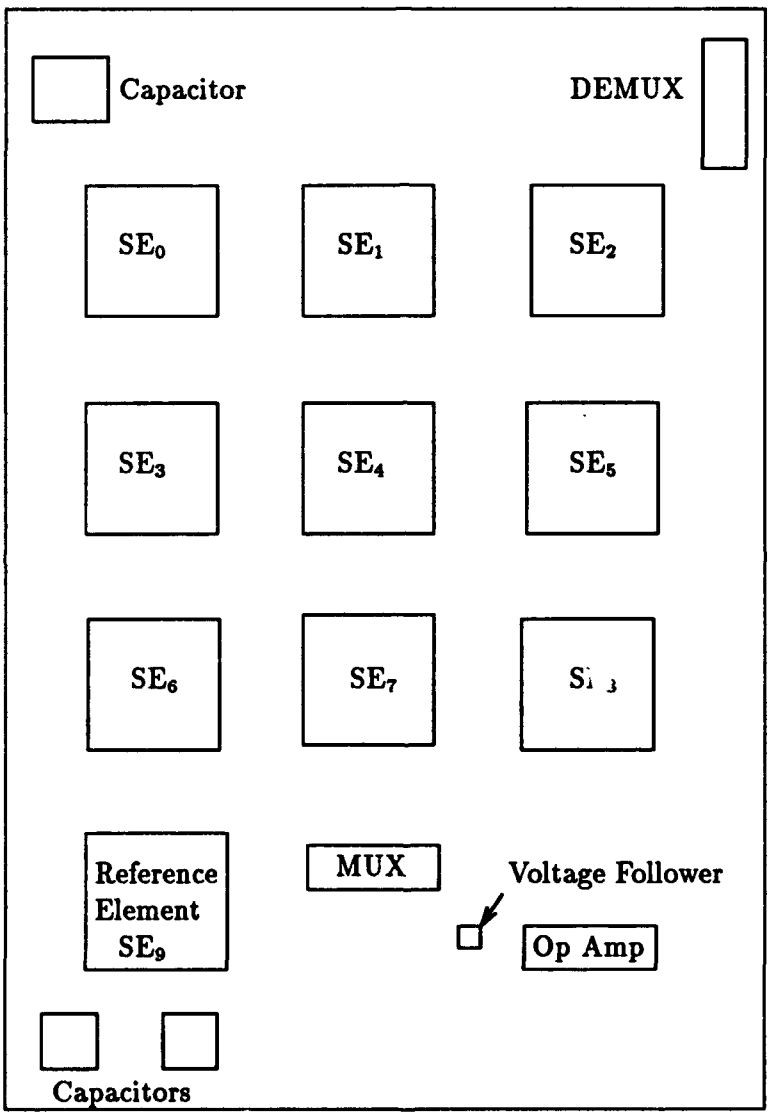

Figure 4.11. Layout of the final IGEFET design depicting the locations of the individual sub-circuits.

Glass cuts were placed in numerous areas on the integrated circuit. Their purpose was to provide a means of troubleshooting internal nodes (those nodes not connected to bonding pads), and to facilitate easy excision of inoperative circuits with an ultrasonic microprobe cutter.

Three capacitors, designed in first- and second-level metal, were located in different areas on the die. They were all different sizes: one was 100 μm x 100 μm, the second was 200 μm x 200 μm, and the third was 400 μm x 400 μm. Their purpose was to provide a means for accurately measuring the thickness and electrical properties of the silicon dioxide layer fabricated between the two metal layers.

Finally, bonding pads were located around the integrated circuit. Due to the large number of nodes in the design that required bonding pads, some sacrifices were made. It would have been preferable to provide separate power supply lines for each sub-circuit. In the final design, however, most circuits shared a common power supply bus. Also, the operational amplifier design required separate offset voltages for each stage. In the final design, all the offset voltage lines were tied together.

IGEFET Integrated Circuit Fabrication. After the design was finalized, a CIF (Caltech Intermediate Form) file was generated and forwarded to the Metal-Oxide-Semiconductor Implementation System (MOSIS) for fabrication. The CIF file generated was for the 2 μm, CMOS, n-well, double polysilicon fabrication technology. A photomicrograph of an IGEFET integrated circuit received from MOSIS is presented in Figure 4.12. Twenty-five packaged integrated circuits were received. The bonding pad arrangement and MOSIS parametric test results are provided in Appendix B. The integrated circuit package pin assignments are listed in Table 4.1.

The SPICE level-4 parameters for the integrated circuit, which were based upon the actual characteristics of the fabricated devices, were included with the MOSIS parametric test results. The SPICE level-4 transistor models necessary to simulate the circuit were derived from the

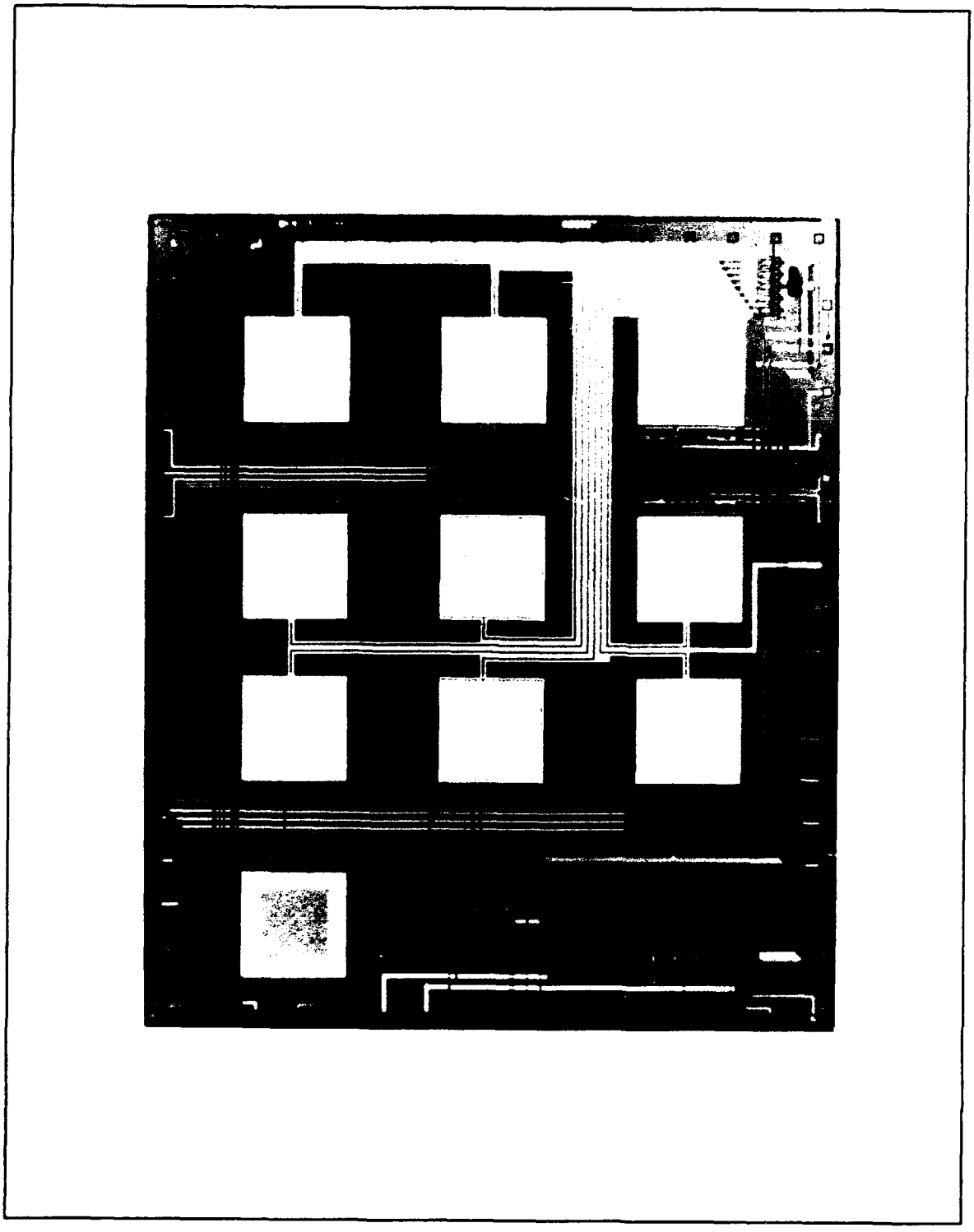

Figure 4.12. Photomicrograph of the IGEFET integrated circuit.

Table 4.1. IGEFET integrated circuit pin assignments.

Pin	Function	Pin	Function
1	SE_8 output	33	FE_3
2	Ground plane	34	SE_3 output
3	FE_5	35	FE_6
4	SE_5 output	36	SE_6 output
5	FE_2	37	V_{DD}
6	SE_2 output	38	V_{BIAS}
7	V_{SS}	39	V_{SS}
8	V_{DD}	40	Reference element output
9	V_{BIAS}	41	Reference element input (FE_2)
10	Demultiplexer input	42	Medium capacitor M1 contact
11	DE_2	43	Medium capacitor M2 contact
12	Ground plane	44	Small capacitor M1 contact
13	Ground plane	45	Small capacitor M2 contact
14	DE_5	46	V_{DD}
15	DE_8	47	V_{SS}
16	DE_7	48	Multiplexer line select A
17	DE_6	49	Multiplexer line select B
18	DE_3	50	Multiplexer line select C
19	D	51	Multiplexer line select D
20	I	52	Multiplexer output
21		53	Voltage follower output
22	e capacitor M1 contact	54	V_{offset}
23	ge capacitor M2 contact	55	V_{SS}
24	FE_0	56	V_{DD}
25	SE_0 output	57	Operational amplifier stage 1 output
26	FE_1	58	Operational amplifier stage 2 output
27	SE_1 output	59	Operational amplifier stage 3 output
28	V_{DD}	60	Operational amplifier stage 4 output
29	V_{BIAS}	61	Operational amplifier stage 5 output
30	V_{SS}	62	FE_7
31	FE_4	63	SE_7 output
32	SE_4 output	64	FE_8

parameters using the program Proc2mod (U.C. Berkeley). The expected gain of the sensor element amplifiers was determined using these models. A plot of the calculated gain is given in Figure 4.13. The calculated gain of the sensor element amplifiers was based upon the bias values determined by Jenkins during his research (4).

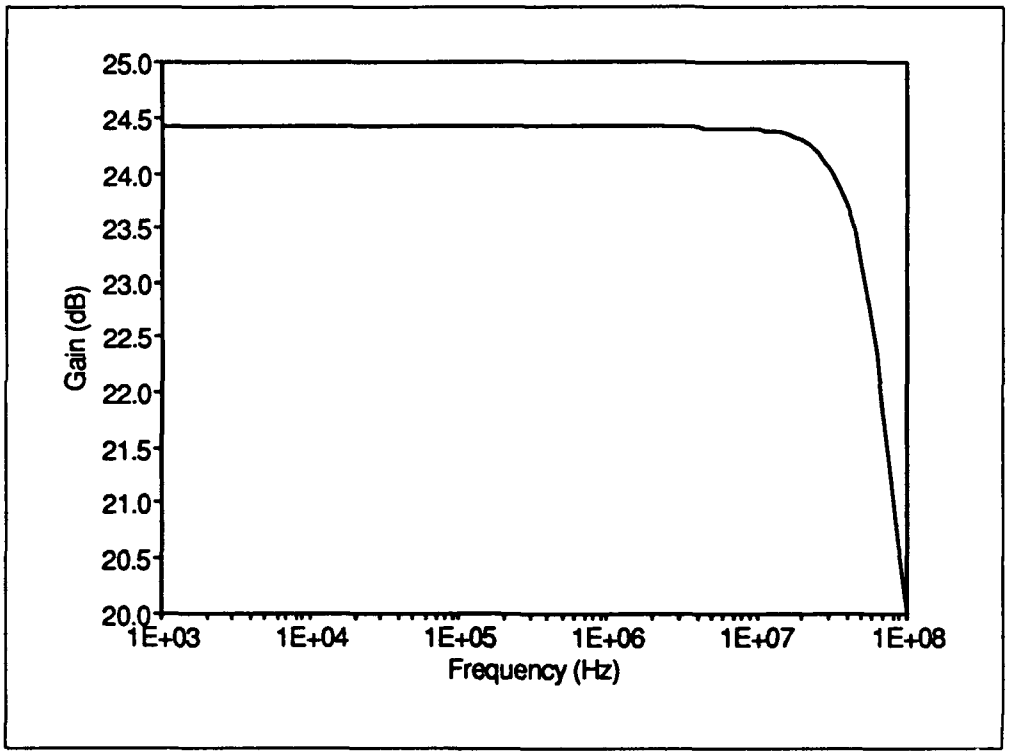

Figure 4.13. Expected gain of the sensor element amplifier.

The optimum bias levels for the circuits were determined experimentally. The values of V_{DD} and V_{SS} were +5 volts and -5 volts, respectively. V_{BIAS} and V_{offset} were determined to be -5 volts. The derivation of these bias levels, and the measured operating characteristics of the IGEFET electronics are detailed in Chapter 5.

IGEFET Performance Instrumentation Configuration

The configuration of the electrical test equipment used to accomplish the measurements of the IGEFET's performance during the resin cure experiments is discussed in this section.

General Considerations. Several different electrical measurements were conducted during the resir cure experiments. These measurements included:

1. Direct current (dc) resistance of the IGE structure.
2. Alternating current (ac) impedance (magnitude and phase) of the IGE structure.
3. Gain and phase delay of the IGE structure.
4. Gain and phase delay of the IGEFET.
5. Gain and phase delay of the reference element.
6. Time-domain response of the IGEFET to a voltage pulse excitation.
7. Frequency-domain response of the IGEFET to a voltage pulse excitation.

In order to maximize the number of measurements performed during the resin's cure cycle, a separate cure was performed for each electrical measurement detailed above. Each different electrical measurement, therefore, constituted a separate resin cure experiment. In addition, since the resin was cured at two temperatures, two experiments were performed for each different electrical measurement—one experiment for each cure temperature. All electrical measurements were referenced relative to the elapsed time during the resin's cure cycle. Also, the resins were cured until the elapsed time of the experiment was at least double the time required to achieve the estimated gelation point.

A Zenith model 248 microcomputer (Zenith Data Systems, St. Joseph, MI) was used to collect the data. Control of the test equipment and retrieval of the performance data was facilitated by and IEEE-488 interface card (Capitol Equipment Corp., model 01000-60300,

Burlington, MA). The listing of the software program used to collect the data is provided in Appendix C.

All necessary power was supplied to the IGEFET with a power supply (Hewlett Packard, model HP6205B, Palo Alto, CA). The power was delivered to the individual IGEFET microcircuits as illustrated in Figure 4.14. The multiplexer and demultiplexer were provided a constant value of decoding logic because it was discovered that repeated switching of these circuits over a prolonged period of time caused them to fail. This issue will be discussed further in Chapter 5. Since these circuits were not utilized, it was necessary to manually select individual SEs for testing. In addition, because of this revised mode of operation, it was not possible to use the voltage follower or the operational amplifier. Consequently, these circuits will not be shown in diagrammatic representations of the test equipment configurations that are subsequently discussed in the chapter.

The interface between the IGEFET and the test equipment was provided by the test cell illustrated in Figure 4.15. The cell was designed by Capt Charles Brothers (39). It provided all required interconnections between the IGEFET and the test equipment. The purpose of the test cell was four-fold. First, it provided a means to connect the IGEFET to the test equipment. This interface included a 64-pin zero insertion-force socket (which held the IGEFET), internal wiring, and BNC connectors to facilitate connection to test equipment via coaxial cable. Second, the test cell eliminated much of the ambient electrical noise which would have made data collection and interpretation more difficult. The cell in which the IGEFET was placed was manufactured from stainless steel. The lid which was fitted in place over the IGEFET was sealed to the body of the test cell with a metal-filled gasket to minimize electrical noise. In addition, the panel containing the connectors was manufactured from aluminum, and its seams were covered with metallic tape. Third, the test cell provided a means for introducing gases to challenge the IGEFET configured as a gas sensor. Finally, the test cell provided the means for establishing the internal temperature

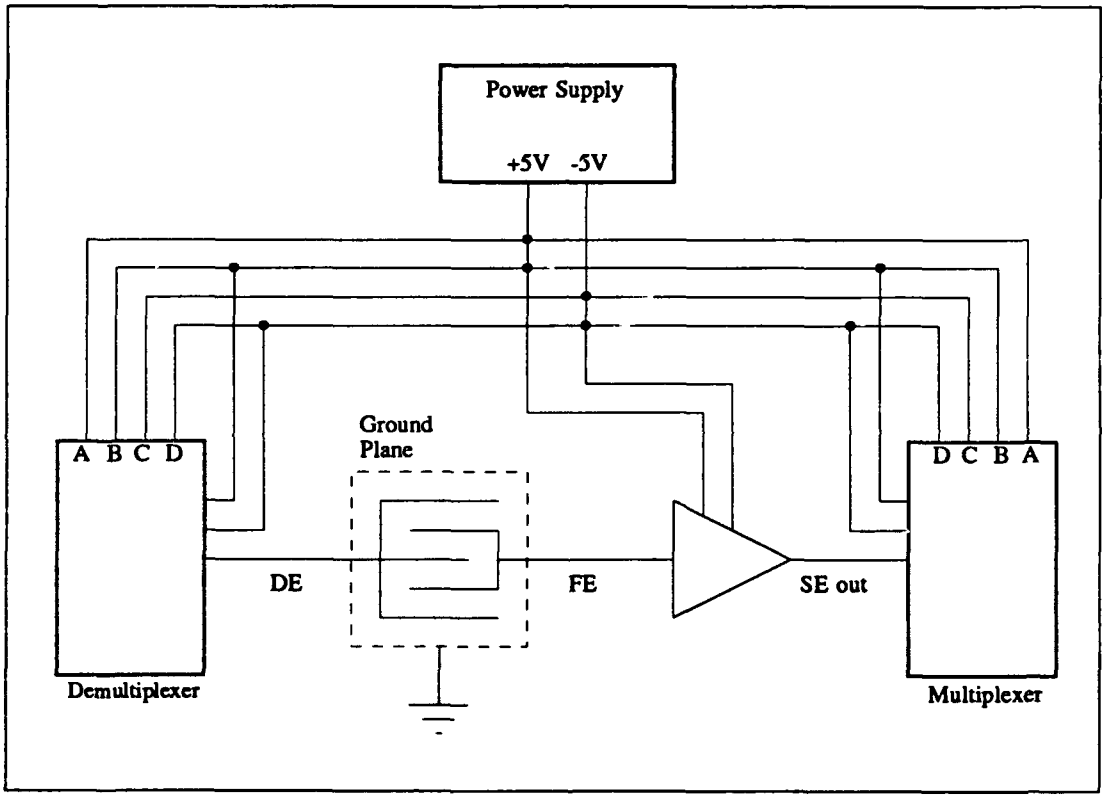

Figure 4.14. Power supply arrangement used for the IGEFET performance data collection.

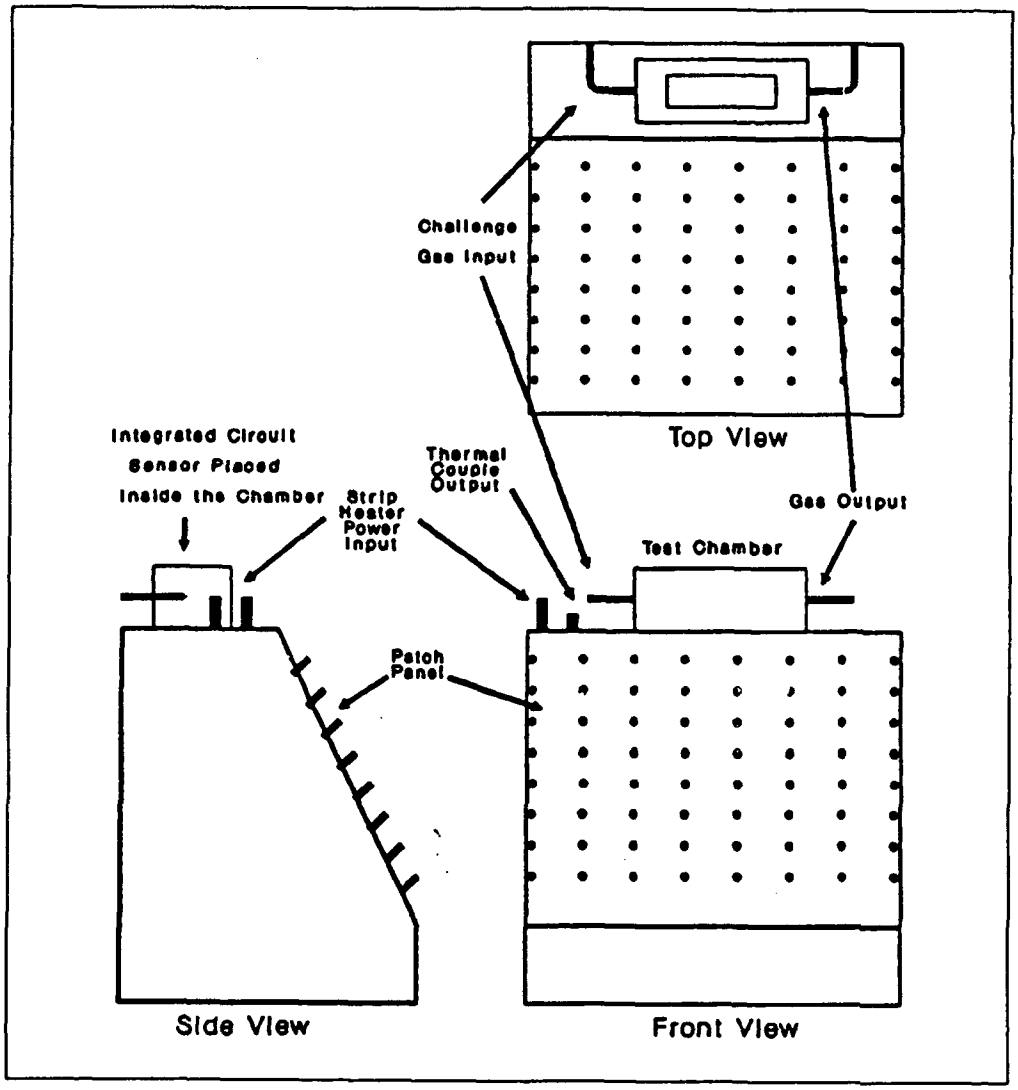

Figure 4.15. Diagram of the IGEFET test cell (39:9).

of the test environment. The cell contained a thermocouple (Omega Engineering, Inc., model SA1-K, Stanford, CT) and a kapton heater strip (Watlow, model KC05020C5, St. Louis, MO), which were attached to the top of the zero insertion-force socket. The IGEFET was then placed in the socket in direct contact with these devices.

During the resin cure experiments, it was necessary to strictly control the humidity in the test cell. Humidity is a factor which can significantly affect the mechanical properties of resins (40). The humidity level was controlled by providing a constant flow of nitrogen through the test cell. The flow was provided by a gas generation and delivery system which was developed by Kolesar (41). The system was used to regulate the flow of nitrogen into the test cell at approximately 250 ml/min. This flow kept the humidity level in the test cell below 5 percent during all experiments. The humidity level was monitored by a hygrometer (Thunder Scientific Corp., model HS-1CHDT-2A, Albuquerque, NM).

Electrical Performance Instrumentation Configurations. The following sections detail the IGEFET electrical performance measurement test equipment configurations.

Direct Current Resistance Measurements. The dc resistance of the IGE structure was measured using an electrometer (Keithly Instruments, Inc., Model 617, Cleveland, OH). The equipment was arranged as illustrated in Figure 4.16. The electrometer was operated in a (V/I)-mode to minimize the effects of leakage resistance and distributed capacitance. This mode of operation also facilitates the measurement of resistances on the order of 10^{16} ohms (42). The dc resistance was measured and recorded with respect to applied bias and time. No power was applied to the IGEFET electronics during these measurements. To measure the dc resistance with respect to the applied bias, the voltage source of the electrometer was increased in 1-volt increments over the interval of 2 volts to 10 volts. Measurements of dc resistance with respect to time were accomplished by recording the resistance of the IGE structure with a 2-volt applied bias, and referencing the measurement to the elapsed time relative to the resin's cure cycle. Prior

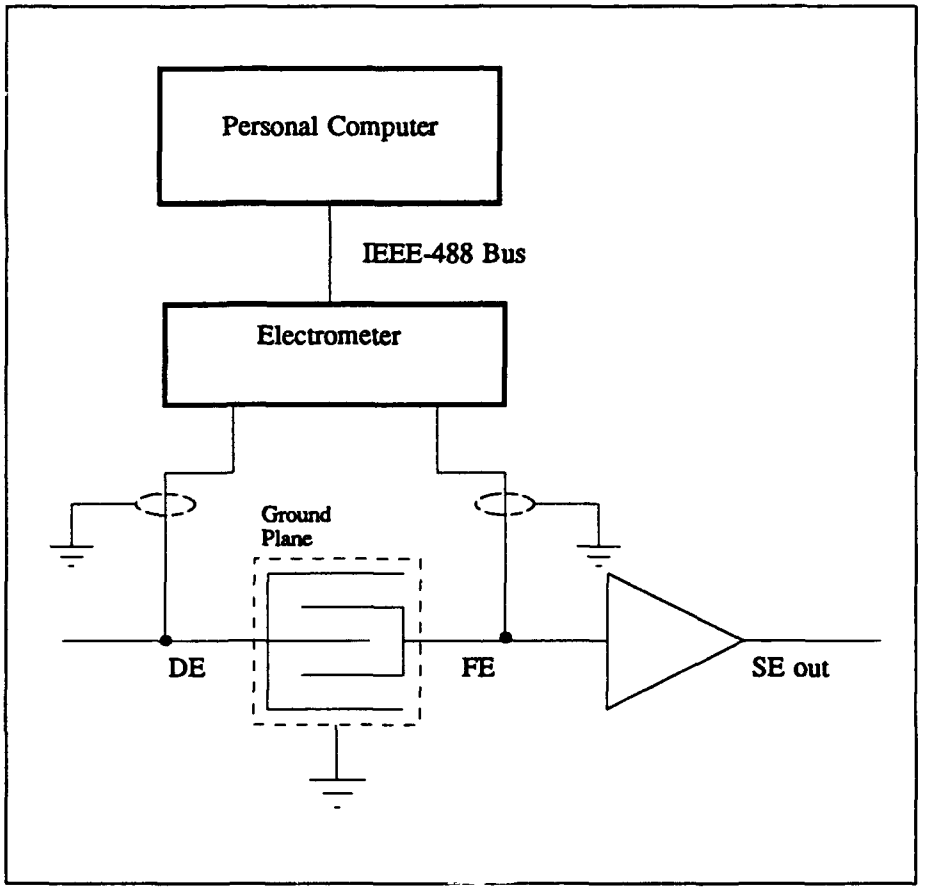

Figure 4.16. IGEFET direct current (dc) resistance instrumentation configuration.

to the application of the resin to the IGE structure and the start of the experiment, the electrometer was calibrated.

Alternating Current Impedance Measurements. The ac impedance measurements of the IGE structure were obtained with an impedance/gain-phase analyzer (Hewlett Packard, model HP4194A, Palo Alto, CA). The analyzer uses a four-wire measurement technique, and it was configured as illustrated in Figure 4.17. Impedance magnitude and phase were collected. These

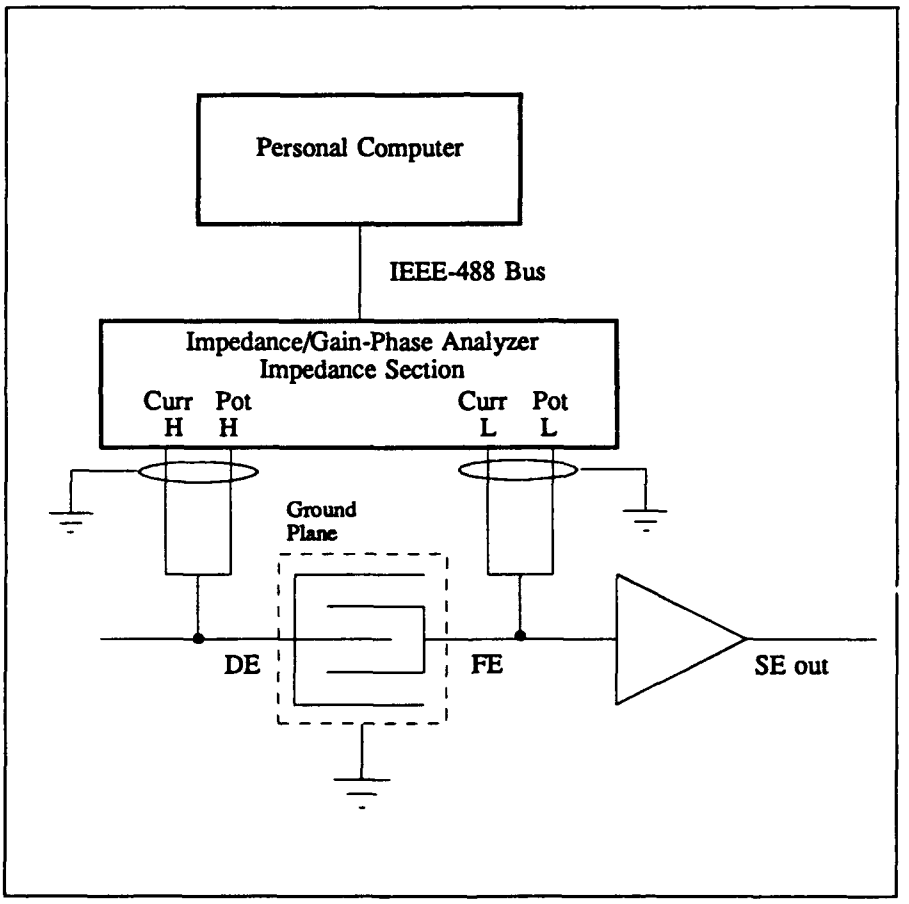

Figure 4.17. IGEFET impedance instrumentation configuration.

measurements were made with a 2-volt dc bias applied across the IGE structure. The real part and imaginary part of the impedance were derived from the magnitude and phase information in a subsequent data reduction exercise. The equations used to derive the real and imaginary

components of the impedance ($Re(Z)$ and $Im(Z)$, respectively) were:

$$Re(Z) = \mid Z \mid \cos\phi, \tag{4.1}$$

and,

$$Im(Z) = \mid Z \mid \sin\phi, \tag{4.2}$$

where $\mid Z \mid$ is the impedance magnitude, and ϕ is the impedance phase. Measurements were accomplished with respect to frequency, which was varied from 100 Hz to 100 KHz. Prior to the start of each impedance experiment, a short-circuit calibration was performed by inserting a jumper wire across the zero insertion-force socket pins corresponding the DE and the FE of the IGE structure. An open-circuit calibration was also performed.

Gain-Phase Measurements. The gain and phase delay of the IGE structure and the IGEFET were also measured with the impedance/gain-phase analyzer (Hewlett Packard, model HP4194A, Palo Alto, CA). The test equipment configuration is depicted in Figure 4.18. Since the electrical characteristics of the resin varied considerably over the course of its cure, it was necessary to manually vary the magnitude of the input signal. A correctly adjusted signal level would provide a favorable signal-to-noise ratio without overloading the analyzer's input. At the beginning of cure, the magnitude of the analyzer's oscillator signal was set at 0.01 volts, and it was gradually increased during successive measurements to a final value of 1 volt. The voltage gain ($20\log_{10}[V_{out}/V_{in}]$) and phase delay ($\phi_{out} - \phi_{in}$) were measured over a frequency range of 10 Hz to 1 KHz. The analyzer was calibrated at the start of each measurement cycle.

Time-Domain Response Measurements. The time-domain response of the IGEFET to a voltage pulse excitation was measured utilizing the configuration illustrated in Figure 4.19. The measurements were made by applying the voltage pulse to the driven-electrode of the IGE structure using a function generator (Wave-Tek Corp., model 148, San Diego, CA) and recording

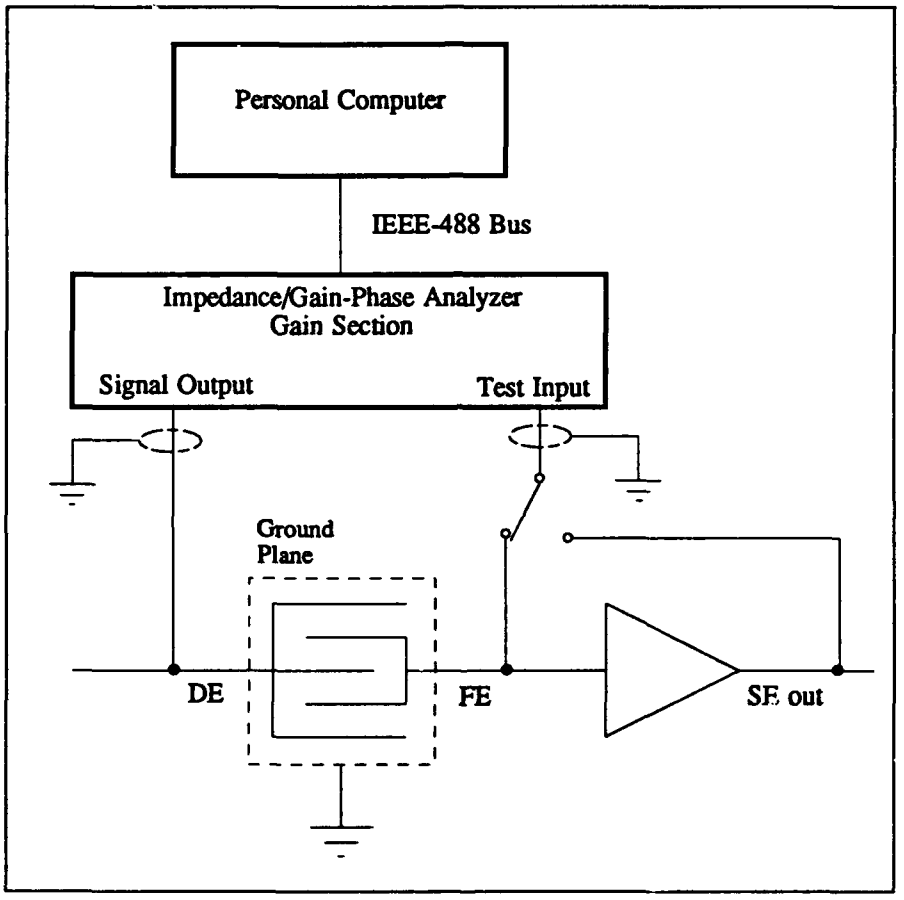

Figure 4.18. IGEFET gain-phase instrumentation configuration. The switch depicted on the test input of the impedance/gain-phase analyzer was not used; it serves only to illustrate the interconnections made for the IGE structure and the IGEFET experiments.

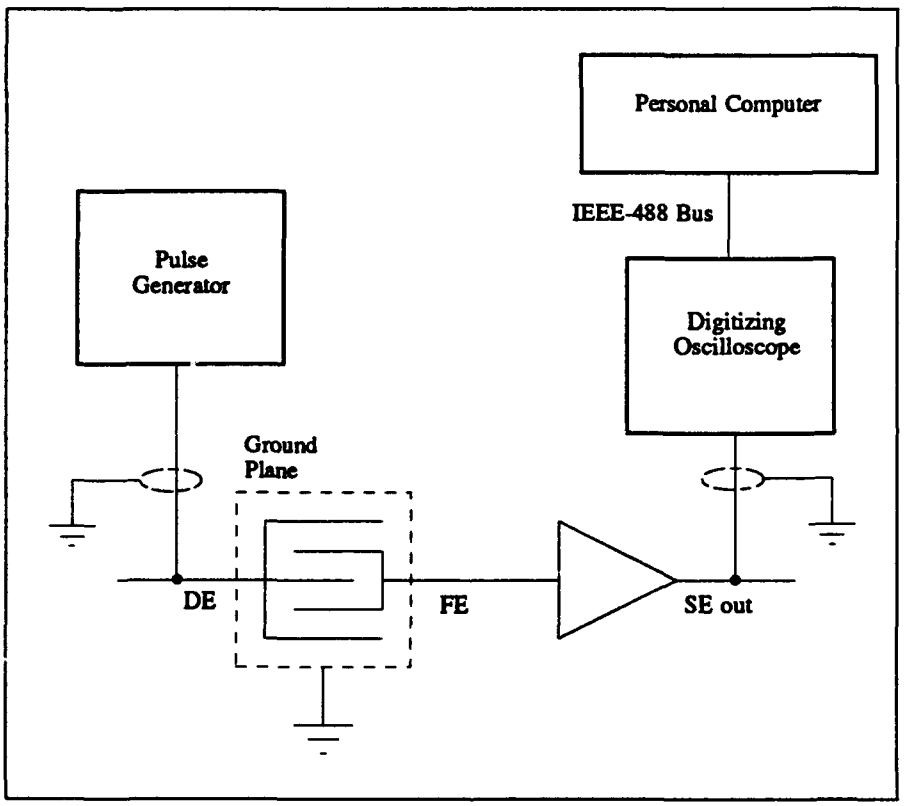

Figure 4.19. IGEFET time-domain response instrumentation configuration.

the output signal with a digital storage oscilloscope (Hewlett-Packard Corp., model HP54501A, Palo Alto, CA).

The time-domain response of a resin contains a great deal of information. After applying the voltage pulse, the nearly instantaneous current transient observed can be attributed to the atomic and electronic polarization mechanisms. Thereafter, a decaying current component manifests itself due to the orientational polarization mechanism. Since some degree of electrical conduction is always present in a resin, the time-domain response also contains a constant current component. The frequency components which correspond to the contribution of these different mechanisms may be extracted using the frequency-domain analysis technique that is described in the next sub-section.

Frequency-Domain Response Measurements. The frequency-domain response of the IGEFET to a voltage pulse applied to the driven-electrode of the IGE structure using a function generator (Wave-Tek Corp., model 148, San Diego, CA) was measured. Because the spectrum analyzer (Hewlett Packard, model HP4195A, Palo Alto, CA) required a 50 ohm input, it was necessary to send the output of the IGEFET to a low-noise amplifier (Stanford Research Systems, model SR560, Sunnyvale, CA). The equipment configuration is illustrated in Figure 4.20. The amplifier provided unity gain over a bandwidth much greater than that provided by the IGEFET, and it provided a 50 ohm output. The output of the low-noise amplifier was passed to the input of the spectrum analyzer. The spectral response of the IGEFET was measured over a frequency span of 10 Hz to 100 KHz.

After the frequency-domain data was collected, the normalized difference Fourier transform spectra were generated. The voltage pulse excitation signal was amplified by the reference element, and its response was stored. This response data was normalized with respect to the largest harmonic component contained in the spectrum. The spectral response of the IGEFET, measured during the resin cure experiments, was normalized with respect to the same harmonic

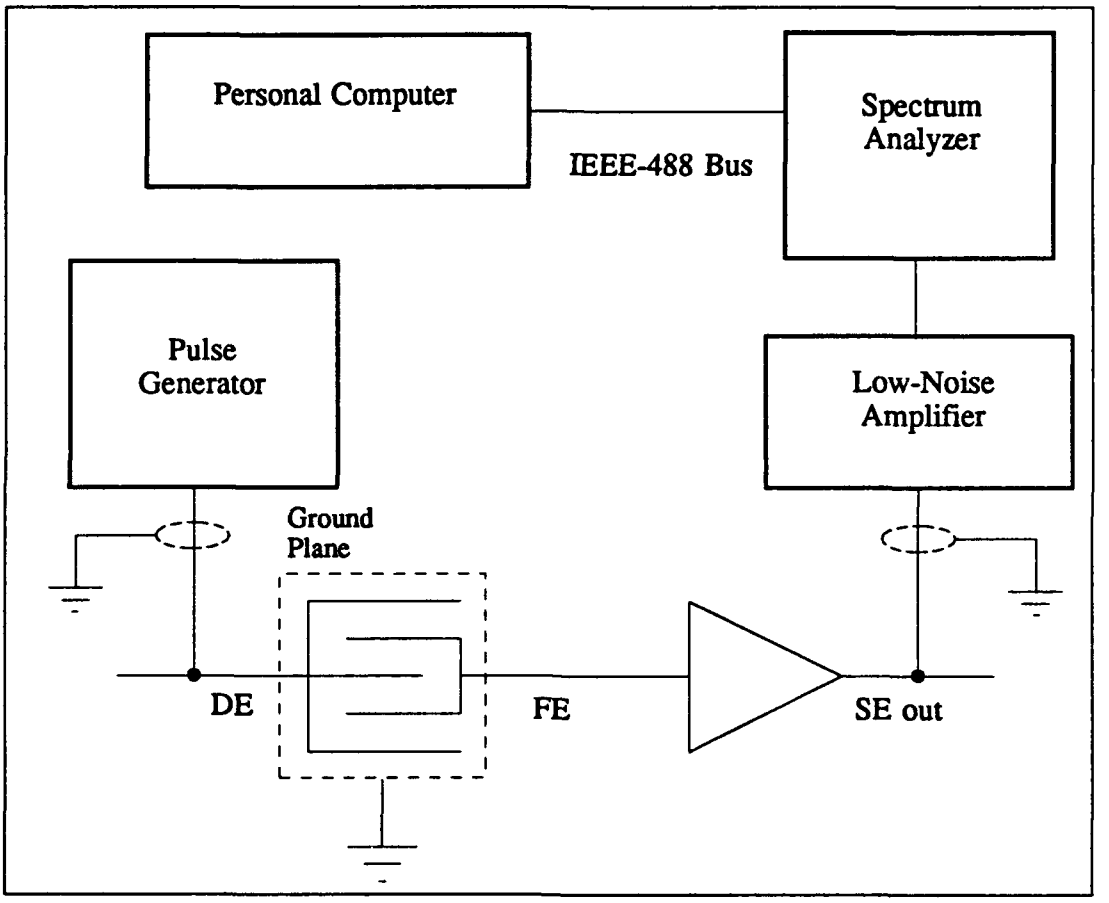

Figure 4.20. IGEFET frequency-domain response instrumentation configuration.

identified from the spectrum of the voltage pulse excitation. The normalized difference Fourier transform spectrum was then calculated by subtracting the normalized IGEFET response from the normalized reference element response, and taking the absolute value of the difference. Consequently, this spectrum provides information regarding the dissipation of energy in the IGE-resin system with respect to the voltage pulse excitation signal.

Experimental Methodology

As discussed in Chapter 1, the IGE structure and IGEFET electrical measurements were performed at two different cure temperatures. These two cure temperatures were determined empirically. The total experimental effort was not simply the collection of electrical performance measurements. That is, prior to conducting the electrical tests, it was necessary to evaluate the mechanical properties of the resin to determine the most advantageous resin cure temperatures. Consequently, this section is divided into two sub-sections; the first will discuss the experimental methodology used during the collection of the mechanical data, and the second is concerned with the evaluation of the IGEFET sensor.

Mechanical Test Procedures. As previously mentioned, prior to the evaluation of the IGEFET sensor as a resin cure monitor, it was necessary to determine the most advantageous resin cure temperatures. From a purely experimental perspective, the temperatures were selected based upon three criteria. First, the temperatures could not be so large as to damage the test cell. Based on the maximum temperature that the zero insertion-force socket could withstand, it was determined that the maximum allowable resin cure temperature was approximately 100°C. Second, the temperatures needed to be sufficiently low to provide a useful amount of data. An excessively high cure temperature would cause the resin to cure too quickly, and this situation would compromise the collection of a useful data. Third, the temperatures needed to be sufficiently large to prevent inordinately long cure times.

The optimum cure temperatures were determined using a dynamic spectrometer (Rheometrics Inc., model RDS-11, Possumtown, Piscataway, NJ). The dynamic spectrometer applies an oscillatory, sinusoidal motion to a sample of resin placed between a pair of parallel plates that are 1.25 inches in diameter. The force is applied directly to the lower plate, and it is transmitted through the resin to the upper plate. A sensor attached to the upper plate measures the amount of force transmitted through the resin.

A sample of the Epoxy 907 resin was prepared according to the vendor's instructions included with the resin: equal amounts of components A and B were applied to a clean, disposable surface (a piece of paper), and they were mixed together for at least three minutes with a wooden tongue depressor. A sufficient amount of the resin (approximately 2 mm thick) was applied to provide a uniform layer between the two plates. The plates were then transferred to an oven under a nitrogen atmosphere to reduce the level of humidity. The oven was then programmed to follow a ramped temperature profile, from room temperature to approximately 130°C, at a rate of 2°C per minute. During the cure of the resin, the lower plate was oscillated at a rate of 10 rad/s. The resultant data, complex viscosity (η^*) versus temperature, was analyzed to determine the optimum range of cure temperatures for the resin. Two of these temperatures were selected based upon the three criteria discussed above.

After the resin cure temperatures to be used during the IGEFET sensor evaluation were selected, it was necessary to determine the gelation time of the resin at each of these temperatures. The dynamic spectrometer was again used, and the procedure was similar to that described above, with the exception that the temperature was programmed to follow an isothermal profile rather than a ramped profile. One isothermal evaluation was performed for each temperature used during the IGEFET sensor evaluation. The data collected was the storage modulus (G') and the loss modulus (G''). The storage modulus and loss modulus correspond to the real part and the imaginary part, respectively, of the resin's complex viscosity. This

information was plotted with respect to time, and the point at which $G' = G''$ was located. This point corresponds to the gelation time of the resin (13).

It is noted here that oscillating the sample at frequencies other than 10 rad/s would result in different interpretations of the gelation time, since the amount of force transmitted through the sample depends upon the rate at which the sample is oscillated. It has been determined empirically, however, that the frequency which provides the best agreement with the actual gelation time is 10 rad/s (13).

A third mechanical test was used to determine the glass transition temperature of the resin. Again, the dynamic spectrometer was used. This time, however, the spectrometer was configured to perform a torsional bar analysis (TBA) of samples cured at each of the two temperatures of interest. Small bars of the resin were made by preparing samples of the resin and placing them in molds made from RTV silicone (General Electric Co., Silicone Products Division, product code RTV664, Waterford, NY). The samples were then cured at the temperatures of interest. The bars were approximately 3 mm high, 13 mm wide, and 42 mm long.

To conduct the TBA, a pair of clamps were substituted for the plates used in the parallel plate tests, and a resin bar was secured with the clamps (a clamp held each end of the bar). The clamps and bar were then enclosed in an oven under a nitrogen atmosphere to reduce the humidity. A 10 rad/s oscillatory motion was applied to the bar, and the oven was thermostatted to the temperature of interest. The storage modulus, loss modulus and the mechanical loss tangent ($\tan \delta_m = G''/G'$) were collected and plotted versus time.

IGEFET Test Procedures. The purpose of this sub-section is to detail the procedures used to collect the IGEFET electrical performance data. In general, the process included preparation of the sensor for the application of the resin, testing each sensor element for correct operation, application of the resin, and collection of the data. These steps are detailed in the following sub-sections.

Preparation of the IGEFET Sensor. As mentioned earlier, several glass cuts were provided in the IGEFET integrated circuit to facilitate excision of inoperative circuits and to permit troubleshooting the sub-circuits. In particular, a glass cut was provided in a location adjacent to each sensor SE amplifier which exposed the metal lines corresponding to the SE's floating-electrode output and SE output, as illustrated in Figure 4.21. The glass cut was

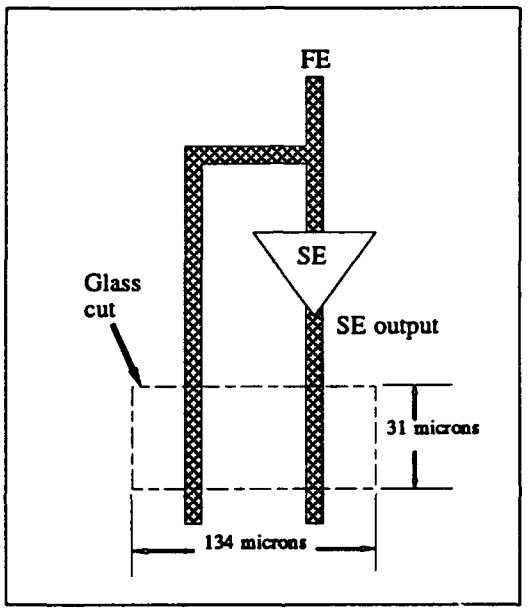

Figure 4.21. Location and size of the glass cut which exposed the floating-electrode and the sensor element output lines.

approximately 31 μm x 134 μm. It was discovered after the first attempt to apply resin to the sensor that the relatively low resistance of the uncured resin provided a short circuit across these signal lines. It became necessary to cover the glass cuts in these locations with a non-conductive wax used in semiconductor processing (Associated Electrical Industries, Limited, Apiezon wax, England). This wax provided adequate insulation for the exposed signal lines. The wax was applied by first shaving a very small amount of it onto a glass microscope slide. The IGEFET sensor was then placed under a microscope equipped with a microprobe station (The Micromanipulator Co., model 6200, Carson City, NV). With the aid of the microscope and

probes, a shard of the wax was manipulated into position above each glass cut adjacent to a sensor element. After each glass cut was covered by one or more pieces of wax, the integrated circuit was placed in a piece of aluminum foil such that all the pins on the circuit protruded through the foil. The integrated circuit was then placed in an oven (Lab-Line Instruments, Inc., model Imperial IV, Melrose Park, IL), and the temperature was thermostatted to approximately 85°C to melt the wax over the glass cut.

Sensor Element Testing. Following the preparation of the integrated circuit for the application of the resin, each SE on the integrated circuit was evaluated for proper operation. This process involved visual and electrical inspection of the IGE structures and electrical testing of each SE amplifier.

The IGE structures were visually inspected under the microscope of a microprobe station. Obvious defects in an IGE structure, such as scratches, disqualified the associated SE from further test and evaluation.

Following the visual inspection, the IGE structures were electrically evaluated using the gain-phase mode of the impedance/gain-phase analyzer. The FE and DE of each structure were expected to be isolated from each other by at least 30 dB relative to the frequency range which spanned 10 Hz to 1 MHz.

The SE amplifiers on the integrated circuit were then electrically inspected. They were expected to provide at least 17 dB of gain with a 3-dB cutoff frequency of at least 80 KHz.

Data Collection. The IGEFET performance evaluation process consisted of fourteen experiments. Each of these experiments required a sample of resin to be deposited on the surface of an IGE structure. While the resin sample cured, a single category of electrical measurement was performed continuously. There were seven types of electrical measurements to be performed, as discussed earlier in this chapter. In addition, the resin cure was evaluated at two different cure

temperatures. Thus, the seven categories of electrical measurements, each performed for two different cure temperatures, constituted the fourteen experiments. The goal of the IGEFET performance evaluation was to locate the gelation point of the resin by analyzing the IGEFET performance data. The performance evaluation was conducted as described below.

First, the IGEFET integrated circuit was secured in the test cell, and the temperature was thermostatted at the desired temperature for the duration of the experiment. The lid was closed and secured, and a 250 ml/min flow of nitrogen was introduced into the test cell. The humidity was then monitored continuously. The humidity level inside the test cell never increased above 5 percent.

After the temperature in the test cell stabilized at the desired level, and prior to the application of the resin, a baseline set of measurements were collected. Prior to the impedance evaluation, the impedance magnitude and phase of the uncoated IGE structure were measured with respect to frequency. Prior to the gain-phase delay evaluation, the gain information was recorded for the uncoated IGE structure, the sensor element, and the reference element. Finally, before the spectral analysis evaluation, the spectral response of the reference element was measured with respect to frequency.

The resin was then mixed according to the vendor's instructions. Equal amounts of components A and B of the resin were extracted from their containers and transferred to a clean piece of paper. They were then mixed for at least three minutes. The lid was removed from the test cell, and a small amount of the resin (enough to completely cover only one IGE structure) was applied with the end of a short piece of 18-gauge insulated electrical wire. The test cell lid was then replaced and secured.

The experimental measurements were initiated immediately after the test cell lid was secured. The measurements were accomplished continuously over a period of time estimated to be

double that of the resin sample's gelation time. The time periods were limited in this manner because the electrical characteristics of the resin changed very little beyond the gelation point.

Summary

The details of the IGEFET design effort, the performance data collection configuration, and experimental methodology were presented in this chapter. The IGEFET design effort was an exercise in combining several features from previously successful designs while incorporating a limited number of changes. An outline of the changes, and the details of the final IGEFET design were discussed. A comprehensive description of the performance data collection configuration was developed in the next section. Finally, the experimental procedures for the collection of the mechanical and electrical performance data were described.

V. Results and Discussion

Introduction

This chapter contains the results of the IGEFET sensor fabrication, the mechanical characterization of the resin, and the resin cure experiments. Each of these phases of the experimental process is discussed in a separate section. The first section presents the electrical characteristics of the IGEFET sensor as received from MOSIS. The second section discusses the results of the mechanical characterization of the resin used in this research. Finally, the third section discusses the results of each of the electrical measurements performed during the resin cure experiments.

Electrical Characteristics of the IGEFET Sensor

A visual and electrical inspection of the IGEFET sensor was performed immediately upon receipt of the integrated circuits from MOSIS. The visual inspection was intended to identify any obvious defects in the sensor. Of particular importance was the condition of the IGE structure. Scratches on the surface of the structure could result in a short circuit between the DE and FE, or they could cause large portions of the electrodes to be electrically isolated from the IGE structure. In general, the condition of the IGE structures was acceptable, although occasional scratches, possibly caused by the wire bonding and packaging processes, were observed.

In order to operate the IGEFET sensor's electronic sub-circuits, values for V_{DD}, V_{SS}, V_{BIAS}, and V_{offset} had to be established. These values were determined empirically. It was assumed that V_{DD} would be in the vicinity of 5 volts, and that V_{SS} and V_{BIAS} would be in the vicinity of -5 volts. In order to simplify the power supply requirements, it was desirable to use the same positive and negative voltage levels throughout the sub-circuits. The values for V_{DD}, V_{SS}, and V_{BIAS} were experimentally determined by adjusting their values to maximize the gain of the SE amplifier. It was determined that using a value of 5 volts for V_{DD}, and -5 volts for V_{SS} and

V_{BIAS}, provided acceptable gain. These values were also convenient because the power supply bias levels used for the multiplexer and the demultiplexer were 5 volts and -5 volts, as well (4:4-21). A plot of the gain and phase delay of the SE amplifier is provided in Figure 5.1. Several

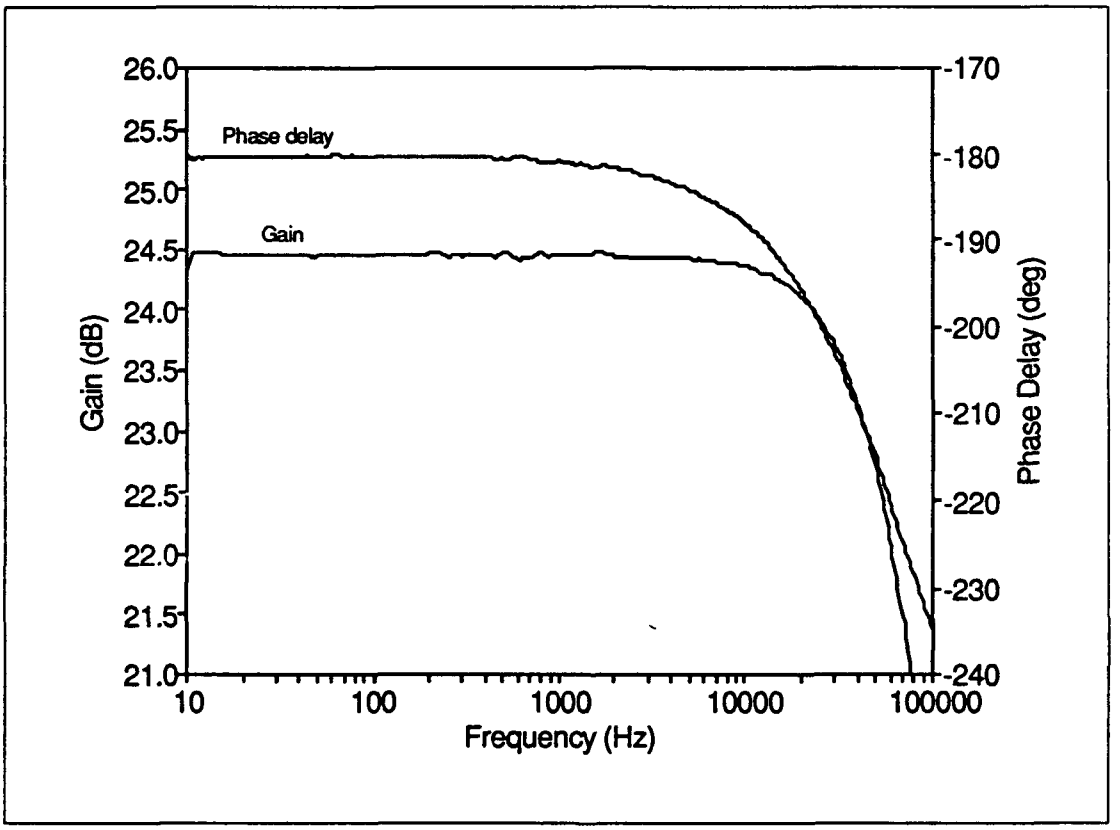

Figure 5.1. Gain and phase delay of the sensor element amplifier at room temperature.

devices were tested, and the SE amplifiers typically provided an average gain of 20 dB with a 3-dB cutoff frequency of approximately 85 KHz.

After evaluating several devices the supply voltages for the operational amplifier were determined to be: $V_{DD} = 5$ volts, $V_{SS} = -5$ volts, $V_{BIAS} = -5$ volts, and $V_{offset} = -5$ volts. Since all of the offset voltages for the five stages were tied together, it was not possible to separately optimize each stage. Hence, the first stage was optimized at the expense of the last

four. The first stage of the operational amplifier provided an average gain of 20 dB with a 3-dB cutoff frequency of 850 KHz.

The voltage-follower circuits did not operate as expected. With the supply voltages configured as described, the gain of the sub-circuit (measured with respect to a signal placed on the FE of the sensor element) was typically on the order of -6 dB. By increasing the supply voltages to 5.5 volts and -5.5 volts, the gain could be increased to approximately 10 dB. This was considered unacceptable. Since the SE amplifiers each had their own output, which could be accessed via the multiplexer, the failure of the voltage-follower circuits to operate acceptably was not considered to be a critical defect.

Once the voltage bias levels necessary to operate the sub-circuits were determined, the IGEFET sensors were evaluated for proper operation. The electrical performance evaluation of the IGEFET sensors was performed in three stages:

1. The electrical isolation of the DE and FE were measured using the gain-phase/impedance analyzer (Hewlett-Packard, model HP4194A, Palo Alto, CA). A minimum isolation of 30 dB was expected.
2. Each SE amplifier was tested, and they were expected to provide an average gain of 20 dB with a 3-dB cutoff frequency of approximately 85 KHz.
3. The operation of the multiplexer was evaluated as follows:

   (a) Upon application of appropriate line select logic values to the multiplexer's decoder, it was required to pass a test signal through the appropriate multiplexer switch. The voltages corresponding to binary logic levels "1" and "0" were 5 volts and -5 volts, respectively. The sensor elements were numbered "0"-to-"9", which corresponded to logic values of "0000"-to-"1001" in binary notation. The test signal was provided by the gain phase/impedance analyzer. The devices were expected to pass the test signal

with a gain of unity. The measured gain for a selected signal was typically slightly negative (on the order of -10 mdB).

(b) Upon application of the appropriate line select logic values to the multiplexer, it was required to block a test signal applied to the unselected lines. Each unselected line was expected to provide a minimum isolation of 30 dB (4:5-3).

4. The operation of the demultiplexer was evaluated using a procedure identical to that described for the multiplexer.

5. The operational amplifier was evaluated, and it was expected to provide an average gain of 20 dB with a 3-dB cutoff frequency of approximately 850 KHz.

During the evaluation of the multiplexer circuits, it was discovered that coupling was occurring between specific IGEFET sensor element outputs. When SE_6 was selected and connected to a test signal, SE_3 provided less than 10 dB of attenuation. Similarly, when SE_2 was selected, SE_1 was not acceptably attenuated. Signals on the lines corresponding to SE_4 and SE_5 exhibited the same problem. This coupling was uni-directional. For example, when SE_3 was selected, there was no coupling to SE_6. The demulitiplexers exhibited the same uni-directional coupling. While the cause of this problem could not be determined, the potential disadvantageous effects of the coupling were eliminated by grounding the FEs of the sensor elements not being interrogated.

Another problem with the multiplexers and demultiplexers was discovered during the IGEFET sensor evaluation experiments. The circuits were prone to fail after several hours of continuous use. The failure manifested itself as a short-circuit to ground. Visual examination of the IGEFET sensor circuits after failure revealed thermal discoloration on the V_{SS} supply to the multiplexer or demultiplexer, which is indicative of very high current levels. No other indications of failure could be discovered. The only resolution to this problem was to discontinue using the multiplexer and demultiplexer. However. this revised operating mode was not facilitated by

removing power from these circuits. That is, since the multiplexer utilized CMOS technology, maximum power was dissipated in the circuit only when the internal logic was switched. Therefore, the decoder logic was set to a constant value, arbitrarily determined to be "1111". Further, it was necessary to have the logic maintained at some known value to prevent inadvertent coupling of the SE output signals through the multiplexer circuit. Finally, this logic level condition also rendered the voltage follower and operational amplifier circuits unusable. In effect, each sensor element had to be manually switched, and the only amplification was provided by the SE amplifier. This technique virtually eliminated the failure mode described above. For this research effort, the gain provided by the SE amplifier (an average gain of 20 dB with a 3-dB cutoff frequency of approximately 85 KHz) was considered acceptable, since the signals utilized and monitored were primarily low frequency (less than 100 KHz).

Mechanical Characterization of the Resin

The purpose of this section is to discuss the results of the evaluation performed to determine the mechanical characteristics of the Epoxy 907 resin used in the subsequent resin cure experiments to evaluate the IGEFET sensor. Three tests were performed, and they will be discussed in separate sub-sections.

Parallel Plate Measurements with a Ramped Temperature Profile. Before any tests could be performed with the resin, the optimum range of cure temperatures needed to be established. This was accomplished by conducting parallel plate tests with a dynamic spectrometer, as described in Chapter 4. The resin was cured in the spectrometer with a ramped temperature profile. The optimum range of temperatures can be discerned by a decrease in the viscosity of the resin prior to gelation (43). The temperature in the oven was ramped from room temperature at a rate of 2°C per minute. The complex viscosity (η^*) was measured with respect to temperature. The results (illustrated in Figure 5.2) indicated that the optimum range of cure temperatures spanned

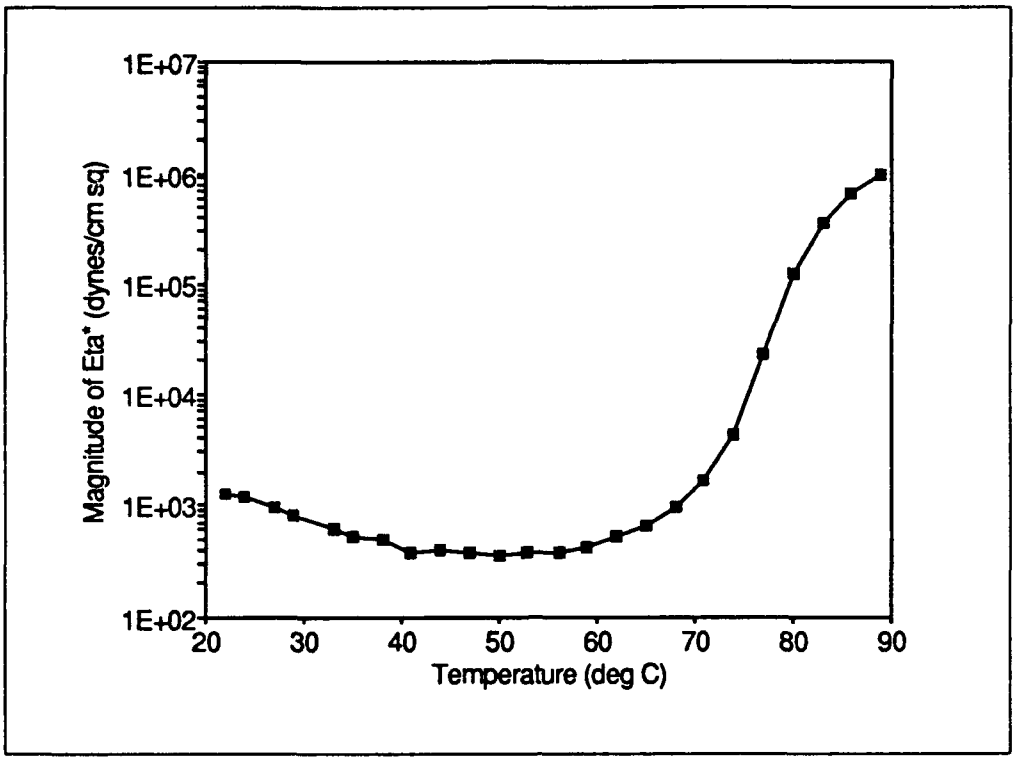

Figure 5.2. Magnitude of the complex viscosity of the resin (η^*) with respect to a ramped temperature profile ("Eta*" is η^*).

approximately 40°C to 60°C. The sudden increase in viscosity after 70°C is indicative of gelation. Based upon the results of this test, two temperatures (45°C and 55°C) were selected for the isothermal resin cure experiments using the IGEFET.

Parallel Plate Measurements with an Isothermal Temperature Profile. After the two cure temperatures (45°C and 55°C) were identified, the gelation times associated with each isothermal profile were determined. The dynamic spectrometer was used for this purpose, and the oven was set for a "ramp and hold" profile to approximate an isothermal cure profile. That is, the temperature in the oven was ramped quickly to the desired cure temperature, and that temperature was maintained for the duration of the test. The evaluation was performed for each of the selected temperatures. The results of the evaluations are illustrated in Figures 5.3 and 5.4. As mentioned in Chapter 4, the point of intersection of the storage modulus (G′) and the loss

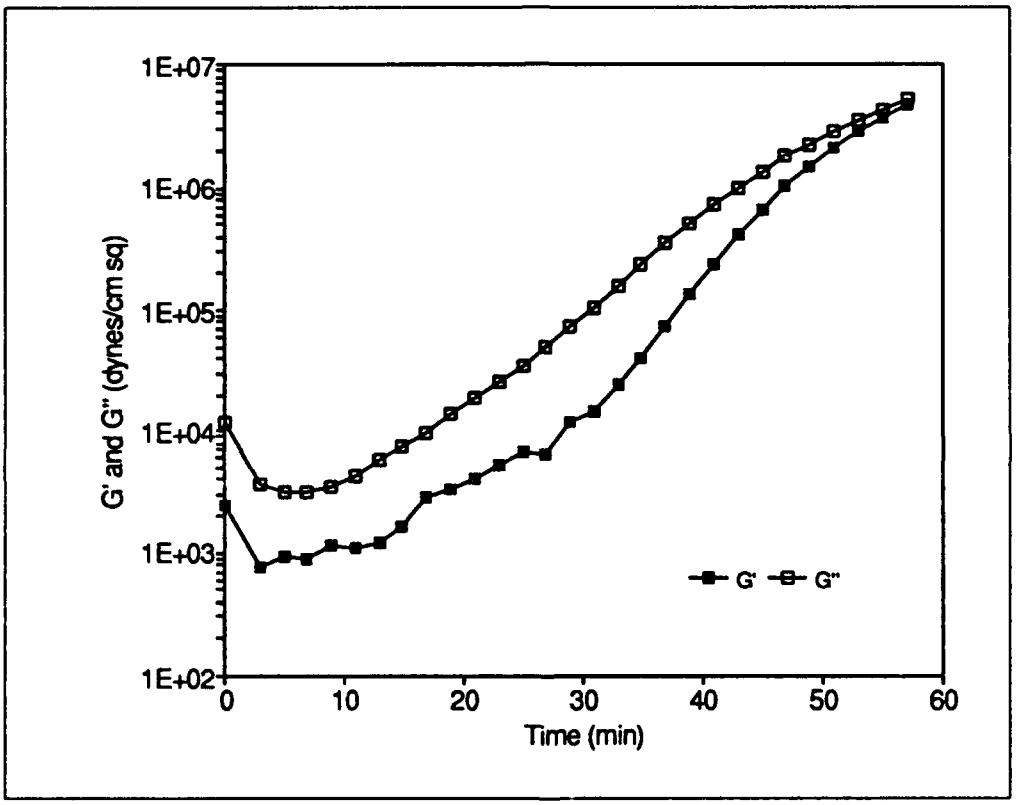

Figure 5.3. Parallel plate mechanical analysis of a resin sample for a 45°C isothermal temperature cure profile.

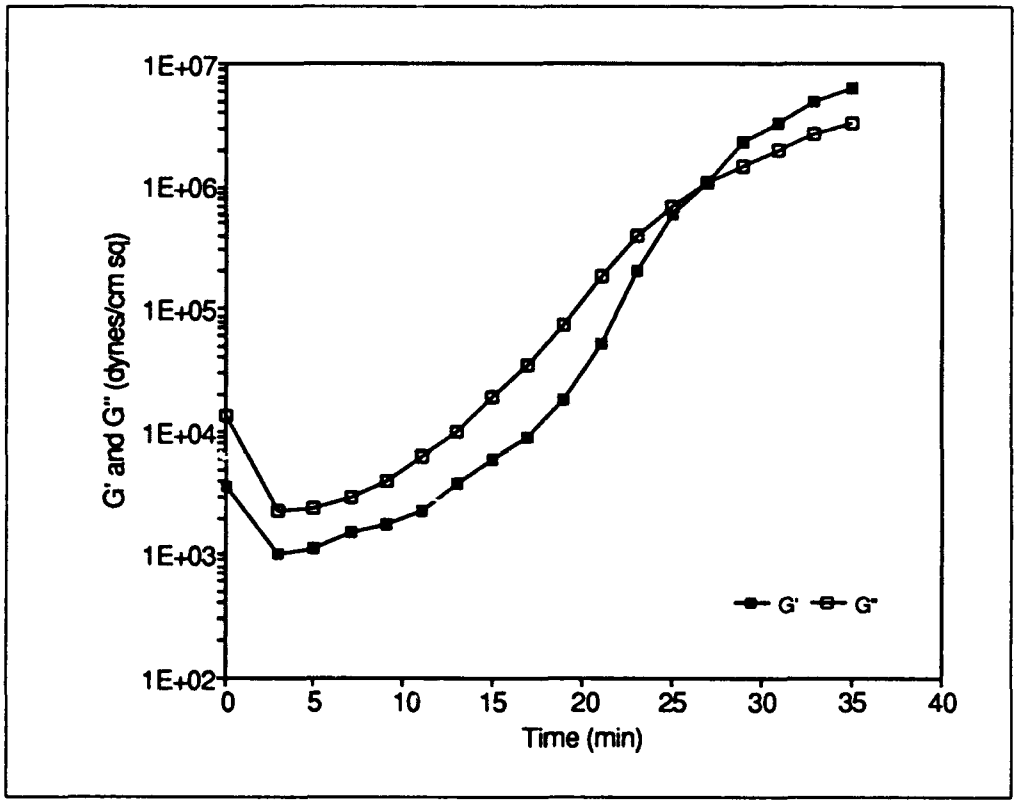

Figure 5.4. Parallel plate mechanical analysis of a resin sample for a 55°C isothermal temperature cure profile.

modulus (G″) can be used as an indicator of the resin's gelation point. From Figure 5.3, the point of intersection for the 45°C profile occurs at approximately 60 minutes. (The evaluation was terminated after 55 minutes because the capability of the equipment was exceeded at that point. However, it is apparent from Figure 5.3 that the point of intersection of the two curves would occur at approximately 60 minutes.) For the 55°C profile, the point of intersection occurred at approximately 26 minutes into the cure, as illustrated in Figure 5.4. The reduction in the viscosity (manifested by a corresponding reduction in G' and G'') for low cure times is typical of curing resin systems (43). The same viscosity reduction is apparent in Figure 5.2. The effect is exaggerated in Figures 5.3 and 5.4 because the temperatures used in these evaluations were ramped very quickly to the desired cure temperature. The temperature in Figure 5.2 was ramped at a relatively slow rate (2°C per minute), and the corresponding viscosity reduction was more gradual.

Torsional Bar Analysis of the Resin. Torsional bar analysis (TBA) was performed on resin samples which were previously cured at 45°C and 55°C. As outlined in Chapter 4, the purpose of TBA is to estimate the glass transition temperature of the material being tested. The results are depicted in Figures 5.5 and 5.6. The glass transition temperature is typically reported as the temperature which corresponds to the maximum value of the mechanical loss tangent ($\tan \delta_m$) (40:64). Analysis of the loss tangent curve in Figure 5.5 reveals that the glass transition temperature for the sample cured at 45°C is approximately 80°C, which is well above the sample's cure temperature. Analysis of the loss tangent curve for the sample cured at 55°C (Figure 5.6) reveals that the glass transition temperature for this resin is approximately 70°C, which is much closer to the sample's cure temperature.

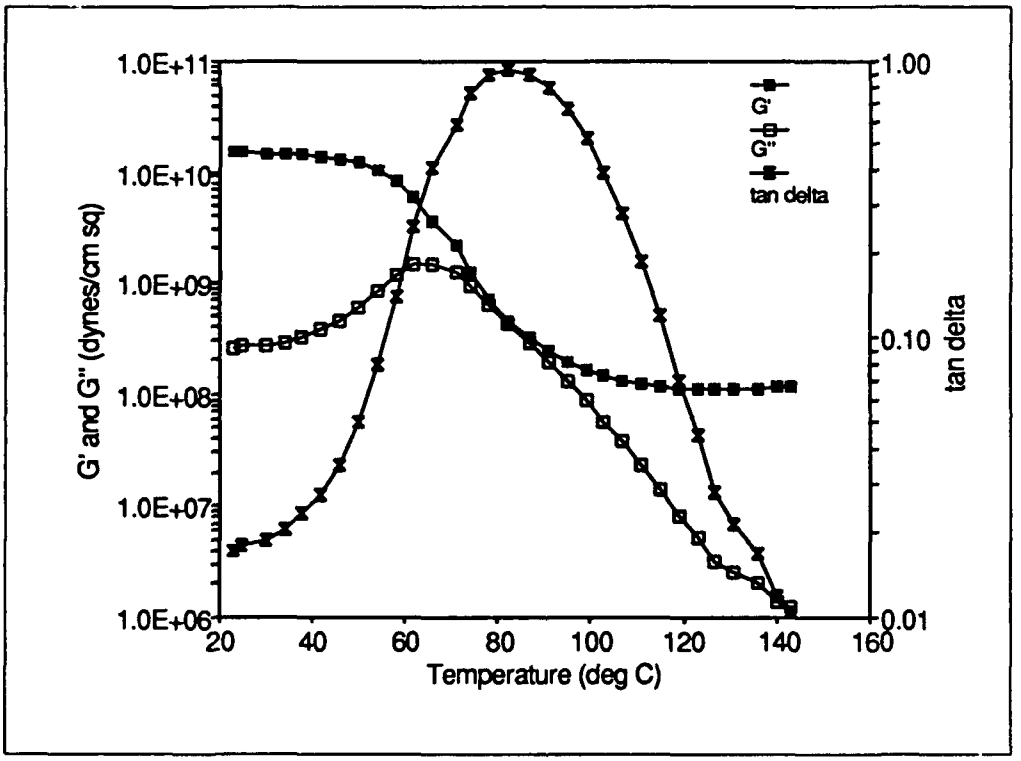

Figure 5.5. Torsional bar analysis for a resin sample cured at 45°C.

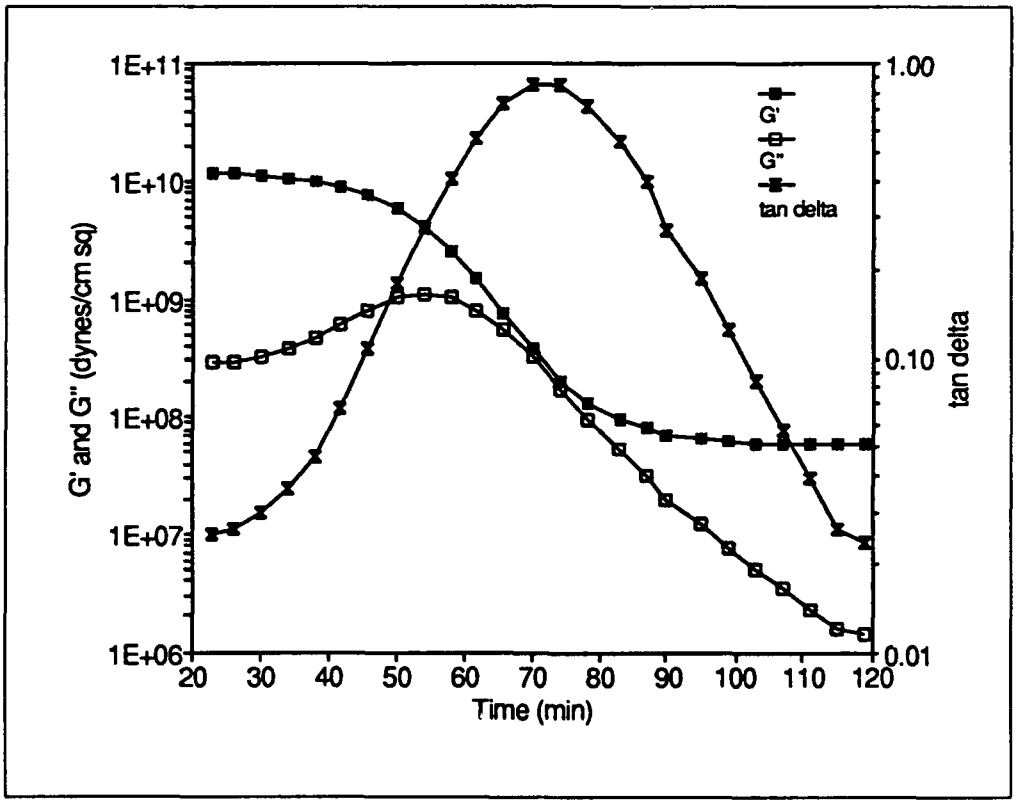

Figure 5.6. Torsional bar analysis for a resin sample cured at 55°C.

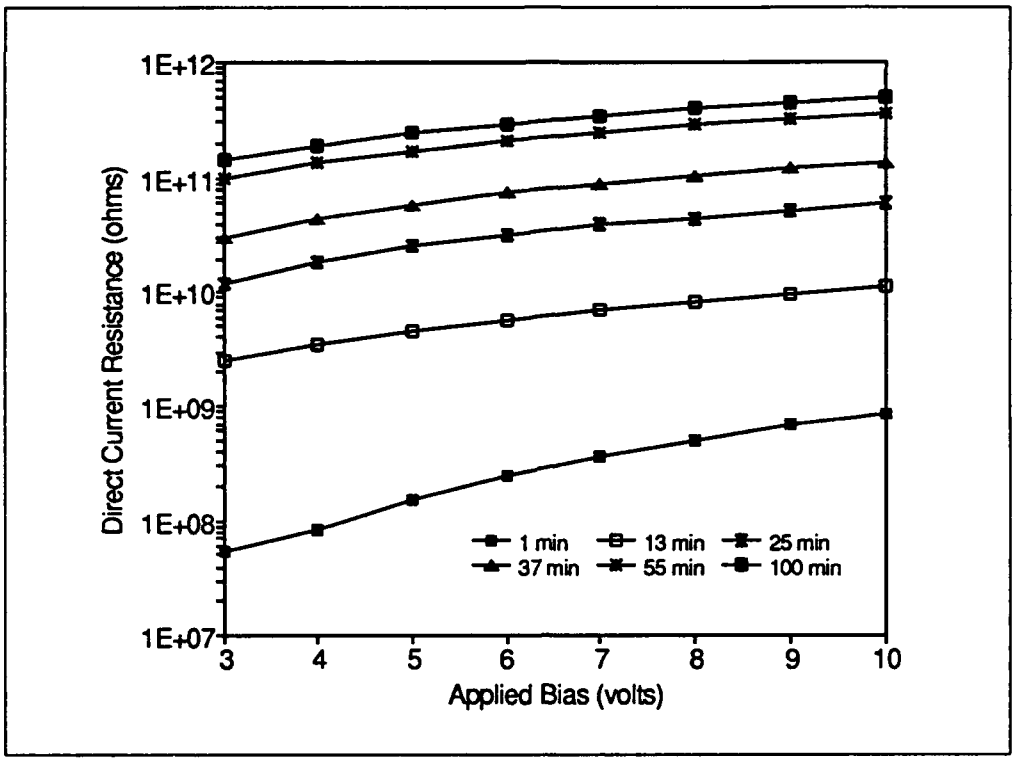

Figure 5.7. Direct current resistance measured with respect to applied bias for a 45°C resin cure.

Resin Cure Experiments

The IGEFET sensor was subjected to seven different electrical tests for each of the two resin cure profiles. This section presents and discusses the results of these tests. First, the direct current (dc) resistance measurements will be discussed. This will be followed by a discussion of the results associated with the impedance, transfer function, and finally, the time- and frequency-domain responses to a pulsed voltage excitation signal.

Direct Current Resistance of the Interdigitated Gate Electrode Structure. The dc resistance of the IGE structure was measured with respect to the applied bias and with respect to time. The results of these measurements conducted during the cure of a resin sample at 45°C are shown in Figures 5.7 and 5.8. The degree of change exhibited in the curves of Figure 5.7 is much greater during the initial portion of the cure, and it is reduced considerably after the 55 minute point.

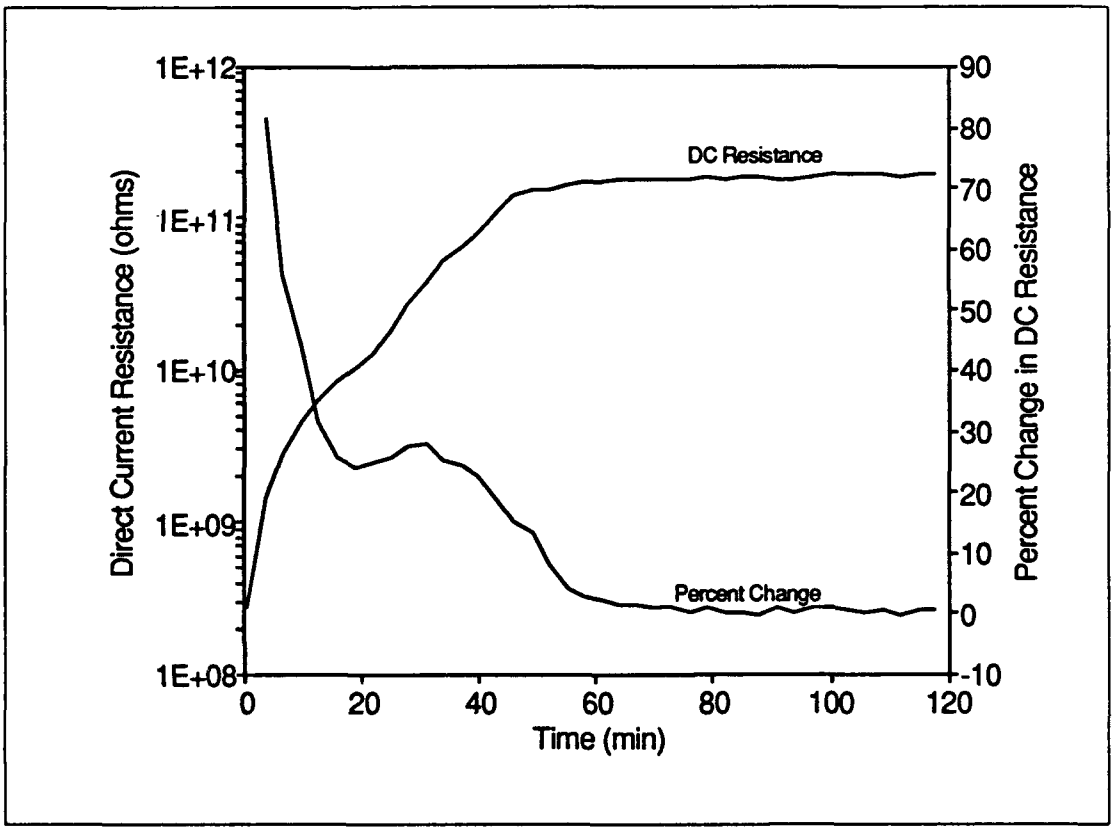

Figure 5.8. Direct current resistance measured with respect to time (2-volt applied bias) for a 45°C resin cure.

This reduction in the rate of change is more effectively depicted in Figure 5.7. That is, the dc resistance of the resin increases dramatically until approximately 55 minutes into the cure. At this point, the rate of change is suddenly reduced. This behavior may be explained in terms of the electrical conductivity mechanisms. DC resistance is a measure of the degree of loss in the material. In an uncured resin, these losses are due primarily to ion transport. These ions are present as unreacted components in the resin, or as byproducts of the resin's synthesis. As the cure reaction progresses, more free ions are consumed in the cross-linking reaction, or they are trapped in the cross-linked polymer, resulting in a conductance decrease, and hence, an increase in the material's dc resistance. The point at which the dc resistance rate of change suddenly decreases may be attributed to the onset of the resin's gelation. The dynamic mechanical tests discussed in the previous section provided an estimate of the gelation time for a 45°C cure of approximately 60 minutes.

The results of the dc resistance measurements for a sample cured at 55°C are given in Figures 5.9 and 5.10. The trend noted in Figures 5.7 and 5.8 for a 45°C cure are more difficult to see in Figures 5.9 and 5.10. In Figure 5.9, in particular, it is difficult to see the decrease in the rate of change of the dc resistance during the course of the cure. Figure 5.10 reveals that the dc resistance of the IGE structure for a 55°C cure did not increase above 2 MΩ. For the lower temperature cure, however, the dc resistance increased to a point in excess of 100 GΩ. This disparity between the results for the two cures is supported by other measurements, as well—most notably the transfer function measurements and the impedance measurements. The obvious conclusion is that there is a greater degree of electrical conduction in this sample compared to the sample cured at 45°C. This may be due to the proximity of the sample's temperature to the glass transition temperature. The temperature may be such that the material is not able to vitrify. If this is the case, the material would remain in the rubbery state indefinitely, and its electrical characteristics would not exhibit the same degree of change as observed with the lower cure temperature.

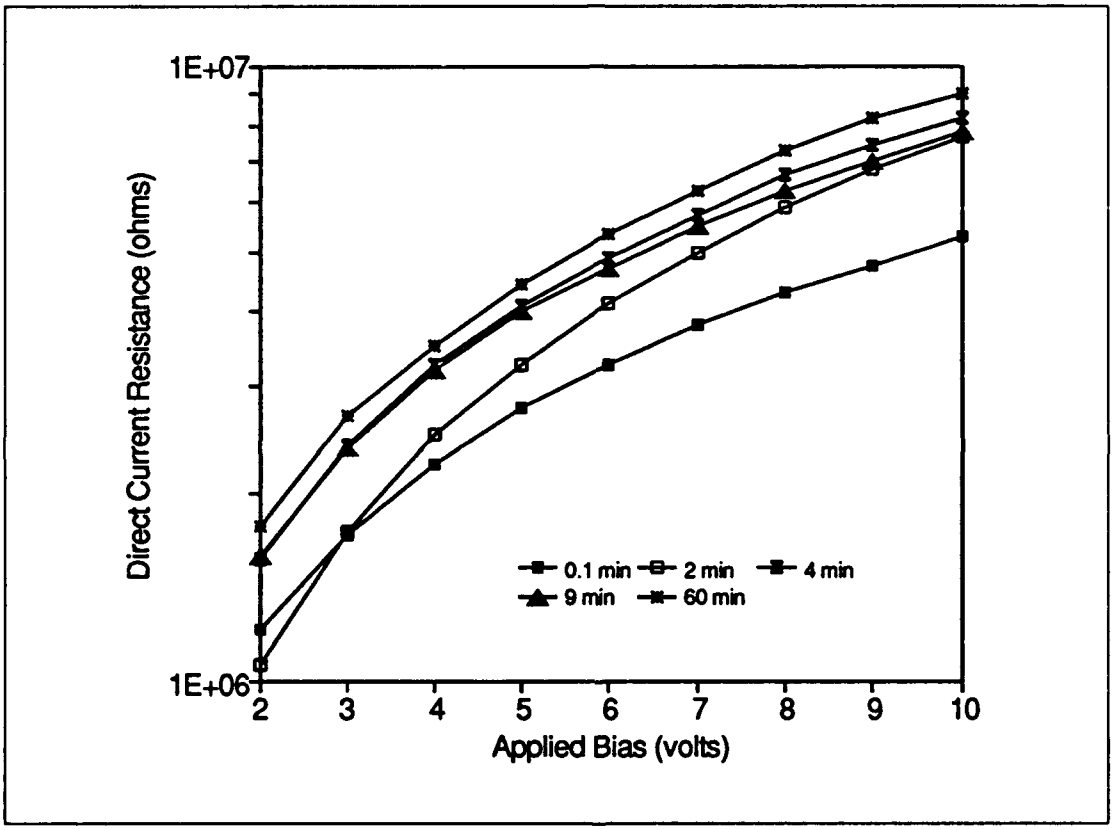

Figure 5.9. Direct current resistance measured with respect to applied bias for a 55°C resin cure.

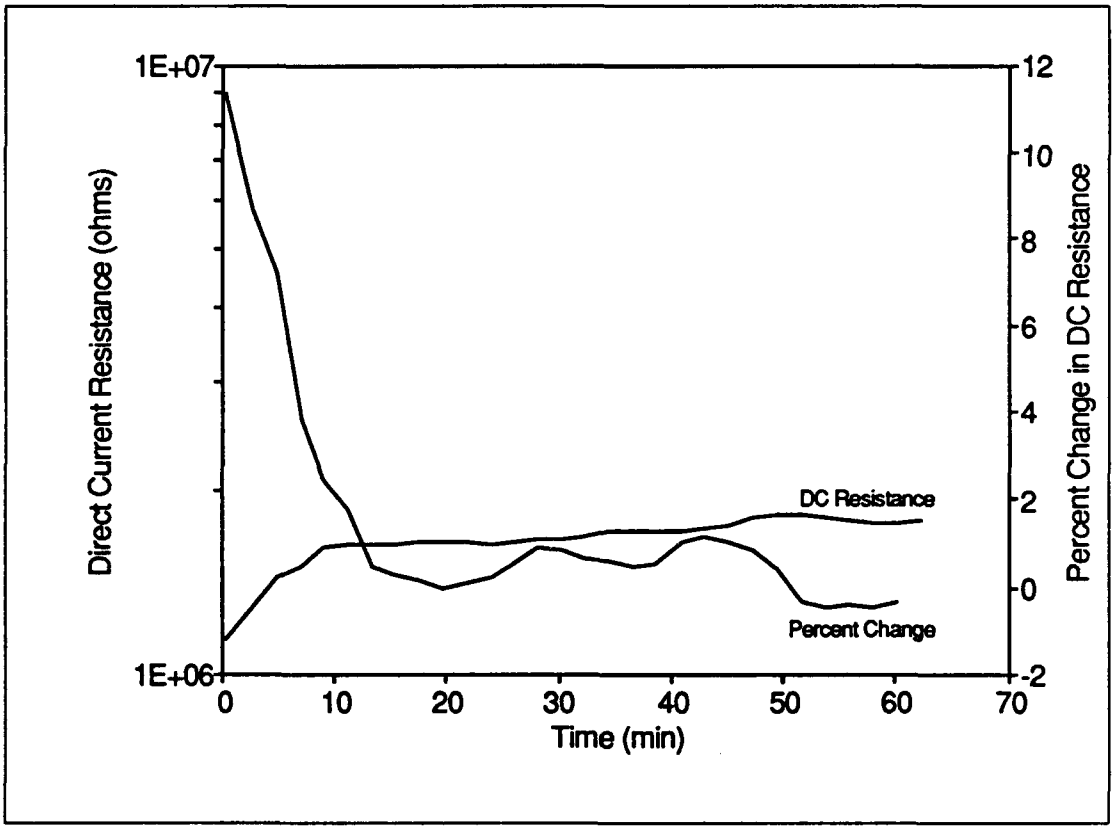

Figure 5.10. Direct current resistance measured with respect to time (2-volt applied bias) for a 55°C resin cure.

Impedance of the Interdigitated Gate Electrode Structure. The impedance magnitude and phase of the IGE structure were measured as discussed in Chapter 4. After the data was collected, the real part and imaginary part of the impedance were extracted, and Cole-Cole plots of the information were generated.

The impedance magnitude and phase for a sample of resin cured at 45°C are plotted in Figures 5.11 through 5.14. These figures show that the impedance magnitude undergoes a steady increase until approximately 60 minutes into the cure cycle. After 60 minutes, there is relatively little change. Again, this is indicative of the onset of gelation in the resin (Figure 5.3). The total current flow in the system is due to contributions from polarization mechanisms and conduction mechanisms. Purely conductive behavior is indicated by a 0 degree phase angle, and purely reactive behavior is indicated by a -90 degree phase angle. The phase information (Figure 5.13) indicates that, at the beginning of the cure process, conduction mechanisms dominate at frequencies up to approximately 10 KHz. However, in the vicinity of 10 KHz, a transition in the phase occurs which indicates a change in the dominant electrical transport mechanism from conduction to that of polarization. Figure 5.14 indicates that after approximately ten minutes of cure time, the polarization mechanisms dominate for frequencies above approximately 300 Hz. After an hour there is very little change in the phase response of the resin.

There is also a well-defined notch in the magnitude of the impedance at approximately 400 Hz which appears after approximately 20 minutes into the cure (Figure 5.12). The notch is most likely attributable to parasitic inductance introduced by the test equipment configuration, which loads the IGE structure, in concert with phenomena at the electrode-resin interface, which will be discussed in greater detail later in this chapter.

The impedance magnitude and phase measurement results for the 55°C cure are presented in Figures 5.15 and 5.16. The trends noted in the 45°C cure are, in general, also present in this information.

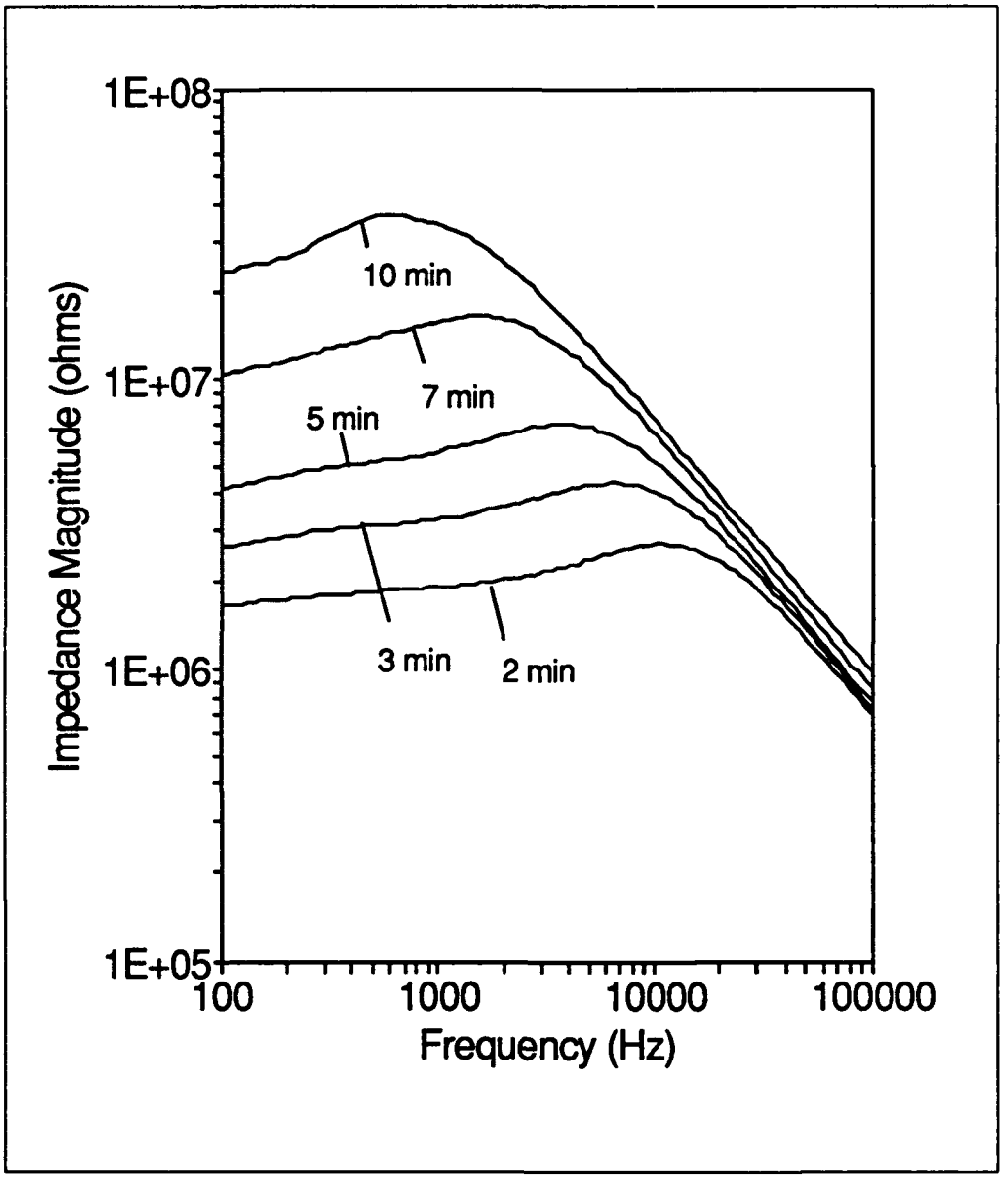

Figure 5.11. Magnitude of the impedance of the interdigitated gate electrode structure for the first ten minutes of a 45°C cure.

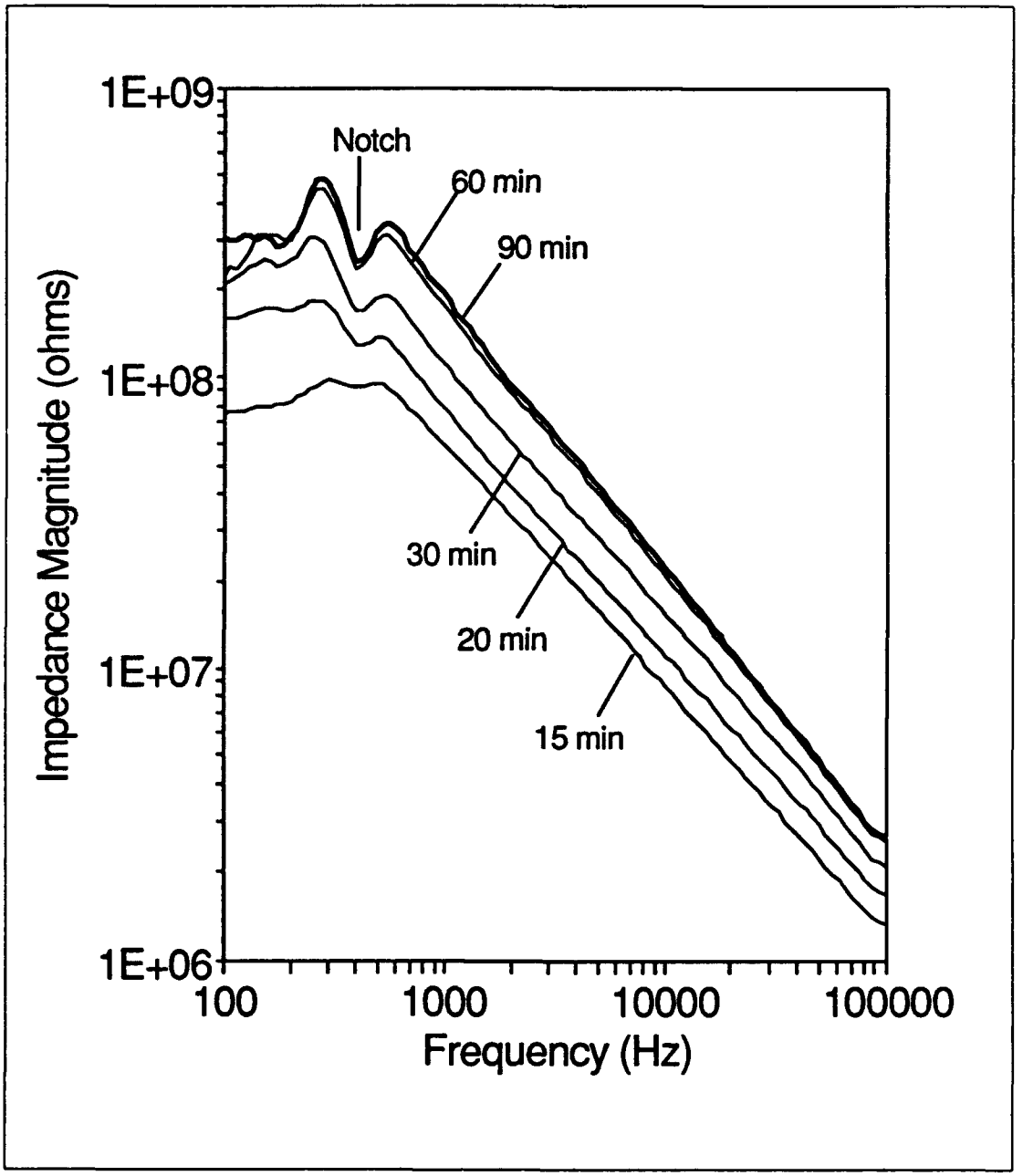

Figure 5.12. Magnitude of the impedance of the interdigitated gate electrode structure after the first ten minutes of a 45°C cure.

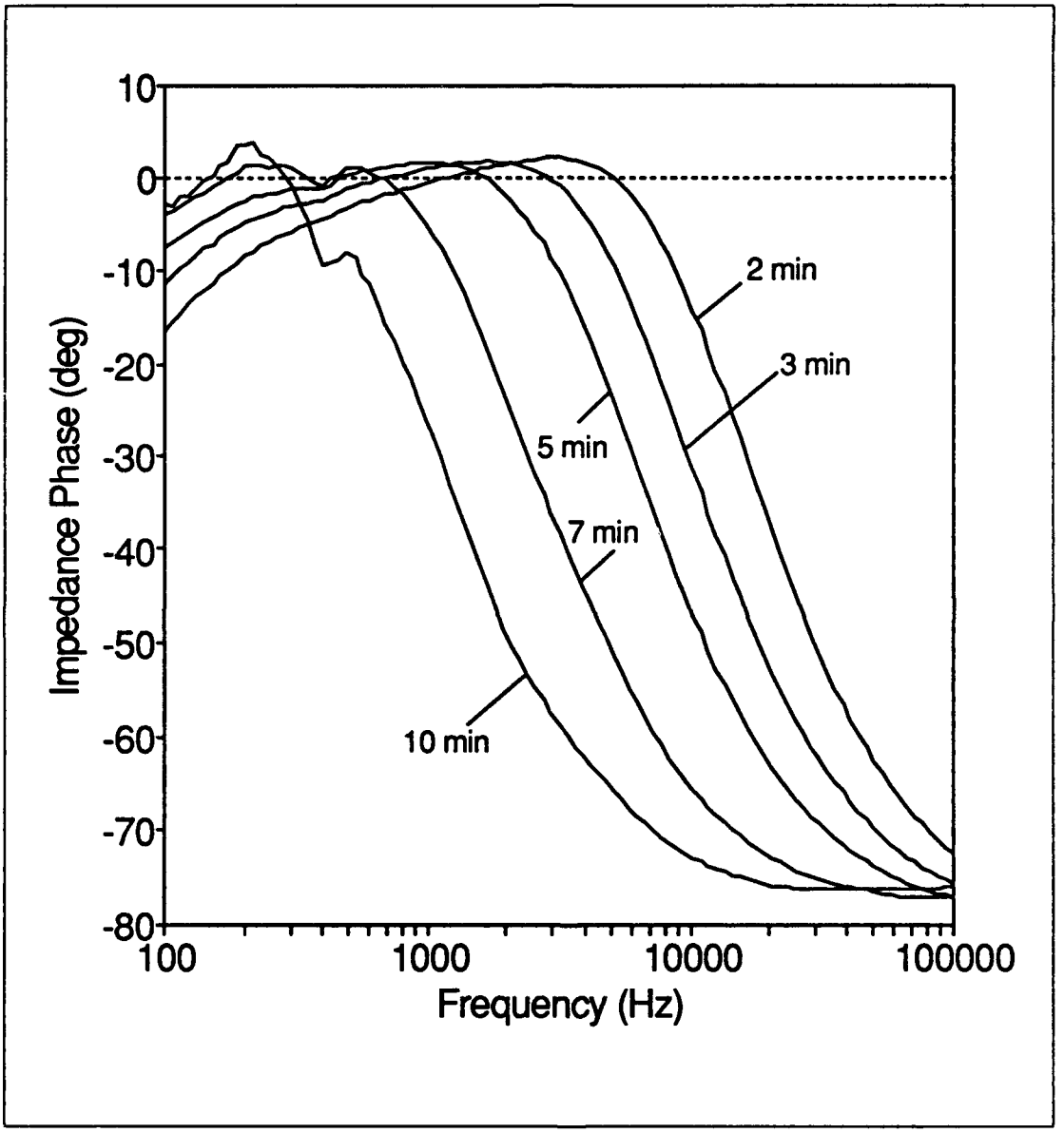

Figure 5.13. Phase of the impedance of the interdigitated gate electrode structure for the first ten minutes of a 45°C cure.

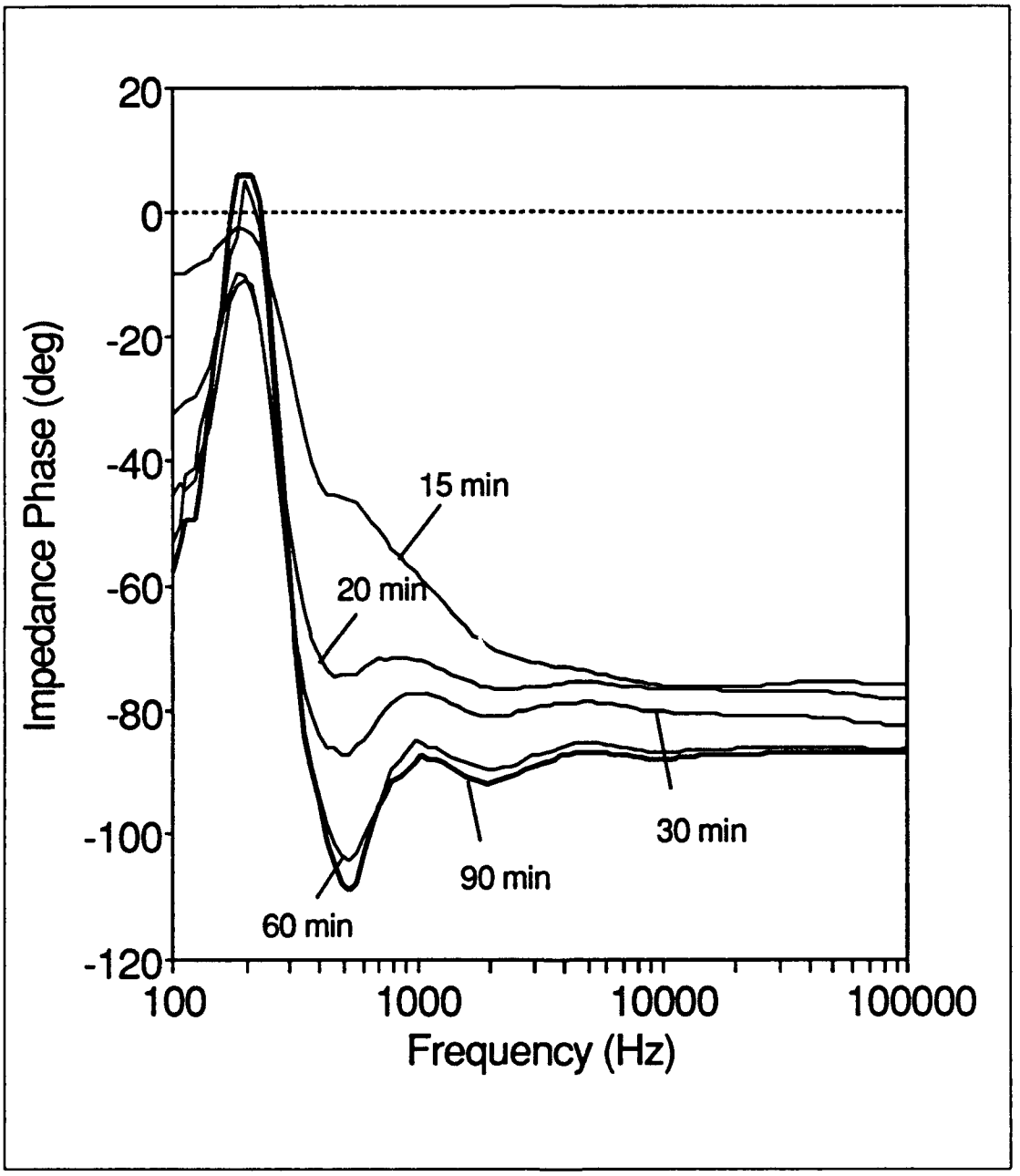

Figure 5.14. Phase of the impedance of the interdigitated gate electrode structure after the first ten minutes of a 45°C cure.

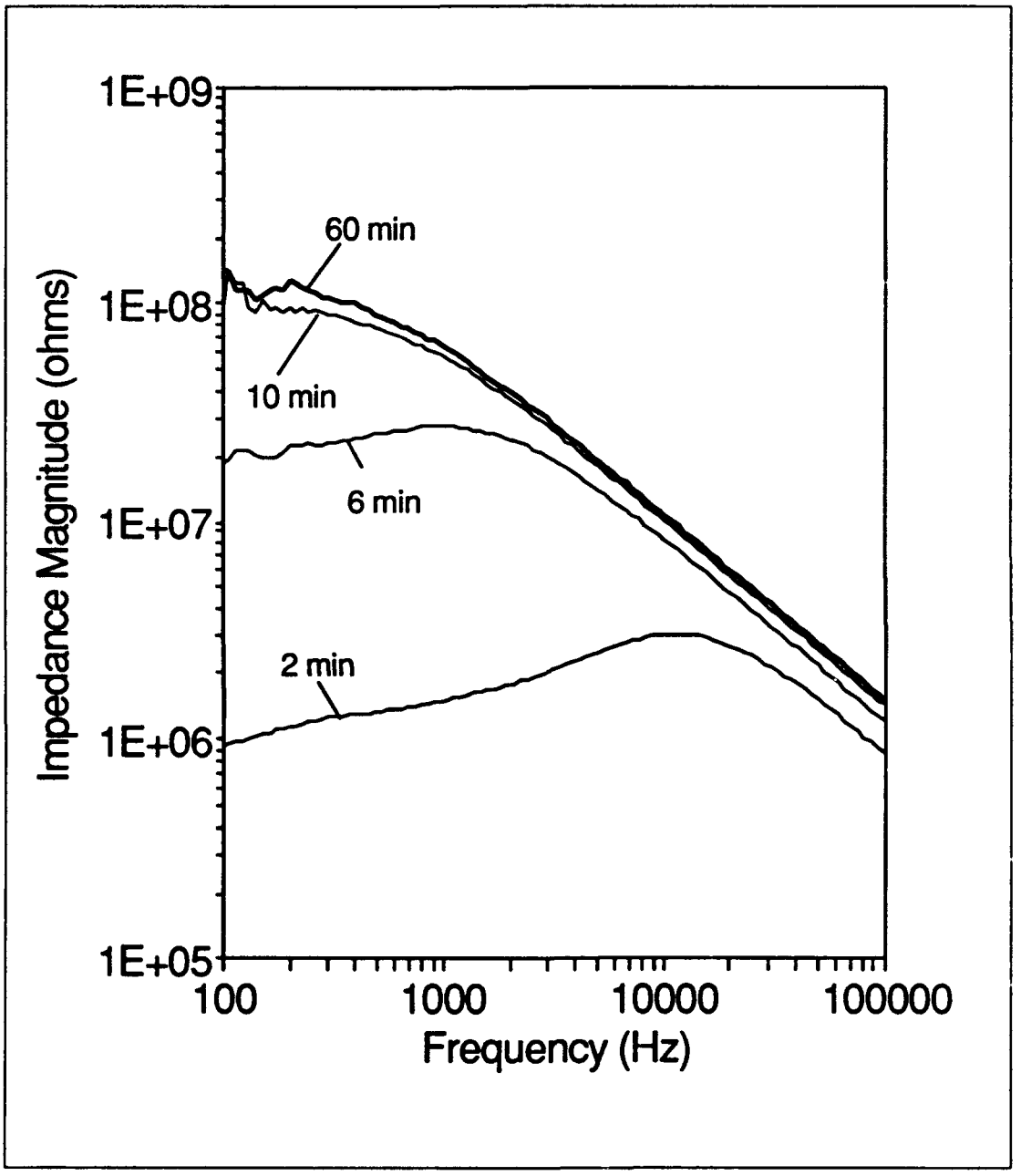

Figure 5.15. Magnitude of the impedance of the interdigitated gate electrode structure for a 55°C cure.

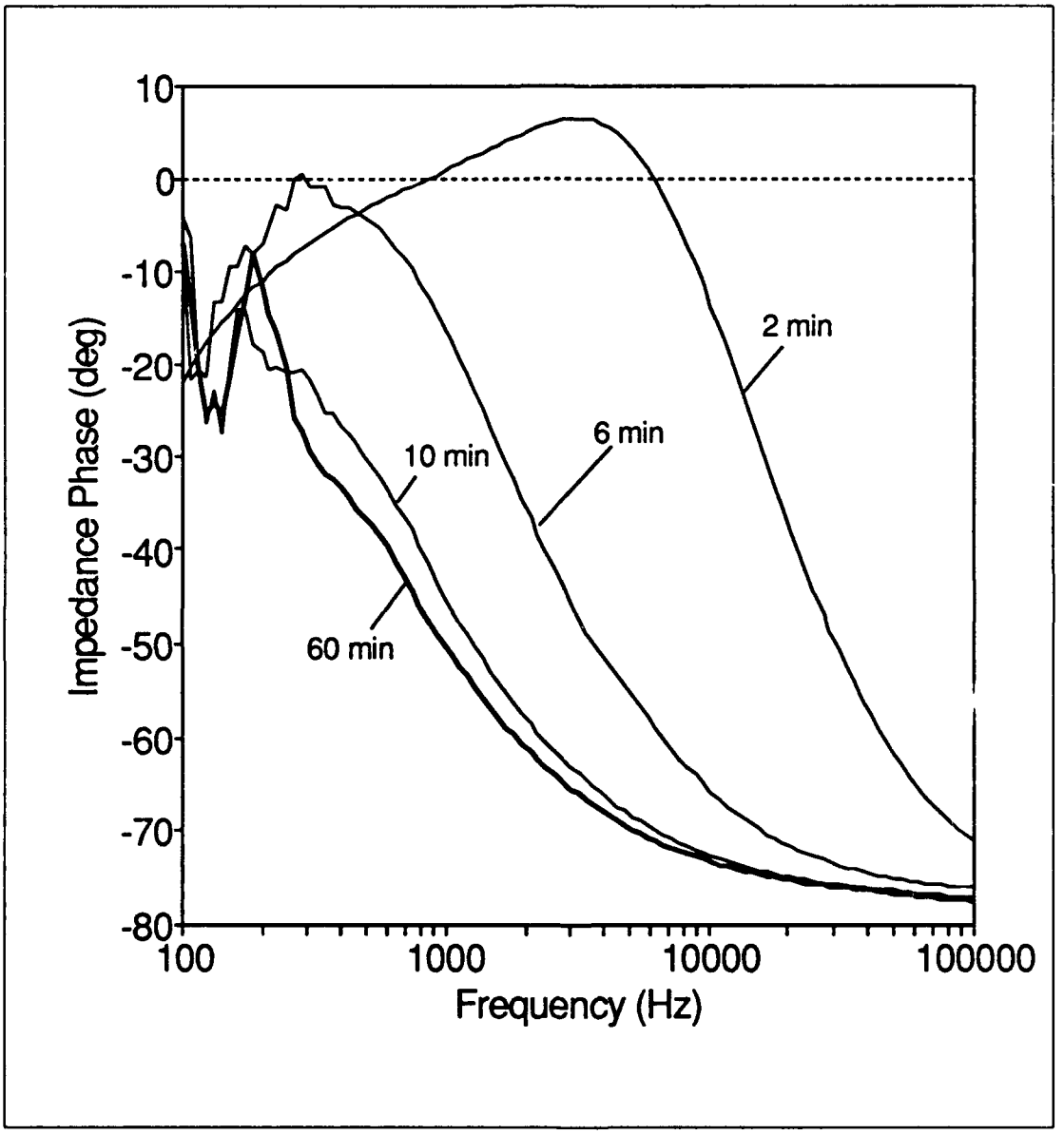

Figure 5.16. Phase of the impedance of the interdigitated gate electrode structure for a 55°C cure.

The real and imaginary components of the impedance were extracted from the magnitude and phase information. The plots of the real and imaginary components of the impedance for a 45°C cure are presented in Figures 5.17 through 5.20. The advantage of this method of representing the impedance information is that it explicitly details the contributions due to the polarization and conduction mechanisms.

The real and imaginary components of the impedance of the IGE structure were also extracted from the 55°C cure, and the results are presented in Figures 5.21 and 5.22. The magnitudes of the real and imaginary components of the impedance are nearly an order of magnitude smaller for the 55°C cure compared to the 45°C cure. This information supports the hypothesis that the material may still be in a rubbery state well into the cure.

Finally, the real and imaginary components of the impedance were used to construct Cole-Cole representations of the resin's impedance at discrete points in the cure cycle. For the 45°C cure cycle, Cole-Cole representations of the impedance at 5 minutes, 9 minutes, and 14 minutes are depicted in Figures 5.23, 5.24, and 5.25, respectively. Cole-Cole plots, in general, are circular arcs which begin at a point corresponding to the material's low frequency (the right-hand portion of the plot) behavior, and the frequency parameter increases as the arc travels in a counter-clockwise direction.

This resin system does not have a single characteristic relaxation time, because the centers of the arcs in these plots are depressed below the horizontal axis. According to MacDonald, the area corresponding to the low frequency portion of the plot in Figure 5.24 is illustrative of the inductive behavior of the material, and is the result of adsorption-reaction processes at the resin-electrode interface (33:112). This inductance could also be the result of a parasitic load inductance associated with the instrumentation and the interconnecting cabling.

According to MacDonald, the adsorption-reaction processes may result in negative resistance behavior, as well. This may explain why the real component of the impedance exhibited the

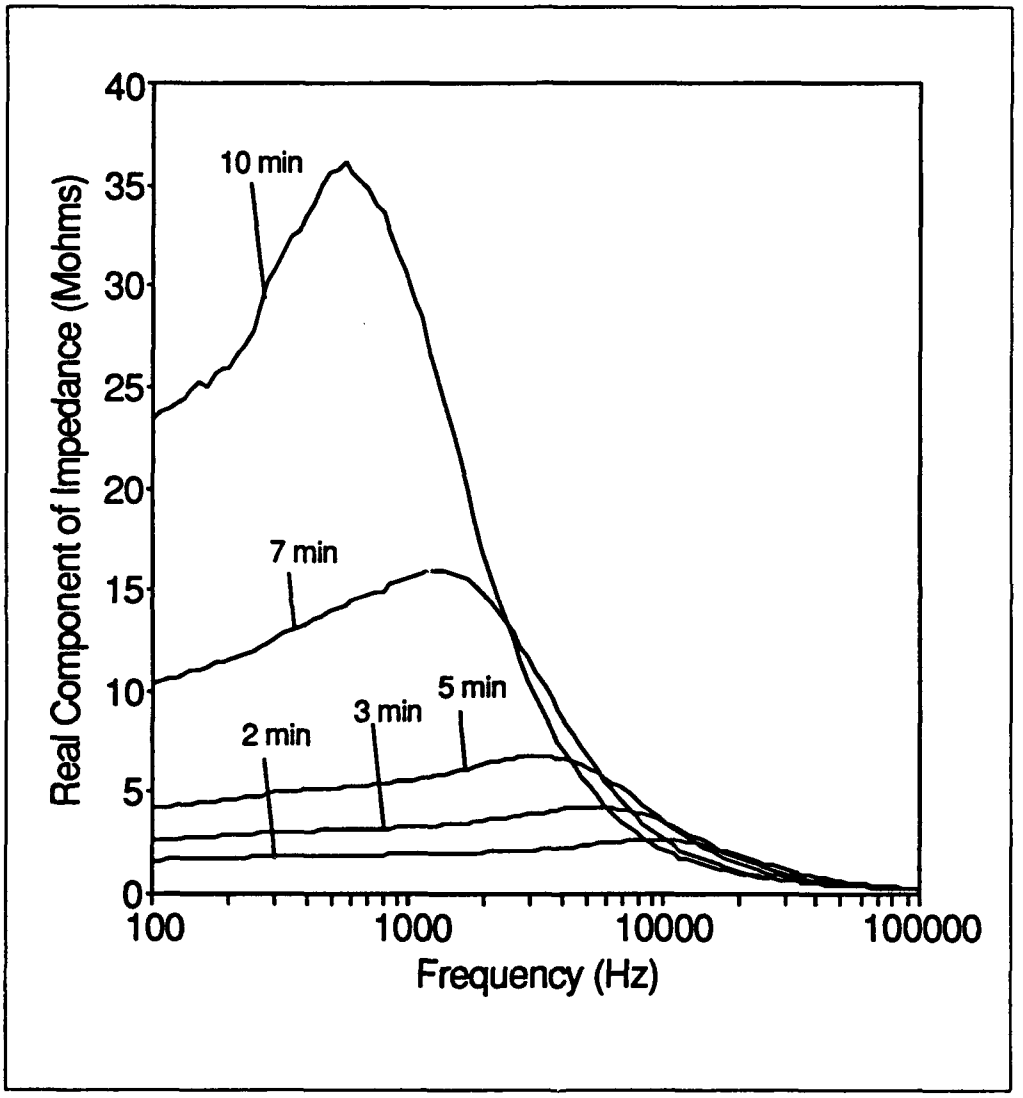

Figure 5.17. Real component of the impedance of the interdigitated gate electrode structure for the first 10 minutes of a 45°C cure.

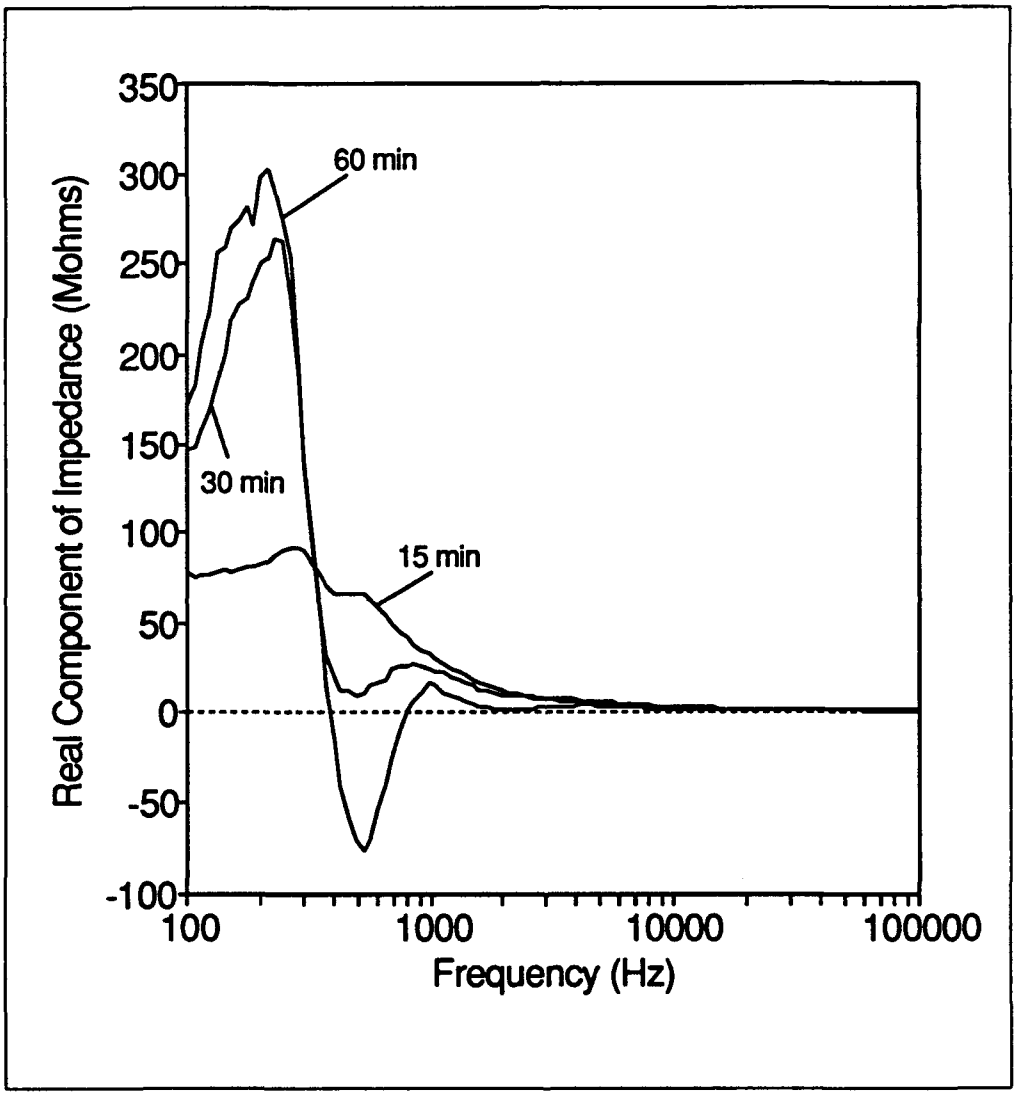

Figure 5.18. Real component of the impedance of the interdigitated gate electrode structure after the first 10 minutes of a 45°C cure.

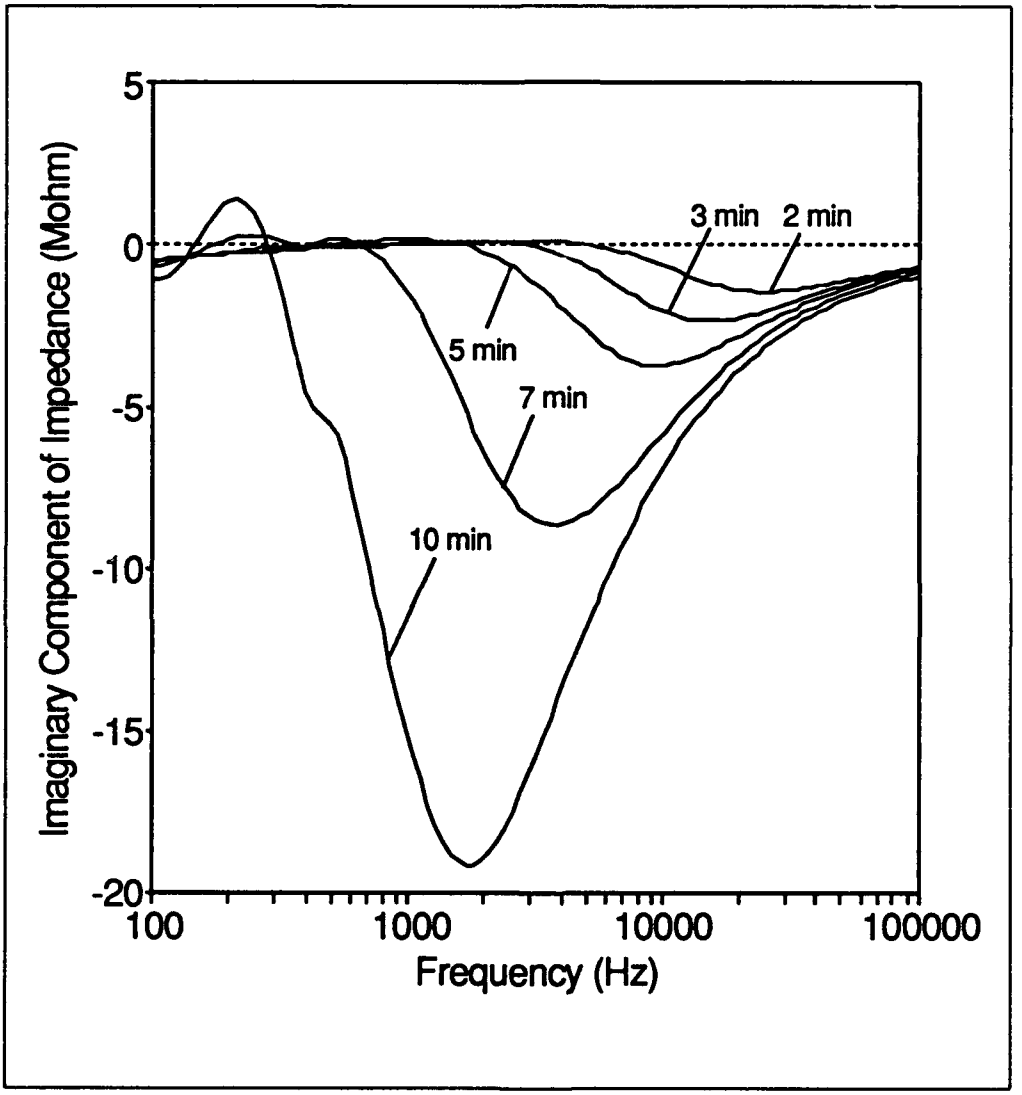

Figure 5.19. Imaginary component of the impedance of the interdigitated gate electrode structure for the first 10 minutes of a 45°C cure.

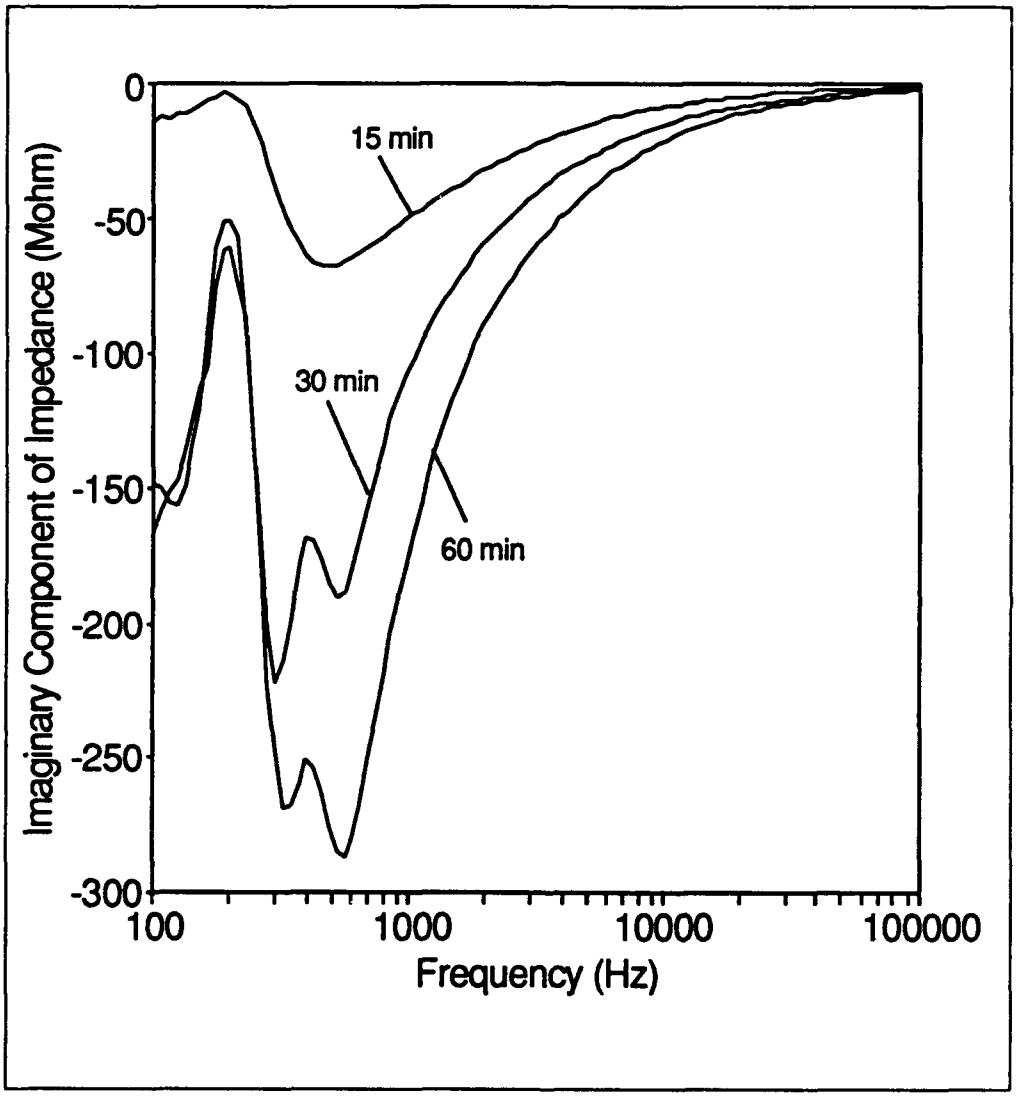

Figure 5.20. Imaginary component of the impedance of the interdigitated gate electrode structure after the first 10 minutes of a 45°C cure.

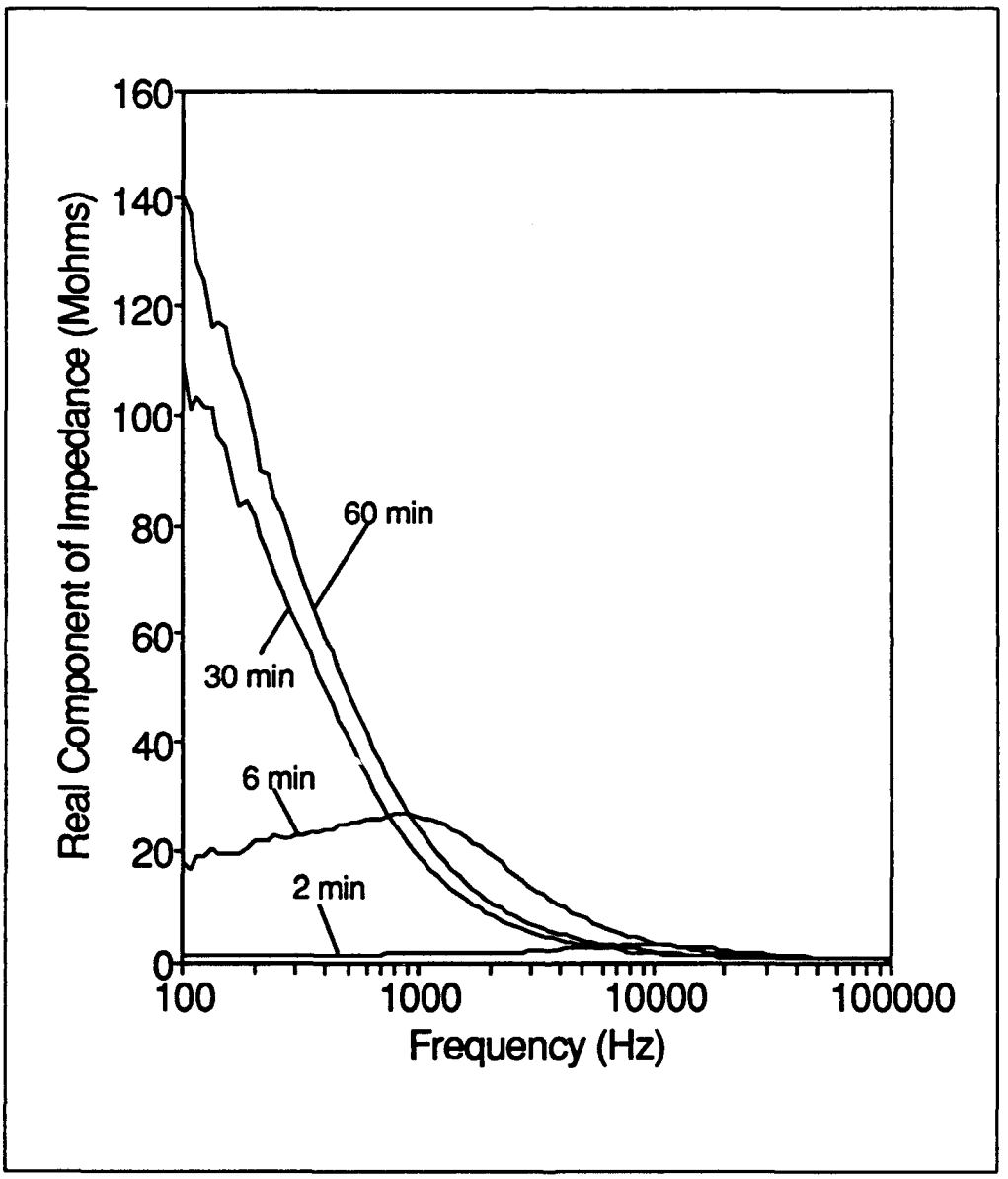

Figure 5.21. Real component of the impedance of the interdigitated gate electrode structure for a 55°C cure.

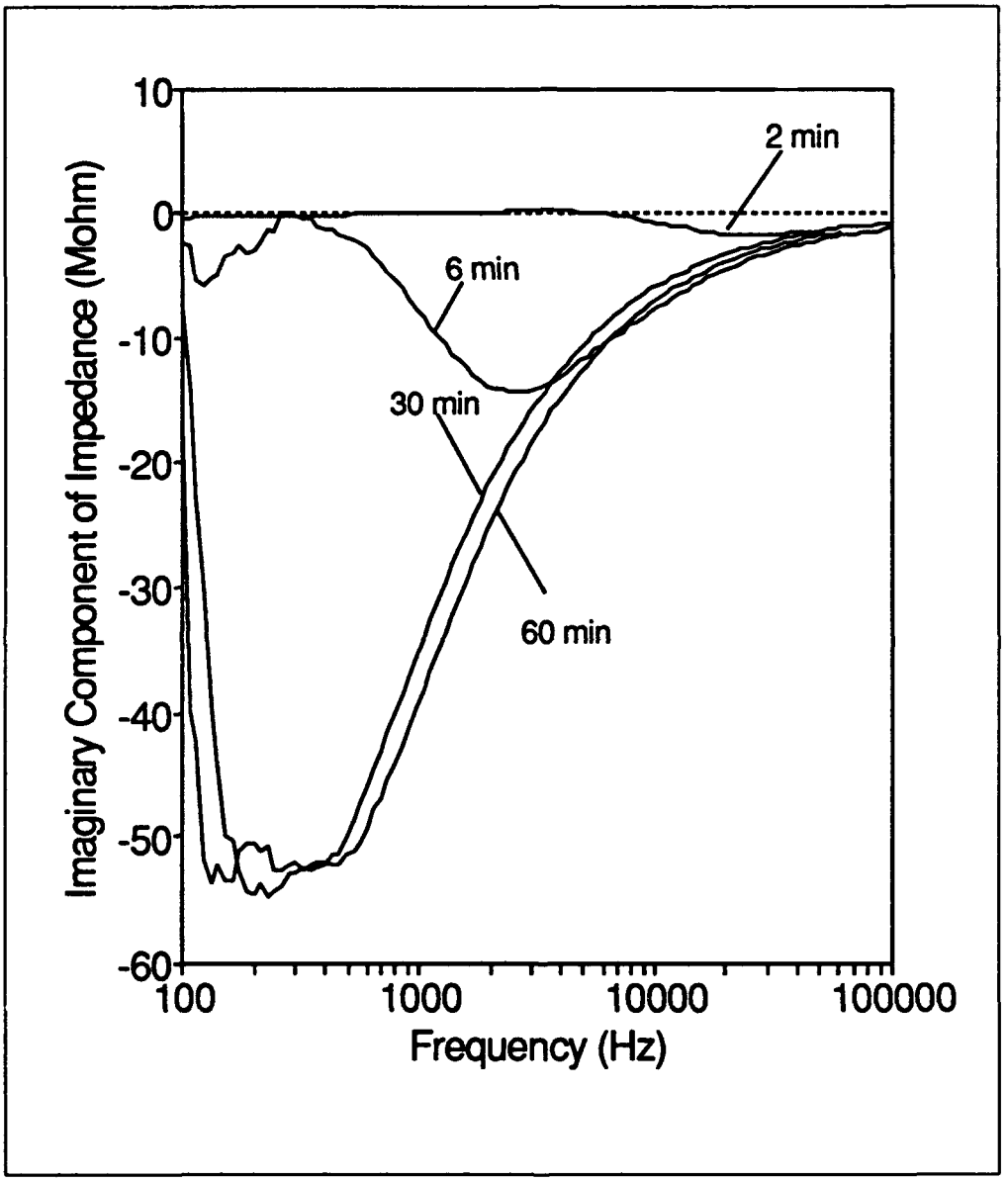

Figure 5.22. Imaginary component of the impedance of the interdigitated gate electrode structure for a 55°C cure.

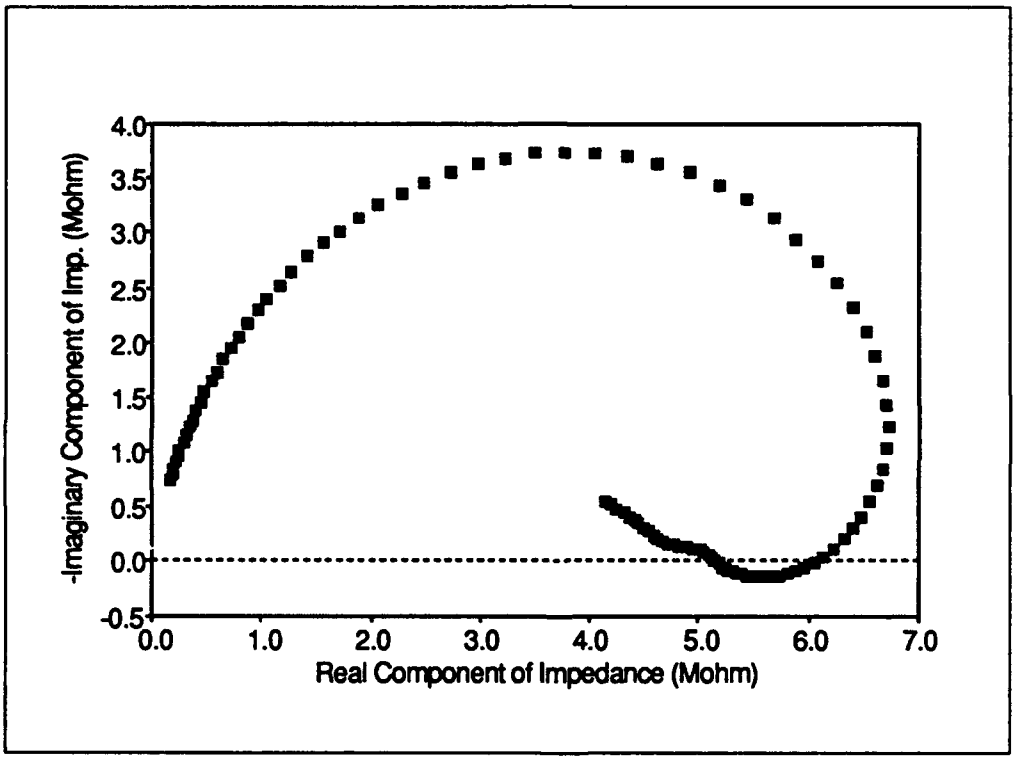

Figure 5.23. Cole-Cole representation of the impedance of the interdigitated gate electrode structure 5 minutes into a 45°C cure cycle (the vertical axis represents the negative of the imaginary component of the impedance).

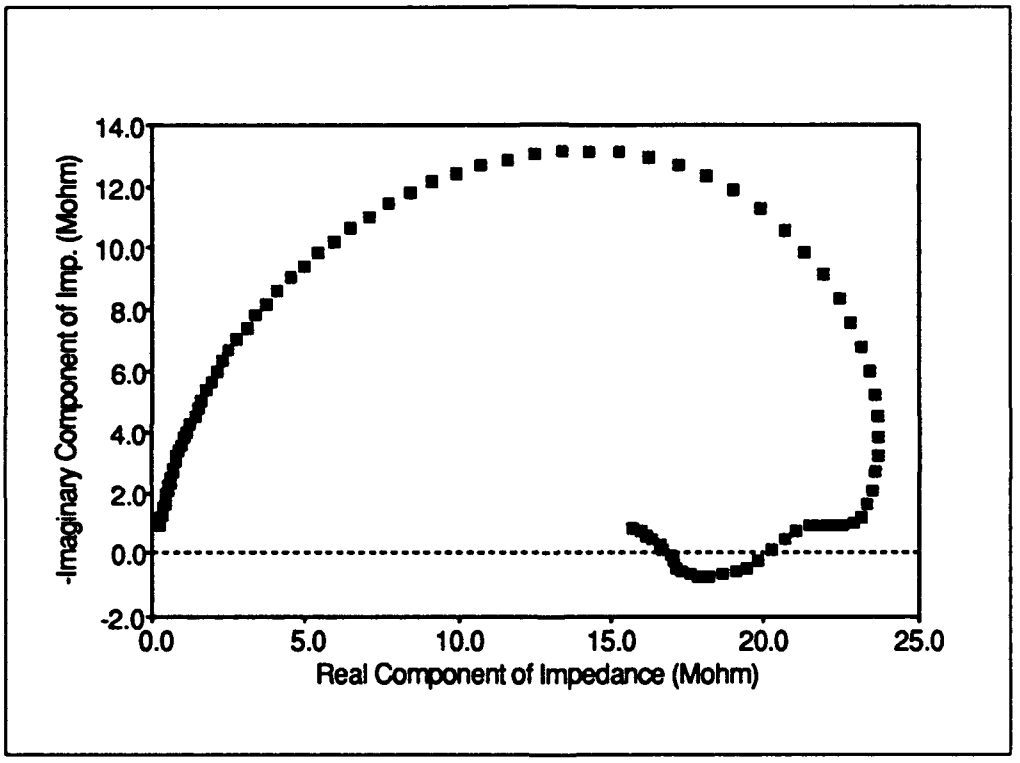

Figure 5.24. Cole-Cole representation of the impedance of the interdigitated gate electrode structure 9 minutes into a 45°C cure cycle (the vertical axis represents the negative of the imaginary component of the impedance).

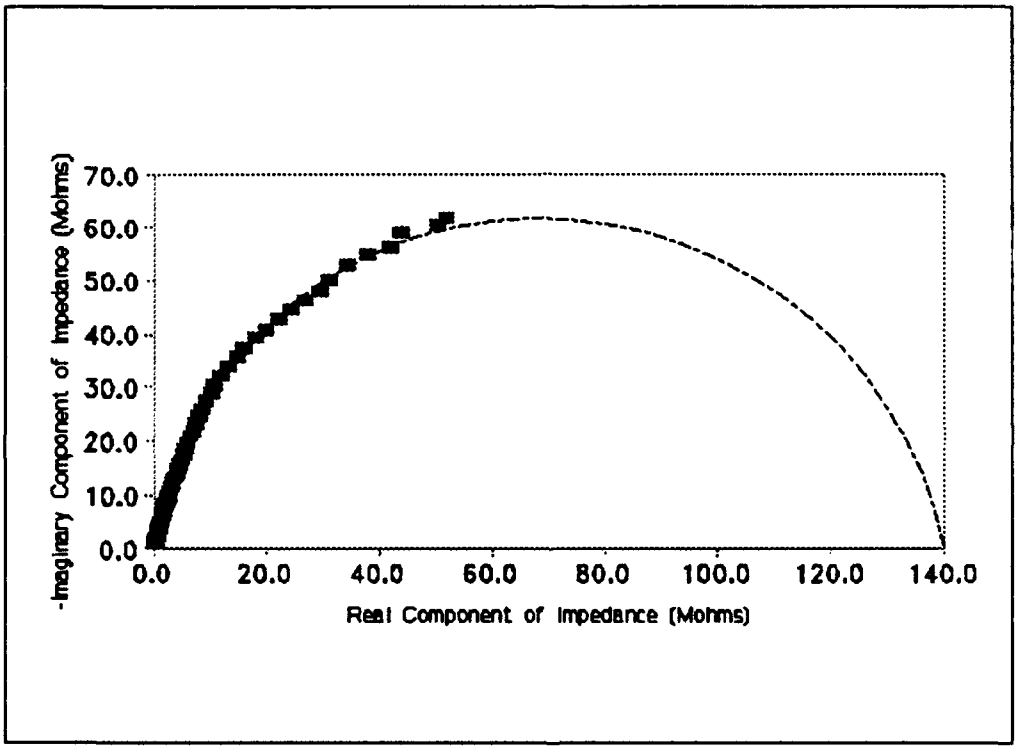

Figure 5.25. Cole-Cole representation of the impedance of the interdigitated gate electrode structure 14 minutes into a 45°C cure cycle (the vertical axis represents the negative of the imaginary component of the impedance).

negative behavior for the 45°C cure cycle at low frequencies (Figure 5.18). In Figure 5.25, the low frequency magnitude of the impedance was such that the measurements were not reliable. That is, given the specific instrument configuration utilized to measure the impedance of the IGE structure, the impedance/gain-phase analyzer's upper limit of a reliabile measurement is approximately 80 MΩ (determined empirically).

From these plots, the mean relaxation time (τ_m) for the material can be estimated. It can be discerned at the point where the imaginary component attains its maximum when $\omega_m \tau_m = 1$, where ω_m is the frequency associated with this point (33:17). In Figure 5.24, the frequency at this point (the apex of the curve) is approximately 16147.8 rad/sec. Solving the above relation for τ_m yields a mean relaxation time for this system of approximately 62 μsec. In contrast, a similar measurement and calculation from the data in Figure 5.25 yields a mean relaxation time of approximately 245 μsec. The relaxation time increase is due to the increase in the average size of the molecules in the polymer, which makes it more difficult for the molecular dipoles to respond to an electromagnetic stimulus.

Similar plots were constructed for the 55°C cure. They are presented in Figures 5.26 through 5.29. This cure cycle produced significantly more well-behaved results because the impedance of the material was not as large as was the case for the low temperature cure. The 2-minute duration plot (Figure 5.26) exhibits the same characteristics as the short duration cure time plot for the low temperature cure (Figure 5.23). Again, this behavior may be attributable to the relatively high conductance of the material during the initial portion of the cure cycle. Utilizing the expression $\omega_m \tau_m = 1$, the mean relaxation time, τ_m, can be calculated as discussed above. The mean relaxation time for the plot corresponding to 10 minutes into the cure is approximately 162 μsec. The mean relaxation time for the plots in Figures 5.28 and 5.29 are nearly the same, approximately 231 μsec.

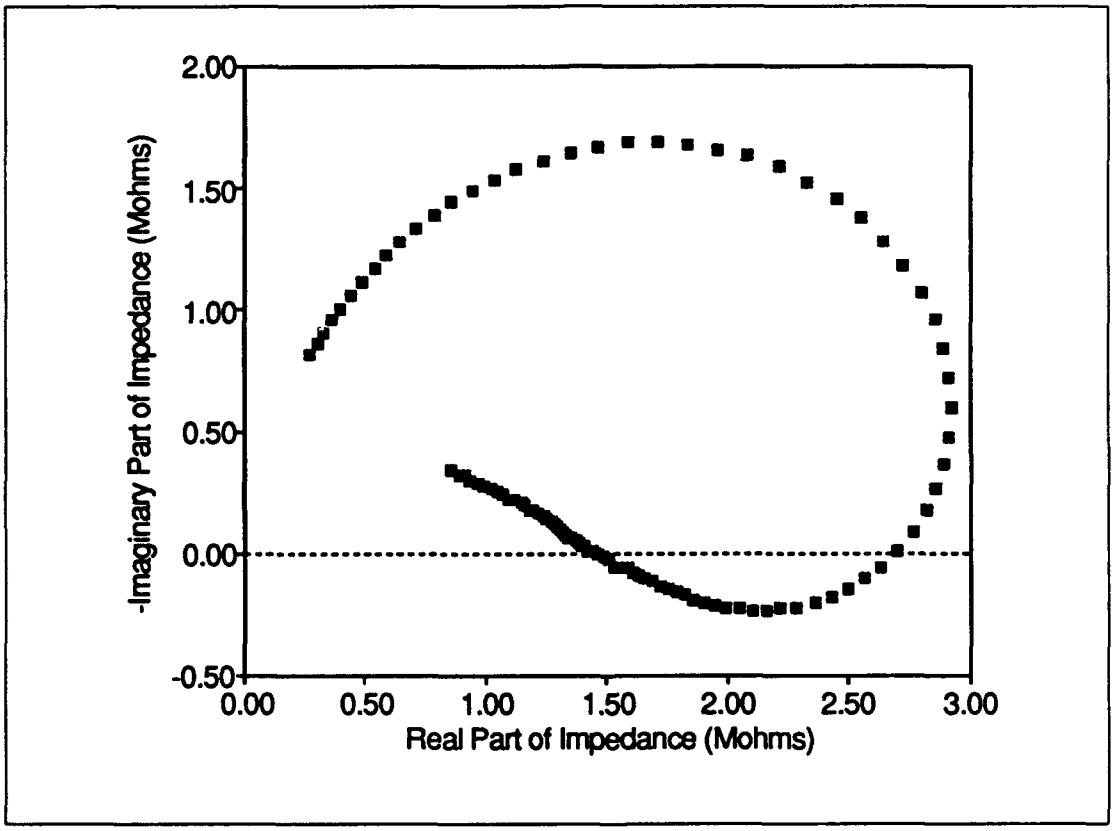

Figure 5.26. Cole-Cole representation of the impedance of the interdigitated gate electrode structure 2 minutes into a 55°C cure cycle (the vertical axis represents the negative of the imaginary component of the impedance).

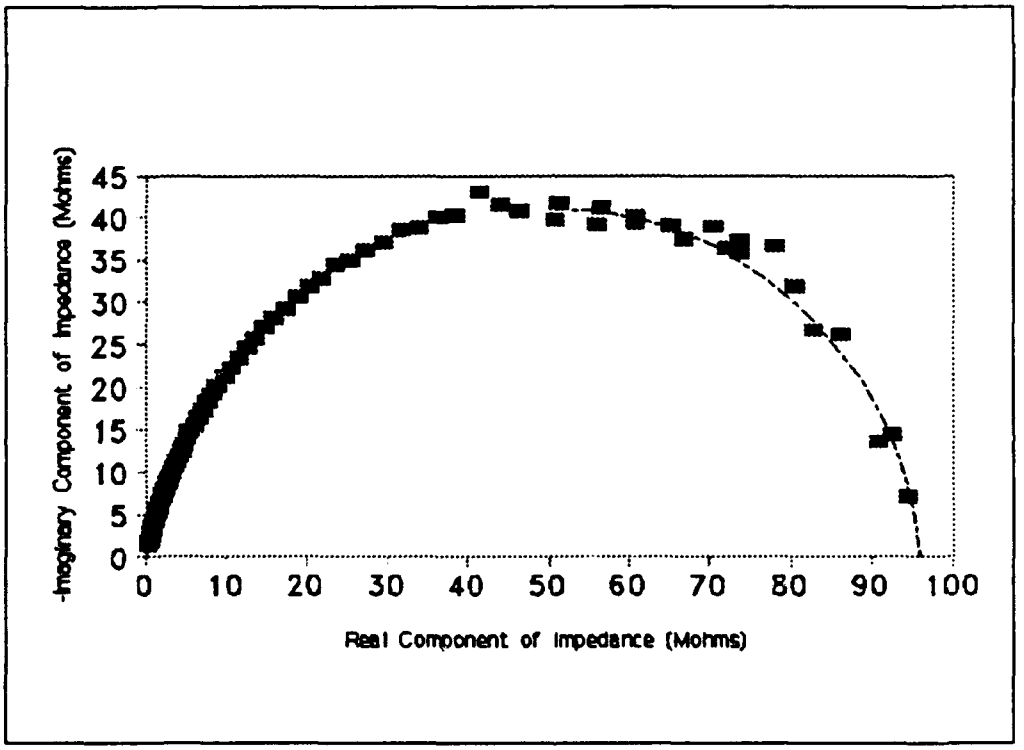

Figure 5.27. Cole-Cole representation of the impedance of the interdigitated gate electrode structure 10 minutes into a 55°C cure cycle (the vertical axis represents the negative of the imaginary component of the impedance).

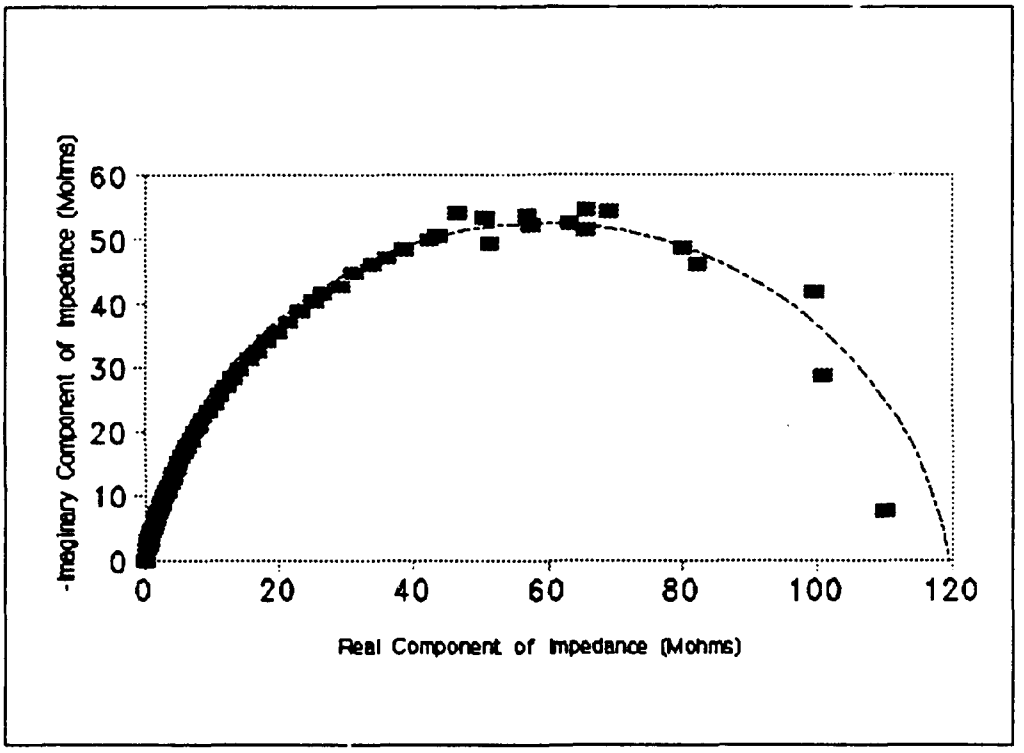

Figure 5.28. Cole-Cole representation of the impedance of the interdigitated gate electrode structure 30 minutes into a 55°C cure cycle (the vertical axis represents the negative of the imaginary component of the impedance).

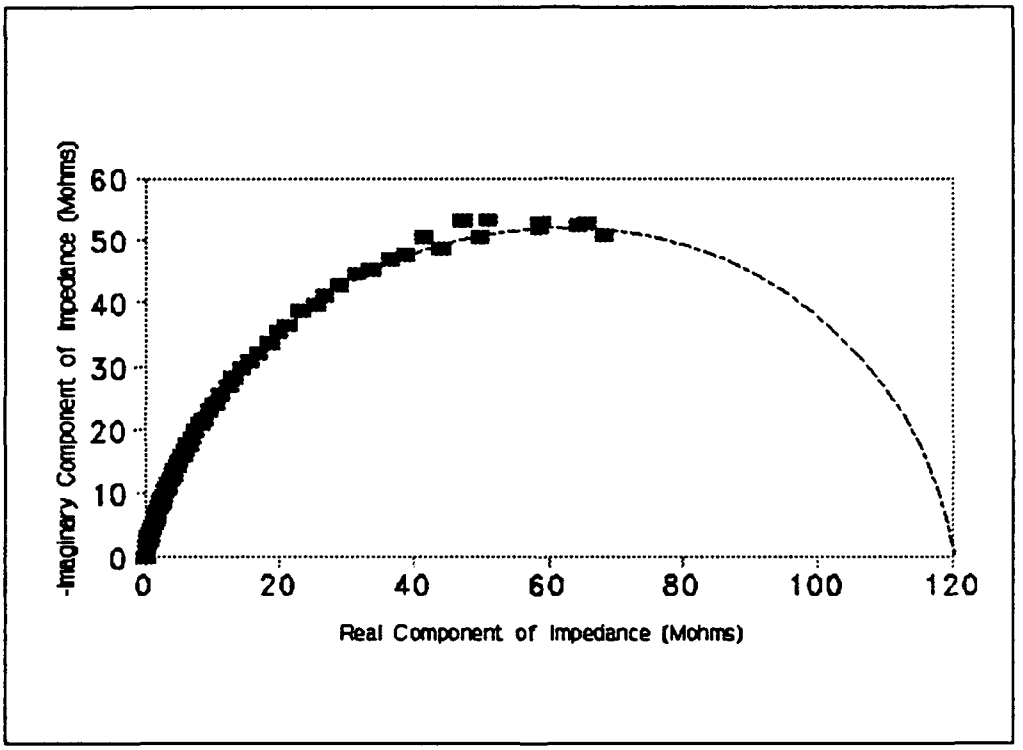

Figure 5.29. Cole-Cole representation of the impedance of the interdigitated gate electrode structure 60 minutes into a 55°C cure cycle (the vertical axis represents the negative of the imaginary component of the impedance).

Transfer Function of the Interdigitated Gate Electrode Structure. The transfer function of the IGE structure was measured for a 45°C cure, and the results are depicted in Figures 5.30 through 5.32. The trends due to the resin's cure, which are evident in this information, support the trends noted in the previous measurements. The gain of the IGE structure (Figure 5.30) decreases with cure time because less energy is transmitted through the material. After the 60 minute cure point, which corresponds to the measured gelation time for the resin at this temperature, the gain of the IGE structure changes very little.

A similar response is exhibited by the phase delay of the system (Figure 5.31). That is, the phase delay undergoes dramatic change initially, but after 60 minutes, exhibits very little change. The phase delay of the IGE structure approaches zero degrees at high frequencies. This response may be clearly understood upon examination of the equivalent circuit model for this structure (see Figure 5.33). The transfer function of the system in Figure 5.33 is given by:

$$T(\omega) = \frac{1 + \jmath\omega R_e C_e}{1 + \jmath\omega R_e (C_e + C_{ox})}. \tag{5.1}$$

As the frequency (ω) approaches infinity, Equation 5.1 reduces to:

$$T(\infty) = \frac{C_e}{C_{ox} + C_e}. \tag{5.2}$$

Thus, for very high frequencies, the IGE structure's equivalent resistance (R_e) may be neglected, and there is no phase shift associated with the resultant transfer function. However, there will always be some current flow due to loss mechanisms at the lower frequencies. Also, since resins are not perfect dielectrics, there will be some finite current flow due to loss mechanisms for a completely cured resin. These loss mechanisms may be represented by the equivalent resistance, R_e. As the frequency, ω, approaches zero (the dc limit), the transfer function (Equation 5.1)

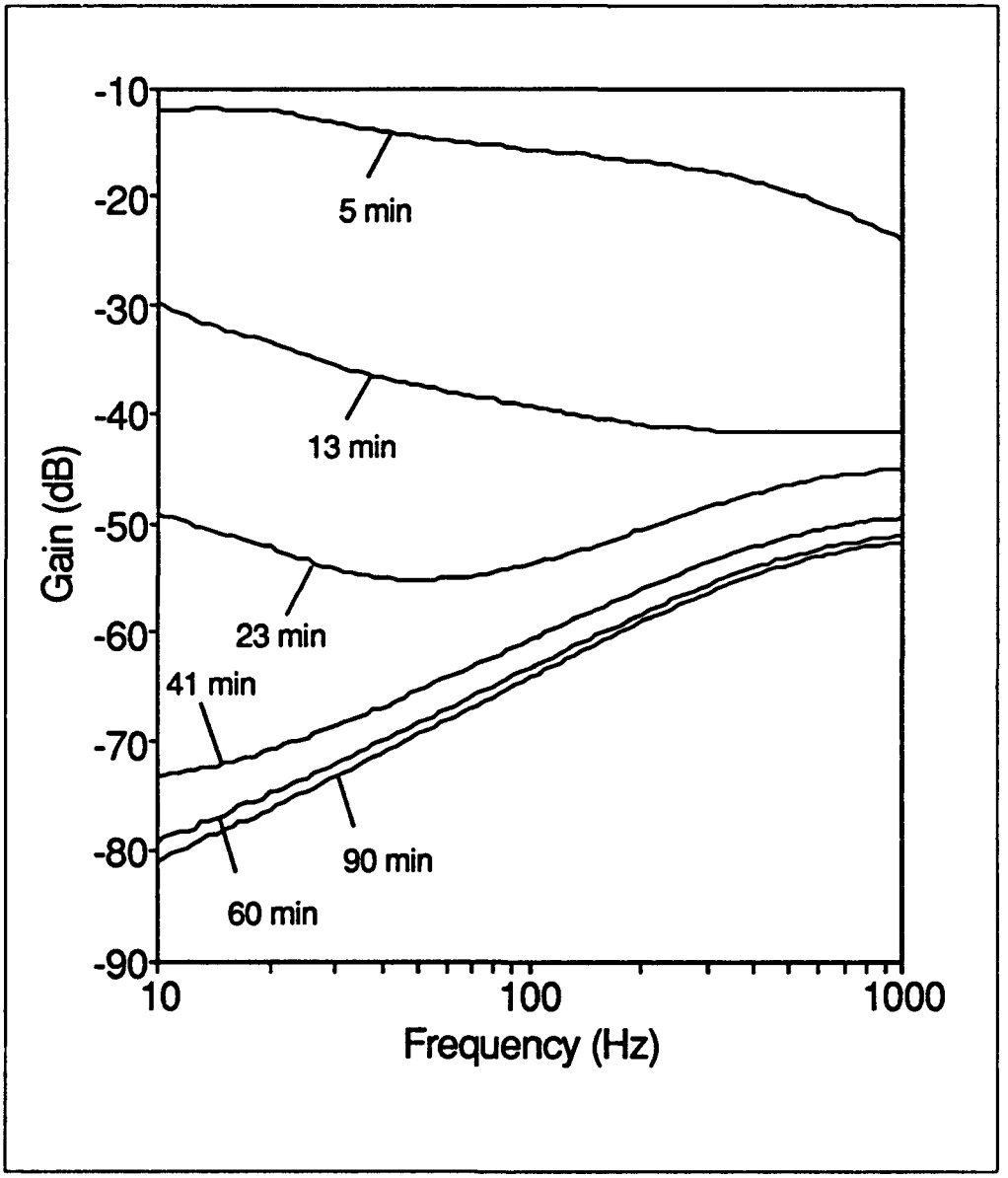

Figure 5.30. Gain of the IGE structure with respect to frequency for a sample cured at 45°C.

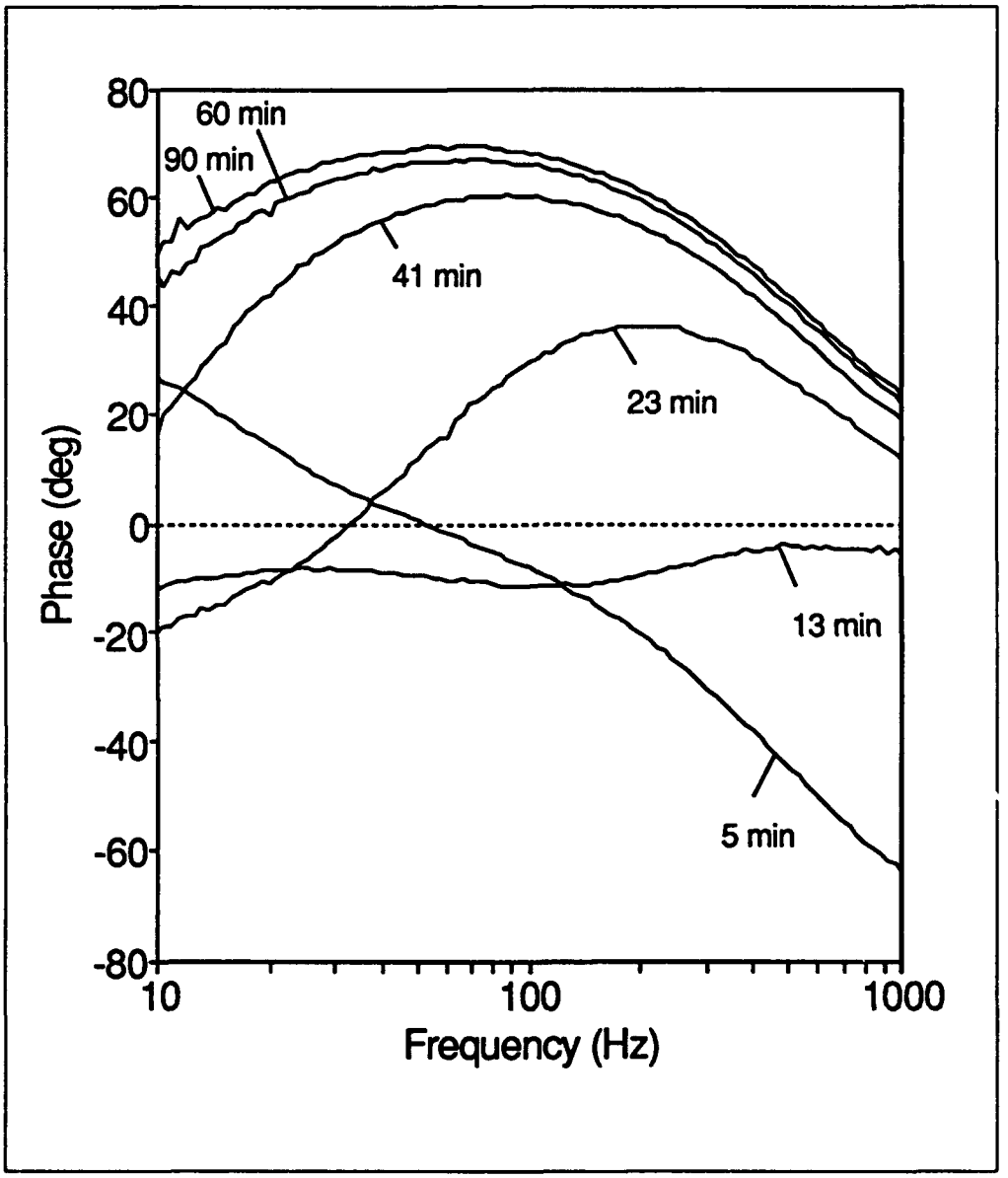

Figure 5.31. Phase delay of the IGE structure with respect to frequency for a sample cured at 45°C.

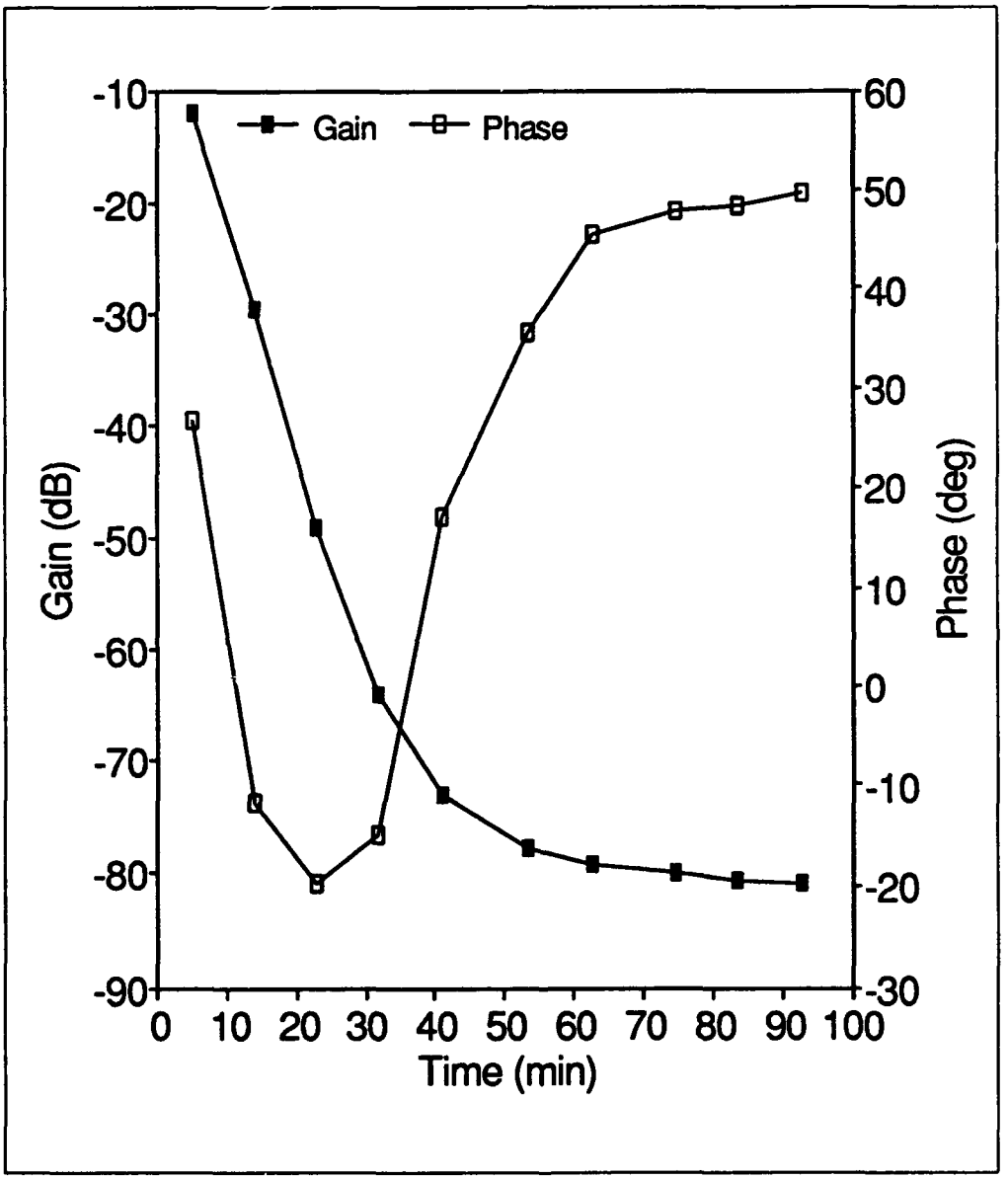

Figure 5.32. Gain and phase delay of the IGE structure with respect to time (frequency equal to 10 Hz) for a sample cured at 45°C.

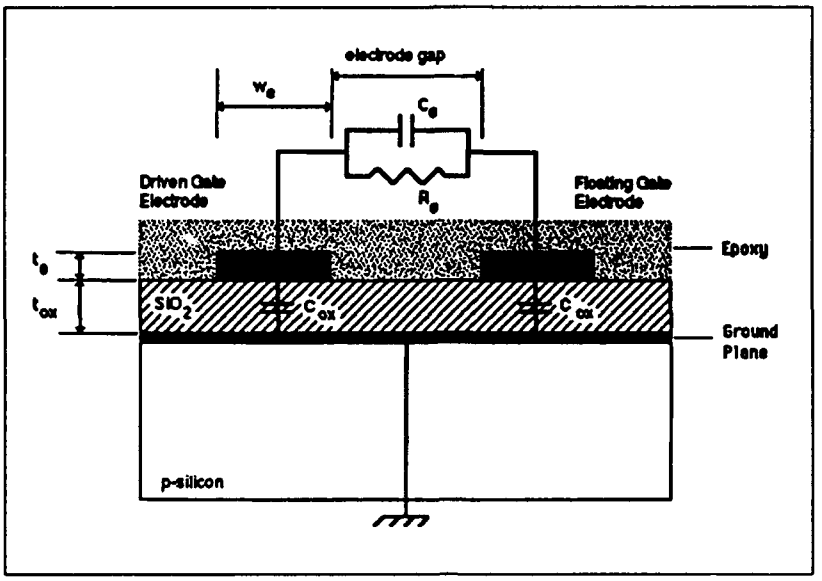

Figure 5.33. Equivalent circuit model of the IGE structure.

becomes:

$$T(0) = 1, \tag{5.3}$$

which also has no associated phase shift. Figure 5.31 illustrates that, at very low and very high frequencies, the phase shift of the system approaches zero.

Since the gain exhibited the greatest degree of change at 10 Hz, the gain and phase data was extracted at this frequency to illustrate the trend toward gelation. This data is plotted in Figure 5.32. It illustrates that, as the cure progresses beyond the estimated gelation time of the sample (60 minutes), the rate of change of the transfer function slows considerably.

Another set of transfer function measurements were made across the IGE structure with a resin sample cured at 55°C. The results of these measurements are presented in Figures 5.34 through 5.36. The results are similar to those of the lower temperature cure. In particular, Figure 5.36 indicates that the onset of gelation occurs at approximately 25 minutes, which corresponds to the gelation time determined by the mechanical methods.

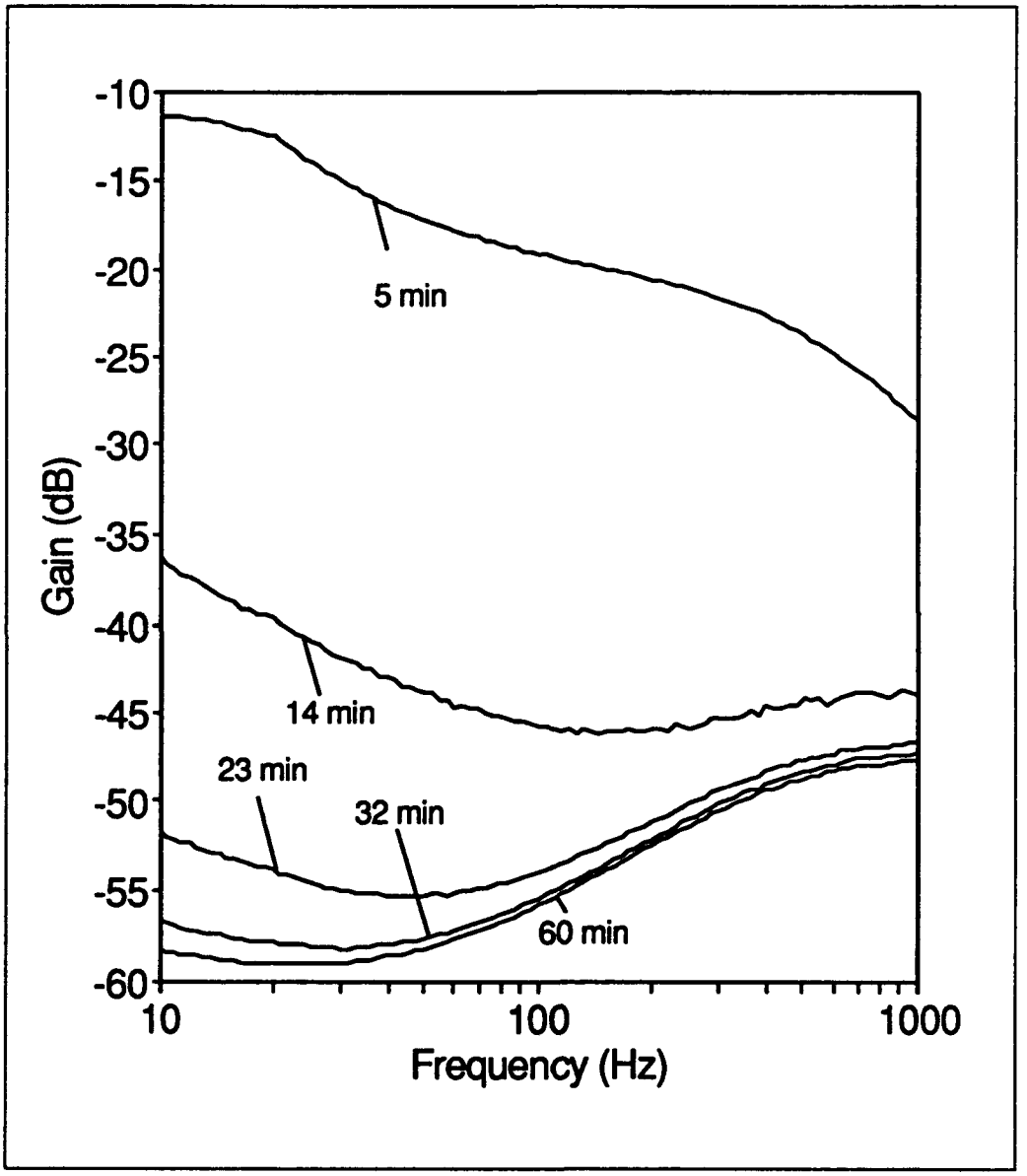

Figure 5.34. Gain of the IGE structure with respect to frequency for a sample cured at 55°C.

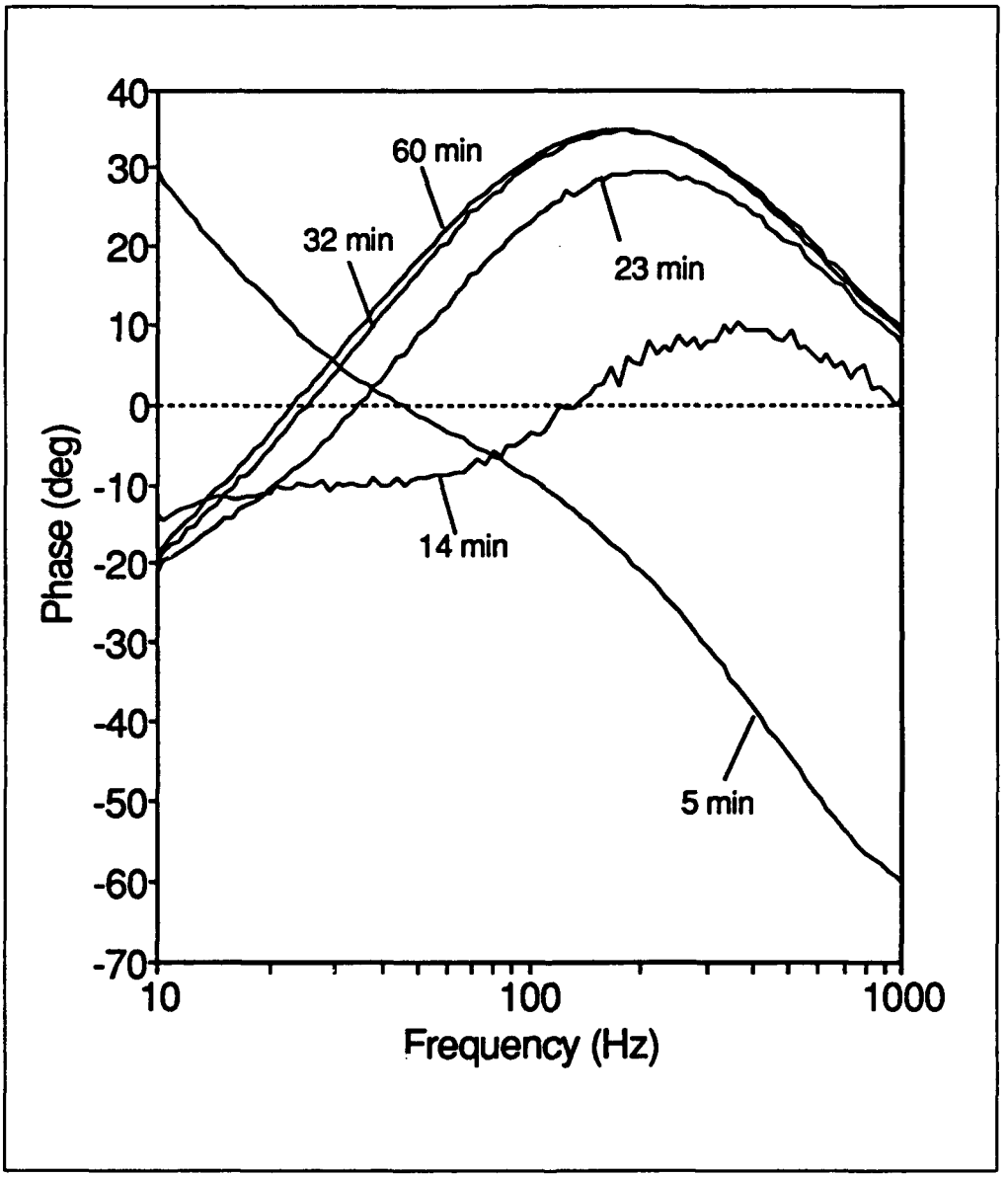

Figure 5.35. Phase delay of the IGE structure with respect to frequency for a sample cured at 55°C.

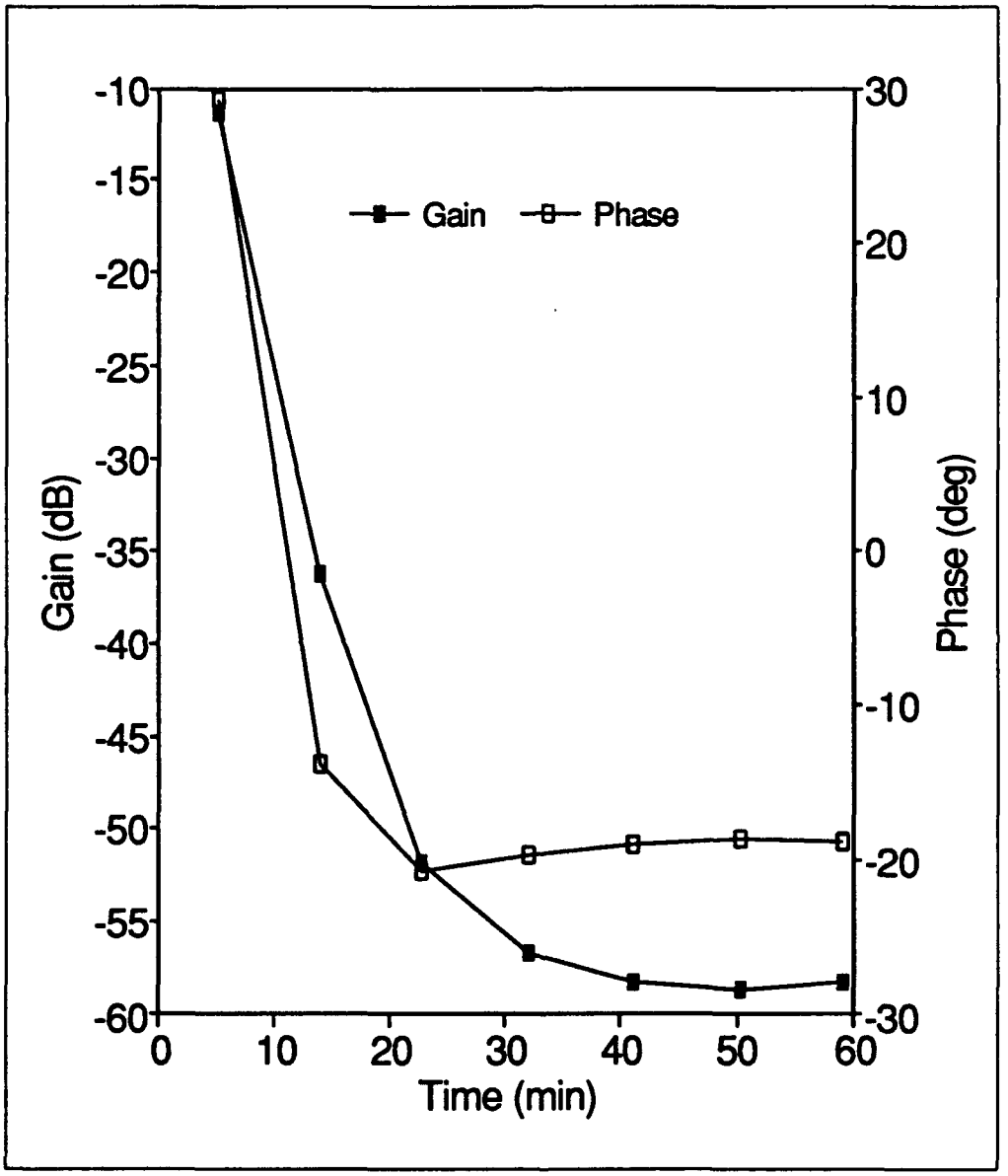

Figure 5.36. Gain and phase delay of the IGE structure with respect to time (frequency equal to 10 Hz) for a sample cured at 55°C.

A comparison between the two cures is presented in Figures 5.37 and 5.38. The gain of the IGE structure after the onset of gelation is much larger for the higher temperature cure. In addition, the phase delay characteristics for the higher temperature cure are markedly different relative to the 45°C cure. This seems to support the hypothesis that the 55°C cure cycle is affected by the proximity of this temperature to the glass transition temperature. That is, the material is softer and the molecular dipoles can respond more readily to electromagnetic stimuli.

Transfer Function of the IGEFET Sensor. The transfer function was measured across the IGEFET sensor for a 45°C cure cycle, and the results are presented in Figures 5.39 through 5.41. The information presented in these figures exhibits the same fundamental characteristics as the information presented for the gain and phase delay measurements of the IGE structure. The gain of the system (Figure 5.39) was increased, due to amplification, and the measurements appear to be less susceptible to noise. The phase delay curves (Figure 5.40) exhibit a characteristic "trough" which appears to decrease with respect to frequency as the cure progresses. The sensor element amplifier inverts the signal present at its input. Figure 5.41 illustrates that the gain and phase delay of the transfer function change very little after approximately 60 minutes into the cure, which coincides with the estimated gelation time of the sample.

The transfer function of the IGEFET sensor was also measured with respect to a 55°C cure cycle. The results of these measurements are presented in Figures 5.42 through 5.44. Again, the characteristics indicative of the onset of gelation (a sudden decrease in the rate of change of the measured electrical parameters) are apparent in these plots. This behavior is best depicted in Figure 5.44. The gain and phase delay slow their rates of change at approximately 25 minutes into the cure.

A comparison between the two cure temperatures is presented in Figures 5.45 and 5.46. The differences between the gain and phase delay characteristics for these two cure temperatures may be indicative of the proximity of the 55°C cure temperature to the glass transition temperature.

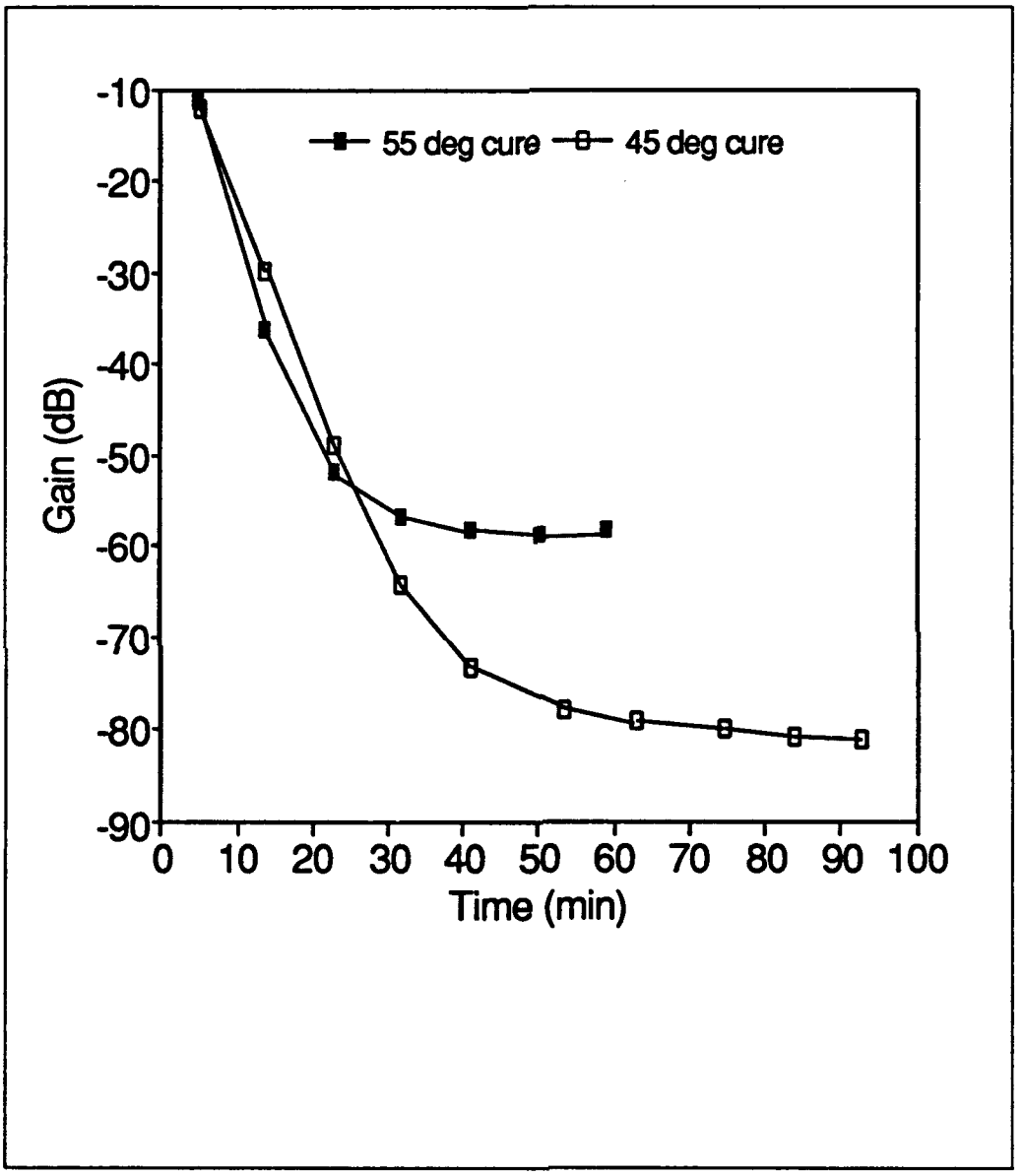

Figure 5.37. Gain of the IGE structure with respect to time (frequency equal to 10 Hz) for samples cured at 45°C and 55°C.

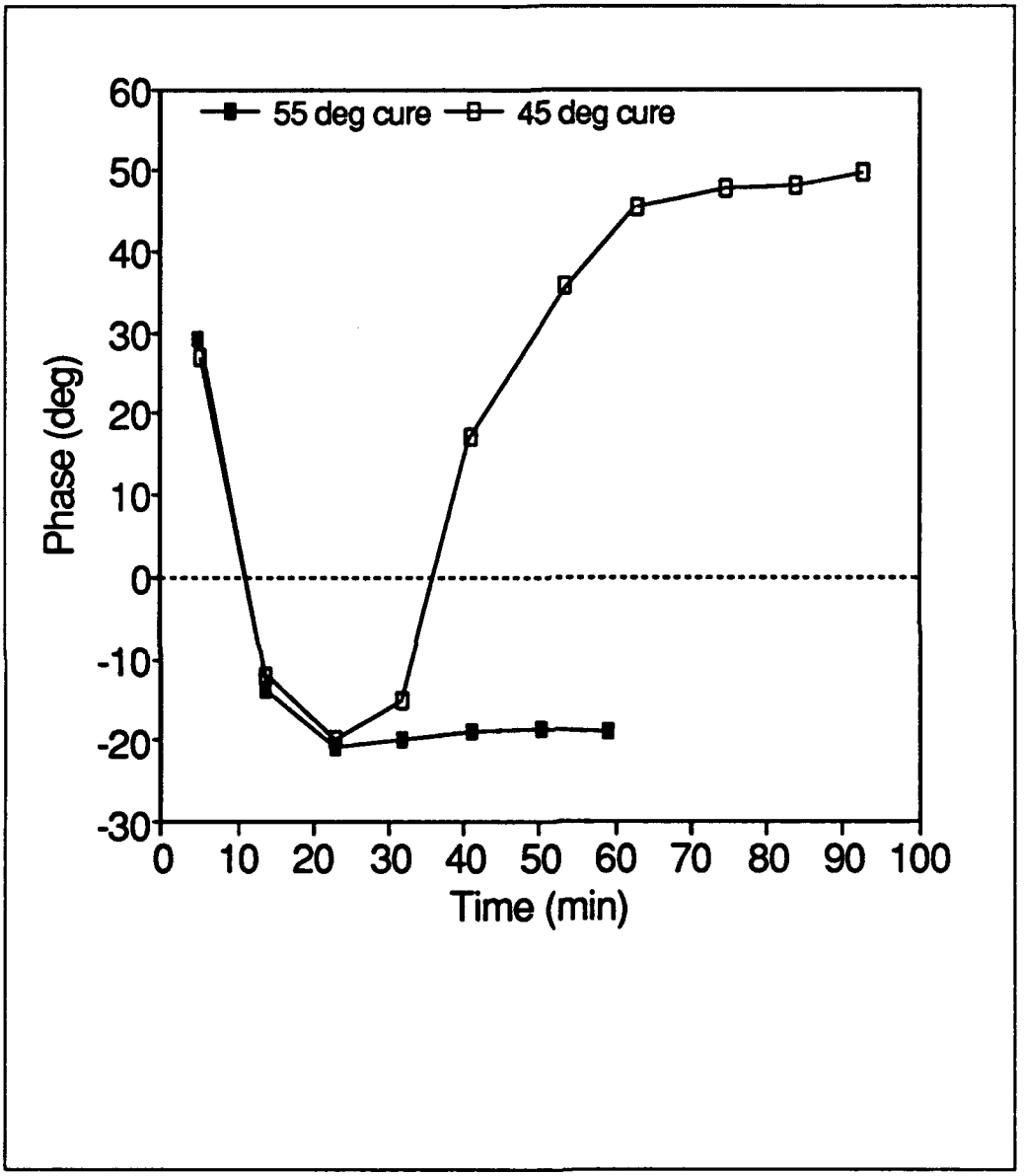

Figure 5.38. Phase delay of the IGE structure with respect to time (frequency equal to 10 Hz) for samples cured at 45°C and 55°C.

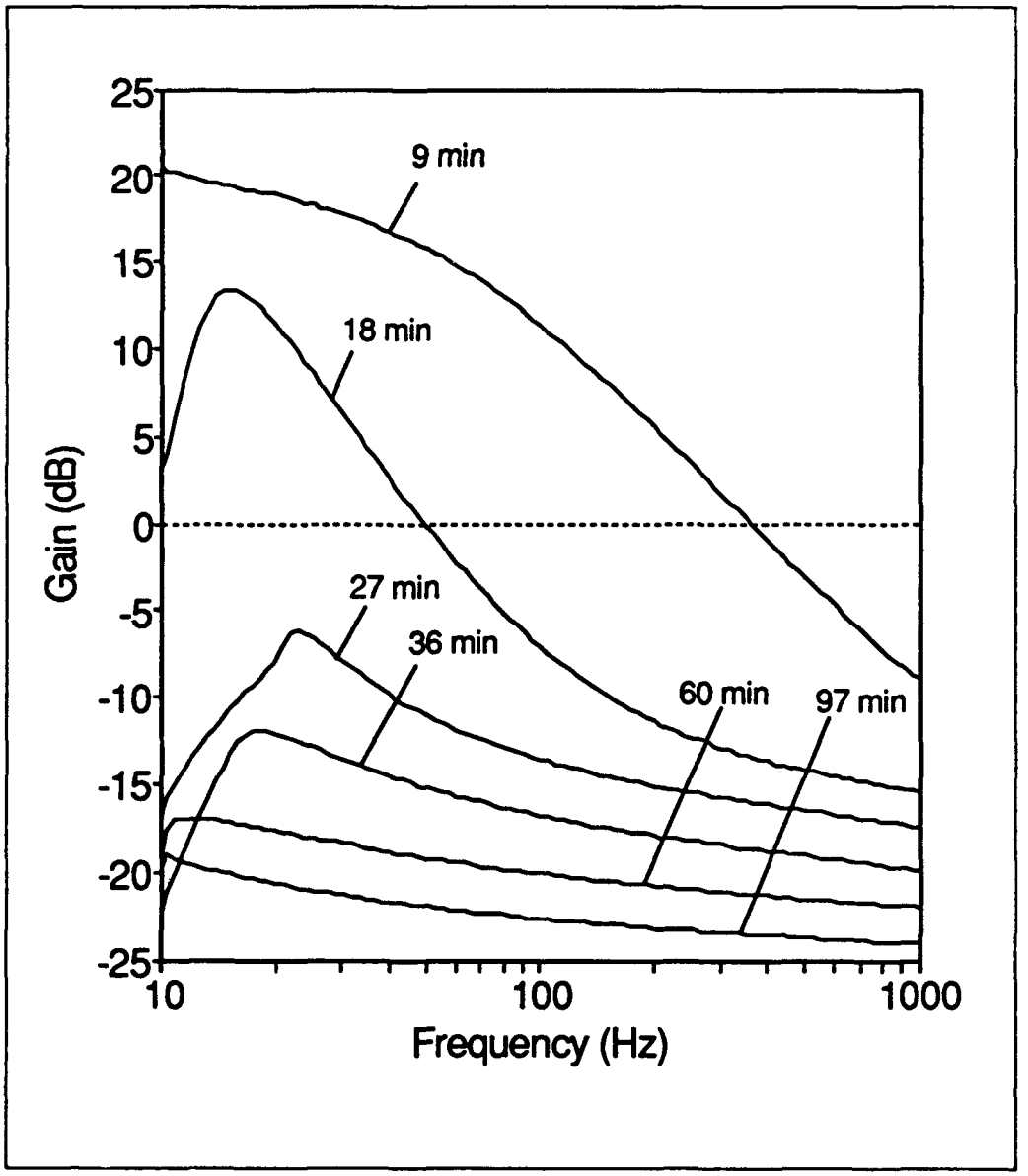

Figure 5.39. Gain of the IGEFET sensor with respect to frequency for a sample cured at 45°C.

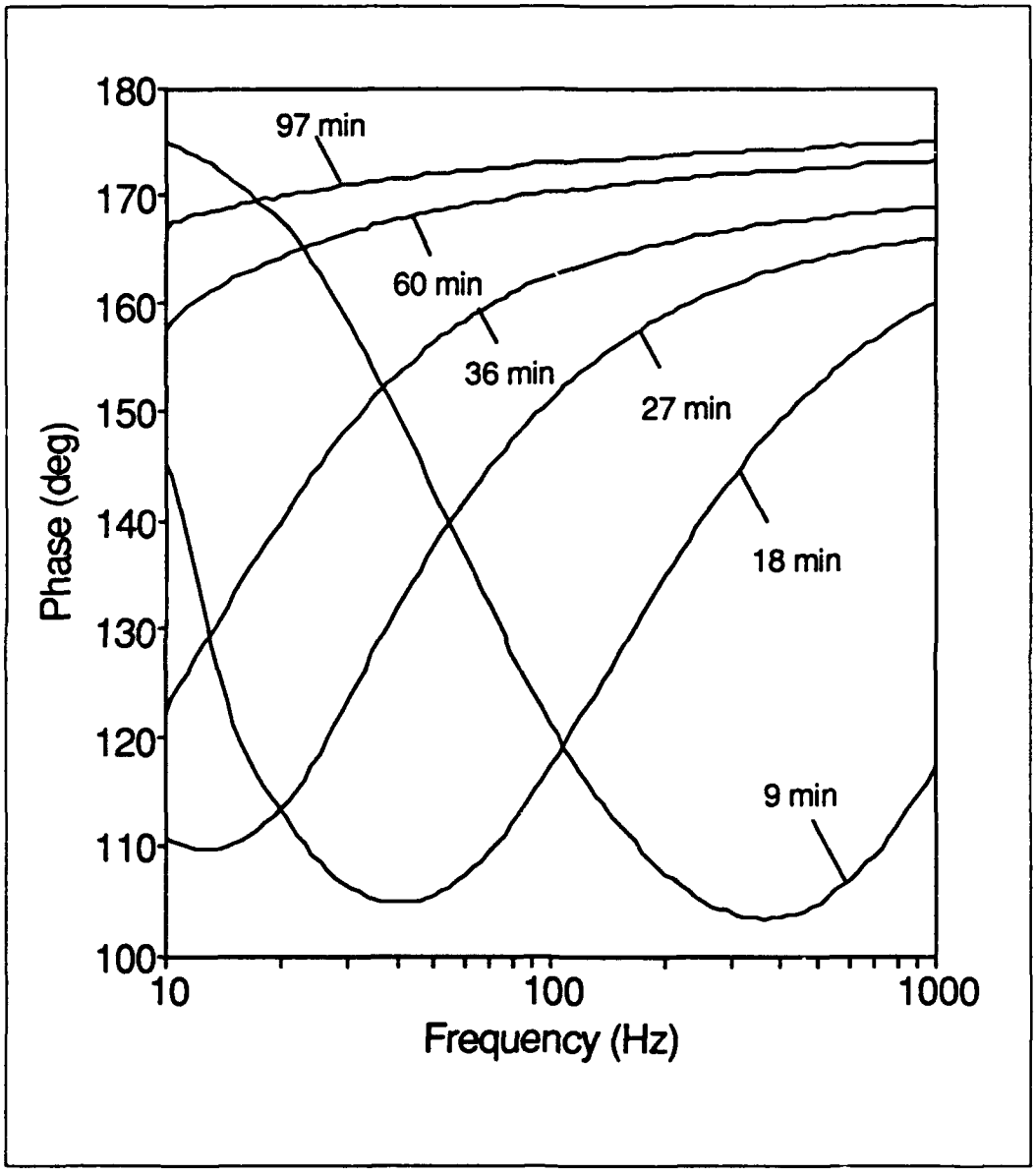

Figure 5.40. Phase delay of the IGEFET sensor with respect to frequency for a sample cured at 45°C.

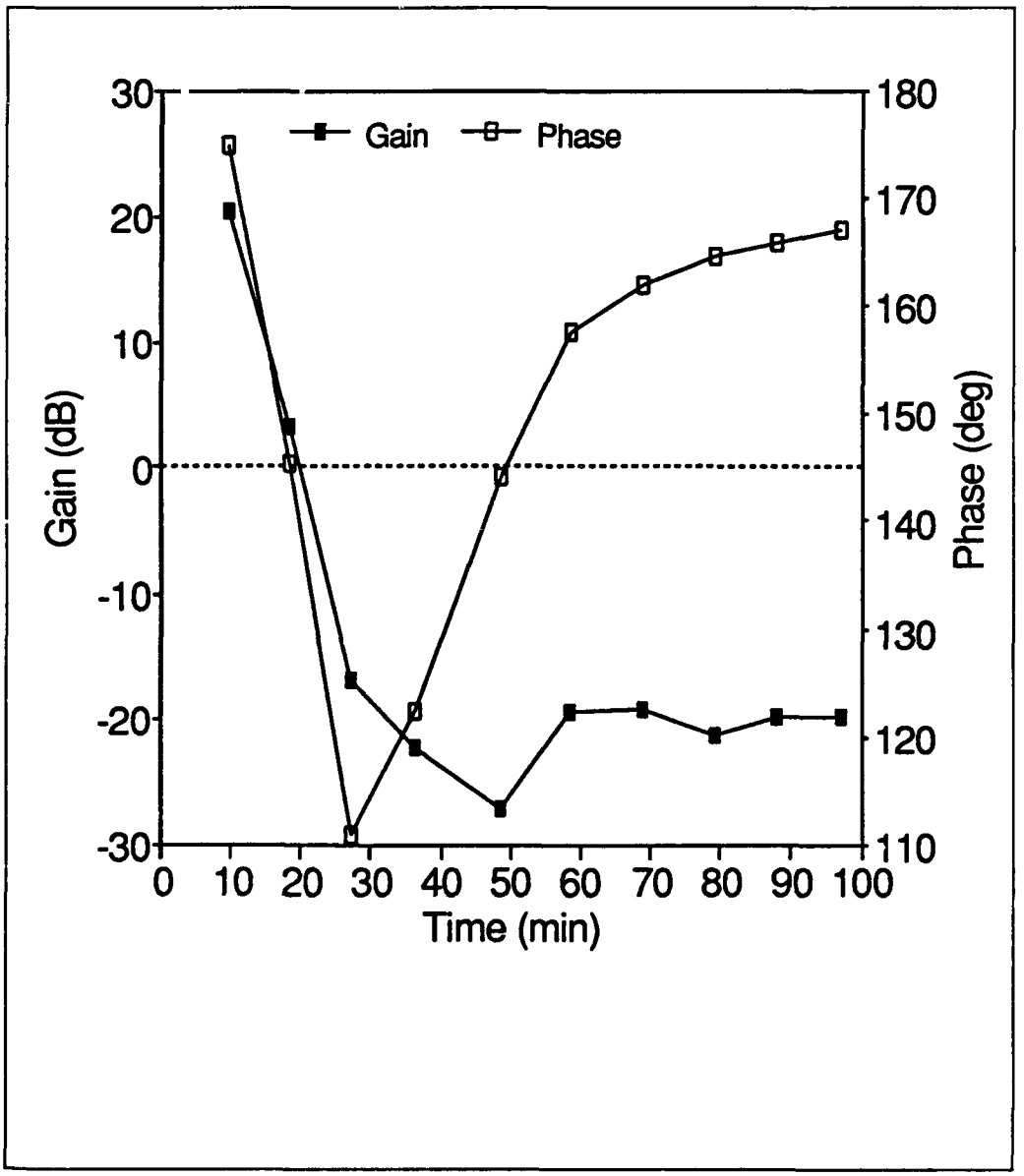

Figure 5.41. Gain and phase delay of the IGEFET sensor with respect to time (frequency equal to 10 Hz) for a sample cured at 45°C.

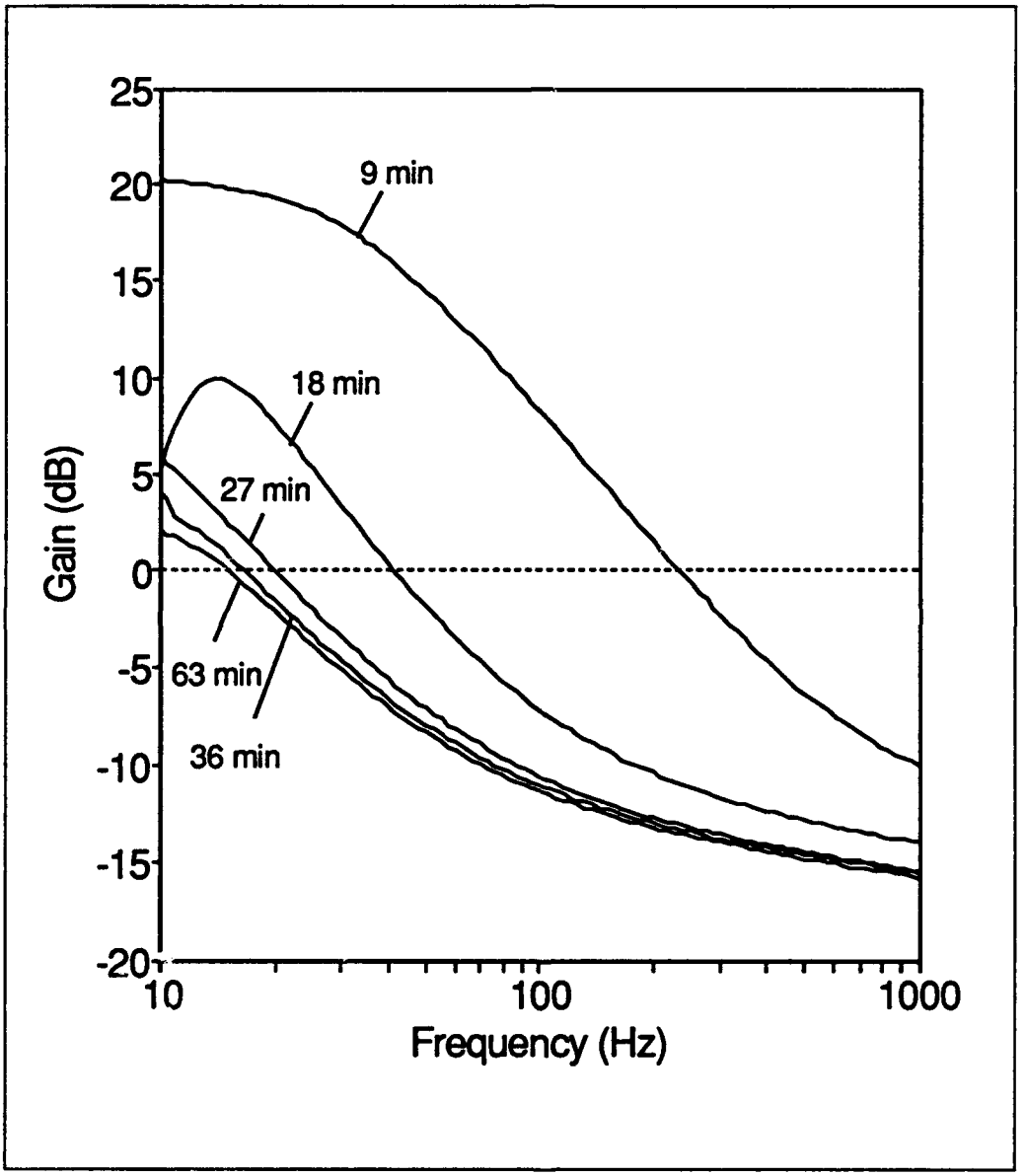

Figure 5.42. Gain of the IGEFET sensor with respect to frequency for a sample cured at 55°C.

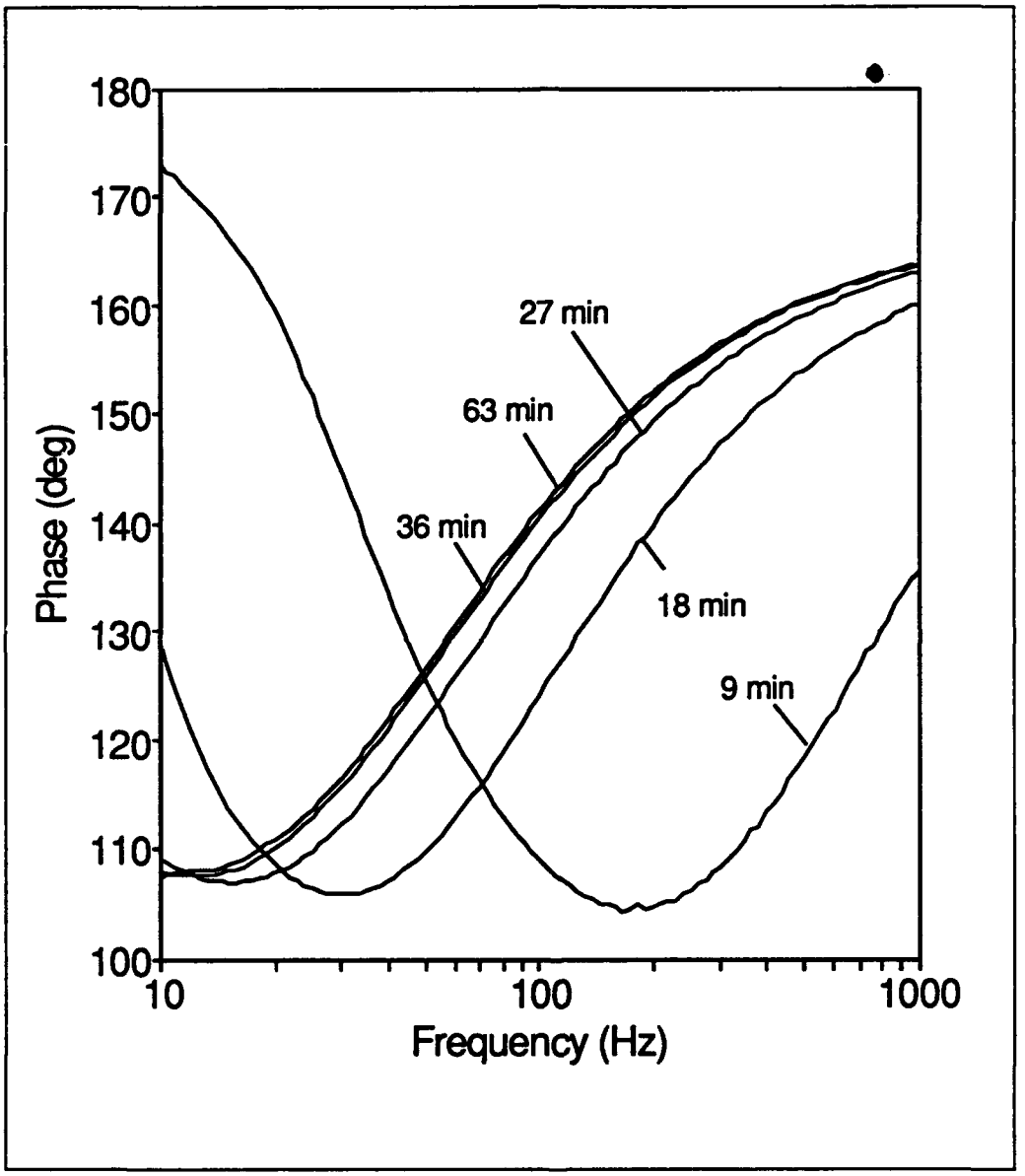

Figure 5.43. Phase delay of the IGEFET sensor with respect to frequency for a sample cured at 55°C.

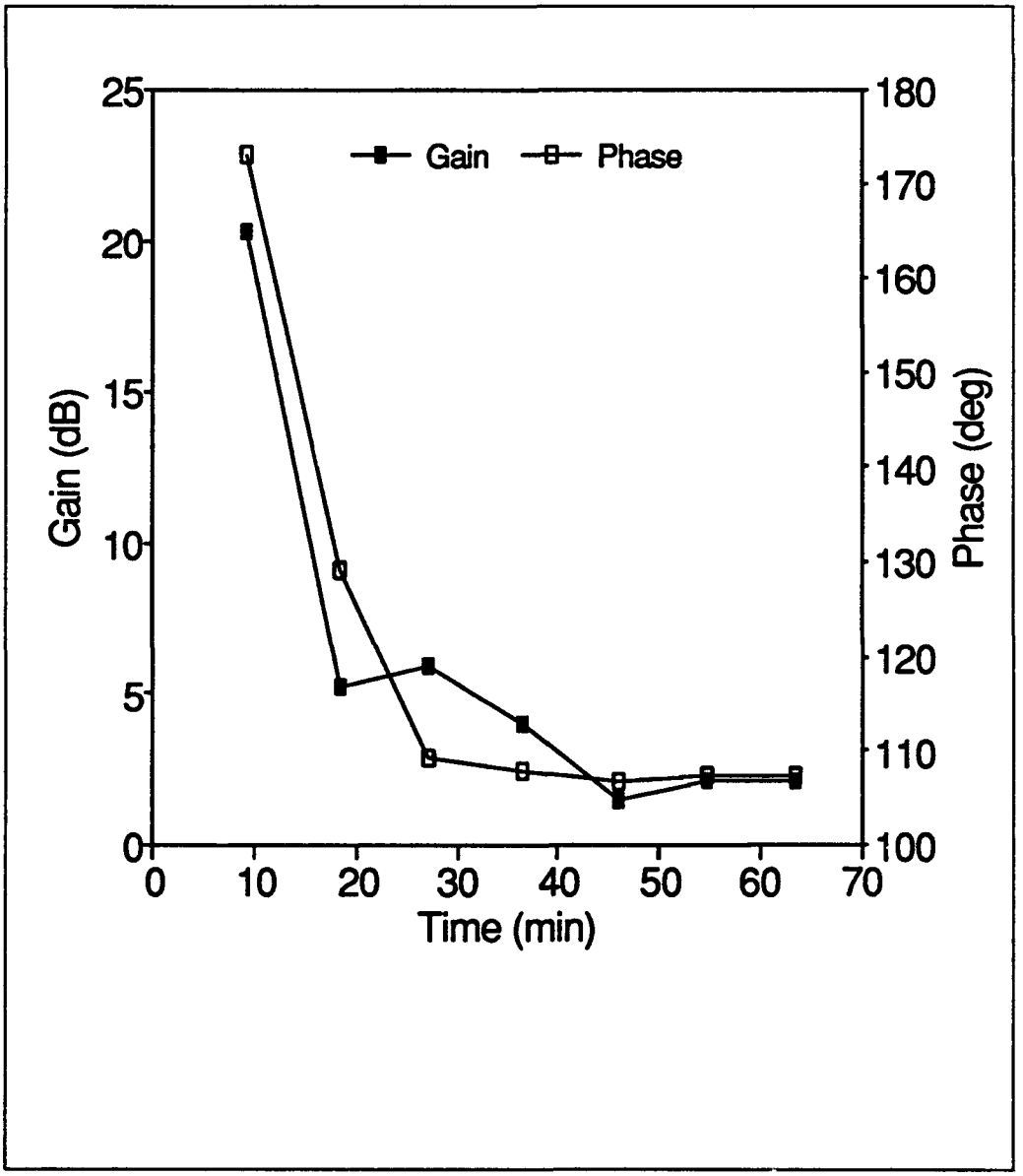

Figure 5.44. Gain and phase delay of the IGEFET sensor with respect to time (frequency equal to 10 Hz) for a sample cured at 55°C.

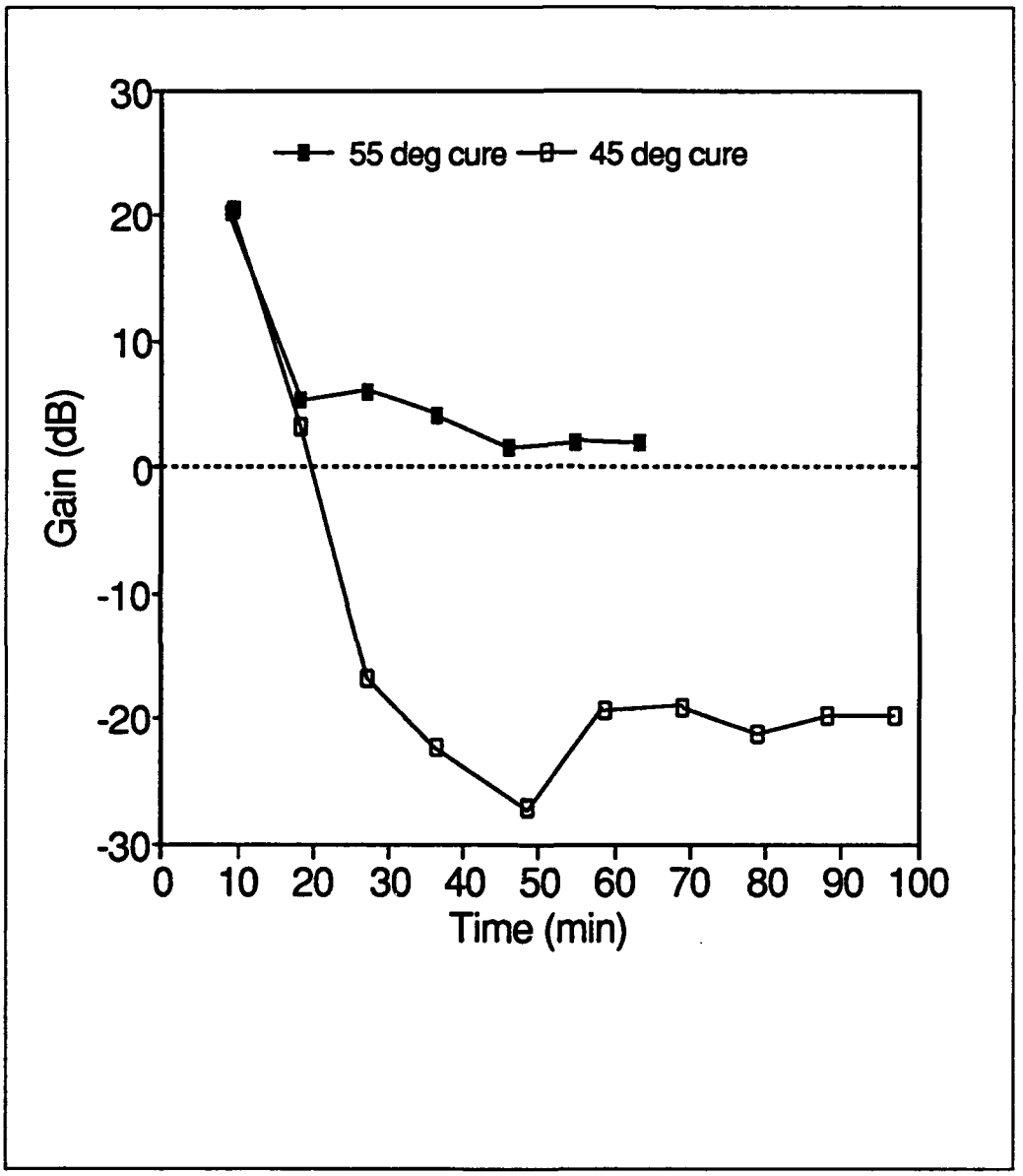

Figure 5.45. Gain of the IGEFET sensor with respect to time (frequency equal to 10 Hz) for samples cured at 45°C and 55°C.

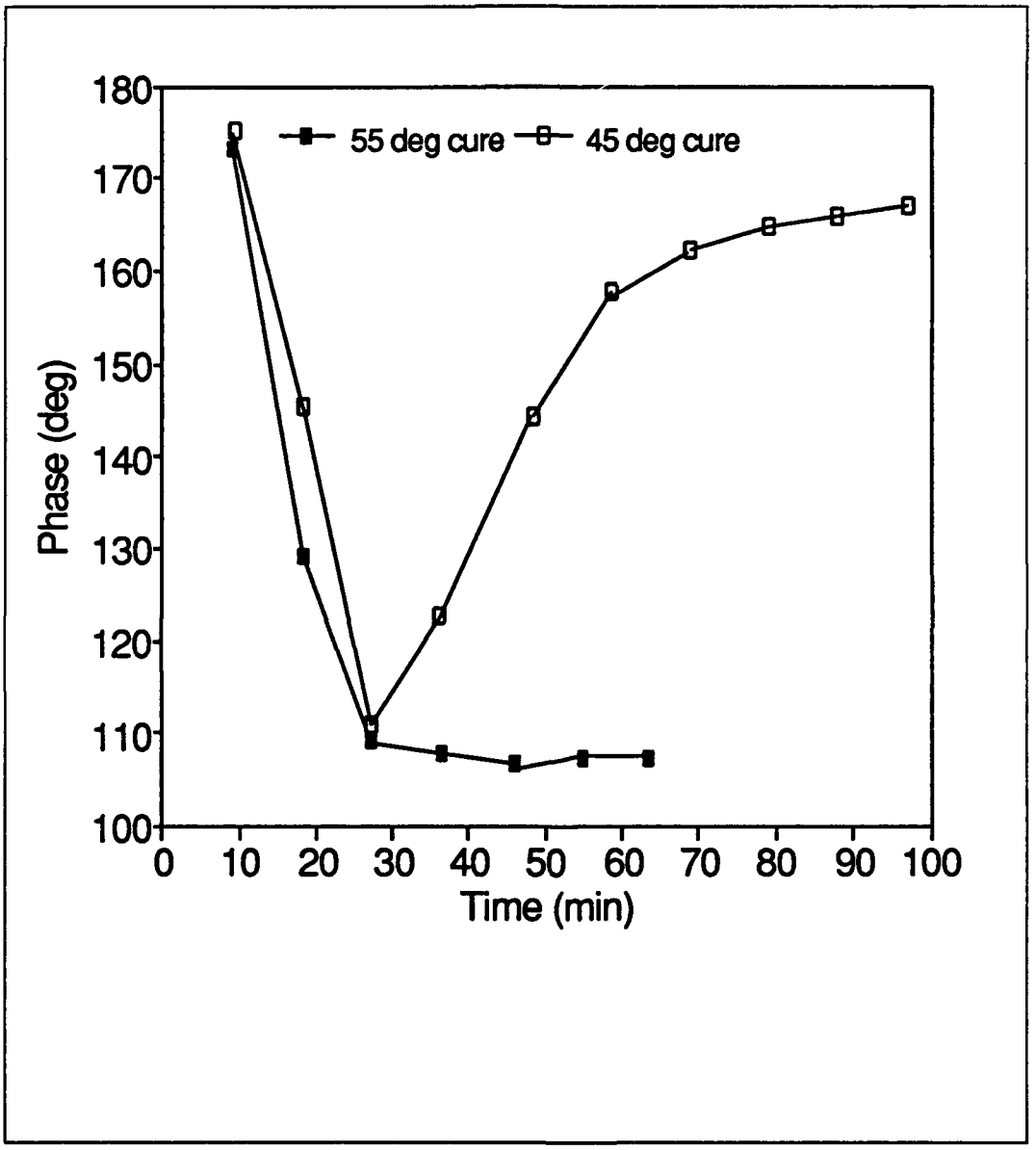

Figure 5.46. Phase delay of the IGEFET sensor with respect to time (frequency equal to 10 Hz) for samples cured at 45°C and 55°C.

Time-Domain Response of the IGEFET Sensor to a Pulsed Voltage Excitation Signal. The time-domain response of the IGEFET sensor to a pulsed voltage excitation signal was measured. The pulse used was a 3-volt, 5-μsec wide, 10 KHz repetitive frequency pulse. The reasons for choosing this signal were twofold. First, it was necessary to use a signal with sufficient energy. That is, the width and height of the pulse were selected such that the output response signal was measurable and well-behaved throughout the cure cycle. Second, in order to effectively dissipate the energy supplied by the excitation signal, it was necessary to use a period that was large compared to the pulse's width. The pulse's amplitude needed to be less than 5 volts to prevent exceeding the bias levels of the SE amplifier transistors. The 3-volt level was selected arbitrarily. The pulse's width was established experimentally. A resin sample was cured. During the cure cycle, the width of the pulse was varied. It was determined that in relation to a 10 KHz repetition frequency, a 5-μsec wide pulse contained enough information, and allowed the IGE-resin system to dissipate the energy prior to the application of a subsequent pulse. The excitation pulse is depicted in Figure 5.47. The results of the measurements for a 45°C cure are illustrated in Figures 5.48 and 5.49. The non-linear initial response of the sensor (the 5 minute contour in Figure 5.48) indicates that a significant amount of energy was not dissipated before the pulse was re-applied. This behavior changed within the first 10 minutes of the cure cycle. A gradual decrease in the amplitude of the output signal is illustrated in Figure 5.49, until, after 60 minutes, relatively little change in the amplitude occurs. This behavior is consistent with the estimated gelation point of the resin.

The time-domain response of the IGEFET sensor to a pulsed voltage excitation for a 55°C cure cycle is illustrated in Figure 5.50. The resin cured at this temperature exhibited a non-linear response during its initial cure times, as well. The system also exhibited a dramatic decrease in the rate of change of the amplitude in the vicinity of the estimated cure time.

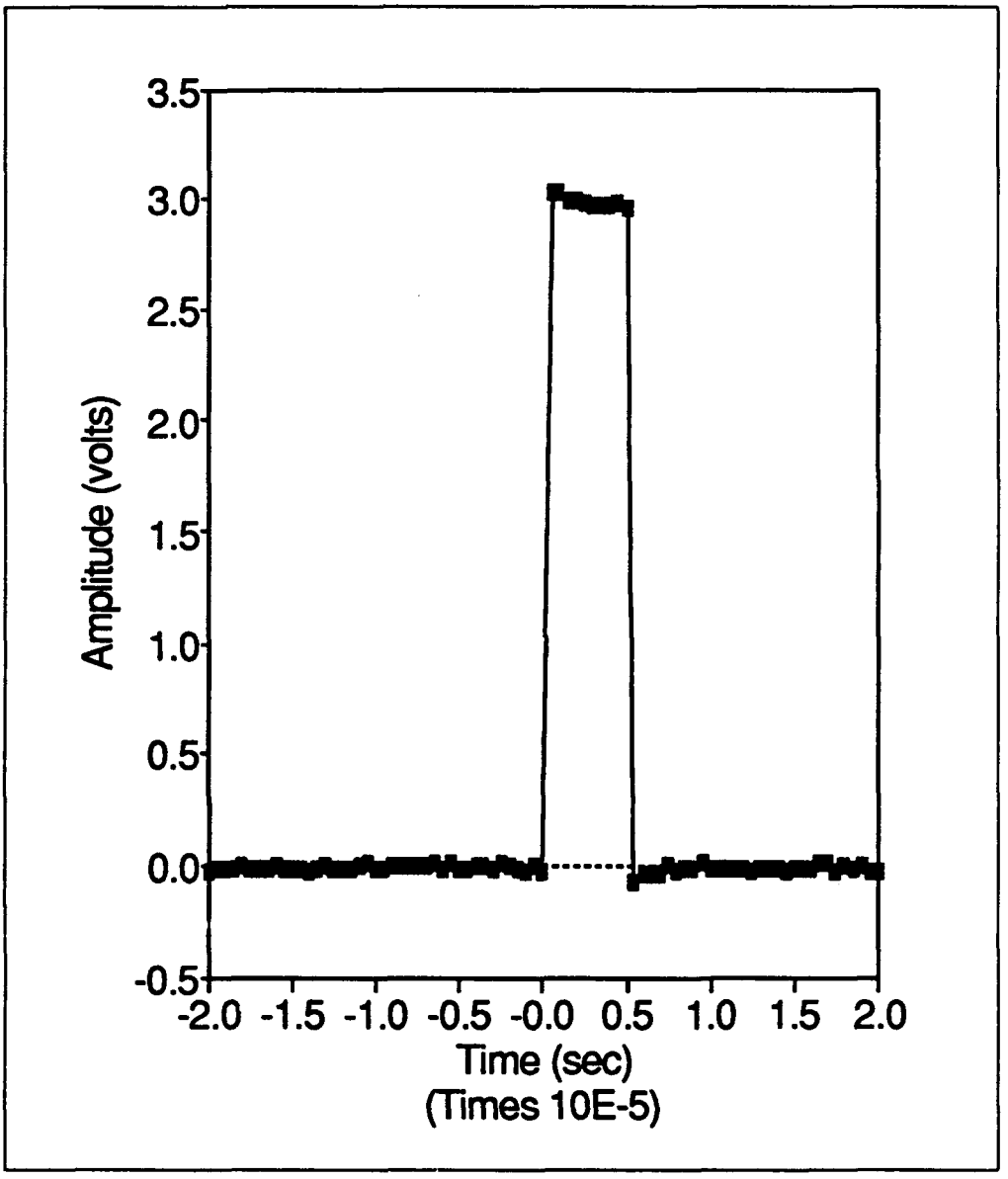

Figure 5.47. Excitation pulse used for the time-domain response measurements (a 40-μsec wide window is illustrated).

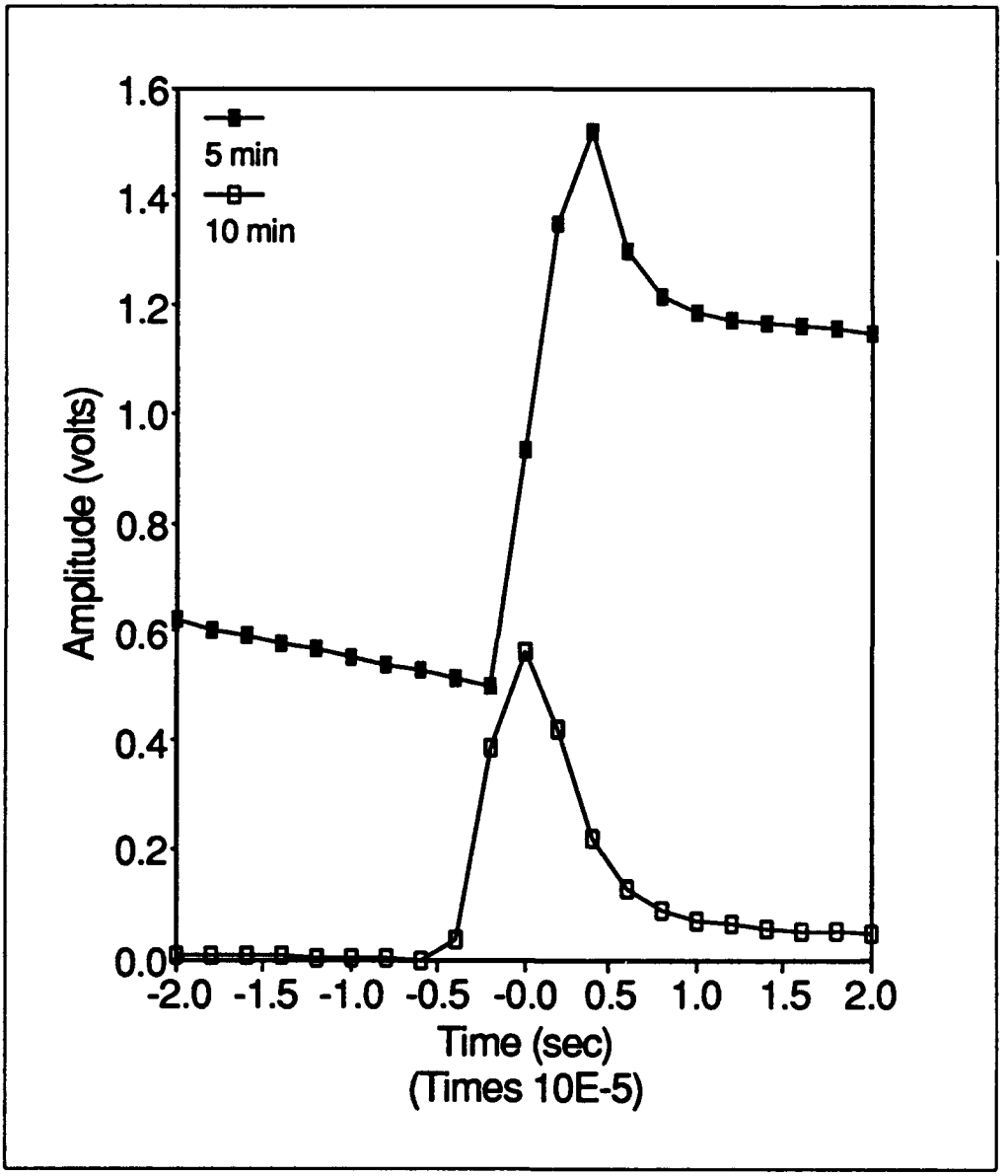

Figure 5.48. Time-domain response of the IGEFET sensor for the first 10 minutes of a 45°C cure cycle (a 40-μsec wide window is illustrated).

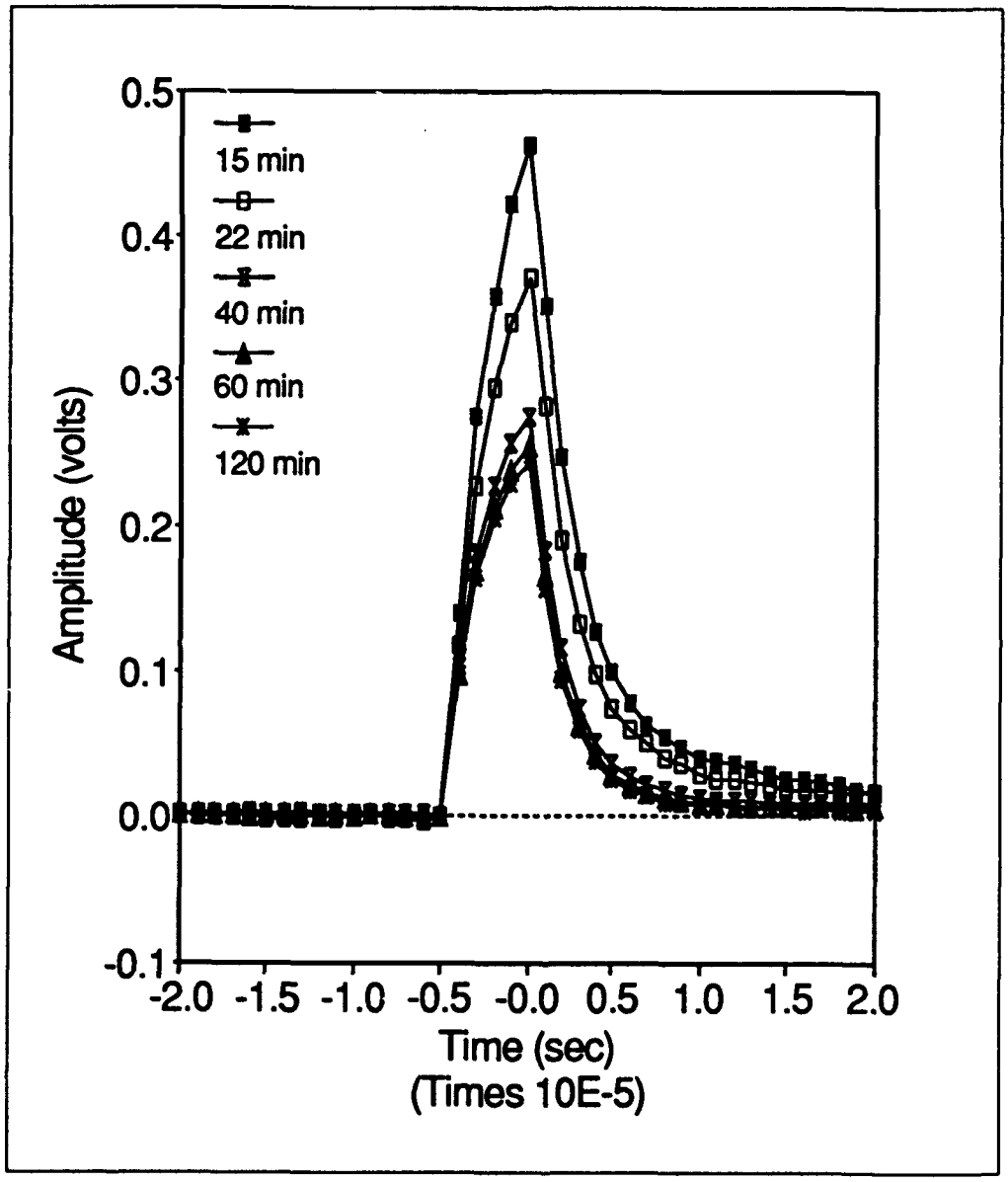

Figure 5.49. Time-domain response of the IGEFET sensor after the first 10 minutes of a 45°C cure cycle (a 40-μsec wide window is illustrated).

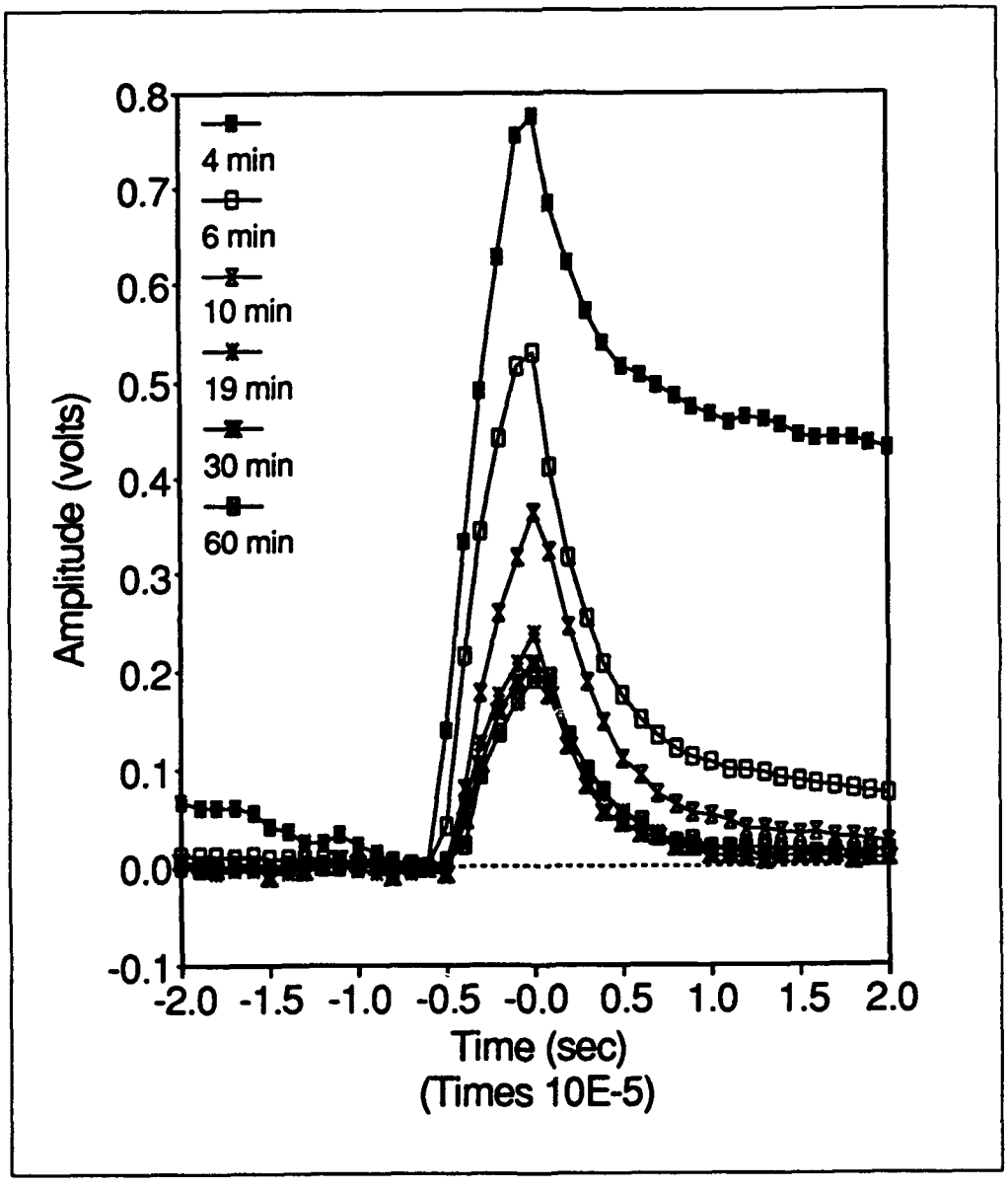

Figure 5.50. Time-domain response of the IGEFET sensor for a 55°C cure cycle (a 40 μsec wide window is illustrated).

Frequency-Domain Response of the IGEFET Sensor to a Pulsed Voltage Excitation Signal. The frequency-domain response of the IGEFET sensor to a pulsed voltage excitation signal was measured. The pulse used in these experiments had a 2 volt magnitude, a 5-μsec width, and a repetition frequency of 5 KHz. These parameters were determined empirically, by applying pulses to cured resin samples and observing their response. It was necessary to use a 2-volt amplitude pulse (as opposed to the 3-volt amplitude pulse used during the time-domain response measurements) because larger levels overloaded the low-noise amplifier. The 10 KHz frequency used in the time-domain study did not provide a sufficient number of harmonics for good resolution. A 5 KHz signal was used because it provided a sufficient number of harmonics within the frequency span of interest. The response was measured from 0 to 100 KHz. In this frequency range, there were 20 harmonics in addition to the fundamental.

The Fourier transform of the input signal (normalized) is depicted in Figure 5.51. Since the 3-dB cutoff frequency for the amplifier was 85 KHz, the amplitudes of the harmonics decrease somewhat in the vicinity of 100 KHz. The normalized Fourier spectrum of the reference element at 45°C is provided in Figure 5.52. The normalized difference Fourier transform spectra for the 45°C cure cycle are provided in Figure 5.53. The low frequency components of the response are manifested in the time-domain curves as slower rise and fall times early in the cure. In general the system exhibits gradual change across all frequencies throughout the cure until approximately 60 minutes into the reaction, when the resin's gelation point was attained. Similar trends were noted in the 55°C cure. The normalized Fourier transform spectum of the reference element at 55°C is illustrated in Figure 5.54. The normalized difference Fourier transform spectra for the 55°C cure cycle are provided in Figure 5.55. The most notable difference between Figures 5.53 and 5.55 is the magnitude of the response. The normalized difference Fourier transform magnitude for the 45°C cure is much larger than that of the 55°C cure.

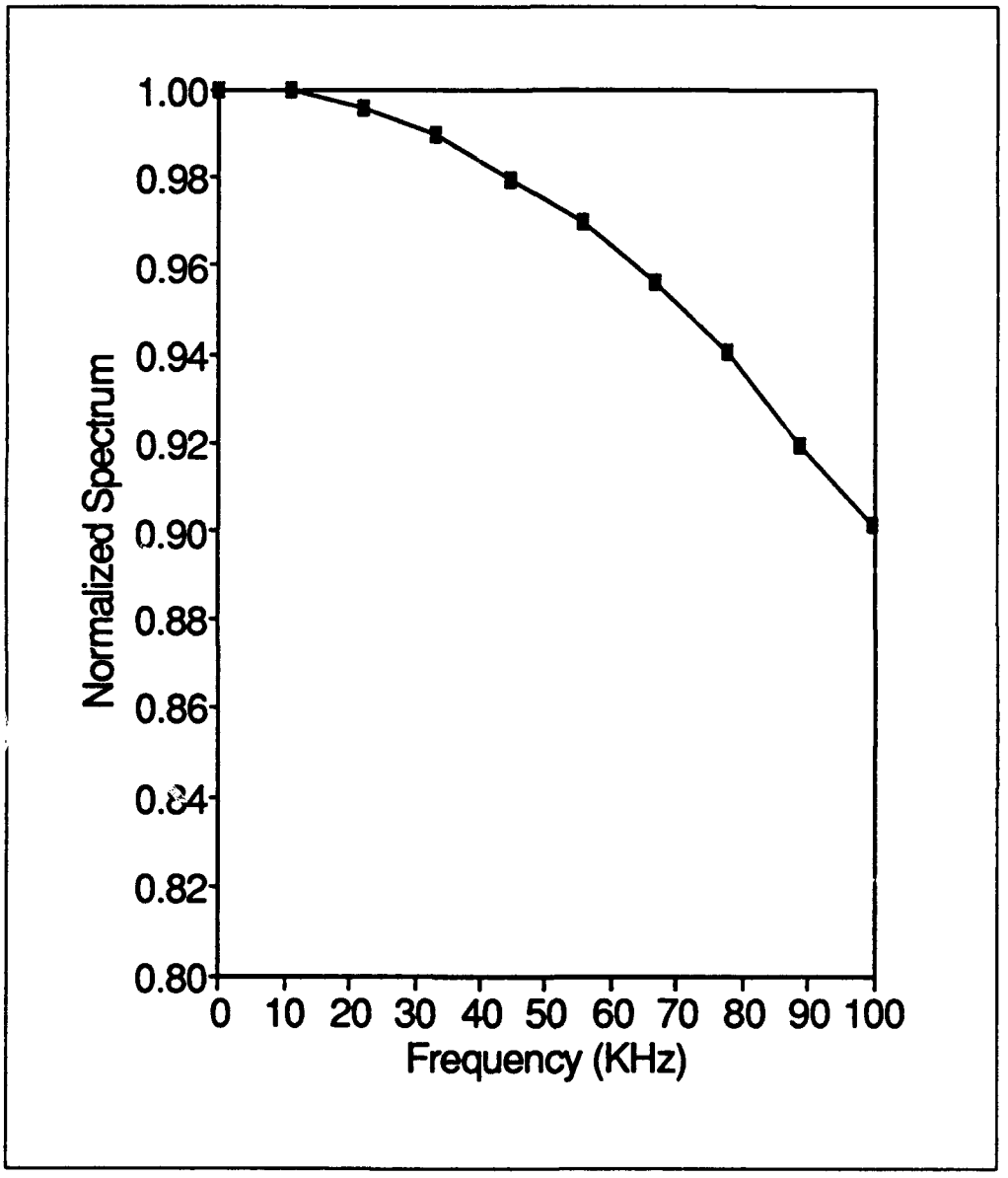

Figure 5.51. Normalized Fourier transform of the input signal used in the frequency-domain analysis.

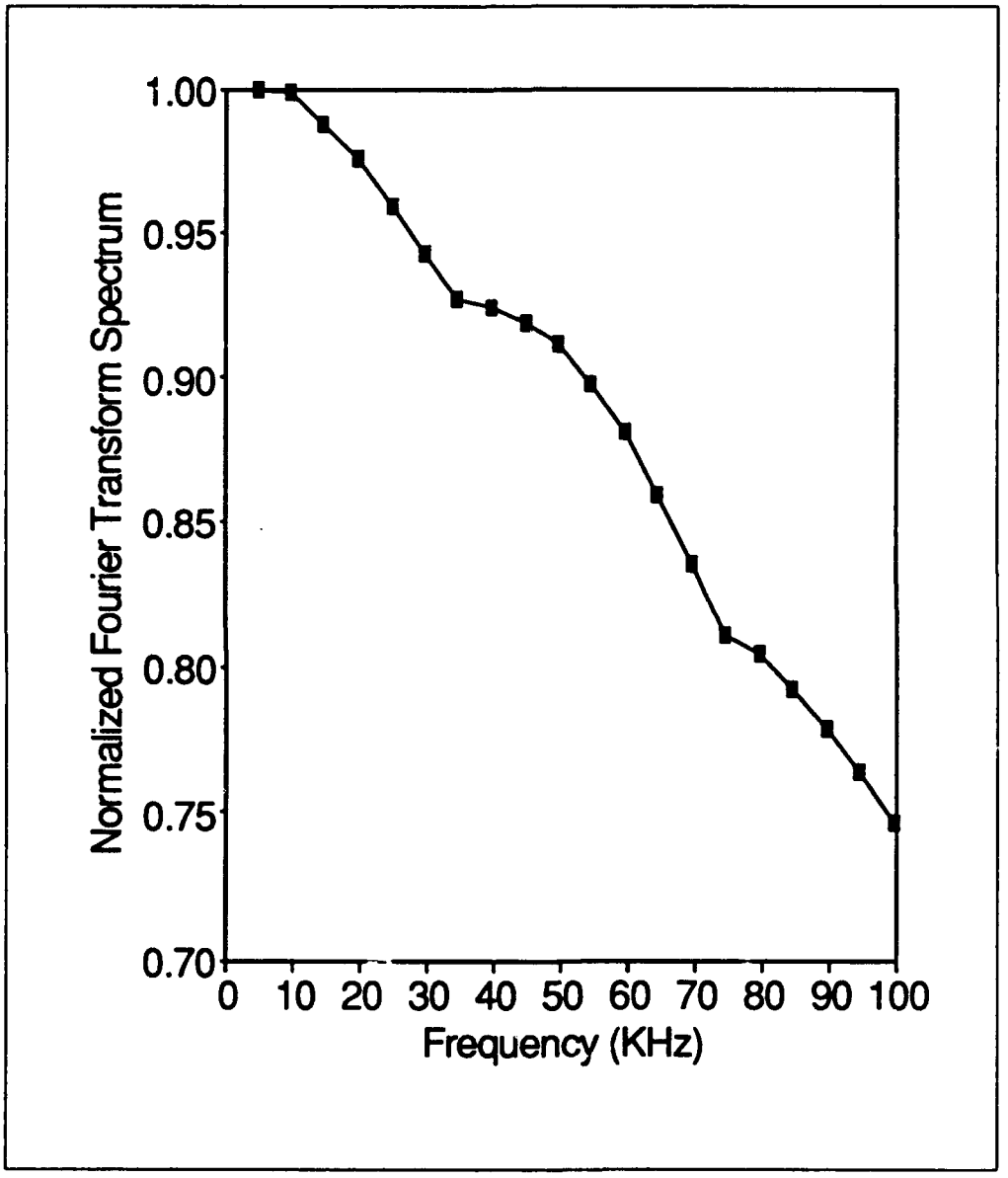

Figure 5.52. Normalized Fourier transform spectrum for the reference element at 45°C.

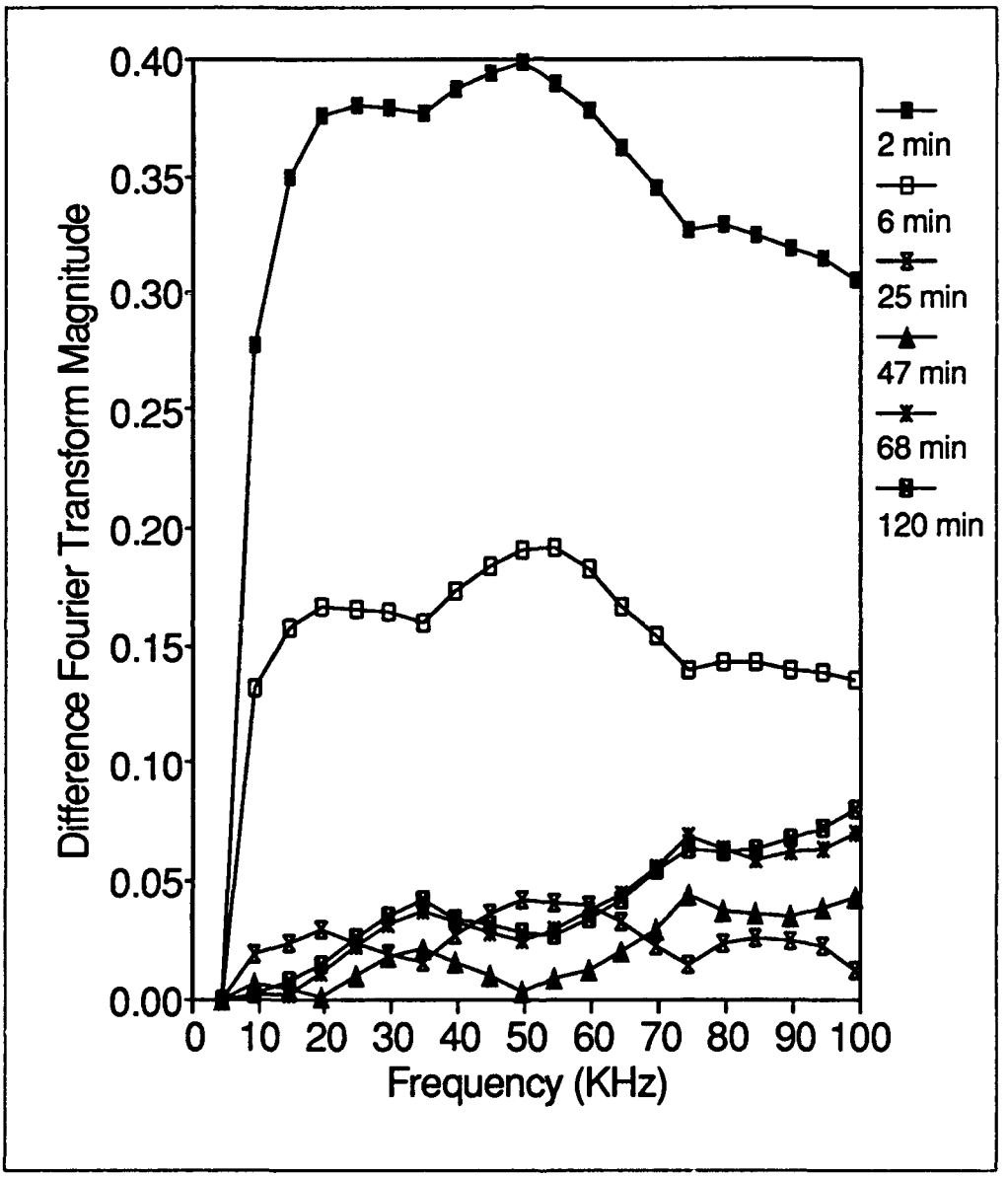

Figure 5.53. Normalized difference Fourier transform magnitude spectra for a 45°C cure.

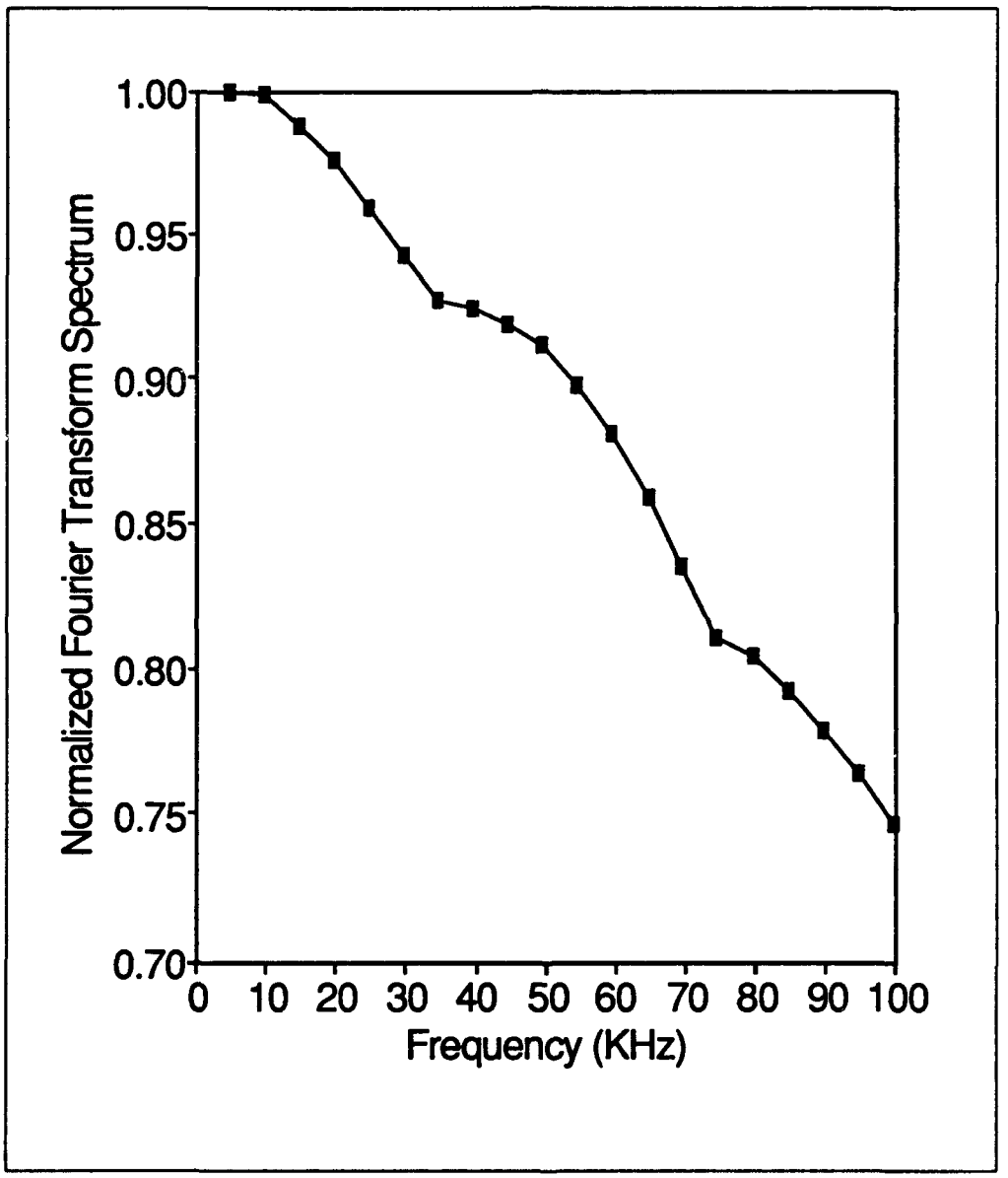

Figure 5.54. Normalized Fourier transform spectrum for the reference element at 55°C.

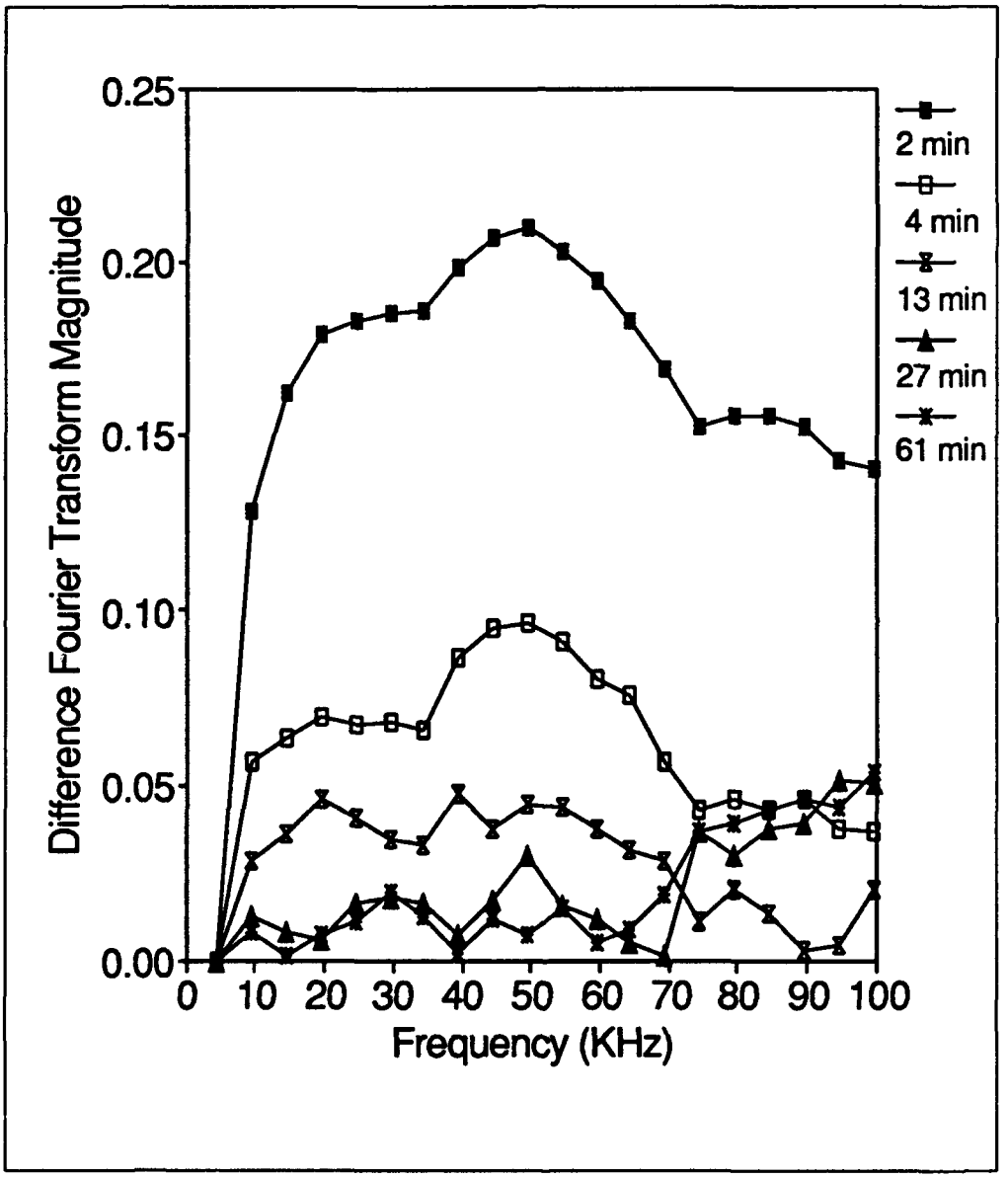

Figure 5.55. Normalized difference Fourier transform magnitude spectra for a 55°C cure.

Summary

The IGEFET integrated circuits were received from MOSIS and electrically tested. Problems were encountered with the multiplexer and demultiplexer circuits, and these circuits were bypassed. The sensor elements were utilized in the IGEFET sensor experiments without further amplification from the voltage follower or operational amplifier circuits.

Mechanical tests were conducted which indicated the range of temperatures for optimum cure, and two of these were selected for this research (45°C and 55°C). Further mechanical tests were performed to estimate the gelation times for these temperatures. Finally, torsional braid analysis was conducted to determine the glass transition temperature for samples cured at 45°C and 55°C.

Electrical tests were conducted to evaluate the IGEFET as a resin cure sensor. Given the results of the electrical tests, it was possible to estimate the gelation time of the resin. The information that appeared to be most useful in the characterization of the material was the impedance information. From a cure monitoring perspective, however, the gain-phase information and the normalized difference Fourier transform spectra provided acceptable results. The data associated with these measurements provided information regarding the gelation time of the resin, and it was easily interpreted. In general, the gelation point was manifested by a decreased rate of change in the measured electrical characteristic.

VI. Conclusions and Recommendations

Conclusions

An interdigitated gate electrode field-effect transistor (IGEFET) was designed, and its electrical performance as a sensor for monitoring the cure cycle of an epoxy resin was evaluated. The resin's molecular structure changed during its cure cycle. The physical change was indicated by altered impedance characteristics, which the IGEFET detected. The research was conducted in three phases. First, the IGEFET sensor was designed, and after it was fabricated, its operating characteristics were evaluated. Second mechanical characteristics of the resin were determined. Finally, the sensor's performance as an *in situ* resin cure monitor was characterized.

The IGEFET sensor design consisted of a 3 × 3 array of sensor elements (SEs). Each sensor element consisted of an interdigitated gate electrode (IGE) structure and an output amplifier. A metallic ground plane was fabricated beneath the IGE structure to provide a degree of ambient noise immunity, and also to facilitate characterizing the capacitance (to ground) of the IGE structure. An input excitation signal was coupled to the driven-electrode of the IGE structure by a demultiplexer, and the floating-electrode was connected to the input gate of the SE amplifier. The SE amplifier was a 3-stage NMOS enhancement-mode device. The output of the SE amplifier was coupled to the sensor's output buffers via a multiplexer. Two output buffers were included in the design, a voltage follower, and an operational amplifier. In addition to these sub-circuits, three capacitors were included in the design to facilitate characterizing the silicon dioxide layer between the IGE structure and the ground plane. The reference element was identical to the SE, except that the IGE structure was replaced by a solid metal plate to mimic the IGE structure's impedance.

The multiplexer and demultiplexer did not operate correctly, and they could not be used. Therefore, the only *in situ* signal amplification was provided by the sensor element amplifiers.

The mechanical characteristics of the resin were evaluated. The purpose of the evaluation was to determine the range of optimum cure temperatures, to determine the gelation time for two selected isothermal cure profiles, and to determine the glass transition temperature of the resin cured at both selected temperatures. A dynamic spectrometer was utilized for all these evaluations. The resin was cured with a ramped temperature profile to determine the optimum range of cure temperatures. The resin's complex viscosity was measured using the parallel plate mode of the dynamic spectrometer. The optimum cure temperature range corresponded to a range of temperatures over which the resin exhibited a reduced viscosity. Two temperatures were selected from this range (45°C and 55°C). Resin samples were then cured at each of these temperatures (again in a parallel plate mode) to determine the resin's characteristic gelation time for both isothermal cure profiles. Torsional bar analysis was performed using samples previously cured at each of the selected temperatures, and the glass transition temperature was determined. The glass transition temperature was 80°C for the samples cured at 45°C, and was 70°C for the samples cured at 55°C.

The IGEFET sensor was then evaluated as a resin cure monitor. This evaluation required seven electrical performance measurements for each of the isothermal cure profiles. The direct current resistance of the IGE structure was measured. The IGE structure's resistance was found to increase rapidly during the cure, and it remained relatively constant after gelation. The impedance of the IGE structure was measured, and it exhibited the same trend as the direct current resistance. That is, a rapid change in the impedance characteristics, followed by relatively little change after gelation, was observed. The electrical impedance measurements indicated that loss mechanisms (due primarily to ionic conduction) dominate the cure initially, and later in the cure, reactance dominates the impedance. The gain and phase delay of the IGE structure and the IGEFET sensor's transfer functions were measured. The results of these measurements corroborated the trends observed in other electrical measurements, specifically, the characteristic decrease in the rate of change of the measured characteristic after the gelation point was attained.

The gain and the phase delay changed dramatically during the initial stages of the cure cycle, but they changed relatively little after the resin's gelation. The time- and frequency-domain response of the IGEFET sensor were measured. They indicated a rapid decrease in energy transmitted through the resin during the cure cycle, followed by little change after the gelation point was attained. In general, the results of the IGEFET experiments corresponded well with the measured mechanical and chemical characteristics of the resin, particularly the time-to-gelation.

The sensor was able to discern important differences between resins cured at different temperatures. The low-temperature cure cycle (45°C) and the high-temperature cure cycle (55°C) exhibited markedly different electrical characteristics. In general, resins cured at both temperatures exhibited similar trends. However, the resin samples cured at 55°C were more lossy, as indicated by the direct current resistance and the impedance measurements. The transfer function of the resins cured at the higher temperature exhibited a much larger gain. These characteristics are indicative of a softer material. The 55°C cure temperature was in the vicinity of the resin's estimated glass transition temperature (70°C). The proximity of the glass transition temperature to the cure temperature may have resulted in the marked differences between the electrical characteristics of the two cure profiles.

In conclusion, the IGEFET sensor's utility as a resin cure monitor was demonstrated. It was able to detect changes in the resin's impedance which were a direct consequence of the cure process. It is clearly possible to estimate the resin's gelation time by analyzing the electrical data. Additionally, the IGEFET sensor was able to discern differences in the electrical characteristics of two resin samples cured at different temperatures.

Recommendations

The IGEFET sensor has clearly demonstrated utility as a resin cure sensor. Future research should be directed toward further improvement of the IGEFET sensor design, and further

evaluation of the sensor with different resins. The specific recommendations for future research include:

1. Eliminate glass cuts over signal lines from future designs. The glass cuts were intended to facilitate the excision of malfunctioning sub-circuits. The original approach for the resin cure evaluation was to coat the entire IGEFET sensor with resin. The glass cuts made this impossible, however, since the resin effectively shorted the exposed signal lines.
2. Place fewer sensor elements on the integrated circuit die, and locate them closer to the center of the integrated circuit. This would facilitate insulating the wire bonds, so that the entire sensor could be coated with resin. The inclusion of nine sensor elements for the IGEFET sensor applied to detect gaseous species is warranted, but it was of little utility for the resin cure studies.
3. Provide separate voltage supply input lines for each subcircuit. Thus, if one voltage supply line fails, only one sub- circuit is affected.
4. Use resins with lower viscosities. The resin used in this research was highly viscous in its uncured state. This characteristic facilitated applying the resin to the IGE structure. However, it precluded the possibility of performing tensile strength tests. The resin was too viscous to permit removal of air bubbles from the material. This operation is typically performed by exposing the resin to a vacuum. Providing the resin flows well, voids can be removed from the resin in this manner. Tensile strength tests require materials without discontinuities such as voids due to air bubbles. Since the material contained numerous voids, it could not be tested for tensile strength.
5. Use resins with a higher relative permittivity. This would permit measurement of the resin's low-frequency impedance after the gelation point, and it would facilitate a more complete electrical characterization of the resin.

6. Develop an automated cure monitoring system. A simple program could be written to measure the change in a particular electrical characteristic with time, and alert the researcher when the gelation time has been attained.

7. Develop the capability to accomplish accurate ramped temperature profile cures cycles. Ramped temperature profiles are more typical in practice than isothermal profiles.

Appendix A. *SPICE Simulation Program*

This appendix contains the SPICE3 code used to simulate the IGEFET's active electronics.

```
IGEFET

***************Subcircuit Models***********************


* Sensing element amplifier

.subckt amp 1 5 4 6

* NODES:
*  1 Vdd
*  5 Vss
*  4 input
*  6 output

*apply substrate bias

Vbias 9 0 dc -5v


*load bias

Ramp1 1 2 6.7e3
Ramp2 1 3 10e3
Ramp3 1 6 7.5e3
M1 2 4 5 9 N l=3U w=9U  as=81P  ad=81P
M2 3 2 5 9 N l=3U w=11U as=81P  ad=81P
M3 6 3 5 9 N l=3U w=12U as=108P ad=108P

.ends amp


*********************************************************


* Voltage Follower

.subckt damp 3 5 1 2 4

* NODES:
* 1 Vin-
* 2 Vin+
* 3 Vdd
* 4 output
```

```
* 5 Vss


*Current mirrors

M1 6 6 3 3 P l=6U w=36U as=324P ad=324P
M2 4 6 3 3 P l=6U w=36U as=324P ad=324P

*Positive input
M3 6 2 7 7 N l=3U w=24U as=216P ad=216P

*Negative input
M4 4 1 7 7 N l=3U w=24U as=216P ad=216P

*Current source
M5 7 0 5 5 N l=3U w=12U as=108P ad=108P

.ends damp


*********************************************************


* MUX  Approximation

*analog switch model

.subckt switch 1 2 3 4

* NODES:
* 1 input
* 2 N-switch control
* 3 P-switch control
* 4 output

* to turn on switch use -5 volts on P-switch
* and +5 on N-switch
* to turn off switch use +5 volts on P-switch
* and -5 on N-switch

* bias the switch substrate

vsubn 5 0 dc -5v
vsubp 6 0 dc 5v

*T-gate switch

m21 4 2 1 5 N l=3U w=15U as=135P ad=135P
m22 1 3 4 6 P l=3U w=15U as=135P ad=135P

.ends switch
```

```
**********************************************************


* Operational Amplifier

.subckt fbdamp 1 2 3 4 6

* NODES:
* 1 Vdd
* 2 Vss
* 3 Vin+
* 4 Voffset
* 6 Vout
* 10 Vin- (feedback)

MP1 5 5 1 1 P L=6u W=36u AD=288p AS=288p
MP2 6 5 1 1 P L=6u W=36u AD=288p AS=288p
MN1 5 3 7 7 N L=6u W=24u AD=192p AS=192p
MN2 6 10 7 7 N L=6u W=24u AD=192p AS=192p
MN3 7 0 2 2 N L=6u W=24u AD=192p AS=192P

R1 6 10 10k
R2 10 4 1k

.ends fbdamp




***************IGEFET Circuit***************************


* Voltages

Vdd 1 0 dc 5v
Vss 2 0 dc -5v


* The input voltage Vin is used to characterize
* the amplifiers' performance.  The input is applied
* at node 3.


Vin 3 0 dc 0.0 ac .01 0 sin(0 .01 1e6 0 0)
*Vin 3 0 dc 0.0 ac .0001 0 pulse(0 .0001 0 1e-6 1e-6 50e-6 100e-6)
```

```
*********************************************************

*  Sensing element amplifiers


* Selected element amplifier

x1 1 2 3 4 amp


* Unselected element amplifiers

*x11 1 2 3 41 amp
*x12 1 2 3 42 amp
*x13 1 2 3 43 amp
*x14 1 2 3 44 amp
*x15 1 2 3 45 amp
*x16 1 2 3 46 amp
*x17 1 2 3 47 amp
*x18 1 2 3 48 amp


* reference element amplifier

*x19 1 2 3 49 amp

*********************************************************


* MUX T-gate model

* turn on gate +5v on N-switch and -5v on P-switch
* turn-off is  -5v on P-switch and +5v on N-switch

* The N-switch is the second node listed
* The P-switch is the third node listed

* Control voltages

VcntrlN 5 0 dc 5v
VcntrlP 6 0 dc -5v


* Selected element output signal

x2 4 5 6 7 switch
```

```
* Unselected element output signals

*x21 41 6 5 7 switch
*x22 42 6 5 7 switch
*x23 43 6 5 7 switch
*x24 44 6 5 7 switch
*x25 45 6 5 7 switch
*x26 46 6 5 7 switch
*x27 47 6 5 7 switch
*x28 48 6 5 7 switch
*x29 49 6 5 7 switch

**********.**************************************************


* Voltage Follower

x3 1 2 9 7 9 damp

* Simulated Load

rload 9 0 1e6
cload 9 0 2e-12


*Node 9 is the voltage follower output node

**********************************************************


* Operational Amplifier

* Stage 1

Voff1 11 0 dc -5V
x2 1 2 7 11 10 fbdamp


* Stage 2

*Voff2 13 0 dc -5V
*x3 1 2 10 13 12 fodamp


* Stage 3

*Voff3 15 0 dc -5V
*x4 1 2 12 15 14 fbdamp
```

```
* Stage 4

*Voff4 17 0 dc -5V
*x5 1 2 14 17 16 fbdamp

* Stage 5

*Voff5 19 0 dc -5V

*MP1 25 25 1 1 P L=6u W=36u AD=288p AS=288p
*MP2 26 25 1 1 P L=6u W=36u AD=288p AS=288p
*MN1 25 16 27 27 N L=6u W=24u AD=192p AS=192p
*MN2 26 28 27 27 N L=6u W=24u AD=192p AS=192p
*MN3 27 0 2 2 N L=6u W=24u AD=192p AS=192P

*R1 26 28 3k
*R2 28 19 10k
*R3 26 0 1000k
*C1 28 0 10pf


* Output of op amp is at node 10


***************Device Models*************************

.model orbit_du2 r rsh = 77.2 defw = 0 narrow = 0
.model orbit_du2 c cj = .00021024 cjsw = 1.8745e-10 defw = 0 narrow = 0
.model orbit_du1 r rsh = 23.1 defw = 0 narrow = 0
.model orbit_du1 c cj = .0003871 cjsw = 4.267e-10 defw = 0 narrow = 0
.model orbit_ml2 r rsh = .027 defw = 0 narrow = 0
.model orbit_ml2 c cj = 0 cjsw = 0 defw = 0 narrow = 0
.model orbit_ml1 r rsh = .054 defw = 0 narrow = 0
.model orbit_ml1 c cj = 0 cjsw = 0 defw = 0 narrow = 0
.model P pmos level=4
+ vfb = -.205514 lvfb = -.112387 wvfb = .319501
+ phi = .651256 lphi = 0 wphi = 0
+ k1 = .42996 lk1 = .060703 wk1 = -.105273
+ k2 = -.0122414 lk2 = .0595048 wk2 = -.0518187
+ eta = -.00775855 leta = .0600061 weta = .0289938
+ muz = 243.186 dl = .555117 dw = -.0268719
+ u0 = .131183 lu0 = .0256252 wu0 = -.0655868
+ u1 = .019488 lu1 = .29191 wu1 = -.102029
+ x2mz = 9.97779 lx2mz = -4.71751 wx2mz = 7.63253
+ x2e = .000646816 lx2e = -.00478671 wx2e = .000828692
+ x3e = .000729091 lx3e = -.00508643 wx3e = 7.79742e-05
+ x2u0 = .00603891 lx2u0 = -.00382796 wx2u0 = .00733918
+ x2u1 = -.000380988 lx2u1 = .00358808 wx2u1 = .0012638
+ mus = 243.886 lmus = 158.17 wmus = -66.7849
+ x2ms = 8.21881 lx2ms = 1.75711 wx2ms = 9.82284
+ x3ms = -1.45603 lx3ms = 18.4551 wx3ms = -10.9435
```

```
+ x3u1 = -.0168526 lx3u1 = .00395624 wx3u1 = .00243354
+ tox = .0405 temp = 27 vdd = 5
+ cgdo = 3.54981e-10 cgso = 3.54981e-10 cgbo = 6.52295e-10
+ xpart = 1
+ n0 = 1 ln0 = 0 wn0 = 0
+ nb = 0 lnb = 0 wnb = 0
+ nd = 0 lnd = 0 wnd = 0
+ rsh = 77.2 cj = .00021024 cjsw = 1.8745e-10
+ js = 0 pb = .7 pbsw = .7
+ mj = .4434 mjsw = .2054 wdf = 0
+ dell = 0
.model N nmos level=4
+ vfb = -.799628 lvfb = .0358389 wvfb = -.0770939
+ phi = .760829 lphi = 0 wphi = 0
+ k1 = 1.09084 lk1 = .0195692 wk1 = .503221
+ k2 = .00314699 lk2 = .0712321 wk2 = .0627686
+ eta = -.00483964 leta = .0111977 weta = .0124884
+ muz = 568.326 dl = .877101 dw = .124542
+ u0 = .0547895 lu0 = .0455111 wu0 = -.044398
+ u1 = .0202084 lu1 = .538695 wu1 = -.224314
+ x2mz = 14.9246 lx2mz = -25.8935 wx2mz = 40.4786
+ x2e = .000511543 lx2e = -.0078186 wx2e = -.00398345
+ x3e = .000571135 lx3e = -.00175635 wx3e = -.00386746
+ x2u0 = .00269152 lx2u0 = -.0119917 wx2u0 = .0208939
+ x2u1 = -.00220636 lx2u1 = .0113252 wx2u1 = .0138775
+ mus = 572.011 lmus = 339.156 wmus = -2.31256
+ x2ms = 5.29578 lx2ms = -15.3472 wx2ms = 85.7263
+ x3ms = -.60994 lx3ms = 64.5514 wx3ms = -32.2786
+ x3u1 = .00515024 lx3u1 = .0574119 wx3u1 = -.0347952
+ tox = .0405 temp = 27 vdd = 5
+ cgdo = 5.60881e-10 cgso = 5.60881e-10 cgbo = 6.89101e-10
+ xpart = 1
+ n0 = 1 ln0 = 0 wn0 = 0
+ nb = 0 lnb = 0 wnb = 0
+ nd = 0 lnd = 0 wnd = 0
+ rsh = 23.1 cj = .0003871 cjsw = 4.267e-10
+ js = 0 pb = .8 pbsw = .8
+ mj = .4626 mjsw = .348 wdf = 0
+ dell = 0

.OPTIONS DEFL=3U DEFW=6U DEFAS=45P DEFAD=45P
+ITL1=500  ITL4=30 ABSTOL=100P VNTOL=100U CHGTOL=1E-14
+NOPAGE  RELTOL=.005 CPTIME=5000
.WIDTH OUT=80

.END
```

Appendix B. *MOSIS Parametric Test Results*

The MOSIS parametric test results and the IGEFET bonding pad arrangement are herein provided.

MOSIS PARAMETRIC TEST RESULTS

RUN: N03U / UNIFICATION
TECHNOLOGY: SCPE

VENDOR: ORBIT
FEATURE SIZE: 2.0um

I. INTRODUCTION. This report contains the lot average results obtained by MOSIS from measurements of the MOSIS test structures on the selected wafers of this fabrication lot. The SPICE LEVEL 2 and BSIM parameters obtained from similiar measurements on these wafers are also attached.

COMMENTS: This looks like a typical Orbit Semiconductor 2.0um run.

II. TRANSISTOR PARAMETERS:

	W/L	N-CHANNEL	P-CHANNEL	UNITS
Vth (Vds=.05V)	3/2	1.021	-.812	V
Vth (Vds=.05V)	18/2	.938	-.788	V
Idss (Vgds=5V)	18/2	2529.0	-1278.0	uA
Vpt (Id=1.0uA)	18/2	16.23	-15.03	V
Vth (Vds=.05V)	50/50	.920	-.800	V
Vbkd (Ij=1.0uA)	50/50	16.3	-16.1	V
Kp (Uo*Cox/2)	50/50	23.5	11.13	uA/V^2
Gamma (2.5v,5.0v)	50/50	1.043	.456	V^0.5
Delta Length		.612	.345	um
Delta Width (Effective=Drawn-Delta)		.127	.214	um

COMMENTS: These parameters seem normal.

III. FIELD OXIDE TRANSISTOR PARAMETERS:

	GATE	SOURCE/DRAIN N + ACTIVE	SOURCE/DRAIN P + ACTIVE	UNITS
Vth (Vbs=0,I=1uA)	Poly	17.5	-12.5	V
Vth (Vbs=0,I=1uA)	Metal1	17.5	-25.7	V
Vth (Vbs=0,I=1uA)	Metal2	17.4	-27.1	V

COMMENTS: These parameters seem normal.

IV. PROCESS PARAMETERS:

	N POLY	P POLY	N DIFF	P DIFF	METAL 1	METAL 2	POLY 2	UNITS
Sheet Resistance	20.4	20.7	22.6	77.4	.053	.026	20.1	Ohm/sq
Width Variation (Measured - Drawn)	-.333	-.324	.052	.024	-.434	.089	.036	um
Contact Resist. (Metal1 to Layer)	8.45	8.91	15.57	36.21	----	.033	9.26	Ohms
Gate Oxide Thickness:	----	----	392.	----	----	----	----	Angst.

COMMENTS: These parameters seem normal.

V. CAPACITANCE PARAMETERS:	POLY	N DIFF	P DIFF	METAL 1	METAL 2	POLY 2	UNITS
Area Cap (Layer to subs)	.068	.394	.209	.031	.020	----	fF/um^2
Area Cap (Layer to Poly)	----	----	----	.040	.021	.462	fF/um^2
Area Cap (Layer to Metall)	----	----	----	----	.034	.040	fF/um^2
Fringe Cap (Layer to subs)	----	.442	.217	----	----	----	fF/um

COMMENTS: These parameters seem normal.

VI. CIRCUIT PARAMETERS:			
Vinv,	K = 1	2.18	V
Vinv,	K = 1.5	2.38	V
Vlow,	K = 2.0	0.00	V
Vhigh,	K = 2.0	4.99	V
Vinv,	K = 2.0	2.54	V
Gain,	K = 2.0	-11.04	
Ring Oscillator Frequency		30.49	MHz (31 stages @ 5.0V)

COMMENTS: The ring oscillator frequency is typical.

N03U SPICE LEVEL 2 PARAMETERS

```
.MODEL CMOSN NMOS LEVEL=2 LD=0.250000U TOX=405.000000E-10
+ NSUB=2.057225E+16 VTO=0.92407 KP=4.971000E-05 GAMMA=0.9692
+ PHI=0.6 UO=582.7 UEXP=0.221281 UCRIT=137749
+ DELTA=2.73272 VMAX=83539.8 XJ=0.250000U LAMBDA=2.357637E-02
+ NFS=2.400030E+12 NEFF=1 NSS=1.000000E+12 TPG=1.000000
+ RSH=23.100000 CGDO=3.197355E-10 CGSO=3.197355E-10 CGBO=6.891152E-10
+ CJ=3.871000E-04 MJ=0.462600 CJSW=4.267000E-10 MJSW=0.348000 PB=0.800000
* Weff = Wdrawn - Delta_W
* The suggested Delta_W is 0.12 um
.MODEL CMOSP PMOS LEVEL=2 LD=0.250000U TOX=405.000000E-10
+ NSUB=4.864740E+15 VTO=-0.799152 KP=2.336000E-05 GAMMA=0.4713
+ PHI=0.6 UO=273.8 UEXP=0.177959 UCRIT=7687.01
+ DELTA=1.11147 VMAX=44954.5 XJ=0.250000U LAMBDA=5.204457E-02
+ NFS=4.247374E+11 NEFF=1.001 NSS=1.000000E+12 TPG=-1.000000
+ RSH=77.200000 CGDO=3.197355E-10 CGSO=3.197355E-10 CGBO=7.204215E-10
+ CJ=2.102400E-04 MJ=0.443400 CJSW=1.874500E-10 MJSW=0.205400 PB=0.700000
* Weff = Wdrawn - Delta_W
* The suggested Delta_W is 0.25 um
```

```
N03U  SPICE BSIM PARAMETERS

NM1 PM1 DU1 DU2 ML1 ML2
*
*PROCESS=orbit
*RUN=n03u
*WAFER=2
*Gate-oxide thickness= 405.0 angstroms
*Geometries (W-drawn/L-drawn, units are um/um) of transistors measured were:
* 3.0/2.0, 6.0/2.0, 18.0/2.0, 18.0/5.0, 18.0/25.0
*Bias range to perform the extraction (Vdd)=5 volts
*DATE=04-25-90
*
*NMOS PARAMETERS
*
-7.99628E-01, 3.58389E-02,-7.70939E-02
 7.60829E-01, 0.00000E+00, 0.00000E+00
 1.09084E+00, 1.95692E-02, 5.03221E-01
 3.14699E-03, 7.12321E-02, 6.27686E-02
-4.83964E-03, 1.11977E-02, 1.24884E-02
 5.68326E+02,8.77101E-001,1.24542E-001
 5.47895E-02, 4.55111E-02,-4.43980E-02
 2.02084E-02, 5.38695E-01,-2.24314E-01
 1.49246E+01,-2.58935E+01, 4.04786E+01
 5.11543E-04,-7.81860E-03,-3.98345E-03
 5.71135E-04,-1.75635E-03,-3.86746E-03
 2.69152E-03,-1.19917E-02, 2.08939E-02
-2.20636E-03, 1.13252E-02, 1.38775E-02
 5.72011E+02, 3.39156E+02,-2.31256E+00
 5.29578E+00,-1.53472E+01, 8.57263E+01
-6.09940E-01, 6.45514E+01,-3.22786E+01
 5.15024E-03, 5.74119E-02,-3.47952E-02
4.05000E-002, 2.70000E+01, 5.00000E+00
5.60881E-010,5.60881E-010,6.89101E-010
1.00000E+000,0.00000E+000,0.00000E+000
1.00000E+000,0.00000E+000,0.00000E+000
0.00000E+000,0.00000E+000,0.00000E+000
0.00000E+000,0.00000E+000,0.00000E+000
*
* Gate Oxide Thickness is 405 Angstroms
*
*
*PMOS PARAMETERS
*
-2.05514E-01,-1.12387E-01, 3.19501E-01
 6.51256E-01, 0.00000E+00, 0.00000E+00
 4.29960E-01, 6.07030E-02,-1.05273E-01
-1.22414E-02, 5.95048E-02,-5.18187E-02
-7.75855E-03, 6.00061E-02, 2.89938E-02
 2.43186E+02,5.55117E-001,-2.68719E-002
 1.31183E-01, 2.56252E-02,-6.55868E-02
 1.94880E-02, 2.91910E-01,-1.02129E-01
 9.97779E+00,-4.71751E+00, 7.63253E+00
 6.46816E-04,-4.78671E-03, 8.28692E-04
 7.29091E-04,-5.08643E-03, 7.79742E-05
 6.03891E-03,-3.82796E-03, 7.33918E-03
-3.80988E-04, 3.58808E-03, 1.26380E-03
 2.43886E+02, 1.58170E+02,-6.67849E+01
 8.21881E+00, 1.75711E+00, 9.82284E+00
-1.45603E+00, 1.84551E+01,-1.09435E+01
-1.68526E-02, 3.95624E-03, 2.43354E-03
4.05000E-002, 2.70000E+01, 5.00000E+00
3.54981E-010,3.54981E-010,6.52295E-010
1.00000E+000,0.00000E+000,0.00000E+000
```

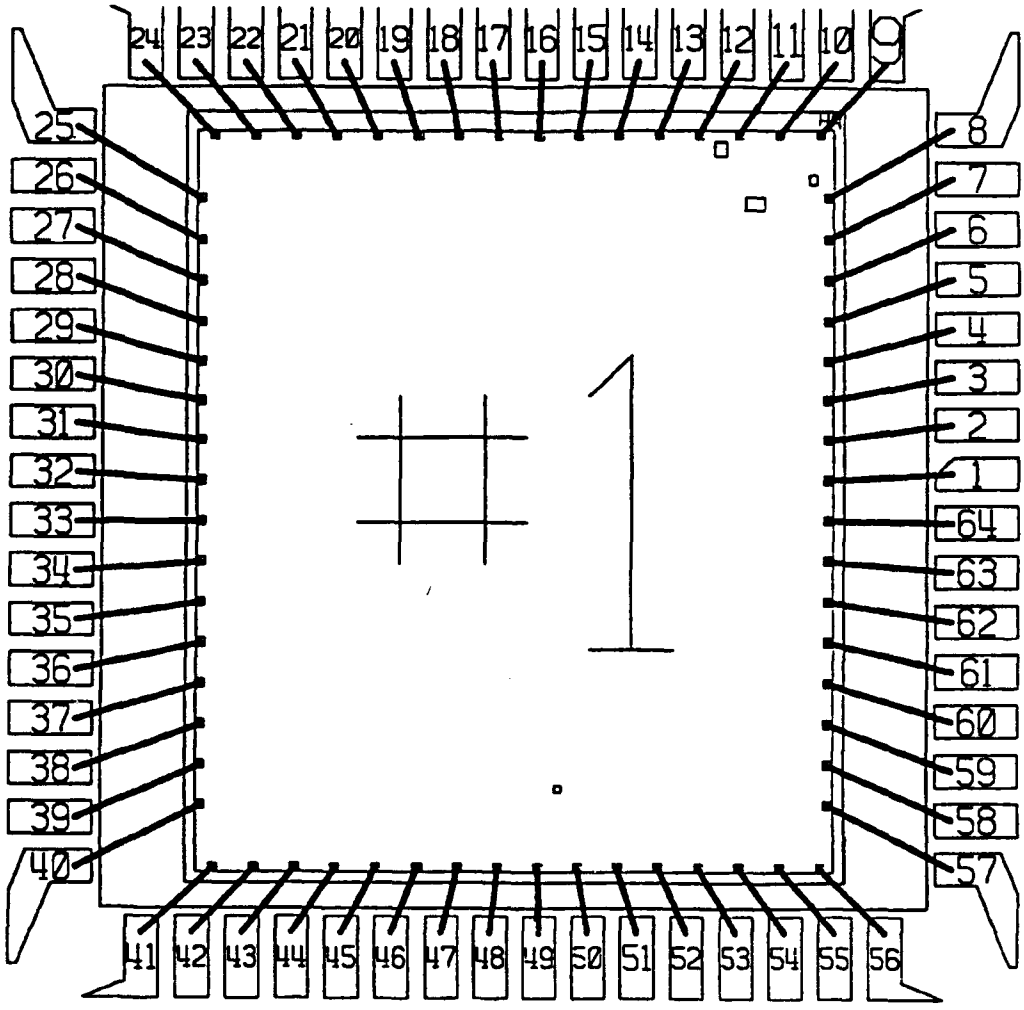

NØ3UHA 1

63-DAR-RES/AFIT-ENG

#1: 29753\IGEFET

DIP64: 3γ PARTS

Appendix C. *Data Collection Software*

This appendix contains a listing of the software used to collect the IGEFET performance data.

Direct Current Data Collection Program

This program (dc.bas) was used to collect the direct current resistance data.

```
10 CLS
20 PRINT "*****************************************************************"
30 PRINT "*                                                               *"
35 PRINT "*        DC RESISTANCE MEASUREMENT PROGRAM                      *"
40 PRINT "*                                                               *"
45 PRINT "*****************************************************************"
50 PRINT ""
60 INPUT "PRESS RETURN WHEN READY TO CONDUCT MEASUREMENTS...",NULL$
70 CLS
100 '****************dc measurement program*********************************
110 '
120 DEF SEG=&HC400
130 INIT%=0
140 TRANSMIT%=3
150 RECIEVE%=6
160 SEND%=9
170 SPOLL%=12
180 ENTER%=21
190 TARRAY%=200
200 RARRY%=203
210 DMA2=206
220 BUSADDRS%=21
230 SYSCONT%=0
240 '
250 MY.ADDR%=21
260 SYS.CONTROL%=0
270 CALL INIT%(MY.ADDR%,SYS.CONTROL%)
280 S$="UNL UNT"
290 CALL TRANSMIT%(S$,STATUS%)
300 K617%=27
310 GOSUB 970                    'GO TO TIMER ROUTINE
320 OPEN "O",#1, "C:\EPOXY\DCBIAS.DAT"
330 OPEN "O",#2, "C:\EPOXY\DCTIME.DAT"
340 INPUT "MATERIAL: ",MATL$
350 INPUT "TEMPERATURE: ",TEMP$
```

```
360 FOR I= 1 TO 2
370  PRINT #I, "DC MEASUREMENT ROUTINE:"
371  PRINT #I, "MATERIAL: ";MATL$
372  PRINT #I, "TEMPERATURE: ";TEMP$
380 NEXT I
390 PRINT #1, "DC RESISTANCE WRT APPLIED BIAS."
400 PRINT #1, ""
410 PRINT #2, "DC RESISTANCE WRT TIME."
420 PRINT #2, ""
430 '***************Initialize electrometer*******************************
440 '
450 '     subroutine dcinitialize
460 '
470 S$="F1"                    'SET TO MEASURE AMPS
480 CALL SEND%(K617%,S$,STATUS%)
490 S$="ROX"                   'SET TO AUTO RANGE
500 CALL SEND%(K617%,S$,STATUS%)
510 S$="Z1X"                  'PERFORM ZERO CORRECT
520 CALL SEND%(K617%,S$,STATUS%)
530 S$="TOX"
540 CALL SEND%(K617%,S$,STATUS%)
550 '
560 S$="F5X"                  'SET TO V/I OHMS MODE
570 CALL SEND%(K617%,S$,STATUS%)
580 S$="V00X"                'SET INTERN  VOLTAGE SOURCE TO 00V
590 CALL SEND%(K617%,S$,STATUS%)
600 '
610 VINIT=1
620 VFINAL=10
630 VSTEP=1
640 '
650 '
660 S$="COX"                    'ENABLE READING
670 CALL SEND%(K617%,S$,STATUS%)
680 S$="O1X"                   'TURN ON VOLTAGE SOURCE
690 CALL SEND%(K617%,S$,STATUS%)
700 '
710 PRINT#1, "ELAPSED TIME: ";ELAPSE.TIME$
720 '
730 CLS
740 PRINT "TAKING MEASUREMENT..."
750 FOR VN=VINIT TO VFINAL STEP VSTEP  'SWEEP THE VOLTAGE
760  S$="V"+STR$(VN)+"X"  'SET THE INTERNAL VOLTAGE SOURCE
770  CALL SEND%(K617%,S$,STATUS%)
780  TEMP$=SPACE$(16)
790    FOR I=1 TO 20000!: NEXT I     'LET ELECTROMETER SETTLE
800  CALL ENTER%(TEMP$,LENGTH%,K617%,STATUS%)
810  DC.RESIST= VAL(RIGHT$(TEMP$,12))
820    PRINT#1, VN;CHR$(44);DC.RESIST
830    IF VN=2 THEN PRINT#2, ELAPSE.TIME;CHR$(44);DC.RESIST
840 NEXT VN
```

```
850 '
860 S$="OOX"                        'TURN OFF VOLTAGE SOURCE
870 CALL SEND%(K617%,S$,STATUS%)
880 S$="VOX"                        'SET VOLTAGE TO ZERO
890 CALL SEND%(K617%,S$,STATUS%)
900 S$="C1X"                        'DISABLE READING
910 CALL SEND%(K617%,S$,STATUS%)
920 '
925  PRINT USING "###.##";ELAPSE.TIME
926 PRINT ""
930 CLS:BEEP: INPUT "ANOTHER MEASUREMENT? [Y]",AN$
940 IF AN$="N" OR AN$="n" THEN 950 ELSE 430
950 CLOSE
960 STOP
970 '***************Timer  initialization routine************************
980 '
990 '     subroutine timer initialization
1000 '
1010 '
1020 ELAPSE.TIME$="00:00:00"
1030 HOURS = 0
1040 MINUTES = 0
1050 SECONDS = 0
1060 '
1070 '    turn on elapse timer
1080 '
1090 '
1100 BEGIN.TIME$=TIME$
1110 BEGIN.HRS= VAL(LEFT$(BEGIN.TIME$,2))
1120 BEGIN.MIN= VAL(MID$(BEGIN.TIME$,4,2))
1130 BEGIN.SEC= VAL(RIGHT$(BEGIN.TIME$,2))
1140 ON TIMER (1) GOSUB 1190   'gosub timer
1150 TIMER ON
1160 '
1170 RETURN
1180 '
1190 '***************TIMER ROUTINE*****************************************
1200 '
1210 '    subroutine timer
1220 '
1230 TIME.NOW$=TIME$
1240 NOW.HRS= VAL(LEFT$(TIME.NOW$,2))
1250 NOW.MIN= VAL(MID$(TIME.NOW$,4,2))
1260 NOW.SEC= VAL(RIGHT$(TIME.NOW$,2))
1270 SECONDS= NOW.SEC-BEGIN.SEC
1280 IF SECONDS >= 0 THEN GOTO 1300            'go two lines down
1290 SECONDS=SECONDS+60: NOW.MIN=NOW.MIN-1
1300 MINUTES=NOW.MIN-BEGIN.MIN
1310 IF MINUTES >= 0 THEN GOTO 1330             'go two lines down
1320 MINUTES=MINUTES+60: NOW.HRS=NOW.HRS-1
1330 IF NOW.HRS<BEGIN.HRS THEN NOW.HRS=NOW.HRS+24
```

```
1340 HOURS=NOW.HRS-BEGIN.HRS
1350 IF SECONDS<10 THEN SECONDS$="0" + RIGHT$(STR$(SECONDS),1)
1360 IF SECONDS >= 10 THEN SECONDS$=RIGHT$(STR$(SECONDS),2)
1370 IF MINUTES<10 THEN MINUTES$="0" + RIGHT$(STR$(MINUTES),1)
1380 IF MINUTES >= 10 THEN MINUTES$=RIGHT$(STR$(MINUTES),2)
1390 'ELAPSE.TIME$= STR$(HOURS) + ":" + MINUTES$ +":" + SECONDS$
1400 '
1410 'THE FOLLOWING ELAPSE.TIME IS IN MINUTES
1420 ELAPSE.TIME=HOURS*60 + MINUTES + SECONDS/60
1430 '
1440 '
1450 RETURN
```

General Data Collection Program

This program (test.bas) was used to collect the impedance, transfer function, and time- and frequency-domain data.

```
10 REM************************************************************
20 REM** PROGRAM TO COLLECT DATA FROM THREE HEWLETT PACKARD     **
30 REM** PIECES OF TEST EQUIPMENT USING THE IEEE-488 BUS.       **
40 REM** HP-54100 OSCILLOSCOPE                                  **
50 REM** HP-4195A SPECTRUM ANALYZER                            **
60 REM**                                                       **
70 REM** Charles P. Brothers Jr.                               **
80 REM** GE-90D                                                **
90 REM**                                                       **
100 REM** NOTES:  The data collection subroutines are a         **
110 REM**   collection of routines written by Capt Thomas       **
120 REM**   Jenkins and the author.                            **
130 REM**                                                      **
140 REM************************************************************
150 '
160 REM -------------- INITIALIZE PROGRAM  ------------------
170 GOSUB 8270          'TIMER INITIALIZATION
180 DEF SEG=&HC400              'PC-488 MEMORY ADDRESS
190 INIT%=0                     'INITIALIZATION CODE
200 TRANSMIT%=3                 'TRANSMIT CODE
210 RECEIVE%=6                  'RECEIVE CODE
220 SEND%=9                     'SEND CODE
230 SPOLL%=12                   'SERIAL POLL CODE
240 PPOLL%=15
250 ENTER%=21
260 TARRAY%=200
270 RARRY%=203
280 DMA2=206
290 BUSADDRS%=21                'IEEE-488 BUS ADDRESS
300 SYSCONT%=0                  'SYSTEM CONTROLLER
310 '
320 REM --------------- INITIALIZE ARRAYS -------------------
330 DIM A(401)
340 DIM X(401)
350 DIM D%(2048)
360 DIM V1POINT(1300)
370 DIM V2POINT(1300)
380 DIM MAG(400)
390 DIM PHS(400)
400 DIM GFREQ(400)
410 '
420 REM ------------- INITIALIZE CONTROLLER -----------------
```

```
430 CALL INIT% (BUSADDRS%,SYSCONT%)
440 CHRFILE$ = "BLANK"
450 '
460 REM ---------- TRANSMIT ----------
470 S$="UNL UNT"              'INITIALIZE BUS
480 CALL TRANSMIT% (S$,STATUS%)
490 IF STATUS%<>0 THEN GOTO 8230
500 '
510 REM ---------- SCREEN MENU ----------
520 CLS : PRINT " "
530 PRINT "         SYSTEM MENU - Choose one "
540 PRINT " "
550 PRINT "     (0)  Enter experiment data header information."
560 PRINT "     (1)  Retreive Data from HP-54100 Oscilloscope"
570 PRINT "     (2)  Retreive Data from HP-4194B in Gain/Phase Mode"
580 PRINT "     (3)  Retreive Data from HP-4194B in Impedance Mode"
590 PRINT "     (4)  Retreive Data from HP-4195A from 1HZ to 10KHZ"
600 PRINT "     (5)  Retreive Data from HP-4195A from 1HZ to 1MHZ"
610 PRINT "     (6)  EXIT TO DOS"
620 PRINT " "
630 PRINT "" :INPUT "ENTER CHOICE:  ",MENU
640 '
650 S$="UNL UNT"              'INITIALIZE BUS
660 CALL TRANSMIT% (S$,STATUS%)
670 IF STATUS%<>0 THEN GOTO 8230
680 '
690 IF MENU=0 THEN GOSUB 810
700 IF MENU=1 THEN GOSUB 1070
710 IF MENU=2 THEN GOSUB 2750
720 IF MENU=3 THEN GOSUB 4300
730 IF MENU=4 THEN GOSUB 5700
740 IF MENU=5 THEN GOSUB 6990
750 IF MENU=6 THEN GOTO 8110
760 '
770 GOTO 520
780 REM ---------- END MENU ----------
790 '
800 REM ---------- GENERATE FILE HEADERS ----------
810 CLS
820 PRINT " "
830 INPUT "ENTER FIVE CHARACTER CODE NAME TO STORE DATA:  ", CHRFILE$
840 INPUT "ENTER FILE HEADER:  ",EXPERIMENT$
850 INPUT "ENTER CHIP TEMPERATURE:  ",CHIPTEMP$
855 INPUT "EXPERIMENT TIME LIMIT (MIN): ",TIME.LIMIT
860 RETURN
870 '
880 '
890 '
900 '
910 '
920 REM************************************************************
```

```
930 REM** SUBROUTINE TO COLLECT OSCILLOSCOPE DATA FROM THE HP   **
940 REM** 54100 DIGITAL OSCILLOSCOPE                            **
950 REM**                                                       **
960 REM** WRITTEN BY: Capt Thomas Jenkins                       **
970 REM**                                                       **
980 REM** Modified by: Charles P. Brothers Jr.                  **
990 REM**              GE-90D                                   **
1000 REM**                                                       **
1010 REM** NOTES: The HP-4194A is set to run SINGLE SWEEP MODE   **
1020 REM**   measurements from the IGEFET electrodes.           **
1030 REM**                                                       **
1040 REM**                                                       **
1050 REM*************************************************************
1060 '
1070 TRACE$ = "C:\EPOXY\DATA\"+CHRFILE$+"SCP.PRN"
1080 OPEN "O",#1, TRACE$
1090 WRITE #1, TRACE$
1100 WRITE #1, EXPERIMENT$
1110 WRITE #1, DATE$
1120 WRITE #1, TIME$
1130 WRITE #1,
1140 WRITE #1, "CHP TEMP=";CHIPTEMP$
1150 WRITE #1, "
1160 WRITE #1, "HP-54100A OSCILLOPE DUMP "
1170 WRITE #1, "   ELAPSED TIME     TIME         VOLTAGE"
1180 CLS
1190 CHOPT = 0
1200 PRINT "    ROUTINE TO CAPTURE SCOPE DISPLAY IN PC FILE"
1210 PRINT "
1220 PRINT "(1) FOR CHAN1, (2) FOR CHAN2, OR ANY OTHER KEY--BOTH"
1230 REM KEY POLL
1240 A$=INKEY$:IF A$="" THEN 1240
1250 IF A$="1" THEN CHOPT=1
1260 IF A$="2" THEN CHOPT=2
1270 K=1  'CHANNEL 1
1280 IF CHOPT <>0 THEN K= CHOPT
1290 '
1300 MY.ADDR%=21
1310 SYS.CONTROL%=0    ' initialize as system ctrlr
1320 CALL INIT%(MY.ADDR%,SYS.CONTROL%)
1330 S$="UNL UNT"        'INITIALIZE BUS
1340 CALL TRANSMIT%(S$,STATUS%)
1350 IF STATUS%<>0 THEN GOTO 8230
1360 ADDR%=15                    ' HP-54100 Oscilloscope address
1370 '
1380 REM -------------------- Send -------------------------
1390 CLS:INPUT "SET UP MEASUREMENT, THEN PRESS ENTER... ",NULL$
1400 CLS:LOCATE 1,1
1410 PRINT"SCOPE GRABBER NOW GRABBING CHANNEL ";K
1420 'S$="CLEAR"
1430 'CALL SEND% (ADDR%,S$,STATUS%)
```

```
1440 'IF STATUS%<>0 THEN 2320
1450 'S$="HEADER OFF"
1460 'CALL SEND% (ADDR%,S$,STATUS%)
1470 'IF STATUS%<>0 THEN 2320
1480 REM ---------- Send ----------
1490 'N$=RIGHT$(STR$(K),1)
1500 'S$="CHANNEL "+N$+"
1510 'CALL SEND% (ADDR%,S$,STATUS%)
1520 'IF STATUS%<>0 THEN 8900
1530 'S$="DISPLAY FORMAT SINGLE"
1540 'CALL SEND% (ADDR%,S$,STATUS%)
1550 'IF STATUS%<>0 THEN 8900
1560 REM ---------- Send ----------
1570 'S$="ACQUIRE TYPE AVERAGE COUNT 1 COMPLETE 90 POINTS 1024;"
1580 'CALL SEND% (ADDR%,S$,STATUS%)
1590 'FOR SCOPEW=1 TO 10000: NEXT SCOPEW 'WAIT FOR SCOPE TO SETTLE
1600 'IF STATUS%<>0 THEN 8900
1610 REM ---------- Send ----------
1620 S$="DIGITIZE CHANNEL"+N$+"
1630 CALL SEND% (ADDR%,S$,STATUS%)
1640 IF STATUS%<>0 THEN 8230
1650 REM ---------- Send ----------
1660 S$="WAVEFORM POINTS?"
1670 CALL SEND% (ADDR%,S$,STATUS%)
1680 IF STATUS%<>0 THEN 8230
1690 REM ---------- Enter ----------
1700 R$=SPACE$(13)            'allocate receive buffer
1710 CALL ENTER% (R$,LENGTH%,ADDR%,STATUS%)
1720 IF STATUS%<>0 THEN 8230
1730 POINTS=VAL(R$):PRINT "THE NUMBER OF WAVE POINTS=";POINTS,
1740 PTMOD=INT(POINTS/100)
1750 PRINT "PTMOD =";PTMOD
1760 IF (PTMOD < 1) THEN PTMOD=1
1770 IF POINTS>1300 THEN PRINT"WARNING: EXCESS POINTS (MAX 1300)"
1780 REM ---------- Send ----------
1790 S$="WAVEFORM XINC?"
1800 CALL SEND% (ADDR%,S$,STATUS%)
1810 IF STATUS%<>0 THEN 8230
1820 R$=SPACE$(30)            'allocate receive buffer
1830 CALL ENTER% (R$,LENGTH%,ADDR%,STATUS%)
1840 IF STATUS%<>0 THEN 8230
1850 XINC=VAL(R$):'---------- Send ----------
1860 S$="WAVEFORM XOR?"
1870 CALL SEND% (ADDR%,S$,STATUS%)
1880 IF STATUS%<>0 THEN 8230
1890 R$=SPACE$(30)            'allocate receive buffer
1900 CALL ENTER% (R$,LENGTH%,ADDR%,STATUS%)
1910 IF STATUS%<>0 THEN 8230
1920 XORG=VAL(R$):'---------- Send ----------
1930 S$="WAVEFORM YREF?"
1940 CALL SEND% (ADDR%,S$,STATUS%)
```

```
1950 IF STATUS%<>0 THEN 8230
1960 R$=SPACE$(13)              'allocate receive buffer
1970 CALL ENTER% (R$,LENGTH%,ADDR%,STATUS%)
1980 IF STATUS%<>0 THEN 8230
1990 YREF=VAL(R$):'------------ Send -------------------------
2000 S$="WAVEFORM YINC?"
2010 CALL SEND% (ADDR%,S$,STATUS%)
2020 IF STATUS%<>0 THEN 8230
2030 R$=SPACE$(13)              'allocate receive buffer
2040 CALL ENTER% (R$,LENGTH%,ADDR%,STATUS%)
2050 IF STATUS%<>0 THEN 8230
2060 YINC=VAL(R$):'------------ Send -------------------------
2070 S$="WAVEFORM YOR?"
2080 CALL SEND% (ADDR%,S$,STATUS%)
2090 IF STATUS%<>0 THEN 8230
2100 REM --------------------- Enter ------------------------
2110 R$=SPACE$(13)              'allocate receive buffer
2120 CALL ENTER% (R$,LENGTH%,ADDR%,STATUS%)
2130 IF STATUS%<>0 THEN 8230
2140 YOR=VAL(R$)
2150 S$="WAVEFORM FORMAT ASCII;WAVEFORM DATA? "
2160 CALL SEND% (ADDR%,S$,STATUS%)
2170 IF STATUS%<>0 THEN 8230
2180 REM --------------------- TRANSMIT ---------------------
2190 S$="MLA TALK 15"
2200 CALL TRANSMIT% (S$,STATUS%)
2210 IF STATUS%<>0 THEN 8230
2220 WRITE #1, "
2230 WRITE #1, "   TIME          VOLTAGE"
2240 WRITE #1,
2250 PRINT " "
2260 PRINT "(INDEX)               TIME                 VOLTAGE"
2270 PRINT "-------------------------------------------------"
2280 FOR I=1 TO POINTS
2290    REM --------------------- Receive ----------------------
2300    R1$=SPACE$(32)              ' allocate receive buffer
2310    IF STATUS%<>0 THEN 8230
2320    TPOINT=XINC*I+XORG
2330    CALL RECEIVE% (R1$,LENGTH%,STATUS%)
2340    IF STATUS%<>0 THEN 8230
2350    IF K=1 THEN V1POINT(I)=((VAL(R1$)-YREF)*YINC)+YOR
2360    IF K=2 THEN V2POINT(I)=((VAL(R1$)-YREF)*YINC)+YOR
2370    IF (I MOD 100)=0 THEN PRINT
"(";I;")",TPOINT;",",V1POINT(I);",",V2POINT(I)
2380    IF (I MOD PTMOD)=0 THEN PRINT#1, USING
"+#.#####^^^^,";ELAPSE.TIME;TPOINT;V1POINT(I);V2POINT(I)
2390 NEXT I
2400 K=K+1 : IF CHOPT<>0 THEN K=3
2410 IF K<3 THEN 1380
2420    IF (I MOD 100)=0 THEN PRINT "(";I;")",TPOINT;",",VPOINT(I)
2430    IF (I MOD PTMOD)=0 THEN PRINT#1, USING "+#.#####^^^^,";TPOINT;VPOINT(I)
```

```
2440 '
2450 INPUT "DO YOU WANT TO TAKE ANOTHER MEASUREMENT? [Y] ",AN$
2460 IF AN$="N" OR AN$="n" THEN 2470 ELSE 1270
2470 S$="LOCAL"
2480 CALL SEND% (ADDR%,S$,STATUS%)
2490 S$="UNL UNT"
2500 CALL TRANSMIT% (S$,STATUS%)
2510 IF STATUS%<>0 THEN 8230
2520 CLOSE
2530 PRINT"FINISHED"
2540 RETURN
2550 '
2560 '
2570 '
2580 '
2590 '
2600 REM*****************************************************************
2610 REM** ROUTINE TO COLLECT GAIN PHASE DATA FROM THE HP-4194B  **
2620 REM** GAIN PHASE ANALYZER.                                  **
2630 REM**                                                      **
2640 REM** WRITTEN BY: Capt Thomas Jenkins                      **
2650 REM**                                                      **
2660 REM** Modified by: Charles P. Brothers Jr.                 **
2670 REM**               GE-90D                                 **
2680 REM**                                                      **
2690 REM** NOTES: The HP-4194A is set to run GAIN PHASE         **
2700 REM**   measurements from the IGEFET electrodes.           **
2710 REM**                                                      **
2720 REM**                                                      **
2730 REM*****************************************************************
2740 '
2750 CLS
2760 PRINT,"  HP4194A GAIN PHASE DATA TRANSFER "
2770 OPEN "O",#1, "C:\EPOXY\DATA\"+CHRFILE$+"GP"+STR$(0)+".PRN"
2780 OPEN "O",#2, "C:\EPOXY\DATA\"+CHRFILE$+"GP"+STR$(1)+".PRN"
2790 '
2800 '------------ GP-IB ADDRESSES OF INSTRUMENTS ------------------
2810 HP4194%=17: HP4192%=9: PRINTER%=1: MY.ADDR%=21: K617%=27
2820 SWITCH%=28
2830 '
2840 SYSCON%=0                          'PC488 ACTS AS CONTROLLER
2850 CALL INIT%(MY.ADDR%,SYSCON%)
2860 '
2870 PRINT " "
2880 PRINT "SETTING-UP 4194 FOR GAIN PHASE MEASUREMENTS -- WAIT..."
2890 '
2900 S$="RQS2"                        'UNMASK AND ENABLE BIT1 FOR SRQ
2910 CALL SEND%(HP4194%,S$,STATUS%)
2920 S$="FNC2"                        'SET 4194 TO GAIN PHASE MODE
2930 CALL SEND%(HP4194%,S$,STATUS%)
2940 S$="PHS2"                        'SET PHASE SCALE TO EXPANSION MODE
```

```
2950 CALL SEND%(HP4194%,S$,STATUS%)
2960 S$="SWM2"                          'SET SWEEP MODE TO SINGLE
2970 CALL SEND%(HP4194%,S$,STATUS%)
2980 S$="SWT2"                          'SET TO LOG SWEEP
2990 CALL SEND%(HP4194%,S$,STATUS%)
3000 S$="MCF1"                          'TURN MARKERS ON
3010 CALL SEND%(HP4194%,S$,STATUS%)
3020 S$="ZIT1"                          'TEST CHANNEL TO 1 MOHMS
3030 CALL SEND%(HP4194%,S$,STATUS%)
3040 S$="ZIR1"                          'TEST CHANNEL TO 1 MOHMS
3050 CALL SEND%(HP4194%,S$,STATUS%)
3060 S$="ATT2"                         'REFERENCE CHANNEL 20DB
3070 CALL SEND%(HP4194%,S$,STATUS%)
3080 S$="ATR2"                         'REFERENCE CHANNEL 20DB
3090 CALL SEND%(HP4194%,S$,STATUS%)
3100 S$="START=10HZ"                    'STRT SWEEP AT 10HZ
3110 CALL SEND%(HP4194%,S$,STATUS%)
3120 S$="STOP=1000HZ"              'SWEEP TO 1KHz
3130 CALL SEND%(HP4194%,S$,STATUS%)
3140 S$="NOA=4"                         'SET AVERAGES TO 4
3150 CALL SEND%(HP4194%,S$,STATUS%)
3160 '
3170 CLS
3180 INPUT "PERFORM THE OFFSET REF STORE, THEN RETURN", NULL$
3190 '
3200 CALL INIT%(MY.ADDR%,SYSCON%)
3210 CALL SPOLL%(HP4194%,POLL%,STATUS%)   'MAKE SURE SRQ NOT SET
3220 S$="ITM2"                          'SET INTEGRATION TIME TO 10 mSEC
3230 CALL SEND%(HP4194%,S$,STATUS%)
3240 S$="X?"                            'READ IN FREQUENCY POINTS
3250 CALL SEND%(HP4194%,S$,STATUS%)
3260 IF STATUS%<>0 THEN 8230
3270 S$="MLA TALK 17"                   '4194 TO OUTPUT
3280 CALL TRANSMIT%(S$,STATUS%)
3290 TEMP$=SPACE$(15)
3300 FOR I=0 TO 400
3310    CALL RECEIVE%(TEMP$,LENGTH%,STATUS%)
3320    GFREQ(I)=VAL(LEFT$(TEMP$,12))
3330 NEXT I
3340 '
3350 CLS
3360 INPUT "NUMBER OF ELECTRODES TO BE SAMPLED:  ",NELECT
3370 FOR N=1 TO NELECT
3380 GAINPH$ = +CHRFILE$+"GP"+STR$(NELECT)+".PRN"
3390 WRITE #N, GAINPH$
3400 WRITE #N, EXPERIMENT$
3410 WRITE #N, DATE$
3420 WRITE #N, TIME$
3430 WRITE #N,
3440 WRITE #N, "CHP TEMP=";CHIPTEMP$
3450 WRITE #N, "
```

```
3460 WRITE #N, "HP-4194A GAIN PHASE DUMP
3470 WRITE #N, "
3480 WRITE #N, "ELAPSED TIME, ELECTRODE, FREQUENCY, Z-MAG, PHASE"
3490 WRITE #N, "
3500 NEXT N
3510 CLS
3520 FOR N=0 TO (NELECT-1)     'LOOP THROUGH THE NUMBER OF ELECTRODES
3530     PRINT "CONNECT ELECTRODE ";N,
3540    PRINT "SET OSC LEVEL, ENSURE OFFSETS ARE TURNED ON, MAKE OTHER"
3550    INPUT "          NECESSARY CHANGES, THEN HIT RETURN.",NULL$
3560     GOSUB 3780     ' GO GET DATA
3570 F=N+1
3580 INPUT "YOU LIKE? [Y] ",AN$
3590 IF AN$="N" OR AN$="n" THEN 3530
3600     '
3610 F=N+1
3620 PRINT#F, "ELAPSED TIME : ";ELAPSE.TIME
3630     FOR I= 0 TO 400
3640 IF (I MOD 4)=0 THEN PRINT#F, USING
"+#.####^^^^,";ELAPSE.TIME;N;GFREQ(I);MAG(I);PHS(I)
3650     IF (I MOD 100) = 0 THEN PRINT N,GFREQ(I),MAG(I),PHS(I)
3660     NEXT I
3670 NEXT N    ' LOOP THROUGH THE ELECTRODE
3680 INPUT "TAKE ANOTHER MEASUREMENT? [Y] ",ANSWER$
3690 IF ANSWER$="N" OR ANSWER$="n" THEN 3700 ELSE 3350
3700 CLOSE
3710 S$="UNL UNT"                'INITIALIZE BUS
3720 CALL TRANSMIT% (S$,STATUS%)
3730 IF STATUS%<>0 THEN GOTO 8230
3740 RETURN
3750 '
3760 '-------------------- HP4194 DATA INPUT ROUTINE ----------------
3770 '
3780 CALL SPOLL%(HP4194%,POLL%,STATUS%)  'MAKE SURE SRQ IS NOT SET
3790 S$="SWTRG"                          'PERFORM SINGLE SWEEP
3800 CALL SEND%(HP4194%,S$,STATUS%)
3810 CALL SPOLL%(HP4194%,POLL%,STATUS%)  'IS SWEEP COMPLETE?
3820 IF ((POLL% AND 64) <> 64) THEN 3810 'IF NOT CONTINUE POLL
3830 '
3840 S$="AUTOA"                          'AUTOSCALE DISPLAY A
3850 CALL SEND%(HP4194%,S$,STATUS%)
3860 S$="AUTOB"                          'AUTOSCALE DISPLAY B
3870 CALL SEND%(HP4194%,S$,STATUS%)
3880 S$="A?"                             'READ IN MAG VALUE
3890 CALL SEND%(HP4194%,S$,STATUS%)      'FROM THE ARRAY REG A
3900 '
3910 S$= "MLA TALK 17"
3920 CALL TRANSMIT%(S$,STATUS%)
3930 TEMP$= SPACE$(13)
3940 FOR I = 0 TO 400
3950     CALL RECEIVE%(TEMP$,LENGTH%,STATUS%)
```

```
3960     MAG(I)=VAL(LEFT$(TEMP$,12))     'EXTRACT MAG VALUE
3970 NEXT I
3980 '
3990 S$="B?"                 'READ IN PHASE FROM ARRAY REGISTER B
4000 CALL SEND%(HP4194%,S$,STATUS%)
4010 S$= "MLA TALK 17"
4020 CALL TRANSMIT%(S$,STATUS%)
4030 FOR I= 0 TO 400
4040     CALL RECEIVE%(TEMP$,LENGTH%,STATUS%)
4050     PHS(I)= VAL(LEFT$(TEMP$,12))     'EXTRACT PHASE VALUE
4060 NEXT I
4070 '
4080 CALL SPOLL%(HP4194%,POLL%,STATUS%)   'MAKE SURE SRQ NOT SET
4090 RETURN
4100 '
4110 '
4120 '
4130 '
4140 '
4150 REM*****************************************************************
4160 REM** ROUTINE TO COLLECT IMPEDANCE DATA FROM THE HP-4194B   **
4170 REM** IMPEDANCE / GAIN PHASE ANALYZER.                     **
4180 REM**                                                     **
4190 REM** WRITTEN BY: Capt Thomas Jenkins                     **
4200 REM**                                                     **
4210 REM** Modified by: Charles P. Brothers Jr.                 **
4220 REM**               GE-90D                                **
4230 REM**                                                     **
4240 REM** NOTES: The HP-4194A is set to run IMPEDANCE         **
4250 REM**   measurements from the IGEFET electrodes.          **
4260 REM**                                                     **
4270 REM**                                                     **
4280 REM*****************************************************************
4290 '
4300 CLS
4310 PRINT,"  HP4194A IMPEDANCE DATA TRANSFER "
4320 '
4330 '------------ GP-IB ADDRESSES OF INSTRUMENTS ------------------
4340 HP4194%=17
4350 HP4192%=9
4360 PRINTER%=1
4370 K617%=27
4380 SWITCH%=28
4390 '
4400 PRINT " "
4410 PRINT "SETTING-UP 4194 FOR IMPEDANCE MEASUREMENTS -- WAIT..."
4420 '
4430 S$="RQS2"                       'UNMASK AND ENABLE BIT1 FOR SRQ
4440 CALL SEND%(HP4194%,S$,STATUS%)
4450 S$="FNC1"                       'SET 4194 TO IMPEDANCE MODE
4460 CALL SEND%(HP4194%,S$,STATUS%)
```

```
4470 S$="PHS2"                          'SET PHASE SCALE TO EXPANSION MODE
4480 CALL SEND%(HP4194%,S$,STATUS%)
4490 S$="SWM2"                          'SET SWEEP MODE TO SINGLE
4500 CALL SEND%(HP4194%,S$,STATUS%)
4510 S$="SWT2"                          'SET TO LOG SWEEP
4520 CALL SEND%(HP4194%,S$,STATUS%)
4530 S$="OSC=0.1V"                      'SET SWEEP OSCILLATOR TO 0.1 VOLT
4540 CALL SEND%(HP4194%,S$,STATUS%)
4550 S$="MCF1"                          'TURN MARKERS OFF
4560 CALL SEND%(HP4194%,S$,STATUS%)
4570 S$="ITM2"                          'SET INTEGRATION TIME TO 5 mSEC
4580 CALL SEND%(HP4194%,S$,STATUS%)
4590 S$="NOA=8"                          'SET AVERAGES TO 8
4600 CALL SEND%(HP4194%,S$,STATUS%)
4610 S$="START=100HZ"                    'STRT SWEEP AT 100 HZ
4620 CALL SEND%(HP4194%,S$,STATUS%)
4630 S$="STOP=1000HZ"              'SWEEP TO 1kHz
4640 CALL SEND%(HP4194%,S$,STATUS%)
4650 '
4660 INPUT "PERFORM THE OFFSET REF STORE, THEN RETURN", NULL$
4670 '
4680 S$="X?"                            'READ IN FREQUENCY POINTS
4690 CALL SEND%(HP4194%,S$,STATUS%)
4700 IF STATUS%<>0 THEN 8230
4710 S$="MLA TALK 17"                   '4194 TO OUTPUT
4720 CALL TRANSMIT%(S$,STATUS%)
4730 TEMP$=SPACE$(15)
4740 FOR I=0 TO 400
4750    CALL RECEIVE%(TEMP$,LENGTH%,STATUS%)
4760    GFREQ(I)=VAL(LEFT$(TEMP$,12))
4770 NEXT I
4780 GATEIMP$ = +CHRFILE$+"IMP.PRN"
4790 OPEN "O",#2, "C:\EPOXY\DATA\"+GATEIMP$
4800 '
4810 CLS
4820 INPUT "NUMBER OF ELECTRODES TO BE SAMPLED:  ",NELECT
4830 WRITE #2, GATEIMP$
4840 WRITE #2, EXPERIMENT$
4850 WRITE #2, DATE$
4860 WRITE #2, TIME$
4870 WRITE #2,
4880 WRITE #2, GATEIMP$
4890 WRITE #2, "CHP TEMP=";CHIPTEMP$
4900 WRITE #2, "
4910 WRITE #2, "HP-4194A IMPEDANCE DUMP"
4920 WRITE #2, "
4930 WRITE #2, "ELAPSED TIME    ELECTRODE     FREQUENCY    Z-MAG       PHASE"
4940 WRITE #2,
4950 CLS
4960 INPUT "CONNECT 4194 ACROSS GATE,   HIT RETURN ", NULL$
4970 'FOR N=0 TO (NELECT-1)    'LOOP THROUGH THE NUMBER OF ELECTRODES
```

```
4980     PRINT "CONNECT ELECTRODE ";N,
4990     PRINT "ENSURE ALL IMPORTANT SETTINGS ARE CORRECT"
5000     INPUT "      THEN PRESS ENTER...",NULL$
5005 CLS
5010     GOSUB 5190    ' GO GET DATA
5015 WRITE #2, ""
5020 'INPUT "YOU LIKE? [Y]? ",AN$
5030 'IF AN$="N" OR AN$="n" THEN 4980
5040     FOR I= 0 TO 400
5050 IF (I MOD 4)=0 THEN PRINT#2, USING
"+#.####^^^^,";ELAPSE.TIME;N;GFREQ(I);MAG(I);PHS(I)
5060 IF (I MOD 100) = 0 THEN PRINT ,ELAPSE.TIME,GFREQ(I),MAG(I),PHS(I)
5070     NEXT I
5080 'NEXT N    ' LOOP THROUGH THE ELECTRODE
5090 IF TIME.LIMIT > ELAPSE.TIME THEN 5010 ELSE 5110
5110 S$="UNL UNT"          'INITIALIZE BUS
5120 CALL TRANSMIT% (S$,STATUS%)
5130 IF STATUS%<>0 THEN GOTO 8230
5140 CLOSE #2
5150 RETURN
5160 '
5170 '------------------- HP4194 DATA INPUT ROUTINE ----------------
5180 '
5190 CALL SPOLL%(HP4194%,POLL%,STATUS%)  'MAKE SURE SRQ IS NOT SET
5200 S$="SWTRG"                          'PERFORM SINGLE SWEEP
5210 CALL SEND%(HP4194%,S$,STATUS%)
5220 CALL SPOLL%(HP4194%,POLL%,STATUS%)  'IS SWEEP COMPLETE?
5230 IF ((POLL% AND 64) <> 64) THEN 5220 'IF NOT CONTINUE POLL
5240 '
5250 S$="AUTOA"                          'AUTOSCALE DISPLAY A
5260 CALL SEND%(HP4194%,S$,STATUS%)
5270 S$="AUTOB"                          'AUTOSCALE DISPLAY B
5280 CALL SEND%(HP4194%,S$,STATUS%)
5290 S$="A?"                             'READ IN MAG VALUE
5300 CALL SEND%(HP4194%,S$,STATUS%)      'FROM THE ARRAY REG A
5310 '
5320 S$= "MLA TALK 17"
5330 CALL TRANSMIT%(S$,STATUS%)
5340 TEMP$= SPACE$(13)
5350 FOR I = 0 TO 400
5360     CALL RECEIVE%(TEMP$,LENGTH%,STATUS%)
5370     MAG(I)=VAL(LEFT$(TEMP$,12))     'EXTRACT MAG VALUE
5380 NEXT I
5390 '
5400 S$="B?"                 'READ IN PHASE FROM ARRAY REGISTER B
5410 CALL SEND%(HP4194%,S$,STATUS%)
5420 S$= "MLA TALK 17"
5430 CALL TRANSMIT%(S$,STATUS%)
5440 FOR I= 0 TO 400
5450     CALL RECEIVE%(TEMP$,LENGTH%,STATUS%)
5460     PHS(I)= VAL(LEFT$(TEMP$,12))     'EXTRACT PHASE VALUE
```

```
5470 NEXT I
5480 '
5490 CALL SPOLL%(HP4194%,POLL%,STATUS%)   'MAKE SURE SRQ NOT SET
5500 RETURN
5510 '
5520 '
5530 '
5540 '
5550 '
5560 '
5570 REM*****************************************************************
5580 REM** PROGRAM TO COLLECT SPECTURM DATA FROM THE HP 4195A     **
5590 REM** SPECTRUM ANALYZER.                                    **
5600 REM**                                                      **
5610 REM** Charles P. Brothers Jr.                               **
5620 REM** GE-90D                                               **
5630 REM**                                                      **
5640 REM** NOTES: The HP-4195A is set to run in one pass         **
5650 REM**   from 0.001HZ to 10 KHZ.                            **
5660 REM**                                                      **
5670 REM**                                                      **
5680 REM*****************************************************************
5690 '
5700 CLS
5710 HPADDR%=18                    'HP-4195A ADDRESS
5720 REM ---------------------- TRANSMIT ----------------------
5730 S$="UNL UNT"         'INITIALIZE BUS
5740 CALL TRANSMIT% (S$,STATUS%)
5750 IF STATUS%<>0 THEN GOTO 8230
5760 CLS : PRINT " "
5770 PRINT "          HP4195A (SPECTRUM ANALYZER) Control Software"
5780 '
5790 REM ------------------- GENERATE FILE HEADER -------------------
5800 CLS
5810 PRINT " "
5820 FILENAM0$="C:\EPOXY\DATA\"+CHRFILE$+"0SPL.PRN"
5825 OPEN "O",#1, FILENAM0$
5835 J = 1
5850 WRITE #J, EXPERIMENT$
5860 WRITE #J, DATE$
5870 WRITE #J, TIME$
5880 WRITE #J,
5920 WRITE #J, "CHP TEMP=";CHIPTEMP$
5950 WRITE #J, "HP-4195A LOW FREQ SWEEP,  0.001 HZ TO 100 HZ"
5960 WRITE #J,
5970 WRITE #J, " ELECTRODE    ELAPSED TIME    FREQUENCY    AMPLITUDE"
5980 WRITE #J,
5990 '
6000 '
6020 REM ---------- BEGIN DATA COLLECTION PASS ----------------------
6030 REM CAPTURE DATA AND TRANSFER TO 1EEE-488 BUS
```

```
6040 '
6050 CLS                    'CLEAR PC SCREEN
6060 PRINT "PLEASE WAIT, SETTING UP ANALYZER..."
6070 REM SETUP HP4195A
6080 S$="FNC2;START=1HZ;STOP=100KHZ;NOP=201;SAP1;SWP1;SWT1;PORT1"
6090 CALL SEND% (HPADDR%,S$,STATUS%)
6100 S$="SWM1;FMT1"
6110 CALL SEND% (HPADDR%,S$,STATUS%)
6160   S$="SWM2;FMT1"
6170   CALL SEND% (HPADDR%,S$,STATUS%)
6180   IF STATUS%=0 THEN GOTO 6250
6190   PRINT "A LONG SWEEP TIME IS HOLDING UP SYSTEM"
6200   IF STATUS%<>8 OR (STATUS%=8 AND SWEEP < 10) THEN GOTO 8230
6210   CALL SPOLL% (HPADDR%,POLL%,STATUS%)
6220   GOTO 6190
6230   '
6240   REM ---------- TRANSMIT ----------
6250   S$="X?"
6260   CALL SEND%(HPADDR%,S$,STATUS%)
6270   S$="MLA TALK 18"
6280   CALL TRANSMIT% (S$,STATUS%)
6290   IF STATUS%<>0 THEN GOTO 8230
6300   REM ---------- RECEIVE ----------
6310   X$=SPACE$(15)              ' allocate RECEIVE buffer
6320   FOR I=0 TO 200
6330     CALL RECEIVE% (X$,LENGTH%,STATUS%)
6340     IF STATUS%<>0 THEN GOTO 8230
6350     X(I)=VAL(X$)
6360   NEXT I
6370   REM ---------- TRANSMIT ----------
6380   S$="UNL UNT"
6390   CALL TRANSMIT% (S$,STATUS%)
6400   S$="A?"
6410   CALL SEND%(HPADDR%,S$,STATUS%)
6420   S$="MLA TALK 18"
6430   CALL TRANSMIT% (S$,STATUS%)
6440   IF STATUS%<>0 THEN GOTO 8230
6450   REM ---------- RECEIVE ----------
6460   REM DRESS-UP THE PC SCREEN OUTPUT
6470   CLS:PRINT " ELAPSED TIME     FREQUENCY      AMPLITITUDE"
6480   '
6490   A$=SPACE$(13)              ' allocate RECEIVE buffer
6500   FOR I=0 TO 200
6510     CALL RECEIVE% (A$,LENGTH%,STATUS%)
6520     IF STATUS%<>0 THEN GOTO 8230
6530     A(I)=VAL(A$)
6540     IF (I MOD 2)=1 THEN PRINT #1, USING
"+#.#####^^^^,";COUNT;ELAPSE.TIME;X(I);A(I)
6550     IF (I MOD 20)=0 THEN PRINT USING "+#.####^^^^";ELAPSE.TIME;X(I);A(I)
6560   NEXT I
6570   '
```

```
6580   S$="SWM1"          ' HP-4195A BACK TO CONTINUOUS SWEEP
6590   CALL SEND% (HPADDR%,S$,STATUS%)
6600   IF STATUS%<>0 THEN GOTO 8230
6610 FOR Z = 1 TO 200000!: NEXT Z
6612 BEEP: INPUT "TAKE ANOTHER MEASUREMENT? [Y] ",AN$
6614 IF AN$="N" OR AN$="n" THEN 6620 ELSE CLS: GOTO 6020
6620 CLOSE
6630 PRINT ""
6640 PRINT " DATA TRANSFER COMPLETE."
6650 '
6660 REM --------------------- TRANSMIT ----------------------
6670 S$="UNL UNT"
6680 CALL TRANSMIT% (S$,STATUS%)
6690 IF STATUS%<>0 THEN GOTO 8230
6700 '
6710 S$="SWM1"       ' HP-4195A BACK TO CONTINUOUS SWEEP
6720 CALL SEND% (HPADDR%,S$,STATUS%)
6730 IF STATUS%<>0 THEN GOTO 8230
6740 '
6750 REM -----------TERMINATE HP-4195A CONTROL ---------------
6760 S$="UNL UNT"
6770 CALL TRANSMIT% (S$,STATUS%)
6780 '
6790 CLS        'CLEAR SCREEN
6800 RETURN
6810 '
6820 '
6830 '
6840 '
6850 '
6860 REM*****************************************************************
6870 REM** ROUTINE TO COLLECT SPECTURM DATA FROM THE HP 4195A     **
6880 REM** SPECTRUM ANALYZER.                                    **
6890 REM**                                                      **
6900 REM** Charles P. Brothers Jr.                              **
6910 REM** GE-90D                                               **
6920 REM**                                                      **
6930 REM** NOTES: The HP-4195A is set to run in one pass        **
6940 REM**   from 0.001HZ to 1.0MHZ.                           **
6950 REM**                                                      **
6960 REM**                                                      **
6970 REM*****************************************************************
6980 '
6990 CLS
7000 HPADDR%=18                    'HP-4195A ADDRESS
7010 '
7020 REM --------------------- TRANSMIT ----------------------
7030 S$="UNL UNT"         'INITIALIZE BUS
7040 CALL TRANSMIT% (S$,STATUS%)
7050 IF STATUS%<>0 THEN GOTO 8230
7060 '
```

```
7070 REM ------------------ GENERATE FILE HEADER -------------------
7080 CLS
7090 PRINT " "
7100 FILENAM$ = +CHRFILE$+"SPH.PRN"
7110 OPEN "O",#1, FILENAM$
7120 WRITE #1, FILENAM$
7130 WRITE #1, EXPERIMENT$
7140 WRITE #1, DATE$
7150 WRITE #1, TIME$
7160 WRITE #1,
7170 WRITE #1, "TEST GAS=";GAS$
7180 WRITE #1, "BTH TEMP=";BATH$
7190 WRITE #1, "FLW RATE=";FLOWR$
7200 WRITE #1, "CHP TEMP=";CHIPTEMP$
7210 WRITE #1, "HUMIDITY=";VHUMD$
7220 WRITE #1, "
7230 WRITE #1, "HP-4195A HIGH FREQ SWEEP,  0.001 HZ TO 1.0 MHZ"
7240 WRITE #1,
7250 WRITE #1, " ELECTRODE    FREQUENCY    AMPLITUDE"
7260 WRITE #1,
7270 '
7280 INPUT "ENTER NUMBER OF ELECTRODES TO BE MEASURED: ",ELECT
7290 REM ---------- BEGIN DATA COLLECTION PASS ---------------------
7300 REM CAPTURE DATA AND TRANSFER TO 1EEE-488 BUS
7310 '
7320 CLS                    'CLEAR PC SCREEN
7330 PRINT "PLEASE WAIT, CAPTURING DATA . . ."
7340 REM SETUP HP4195A
7350 S$="FNC2;START=.001HZ;STOP=1MHZ;NOP=401;SAP1;SWP1;SWT1;PORT1;PWR1"
7360 CALL SEND% (HPADDR%,S$,STATUS%)
7370 S$="SWM1;FMT1"
7380 CALL SEND% (HPADDR%,S$,STATUS%)
7390 FOR COUNT = 0 TO (ELECT - 1)
7400   PRINT "CONNECT ELECTRODE ";COUNT,
7410   INPUT "HIT RETURN", NULL$
7420   INPUT " WAIT FOR DISPLAY TO STABILIZE,  HIT RETURN ",NULL$
7430   S$="SWM2;FMT1"
7440   CALL SEND% (HPADDR%,S$,STATUS%)
7450   IF STATUS%=0 THEN GOTO 7520
7460   PRINT "A LONG SWEEP TIME IS HOLDING UP SYSTEM"
7470   IF STATUS%<>8 OR (STATUS%=8 AND SWEEP < 10) THEN GOTO 8230
7480   CALL SPOLL% (HPADDR%,POLL%,STATUS%)
7490   GOTO 7460
7500   '
7510   REM --------------------- TRANSMIT ----------------------
7520   S$="X?"
7530   CALL SEND%(HPADDR%,S$,STATUS%)
7540   S$="MLA TALK 18"
7550   CALL TRANSMIT% (S$,STATUS%)
7560   IF STATUS%<>0 THEN GOTO 8230
7570   REM --------------------- RECEIVE ----------------------
```

```
7580   X$=SPACE$(15)              ' allocate RECEIVE buffer
7590   FOR I=0 TO 400
7600     CALL RECEIVE% (X$,LENGTH%,STATUS%)
7610     IF STATUS%<>0 THEN GOTO 8230
7620     X(I)=VAL(X$)
7630   NEXT I
7640   REM --------------------- TRANSMIT ----------------------
7650   S$="UNL UNT"
7660   CALL TRANSMIT% (S$,STATUS%)
7670   S$="A?"
7680   CALL SEND%(HPADDR%,S$,STATUS%)
7690   S$="MLA TALK 18"
7700   CALL TRANSMIT% (S$,STATUS%)
7710   IF STATUS%<>0 THEN GOTO 8230
7720   REM --------------------- RECEIVE ----------------------
7730   REM DRESS-UP THE PC SCREEN OUTPUT
7740   CLS:PRINT " FREQUENCY      AMPLITITUDE"
7750   '
7760   A$=SPACE$(13)              ' allocate RECEIVE buffer
7770   FOR I=0 TO 400
7780     CALL RECEIVE% (A$,LENGTH%,STATUS%)
7790     IF STATUS%<>0 THEN GOTO 8230
7800     A(I)=VAL(A$)
7810     IF (I MOD 4)=1 THEN PRINT #1, USING "+#.#####^^^^,";COUNT,X(I),A(I)
7820     IF (I MOD 40)=0 THEN PRINT X(I);"HZ ";A(I);"dbM"
7830   NEXT I
7840   '
7850   S$="SWM1"          ' HP-4195A BACK TO CONTINUOUS SWEEP
7860   CALL SEND% (HPADDR%,S$,STATUS%)
7870   IF STATUS%<>0 THEN GOTO 8230
7880 NEXT COUNT
7890 CLOSE #1
7900 PRINT ""
7910 PRINT " DATA TRANSFER TO '";FILENAM$;"' COMPLETE."
7920 '
7930 REM --------------------- TRANSMIT ----------------------
7940 S$="UNL UNT"
7950 CALL TRANSMIT% (S$,STATUS%)
7960 IF STATUS%<>0 THEN GOTO 8230
7970 '
7980 S$="SWM1"       ' HP-4195A BACK TO CONTINUOUS SWEEP
7990 CALL SEND% (HPADDR%,S$,STATUS%)
8000 IF STATUS%<>0 THEN GOTO 8230
8010 '
8020 REM -----------TERMINATE HP-4195A CONTROL ---------------
8030 S$="UNL UNT"
8040 CALL TRANSMIT% (S$,STATUS%)
8050 RETURN
8060 '
8070 '
8080 '
```

```
8090 '
8100 '
8110 REM ------------------- TERMINATE PROGRAM ----------------
8120 '
8130 S$="UNL UNT"
8140 CALL TRANSMIT% (S$,STATUS%)
8150 CLS        'CLEAR SCREEN
8160 SYSTEM
8170 '
8180 '
8190 '
8200 '
8210 '
8220 REM ------------------- ERROR MESSAGE --------------------
8230 PRINT "COMM PROBLEM -- CHECK IEEE-488 CONNECTIONS,
8240 PRINT "                MAKE SURE EQUIPMENT IS ON AND CONNECTED
8250 PRINT "                THEN RESTART PROGRAM."
8260 STOP
8270 REM------------------- TIMER INITIALIZATION--------------
8280 '
8290 ELAPSE.TIME$="00:00:00"
8300 HOURS = 0
8310 MINUTES = 0
8320 SECONDS = 0
8330 '
8340 'TURN ON ELAPSE TIMER
8350 '
8360 BEGIN.TIME$ = TIME$
8370 BEGIN.HRS=VAL(LEFT$(BEGIN.TIME$,2))
8380 BEGIN.MIN=VAL(MID$(BEGIN.TIME$,4,2))
8390 BEGIN.SEC=VAL(RIGHT$(BEGIN.TIME$,2))
8400 ON TIMER (1) GOSUB 8440
8410 TIMER ON
8420 RETURN
8430 '
8440 REM--------------------- TIMER UPDATE ---------------------
8450 '
8460 TIME.NOW$=TIME$
8470 NOW.HRS = VAL(LEFT$(TIME.NOW$,2))
8480 NOW.MIN = VAL(MID$(TIME.NOW$,4,2))
8490 NOW.SEC = VAL(RIGHT$(TIME.NOW$,2))
8500 SECONDS = NOW.SEC-BEGIN.SEC
8510 IF SECONDS >= 0 THEN 8530
8520 SECONDS=SECONDS+60: NOW.MIN=NOW.MIN-1
8530 MINUTES = NOW.MIN-BEGIN.MIN
8540 IF MINUTES >= 0 THEN 8560
8550 MINUTES=MINUTES+60: NOW.HRS=NOW.HRS-1
8560 IF NOW.HRS<BEGIN.HRS THEN NOW.HRS=NOW.HRS+24
8570 HOURS = NOW.HRS-BEGIN.HRS
8580 IF SECONDS < 10 THEN SECONDS$ = "0" + RIGHT$(STR$(SECONDS),1)
8590 IF SECONDS >= 10 THEN SECONDS$ = RIGHT$(STR$(SECONDS),2)
```

```
8600 IF MINUTES < 10 THEN MINUTES$ = "0" + RIGHT$(STR$(MINUTES),1)
8610 IF MINUTES >= 10 THEN MINUTES$ = RIGHT$(STR$(MINUTES),2)
8620 ELAPSE.TIME=HOURS*60 + MINUTES + SECONDS/60
8630 RETURN
```

Bibliography

1. Margolis, James M. *Advanced Thermoset Composites: Industrial and Commercial Applications.* New York: Van Nostrand Reinhold Company, 1986.
2. Fanconi, B. *et al.* "Cure Monitoring for Polymer Matrix Composites," *Sagamore Army Materials Research Conference Proceedings, 31*: 275–91 (1986).
3. Wiseman, Capt John M. *Investigation of the Impedance Modulation of Thin Films with a Chemically-Sensitive Field-Effect Transistor.* MS Thesis, AFIT/GE/ENG/88D-6.61. School of Engineering, Air Force Institute of Technology, Wright-Patterson AFB, OH, 5 December 1988.
4. Jenkins, Capt Thomas J. *Evaluation of Doped Phthalocyanines and a Chemically-Sensitive Field-Effect Transistor for Detecting Nitrogen Dioxide.* MS Thesis, AFIT/GE/ENG/89D-18. School of Engineering, Air Force Institute of Technology, Wright-Patterson AFB, OH, 4 December 1989.
5. Shin, Capt Jenny E. *Evaluation of Chemically-Sensitive Field-Effect Transistors for Detection of Organophosphorous Compounds.* MS Thesis, AFIT/GE/ENG/89D-47. School of Engineering, Air Force Institute of Technology, Wright-Patterson AFB, OH, 5 December 1989.
6. Kolesar, Edward S. and John M. Wiseman. "Epoxy Cure Monitoring with an Interdigitated Gate Electrode Field Effect Transistor," *Sensors Expo West Proceedings,* 101B-1 to 101B-7 (March 1990).
7. Kolesar, E. *Chemically-Sensitive Field-Effect Transistor.* Thesis Proposal No. VI.13. School of Engineering, Air Force Institute of Technology, Wright-Patterson AFB OH, October 1988.
8. Billmeyer, Fred W., Jr. *Textbook of Polymer Science* (Second Edition). New York: John Wiley and Sons, 1971.
9. Mopsik, F. I. *et al.* "Dielectric Measurements for Cure Monitoring," *Materials Evaluation, 47*: 448–453 (April 1989).
10. Sheppard, Norman Fred, Jr. *Dielectric Analysis of the Cure of Thermosetting Epoxy/Amine Systems.* PhD Dissertation. Massachusetts Institute of Technology, Cambridge, MA, 1986.
11. Lee, H. *Optimization of a Resin Cure Sensor.* MS Thesis. Massachusetts Institute of Technology, Cambridge, MA, 1982.
12. Lee, Henry and Kris Neville. *Handbook of Epoxy Resins.* New York: McGraw-Hill Book Company, 1967.
13. Tung, Chiang-Ying and Paul J. Dynes. "Relationship between Viscoelastic Properties and Gelation in Thermosetting Systems," *Journal of Applied Polymer Science, 27*: 569–574 (1982).
14. Von Hippel, Arthur R. *Dielectrics and Waves.* New York: John Wiley and Sons, 1954.
15. Wang, F. W. *et al.* "Fluorescence Monitoring of Viscosity and Chemical Changes During Polymerization," *American Chemical Society Symposium Series on Photophysics of Polymers,* edited by C. E. Hoyle and J. M. Torkelson. Washington, D.C.: American Chemical Society, 1987.

16. Sung, C. S. P. "Application of Reactive Dye Labeling Technique for Cure Characterization of Epoxy Networks," *American Chemical Society Symposium Series on Photophysics of Polymers*, edited by C. E. Hoyle and J. M. Torkelson. Washington, D.C.: American Chemical Society, 1987.

17. Sung, C. S. P., W. Tang, and N. H. Sung. *In-Situ Cure Monitoring of Composites by Fiber-Optic Molecular Sensors.* Medford, MA: Tufts University, Office of Naval Research, August 1989 (AD-A211495).

18. Kranbuehl, D. *et al.* "Dynamic Dielectric Analysis: Nondestructive Material Evaluation and Cure Cycle Monitoring," *Polymer Engineering and Science, 26*: 338–345 (March 1986).

19. Wohltjen, Hank *et al.* "A Vapor-Sensitive Chemiresistor Fabricated with Planar Microeletrodes and a Langmuir-Blodgett Organic Semiconductor Film," *IEEE Transactions on Electron Devices, 32*: 1170–1174 (July 1985).

20. Senturia, Stephen D. "The Role of the MOS Structure in Integrated Sensors," *Sensors and Actuators, 4*: 507–526 (1983).

21. Janata, Jiri. *Principles of Chemical Sensors.* New York: Plenum Press, 1989.

22. Senturia, Stephen D. *et al.* "The Charge-Flow Transistor: A New MOS Device," *Applied Physics Letters, 30*: 106–108 (15 January 1977).

23. Senturia, Stephen D. *et al. The Feasibility of Electrical Monitoring of Resin Cure with the Charge-Flow Transistor.* Cambridge, MA: Massachusetts Institute of Technology, Office of Naval Research, December 1979 (AD-A081977).

24. Senturia, Stephen D. *et al.* "Monolithic Integrated Circuit Implementation of the Charge-Flow Transistor Oscillator Moisture Sensor," *Sensors and Actuators, 2*: 59–71 (1981).

25. Garverick, Steven L. and Stephen D. Senturia. "An MOS Device for AC Measurements of Surface Impedance with Application to Moisture Monitoring," *IEEE Transactions on Electron Devices, 29*: 90–94 (January 1982).

26. Sheppard, Norman F. *et al.* "Microdielectrometry: A New Method for *In Situ* Cure Monitoring," *26th National SAMPE Symposium*, 65–76 (April 1981).

27. Senturia, Stephen D. *et al. Electrical Monitoring of Polymerization Reactions with the Charge-Flow Transistor.* Cambridge MA: Massachusetts Institute of Technology, Office of Naval Research, 31 May 1984 (AD-A142267).

28. Janata, Jiri *et al.* "Chemically Sensitive Field-Effect Transistor to Detect Organophosphorous Compounds and Pesticides." *Aviation, Space, and Environmental Medicine, 52*: 666–671 (November 1981).

29. Janata, Jiri and Dieter Gehmlich. *CHEMFET Chemical Warfare Agent Detector.* Salt Lake City, UT: University of Utah, December 1983 (AD-A139636).

30. Blythe, A. R. *Electrical Properties of Polymers.* Cambridge: Cambridge University Press, 1979.

31. Anderson, J. C. *Dielectrics.* New York: Reinhold Publishing Company, 1964.

32. Debye, P. *Polar Molecules.* New York: The Chemical Catalog Company, Inc., 1929.

33. MacDonald, J. Ross. *Impedance Spectroscopy.* New York: John Wiley and Sons, 1987.

34. Cole, Kenneth S., and Robert H. Cole. "Dispersion and Absorption in Dielectrics. I. Alternating Current Characteristics." *Journal of Chemical Physics, 9*: 341–351 (April 1941).

35. Miller-Stephenson Chemical Company, Incorporated. *Epoxy Systems: Technical Information.* Danbury CT, undated.

36. Bobalek, E. G. *et al.* "Some Implications of the Gel Point Concept to the Chemistry of Alkyd Resins." *Journal of Applied Polymer Science, 8*: 625–657 (1964).

37. Blair, Scott. *Elementary Rheology.* London: Academic Press, 1969.

38. Eirich, Frederick R. *Rheology: Theory and Applications*, Volume 2. New York: Academic Press, 1958.

39. Brothers, Capt Charles P. *Evaluation of an Interdigitated Gate Electrode Field-Effect Transistor for Detecting Organophosphorus Compounds.* MS Thesis, AFIT/GE/ENG/90D-07. School of Engineering, Air Force Institute of Technology, Wright-Patterson AFB OH, December 1990.

40. Roller, Mark B., and John K. Gillham. "Application of Dynamic Mechanical Testing to Thermoset and Coatings Research and Development." *Journal of Coatings Technology, 50*: 57–68 (January 1978).

41. Kolesar, E. and R. Walser. "Organophosphorus Compound Detection with a Supported Copper + Cuprous Oxide Island Film. 1. Gas-Sensitive Film Physical Characterisics and Direct Current Studies," *Analytical Chemistry, 60*: 1731–1736 (September 1988).

42. Keithly Instruments, Incorporated. *Instruction Manual, Model 617 Programmable Electrometer.* Cleveland, OH, 1984.

43. Abrams, Francis, Chemical Engineer. Personal interview. Wright Research and Development Center, Materials Laboratory (WRDC/MLBC), Wright-Patterson AFB OH, 3 May 1990.

44. Miller-Stephenson Chemical Company, Incorporated. Telephone interview. Danbury, CT, 21 September 1990.

REPORT DOCUMENTATION PAGE

Form Approved
OMB No. 0704-0188

1. AGENCY USE ONLY (Leave blank)	2. REPORT DATE	3. REPORT TYPE AND DATES COVERED
	December 1991	Master's Thesis

4. TITLE AND SUBTITLE
EVALUATION OF AN INTERDIGITATED GATE ELECIRODE FIELD-EFFECT TRANSISTOR FOR IN SITU RESIN CURE MONITORING

5. FUNDING NUMBERS

6. AUTHOR(S)
Thomas E. Graham, Captain, USAF

7. PERFORMING ORGANIZATION NAME(S) AND ADDRESS(ES)
Air Force Institute of Technology, WPAFB, OH 45433-6583

8. PERFORMING ORGANIZATION REPORT NUMBER
AFIT/GE/ENG/91D-55

9. SPONSORING/MONITORING AGENCY NAME(S) AND ADDRESS(ES)
Wright Laboratory, Materials Directorate (WL/MLBC)
WPAFB OH 45433-6583

10. SPONSORING/MONITORING AGENCY REPORT NUMBER

11. SUPPLEMENTARY NOTES

12a. DISTRIBUTION/AVAILABILITY STATEMENT
Approved for public release; distribution unlimited

12b. DISTRIBUTION CODE

13. ABSTRACT *(Maximum 200 words)*

The purpose of this study was to design an Interdigitated Gate Electrode Field-Effect Transistor (IGEFET) and evaluate its performance as an in situ resin cure monitor. A commercially available resin was selected for the research, and rheological studies were performed to identify the resin's gelation point during isothermal cures at two selected temperatures. Additional rheological studies were performed to identify the resin's glass transition temperature. The interdigitated gate electrode of the IGEFET was coated with samples of the resin, and electrical measurements were performed while the resin cured. The chemical changes which occur in the resin as a result of curing were manifested in the interdigitated gate electrode's electrical characteristics. The results reveal that the IGEFET is capable of sensing the electrical impedance changes, and hence the chemical changes, which occur during the resin's cure. In particular, the chemical changes due to gelation are evident in the IGEFET's electrical response data. In addition, the resin which was cured at the higher temperature was close to its glass transition temperature, and hence softer than the resin cured at the lower temperature, and the IGEFET was capable of detecting this difference.

14. SUBJECT TERMS
IGEFET, Resin Cure Monitoring, Epoxy, CHEMFET, Impedance Spectroscopy, These + field effect transistor

15. NUMBER OF PAGES
209

16. PRICE CODE

17. SECURITY CLASSIFICATION OF REPORT	18. SECURITY CLASSIFICATION OF THIS PAGE	19. SECURITY CLASSIFICATION OF ABSTRACT	20. LIMITATION OF ABSTRACT
Unclassified	Unclassified	Unclassified	UL